Cranfield University

School of Engineering
Department of Process and Systems Engineering

Multiphase Flow Measurement in the Slug Regime Using Ultrasonic Measurements Techniques and Slug Closure Model

Salem Al-lababidi

PhD Thesis

June, 2006

Cranfield University

School of Engineering

Ph.D. THESIS

Academic Year 2002-2006

Salem Al-lababidi

Multiphase Flow Measurement in the Slug Regime Using Ultrasonic Measurements Techniques and Slug Closure Model

Supervisor: Professor. M.L.Sanderson

Academic Year 2006

This thesis is submitted in partial fulfilment of the requirements for the degree of Doctor of Philosophy

ABSTRACT

Multiphase flow in the oil and gas industry covers a wide range of flows. Thus, over the last decade, the investigation, development and use of multiphase flow metering system have been a major focus for the industry worldwide. However, these meters do not perform well in slug flow conditions.

The present work involves experimental investigations of multiphase flow measurement under slug flow conditions. A two-phase gas/liquid facility was designed and constructed at Cranfield University. It consisted of a 0.05 m diameter 25 m long horizontal pipeline with the necessary instrumentation.

An ultrasonic multiphase metering concept has been proposed and investigated. The concept was based on the combination of non-invasive and non-intrusive ultrasonic sensors and a slug closure model. The slug closure model was based on the "slug unit" model to infer the gas and liquid phase volumetric flowrates.

The slug characteristics obtained by non-invasive and non-intrusive ultrasonic techniques were inputs to slug closure model which calculates the factors $K_{1\,(Liquid)}$, $K_{2\,(Liquid)}$, $K_{3\,(Gas)}$ and $K_{4\,(Gas)}$. These factors are function of the slip ratio in the slug body, flow profile (C_o), drift velocity (V_d), liquid holdup and gas void fraction in slug body, slug length, film length, and the total length of the slug unit. Based on ultrasonic sensor measurements, the slug translational velocity was estimated and the slug closure model then calculates the gas and liquid phase volumetric flowrates.

Air water slug flow data were gathered and processed for a range of superficial velocities V_{SL}=0.3 to 1.03 ms^{-1} and V_{SG}=0.6 to 3.01 ms^{-1}. The overall goal of a 5% relative error metering for both phases was not achieved for the conditions tested. The liquid phase percentage errors were from -63.6% to 45.4% while the gas phase percentage errors were from 42% to -14.6%.

Key words: slug flow, slug characteristics, slug closure model, non-invasive ultrasonic, non-intrusive ultrasonic, clamp-on transit time ultrasonic flowmeter.

PAGE NUMBERING AS ORIGINAL

ACKNOWLEDGEMENTS

I wish to express my sincere thanks and gratitude to my supervisor Professor Mike Sanderson for his unconditional support, valuable and continuous advice, guidance, thoughtfulness and assistance throughout the duration of this work. I would like to thank Dr. Hoi Yeung for his advice and kind supports.

My thanks also go to Hermann Gmeiner Academy, Austria represented by Mr. Kutine, Daniel Fox and Gabriel Alexander for the provision of the scholarship and financial support for the duration of my study at Cranfield University.

My thanks and appreciation is due to the all members of staff in the Department o f Process and Systems Engineering for their great support and encouragement throughout this work.

My gratitude belongs to my family, whose love, encouragement, support and faith meant a very great deal to me. I would like to express my appreciation for all the kind support they have offered. It would have been much harder without such support.

Finally, but no means least, I would like to express my gratefulness and gratitude to my friends for their unconditional support, encouragement and tolerance over the life of this PhD. Without them, it would simply not have been possible.

Table of Contents

List of Figures

List of Figures

List of Tables

Nomenclature

Symbol	Denotes	Units
A_{pipe}	pipe cross-section area	m^2
L_S	slug liquid body length	m
L_F	film zone length	m
L_U	slug unit length	m
E_{LS}	slug liquid body holdup	(-)
E_{LF}	liquid film holdup	(-)
V_{SL}	superficial liquid velocity	ms^{-1}
V_{SG}	superficial gas velocity	ms^{-1}
V_{LS}	local liquid slug body velocity	ms^{-1}
V_{GS}	local dispersed bubble in liquid slug body velocity	ms^{-1}
V_{LF}	liquid film velocity	ms^{-1}
V_{GF}	gas velocity in film zone	ms^{-1}
V_T	slug translational velocity	ms^{-1}
V_{mix}	mixture velocity	ms^{-1}
ΔP_U	slug unit pressure drop	Pa
ΔP_S	slug region pressure drop	Pa
ΔP_{Film}	film region pressure drop	Pa
ΔP_{acc}	accelerating pressure drop	Pa
t_{Slug}	time for the passage of a slug body	s
t_{Film}	time for the passage of a film zone	s
$t_{Slug(U)}$	slug body time measured by ultrasonic	s
$t_{Film(U)}$	film zone time measured by ultrasonic	s

Nomenclature

C	distribution parameter (unaerated slug body)	(-)
C_o	distribution parameter (aerated slug body)	(-)
V_d	slug flow drift velocity	ms^{-1}
$K_{1\ (Liquid)}$ and $K_{2\ (Liquid)}$,	slug closure model factors for liquid phase	-
$K_{3\ (Gas)}$ and $K_{4\ (Gas)}$.	slug closure model factors for gas phase	-
Re_S	slug Reynolds number	-
s	slip parameter	-
υ	slug frequency	Hz
ρ_m	mixture density	$kg\ m^{-3}$
ρ_l, ρ_g	liquid phase and gas phase density	$kg\ m^{-3}$
μ_l, μ_g	liquid phase and gas phase viscosity	Nm^{-2}
σ	Liquid surface tension	Nm^{-1}
Fr	Froude number	-
Bo	Bond number	-

Chapter 1

Introduction

1.1 Reasons behind this Thesis

Recent years have seen the increasing acceptance of ultrasonic flow measurement techniques in the oil and gas industry as demonstrated in the recent international conferences (FLOMEKO, North Sea Flow Measurement Workshop) which up to half of the papers presented were related to ultrasonic flow metrology.

Ultrasonic techniques have significant potential benefits over the traditional mechanical flow measurements including higher reliability, greater rangeability, lower maintenance requirements and on-line maintenance possibility. The most significant benefit of ultrasonic flow meters is that they are non-invasive or non-intrusive.

The advantages of the ultrasonic technique encouraged many researchers to carry out further theoretical and experimental investigations to implement this fascinating technique to oil and gas multiphase flow measurements. The present work was driven with the hope to introduce a new ultrasonic metering concept for the oil and gas industry.

1.2 Background

Multiphase flow in oil and gas industries covers a wide range of flow conditions. Over the last decade, the investigations and developments of multiphase flow metering system for use in oil fields have been a major focus for the industry worldwide.

An offshore production facility consists of several satellite wells. The contents of each well are combined and passed onshore via a common pipeline. Each satellite well produces variable quantities of oil, water and gas during its lifetime. However, if

different companies own these wells, their flowrates and compositions must be monitored before any mixing takes place. This factor is one of the main reasons behind the increased importance of multiphase flowmeters.

Within the oil and gas industry, it is generally recognized that the implementation of multiphase flow metering could lead to great benefits in terms of well testing, reservoir management, production allocation, production monitoring, capital expenditure and operational expenditure. So it can be concluded that using multiphase flowmeters can lead to:

- Reduction in the capital cost as the outputs of several wells can be grouped together after being metered at the well discharge.

- Reduction in capital cost of new offshore platforms by replacing the bulky and heavy test separators.

- Better reservoir management, production allocation and optimisation of total oil production over the lifetime of the field. This could mean the continued production for otherwise uneconomical wells rather than abandonment leaving behind a high proportion of the oil untapped.

An ideal multiphase flowmeter would be able to measure to the required accuracy over the range of component fractions and flow rates. The general agreement amongst the major oil companies is that a satisfactory multiphase meter would need to measure over 0-99% gas volume flowrate and 0-90% water cut. The ideal multiphase flowmeter should have several attributes apart from the ability to measure up to the required accuracy level as listed below:

- In order to minimise erosion of the device, to avoid pressure drop and difficulties with pipe cleaning operations, the flowmeter should not physically interfere with the flow. In other word, it should be non-intrusive meter.

- Multiphase flowmeter should be robust, reliable and require little maintenance, especially for subsea metering applications where maintenance operations are costly.

- It should also be flow regime independent, i.e. unaffected by changes in the prevailing flow regime.

- Another important factor to consider when designing a multiphase flow meter is cost. The price of multiphase flowmeter should be within the current market price (approximately £100 - 200k for surface and £200 - 400k for subsea per unit).

The measurement accuracy obtained by multiphase flowmeter should be at least comparable to the test separation method. In practice, about 5% relative error accuracy in the phase mass flowrates and about 2% absolute accuracy in the water cut are desired.

However, from practical point of view, the wide variety of possible flow regimes for oil, water and gas mixtures makes these requirements hard to be achieved. Therefore, there is still much work to be done in this area.

1.3 Thesis Overview

Recent years have seen the increasing acceptance of deploying ultrasonic flow measurements technique in oil and gas industries. However, the implementation of the ultrasonic technique is still restricted to the single phase pipelines such as export pipelines.
This thesis presents a new metering concept to measure multiphase flow in pipeline using combinations of non-invasive and non-intrusive ultrasonic sensors.

Due to the fact that multiphase flow system has a wide range of flow conditions and cannot be addressed within a single study, this thesis concentrates only on two-phase gas/water flow in horizontal pipelines.

During the production well lifetime, the gas and liquid phases will typically adopt a slug flow pattern. This thesis describes the development of ultrasonic metering concept for metering two-phase air/water under slug flow conditions.

1.4 Thesis Objectives

This thesis experimentally investigates the development of an ultrasonic metering system through the use of a combination of non-invasive and non-intrusive ultrasonic sensors to measure the gas and liquid phase volumetric flowrates under slug flow conditions in a 2-inch horizontal pipeline. The main objectives of this thesis are:

- Literature review of the multiphase metering systems and ultrasonic applications in multiphase flow measurement.

- Literature review in slug flow characteristics and modelling of slug flow.

- Develop a slug closure model to infer the gas and liquid phase volumetric flowrates.

- Measuring the slug flow characteristics by non-invasive and non-intrusive ultrasonic sensors.

- Design and build a two-phase gas/liquid facility and its instrumentations to assess the performance of the ultrasonic metering concept under two-phase gas/liquid slug flow conditions.

Based on the outcome from the last objectives, a set of proposal for future study is presented.

1.5 Thesis Structure

The remainder of this thesis is divided into 6 chapters, the content of which are described below.

Chapter 2, 'Review of Multiphase Flow Measurement Techniques'.

In the first part of this Chapter, the definition of multiphase flow, flow regimes and flow map in horizontal pipes are introduced. The second part of the Chapter introduces the reader to the concept of measurement strategies followed in multiphase flow systems. The third part of the Chapter introduces the techniques of multiphase flow measurements currently available. The fourth part concentrates on the ultrasonic measuring techniques and their application in multiphase flow. This part of the chapter is demonstrated through the latest patents in the applications of ultrasonic for multiphase flow measurements.

Chapter 3, 'Slug Closure Model and Ultrasonic Metering Concept

This chapter is separated into four main parts. The first part describes the slug flow initiation and dissipation process in two-phase gas/liquid in horizontal pipelines. Empirical correlations for slug flow characteristics including slug body velocity, slug body liquid holdup, slug frequency, and slug length are presented in the second part of this Chapter. In the third part of this chapter, the development of the slug closure model based on the slug unit "steady-state" model is presented. Then the ultrasonic metering concept is detailed in the fourth part of this Chapter.

Chapter 4, 'Experimental Set-up',

In the first part of this Chapter, the water and gas supply system and their instrumentations are presented. The conductivity ring design and its calibration process, non-invasive ultrasonic sensors and their signal conditioning unit, the non-intrusive ultrasonic level sensor and its electronic circuit are described in the second part of this Chapter. This is followed by the experimental test campaigns and the data acquisition systems are presented.

Chapter 5, 'Slug Characteristics Measurements by Ultrasonic Techniques'.

This chapter describes firstly the ultrasonic signals generated under slug body and film zone. Then in the second part, the measurement of the slug frequency using non-invasive ultrasonic sensor is presented. The third part describes the measurement of the slug translational velocity using non-invasive ultrasonic sensor. The slug body length and the film region length are measured by non-invasive ultrasonic sensor and they are presented. The fifth part of this Chapter presents the slug body liquid holdup and the film liquid holdup measurements by non-intrusive ultrasonic sensor. The sixth part of this chapter then describes the method used to extract the flow profile C_0 and the drift velocity V_d.

Chapter 6, 'Ultrasonic Multiphase Metering Performance Assessment'.

This chapter describes the performance assessment of the proposed metering concept. Experimental data are obtained from the two-phase gas/liquid facility, for the range of liquid superficial velocities V_{SL}=0.3 to 1.03 ms^{-1} and gas superficial velocities V_{SG}=0.6 to 3.01 ms^{-1}. These data are processed to calculate the slug closure model factors $K_{1\ (Liquid)}$, $K_{2\ (Liquid)}$, $K_{3\ (Gas)}$ and $K_{4\ (Gas)}$, the gas and liquid phase volumetric flowrates, and the relative predication errors.

Chapter 7, 'Conclusions and Recommendations for Future Work',

The thesis concluded by summarising the conclusions of all the previous chapters. A discussion of future work is also included.

Chapter 2

Review of Multiphase Flow Measurement Techniques

This chapter provides a selective background of the experimental and the theoretical approach to a number techniques applied in area of multiphase flow measurements including ultrasonic transit time methods.

The chapter starts with the definition of multiphase flows and the fundamentals of multiphase flow system in pipeline, Section 2.1. The current status of multiphase flow measurements is discussed in Section 2.2.

In Section 2.3, different direct measurement techniques for phase fraction, phase velocity and phase density using different measurement techniques are discussed.

The review of ultrasonic techniques used in multiphase flow measurement is presented in Section 2.4. Finally, the chapter summary is presented in Section 2.5.

2.1 Multiphase Flows

The simultaneous flow of two or more phases in pipe is termed multiphase flow. Multiphase flow systems are of great industrial significance and are commonly found in the chemical, process, nuclear, hydrocarbon and food industries. The subject has received widespread research attention, particularly over the past five decades.

In multiphase flows, the flow behaviour is much more complex than for single-phase flow. The phases tend to separate because of differences in density. Shear stresses at the pipe wall are different for each phase as a result of their different densities and viscosities. The most distinguishing aspect of multiphase flow is the variation in the physical distribution of the phases in the flow conduit, a characteristic known as flow pattern or flow regime.

2.1.1 Horizontal Gas-Liquid Flow Regimes

Gas/Liquid flow regimes in horizontal pipes are summarised in Figure 2-1, from top to bottom in order of increasing gas flow rate.

- *Bubble Flow*: In bubble flow, small gas bubbles flow along the top of the pipe.

- *Elongated Bubble Flow*: Collisions between the individual bubbles occur more frequently with increasing gas flow rate and they coalesce into elongated "plugs". This is often called plug flow.

- *Smooth Stratified Flow*: The gas plugs coalesce to produce a continuous gas flow along the top of the pipe with a smooth gas-liquid interface typical of stratified flow at relatively low flow rates.

- *Wavy Stratified Flow*: In most situations, the gas-liquid interface is rarely smooth with ripples appear on the liquid surface. The amplitude increases with increased gas flow rate.

- *Slug Flow*: When the amplitude of the waves travelling along the liquid surface becomes sufficiently large enough for them to bridge the top of the pipe, the flow enters the slug flow regime. The gas flows as intermittent slugs and with smaller bubbles entrained in the liquid.

- *Annular Flow:* Occurs when gas flow rate is large enough to support the liquid film around the pipe walls. Liquid is also transported as droplets distributed throughout the continuous gas stream flowing in the centre of the pipe. The liquid film is thicker along the bottom of the pipe because of the effect of gravity.

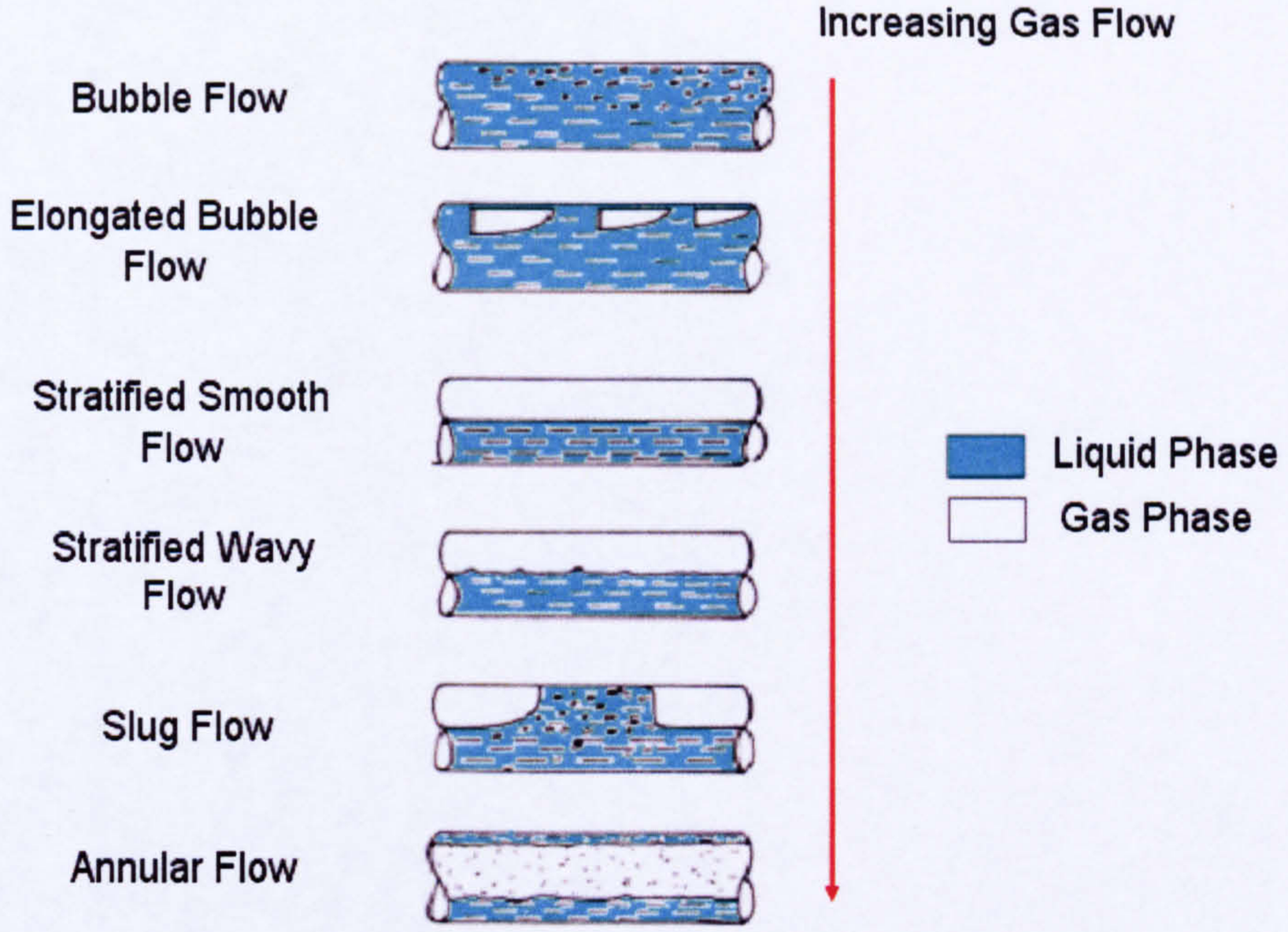

Figure 2-1: Flow Regimes of Gas/ Liquid Horizontal Flow

2.1.2 Gas-Liquid Flow Regimes Map in Horizontal Flow

The most distinguish aspect of multi-phase flow is the variation of the physical distribution of the phases in the flow conduit, a characteristic known as flow pattern or flow regime. The flow pattern that exists depends on the relative magnitudes of the forces that act on the fluids. These forces such as buoyancy, turbulence, inertia, and surface-tension forces, all vary significantly with flow rates, pipe diameter, inclination angle, and fluid properties of the phases.

Flow pattern is often displayed using a flow pattern map, which is a two-dimensional map depicting flow regime transition boundary. The selection of appropriate coordinates to present clearly and effectively the different flow regimes has been a research topic for a long time. The dimensional coordinates such as superficial velocities are much more generally used in practice as the one by Taitel *et al.* (1976).as shown in Figure 2-2.

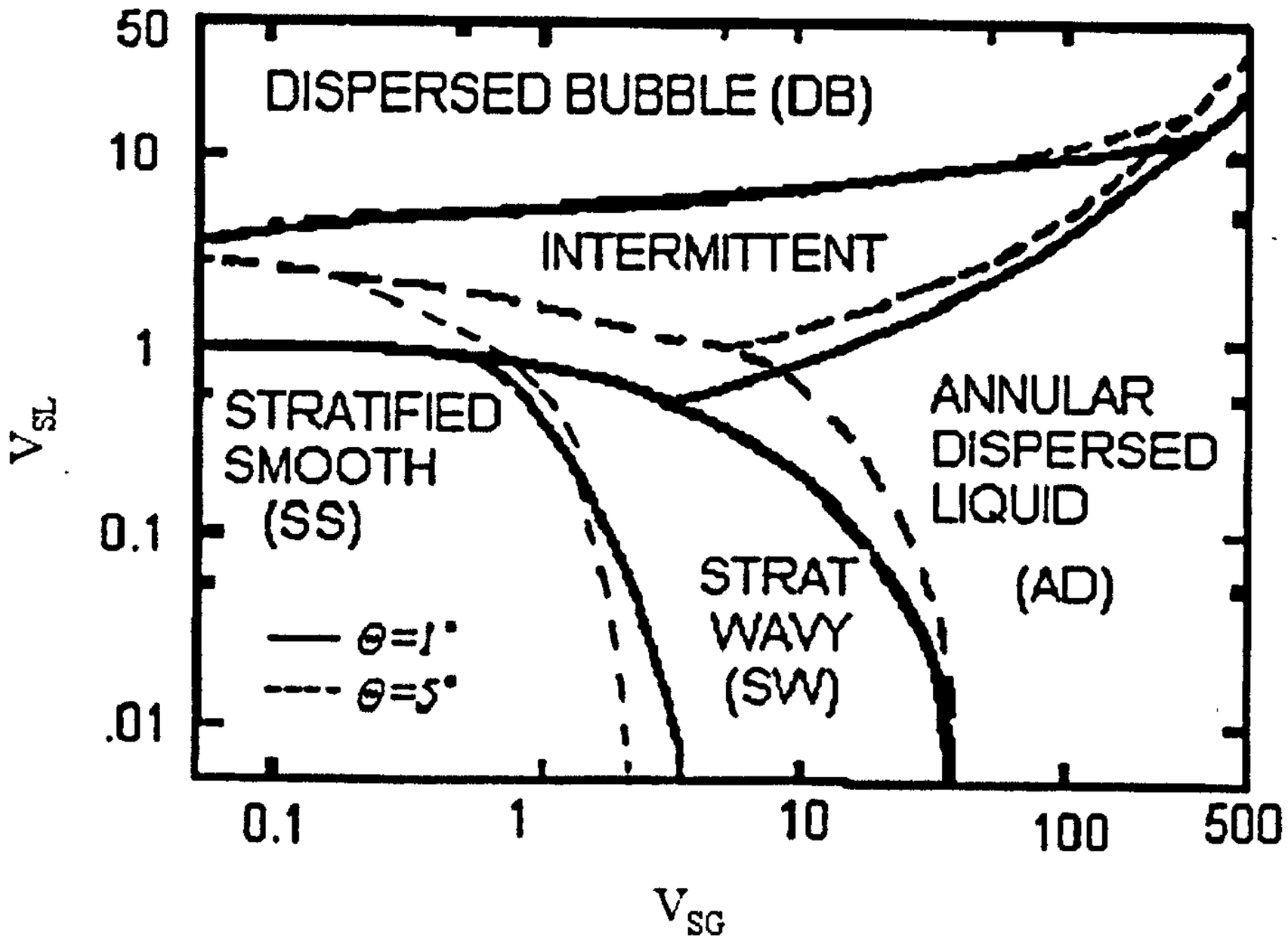

Figure 2-2: Horizontal Flow Regimes Map by Taitel *et al.* (1976)

2.2 Current Status in Multiphase Flow Measurements

Multiphase metering methods can be classified into two major groups. The first group is the conditioning methods where the condition of the phases in the pipe is changed (phases partial separations or phases mixing) upstream of the metering point. The second group is the direct method, where the phase parameter measurements are achieved without a pre-conditioning process.

In a partially separation system, as the name suggests, is based on partially separate the flow, usually into predominately liquid and predominately gas streams, before measurement. Since the separation is only partial, some liquid expected to travel with the gas stream. As a result, each flow stream only needs to be measured over a limited range of phase fractions as shown in Figure 2-3a.

In homogenous based systems, the flow is pre-mixed to try to ensure that all measurements are made on a homogenous flow, hence removing the problem of flow regime dependency and reducing the number of and difficulties of measurement required. Figure2-3b shows an example of a commercially available three-phase flowmeter which uses this strategy. The Framo multiphase flowmeter uses a tank mixer to homogenize the flow both radially and axially. The homogenized flow then passes through a Venturi meter which is used to measure the velocity of the mixture, and a dual-energy-ray attenuation meter which uses two different energy levels of the Barium 133 isotope to determine the oil, water and gas fractions.

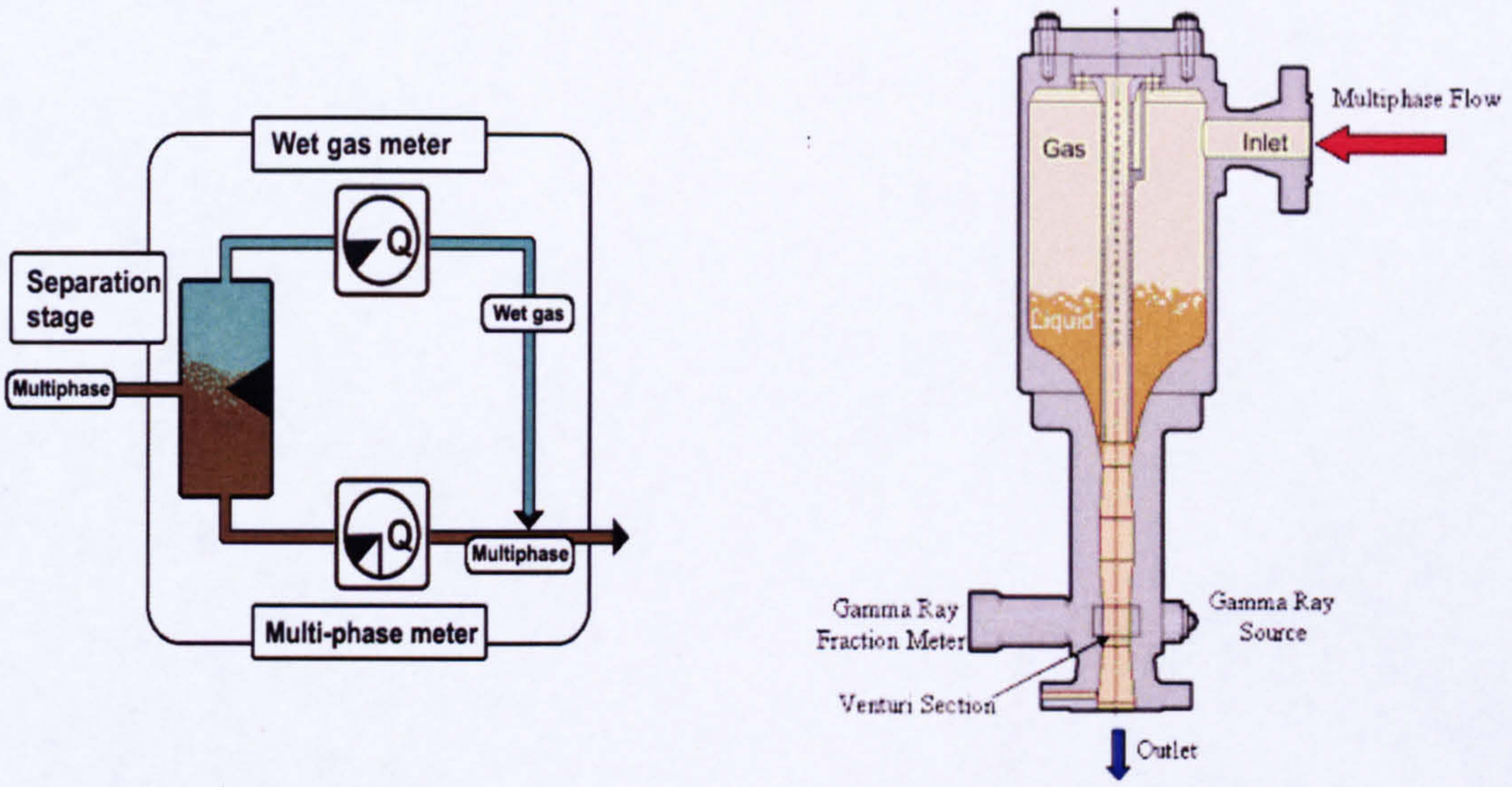

a. Partial Separation System b. Homogenisation System

Figure 2-3: Preconditioning System (Thorn *et al.* 1997)

2.2.1 Measurement Strategies - Inferential Approach

The primary information required by a user of multiphase meters is the mass flow rate of the each phase. An ideal multiphase flow meter would make independent direct measurements of each of these quantities. Unfortunately, direct mass flowmeters for use with two phase flows are rare and do not exist at all for three phase flows.

An alternative to direct mass flow measurement is to use an inferential method. An inferential mass method requires both the instantaneous velocity and cross sectional fraction of each component to be know in order to calculate the individual component mass flowrates and total mixture mass flowrate (Thorn *et al.* 1997). Figure 2-4 shows a schematic of such an approach. Two types of parameters are monitored by a multiphase metering system:

1. Primary parameters:
    - Phase fraction (e.g. void fraction, water cut);
    - Phase velocity (the velocity of each phase as they cannot be assumed to be travelling at the same velocity);
    - Phase density.
2. Secondary parameters:
    - Flow regime (this may be considered as a primary parameter if a flow dependent sensing technique is used);

- Phase viscosity;
- Phase salinity;
- Phase permittivity/ conductivity.

Density information of the oil, water and gas components are readily available from other parts of the production process, e.g. densitometer readings or estimated from PVT diagrams using measured pressure and temperature. Therefore, the problem is to measure the oil, water, and gas velocities and two of the component fractions. The third component fraction (oil fraction) is deduced from the fact that the sum of the three phase fractions is equal to unity.

$$m = \alpha_g \times V_g \times \rho_g \times A_{pipe} + \alpha_w \times V_w \times \rho_w \times A_{pipe} + \alpha_o \times V_o \times \rho_o \times A_{pipe} \quad (2.1)$$

where

m is the total mass flow rate,

ρ_g, ρ_w and ρ_o are the densities of gas, water and oil,

V_g, V_w and V_o are the velocities of gas, water and oil,
A_{pipe} is the pipe cross section area.

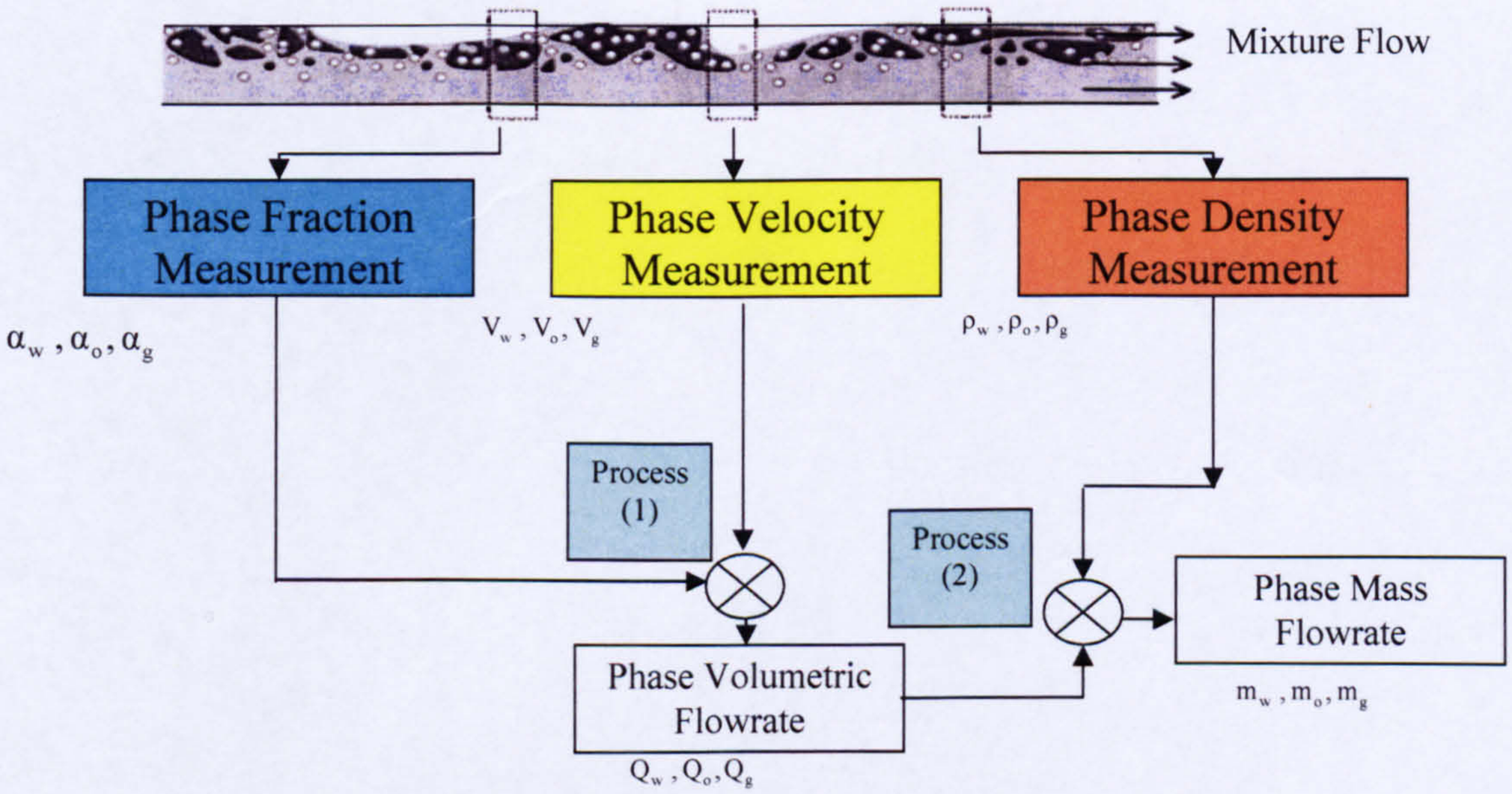

Figure 2-4: Inferential Multiphase Flow Measurement Strategy (Thorn *et al.* 1997)

2.3 Direct Measurements Techniques in Multiphase Flow

2.3.1 Phase Fraction Measurement

The two most commonly used methods for measuring gas and liquid fractions in a multiphase flow are based on gamma-ray attenuation and electrical impedance techniques.

2.3.1.1 Gamma Ray Attenuation (Absorption) Measurement

The basic principle for the gamma-ray attenuation technique is the fact that the intensity of a collimated beam decreases exponentially as it passes through matter.

There are different gamma ray systems which are used in multiphase flow metering including, single-beam, dual-beam or multiple-beam gamma ray systems. Gamma ray attenuation measurement is applicable to all possible combinations of two-phase and three-phase flows (Corneliussen *et al*. 2005).

2.3.1.1.1 Single-Beam Gamma Ray Attenuation (Absorption)

The single energy gamma ray attenuation measurement is based on the attenuation of a narrow beam of gamma ray of energy as shown in Figure 2-5.

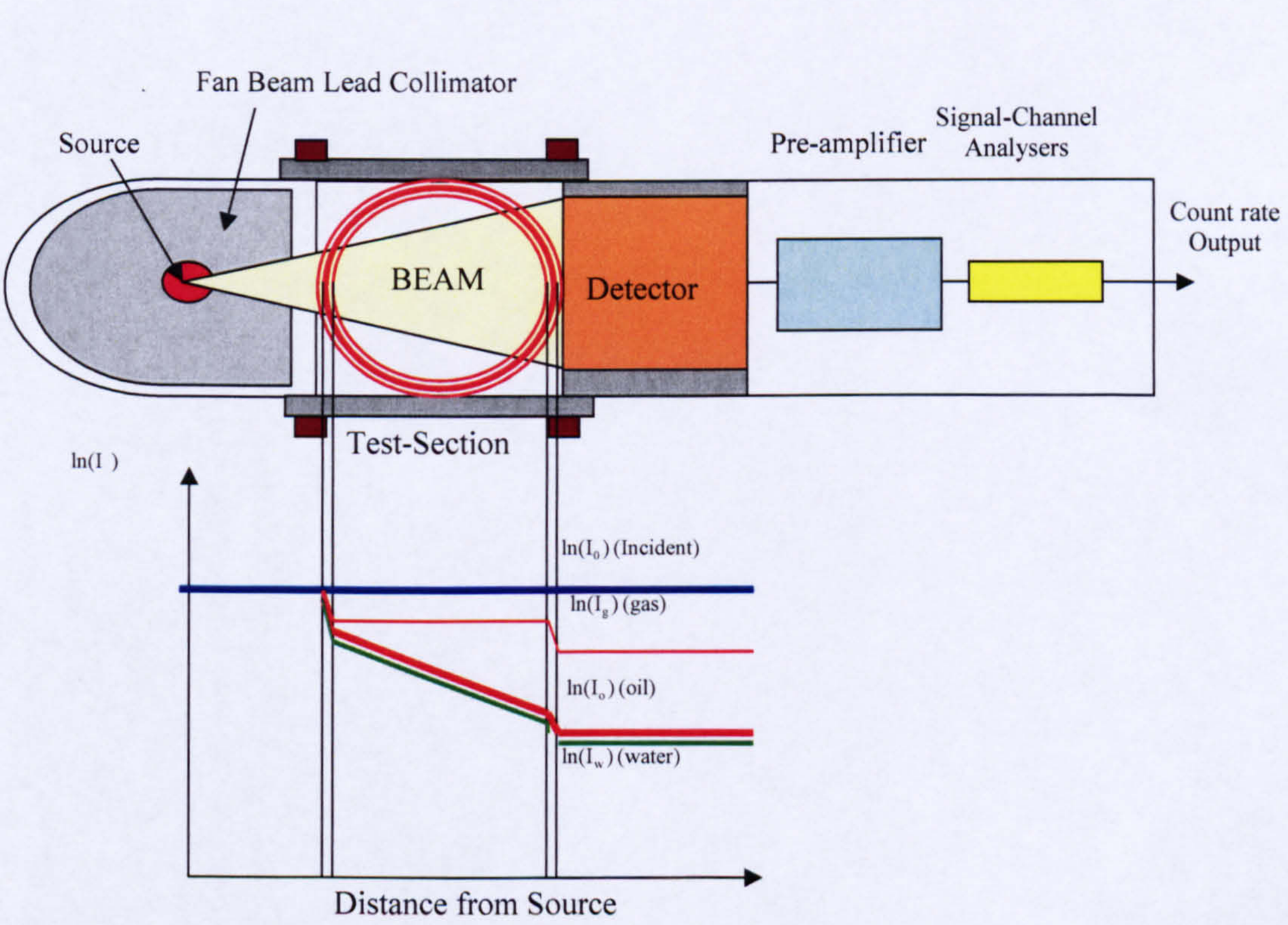

Figure 2-5: Single-Beam Gamma Ray Densitometer

Single energy gamma ray attenuation can be used in liquid/liquid system (oil/water) or liquid/gas system. In a pipe, with inner diameter d, the intensity of the beam of radiation after it has passed through the mixture of two-phase flow is given by:

$$I_m(e) = I_v(e) \times \exp[-\sum_{i=1}^{2} \alpha_i \times \mu_i(e) \times d] \qquad (2.2)$$

where

$I_m(e)$ is the measured countrate,

$I_v(e)$ is the count rate when the pipe is empty,

μ_i is the linear attenuation coefficients for the two phases.

Apart from fractions of the phases α_i, the attenuation coefficients μ_i are also initially unknown. However, the latter can be found by calibration where the meter is filled with individual fluids. In both cases the following two equations for water and oil can be used:

$$I_w = I_v \times \exp[-\alpha_w \times \mu_w \times d] \qquad (2.3)$$

$$I_o = I_v \times \exp[-\alpha_o \times \mu_o \times d] \qquad (2.4)$$

These two calibration points together with the relation $\alpha_w + \alpha_o = 1$ can be rewritten as an expression for the water fraction in two-phase liquid/liquid mixture (or the water cut):

$$\alpha_w = \frac{\ln(I_w) - \ln(I_m)}{\ln(I_w) - \ln(I_o)} \qquad (2.5)$$

2.3.1.1.2 Dual-Energy Gamma Ray Attenuation (Absorption)

In order to determine oil, water and gas fractions, two independent measurements are required using dual or multiple energy technique. This technique has been investigated by a number of researchers (Abouelawafa and Kendall. 1980; Roach and Watt. 1996; Van Santen *et al.* 1995 and Hewitt *et al.* 1995).

The basics of dual energy gamma ray absorption measurement are similar to the single energy gamma ray attenuation concept, but now two gamma energies e_1 and e_2 are used. In a pipe, with inner diameter d, containing a mixture of water, oil and gas with fractions α_g, α_w and α_o, the measured count rate $I_m(e)$ is:

$$I_m(e) = I_V(e) \times \exp[-\sum_{i=1}^{3} \alpha_i \times \mu_i(e) \times d] \quad (2.6)$$

where

$I_V(e)$ is the count rate when the pipe is empty,

μ_i is represent the linear attenuation coefficients for the three phases (μ_g, μ_w, μ_o).

For two energy levels, e_1 and e_2, provided the linear attenuation coefficients between water, oil, and gas are sufficiently different, two independent equations are obtained. The third equation is simply the fact that the sum of the three phase fractions in closed conduit should equal to unity as given:

$$\alpha_g + \alpha_w + \alpha_o = 1 \quad (2.7)$$

A full set of linear equations is given below. R_O, R_W, Rg, and Rm represent the logarithm of the count rates for water, oil, gas and mixture, respectively, at energies e_1 and e_2.

$$\begin{bmatrix} R_w(e_1) & R_o(e_1) & R_g(e_1) \\ R_w(e_2) & R_o(e_2) & R_g(e_2) \\ 1 & 1 & 1 \end{bmatrix} \times \begin{bmatrix} \alpha_w \\ \alpha_o \\ \alpha_g \end{bmatrix} = \begin{bmatrix} R_m(e_1) \\ R_m(e_2) \\ 1 \end{bmatrix} \quad (2.8)$$

The elements in the matrix are determined in a calibration process by filling the pipe with 100% water, 100% oil, and 100% gas (air) or alternatively by calculations based on the fluid properties. Together with the measured count rates at the two energy levels from a multiphase mixture it is possible to calculate the unknown phase fractions. In Figure 2-6 shows a typical response triangle with a dual energy source (18 keV and 60 keV) for water, oil and gas mixture.

The corners of the triangle are the water, oil and gas calibrations, and any point inside this triangle represents a particular composition of water, oil and gas (Rafa *et al.* 1989). The shape of the triangle depends mainly on the energy levels used (thus specific radioactive source), pipe diameter and detector characteristics; however, fluid properties may also influence the triangular shape. If the count levels are too close the triangle will transform into a line and therefore cannot be used for a three-phase composition measurement.

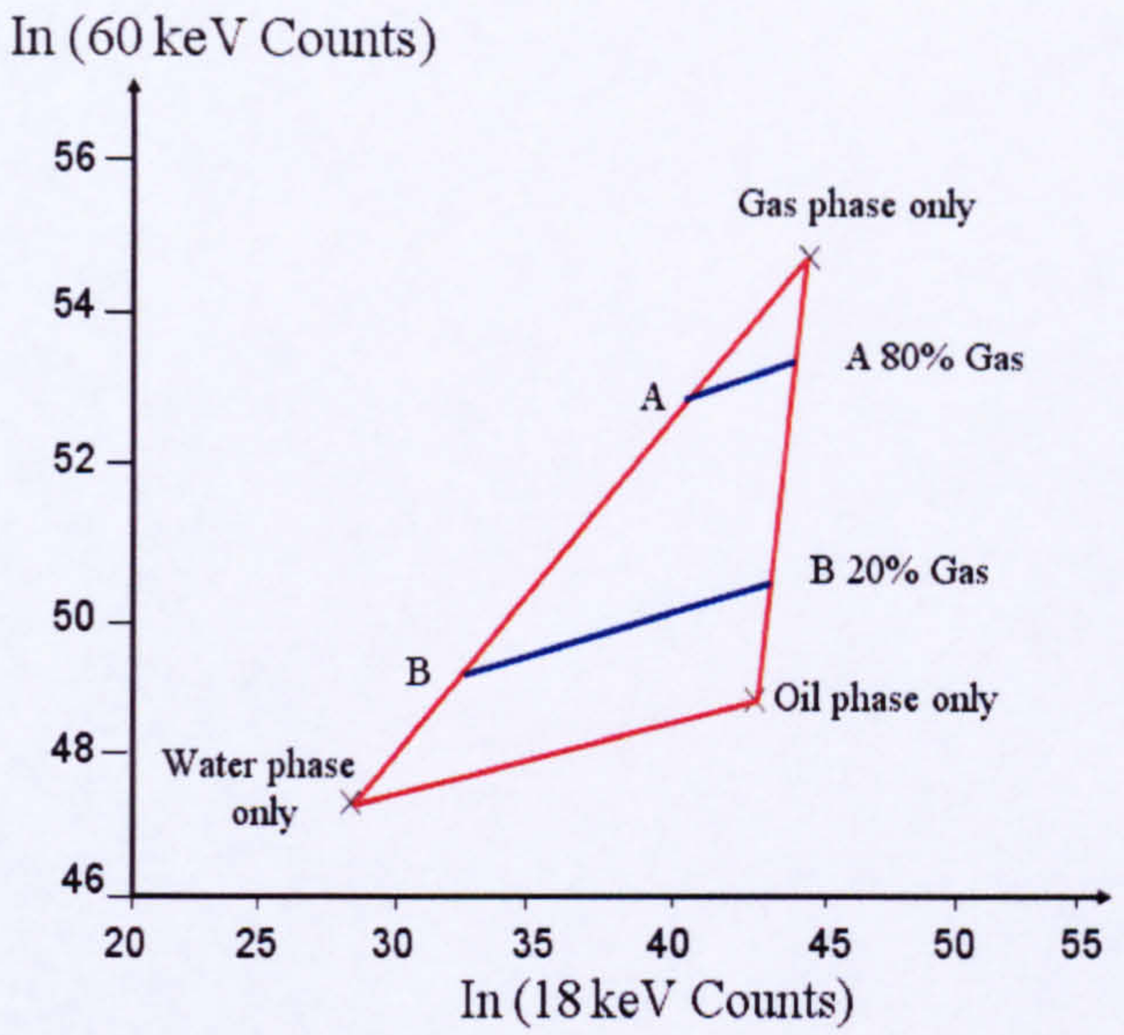

Figure 2-6: Dual Energy Gamma Ray Response Triangle (Rafa *et al*. 1989)

2.3.1.2 Electrical Impedance Measurements

The main principle of electrical impedance methods for component fraction measurements is that the fluid flowing in the measurement section of the pipe is characterised as an electrical conductor. By measuring the electrical impedance across the pipe diameter (using e.g. contact or non-contact electrodes), properties of the fluid mixture, conductance and capacitance, can be determined. The measured electrical quantity of the mixture then depends on the conductivity and permittivity of the oil, gas and water components, respectively. Figure 2-7 shows the basic principle of impedance method to measure component fraction.

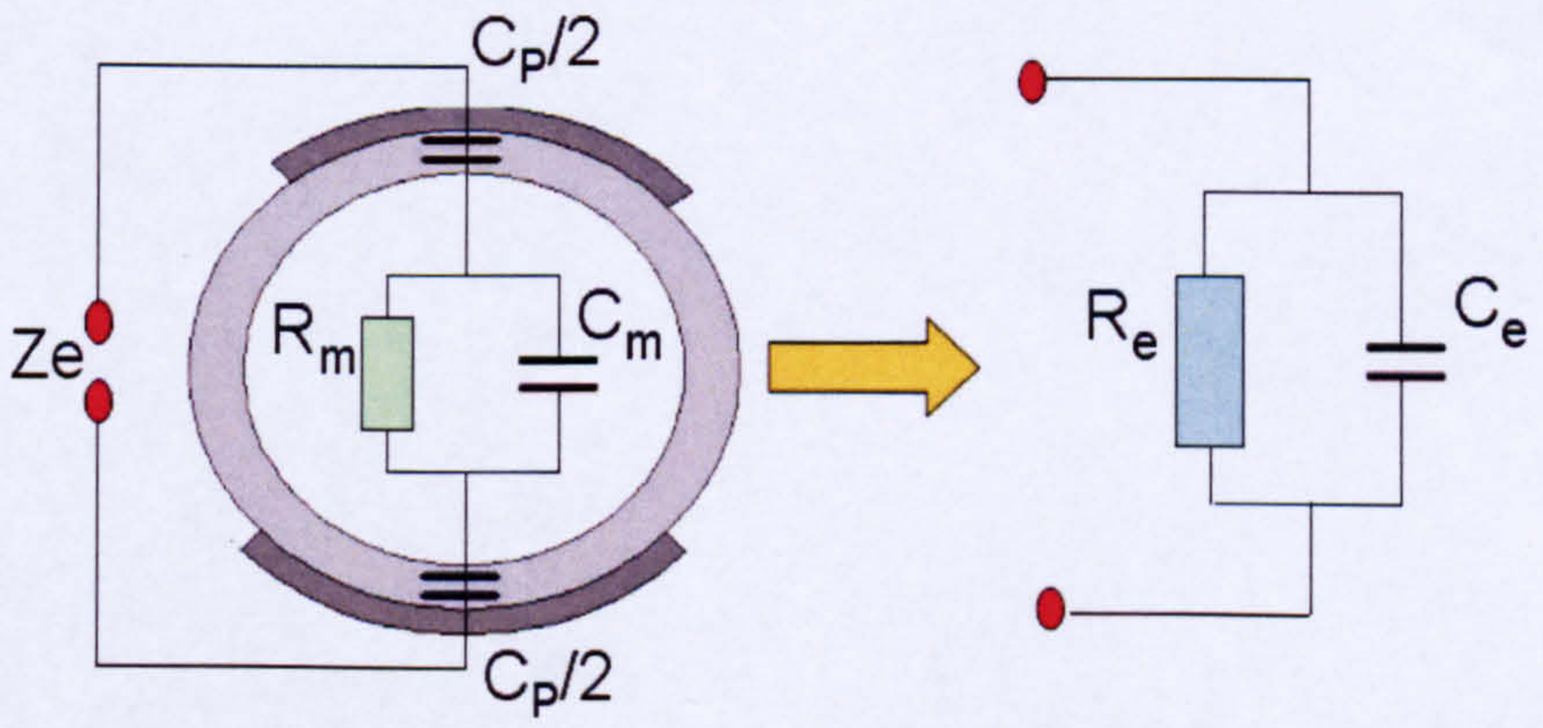

Figure 2-7: Impedance for Component Fraction Measurement (Thorn *et al*. 1997)

If the electrical impedance Z_e is measured across two electrodes, between which an oil/water/gas mixture is flowing, the measured resistance R_e and capacitance C_e are given by:

$$R_e = \frac{1+\omega^2 R_m^2 (C_m + C_P)^2}{\omega^2 R_m C_P^2} \qquad (2.9)$$

$$C_e = \frac{[1+\omega^2 R_m^2 C_m (C_m + C_P)^2] C_P}{1+\omega^2 R_m (C_m + C_P)^2} \qquad (2.10)$$

The resistance R_m and capacitance C_m of the mixture flowing through the pipe depends on the permittivity and conductivity of the oil, water and gas components, the void fraction and water fraction of the flow, and the flow regime.

The measured resistance and capacitance not only depends on R_m and C_m but also on the excitation frequency ω of the detection electronics and the geometry and materials of the sensor. For a particular sensor geometry (and hence fixed C_P) and flow regime, the measured impedance will be a direct function of the flow component ratio.

In oil continuous mixture R_e is large and can be difficult to measure reliably. For the flows in which water is the continuous phase, a short circuiting effect will occur, caused by the conductive water, if the sensor excitation frequency, fc, is less than:

$$f_c < \frac{\sigma_w}{2\pi\varepsilon_o\varepsilon_w} \qquad (2.11)$$

where

σ_w and ε_w are the conductivity and permittivity of the water component respectively.

For process water this would mean a frequency below that of microwave frequencies. Therefore, impedance method is limited to oil or water in continuous phase.

However impedance based methods suffer from two important limitations - they cannot be used over the full component fraction range and are flow regime dependent. This dependency is eliminated by one of two methods: (1) homogenisation of the phase, before the measurement is made and (2) development of electrodes which minimise the dependency upon the flow geometry.

Various methods have been used to reduce the flow regime dependency effects of impedance sensors as shown in Figure 2-8. In this figure four different designs of non-intrusive sensor are illustrated. These styles have been developed recently, and that to minimise the flow geometry dependency,

1. Arc electrodes, (Xie *et al.* 1990), for resistive and capacitive cross-section measurement, Figure 2-8 (a). In this design the guard electrodes are installed at either side of the electrodes, in order to reduce the sensitivity to axial flow distributions.

2. Ring electrodes (Andreussi *et al.* 1988), for resistive measurement and to achieve a uniform electric field structure within the sensing volume, the ring electrodes trade-off a localised cross-section measurement. Figure 2-8 (b).

3. Helical electrodes (Abouelwafa and Kendall. 1980), Figure 2.8 (c). In this model, the electrodes twist round the pipe, to overcome flow geometry dependence.

4. Rotating field electrodes (Merilo *et al.* 1977), as shown in Figure 2-8 (d), this design achieves a similar effect to helical electrodes. Here, three electrode pairs are driven at 120° phase intervals, to produce a rotating field vector in the pipe centre.

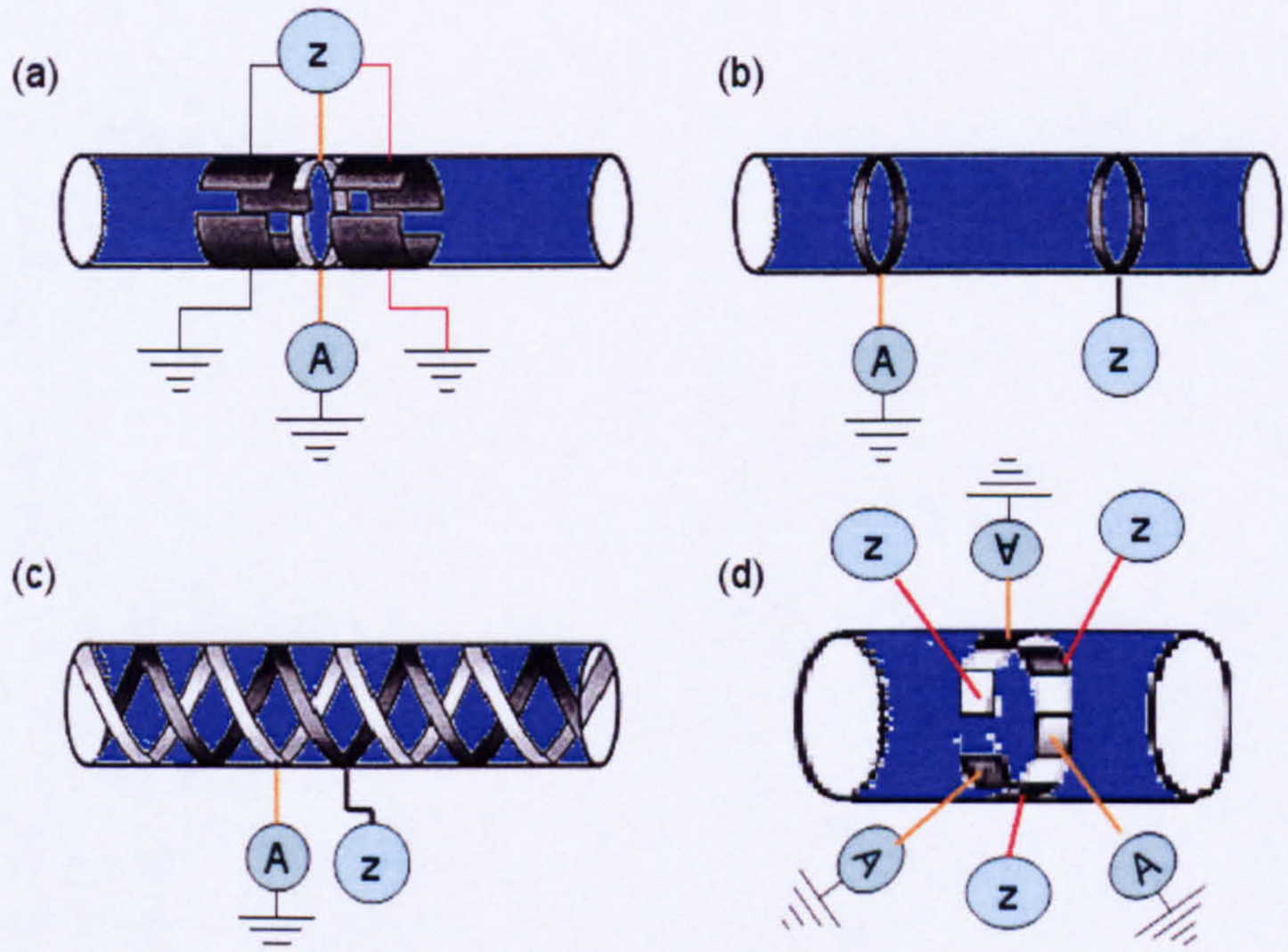

Figure 2-8: Non-Intrusive Impedance Measurement

2.3.2 Phase Velocity Measurement

2.3.2.1 Differential Pressure Meters

Olsen (1993) stated that several concepts of multiphase meters adopt the differential pressure type component to determine the total speed of the multiphase mixture. The types employed most frequently are Venturi meter and the orifice plate, (Zhang *et al.* 2005).

The principle of an orifice meter is based on the difference between the pressure in upstream and downstream of an orifice plate; this change in Venturi meter does not occur immediately as in as orifice, but the change in pressure is caused by the internal changed area. Figure 2-9 shows the geometrical designs for the differential pressure flowmeters where (a) is the Venturi meter, and (b) is the orifice plate meter.

The flow through the Venturi, see Figure 2-10 (a), illustrates the well-behaved nature of a flow when the area changes blend reasonably smoothly from one size to another. Converging flow is particularly well-behaved, while diverging flow for diffusion, with small enough angle, will continue to remain generally in one direction. As the velocity increases, due to the smaller area, so pressure decreases, and vice versa. However, pressure recovery is dependent on the smoothness of the expanding flow.

In contrast, the flow through the orifice plate is far from smooth; see Figure 2-10 (b). The abrupt changes are caused by the orifice plate, which, while causing the flow to contract as it passes through the orifice, may also trigger a small recirculation zone in the corner upstream of the plate and will initiate a large recirculation zone downstream of the plate around the central jet area. In addition to this the flow downstream of the plate is highly disturbed and the diffusion will result in high pressure losses.

As a result, the Venturi has an influence on flow regimes, the smallest pressure loss, and the shortest straight pipe upstream and downstream. Considering the great technical importance as well as pure scientific interest, two-phase flow through Venturi has been widely studied both experimentally and theoretically by Xu *et al.* (2003), Steven (2002) and Moura and Marvillet. (1997).

To determine the liquid flowrate (Q_L) for the mixture flow (homogenous flow) in a liquid-gas flow, a Venturi meter can be used as given in the following equation (Hammer and Nordtvedt ,1991):

$$Q_L \propto \sqrt{\frac{(1-\alpha)\times\Delta P}{\rho_l}} \qquad (2.12)$$

where
ΔP is the differential pressure between the upstream tapping and the throat tapping of the Venturi meter,
α is the gas fraction, and liquid density (ρ_l) at the upstream pressure tapping cross-section are known.

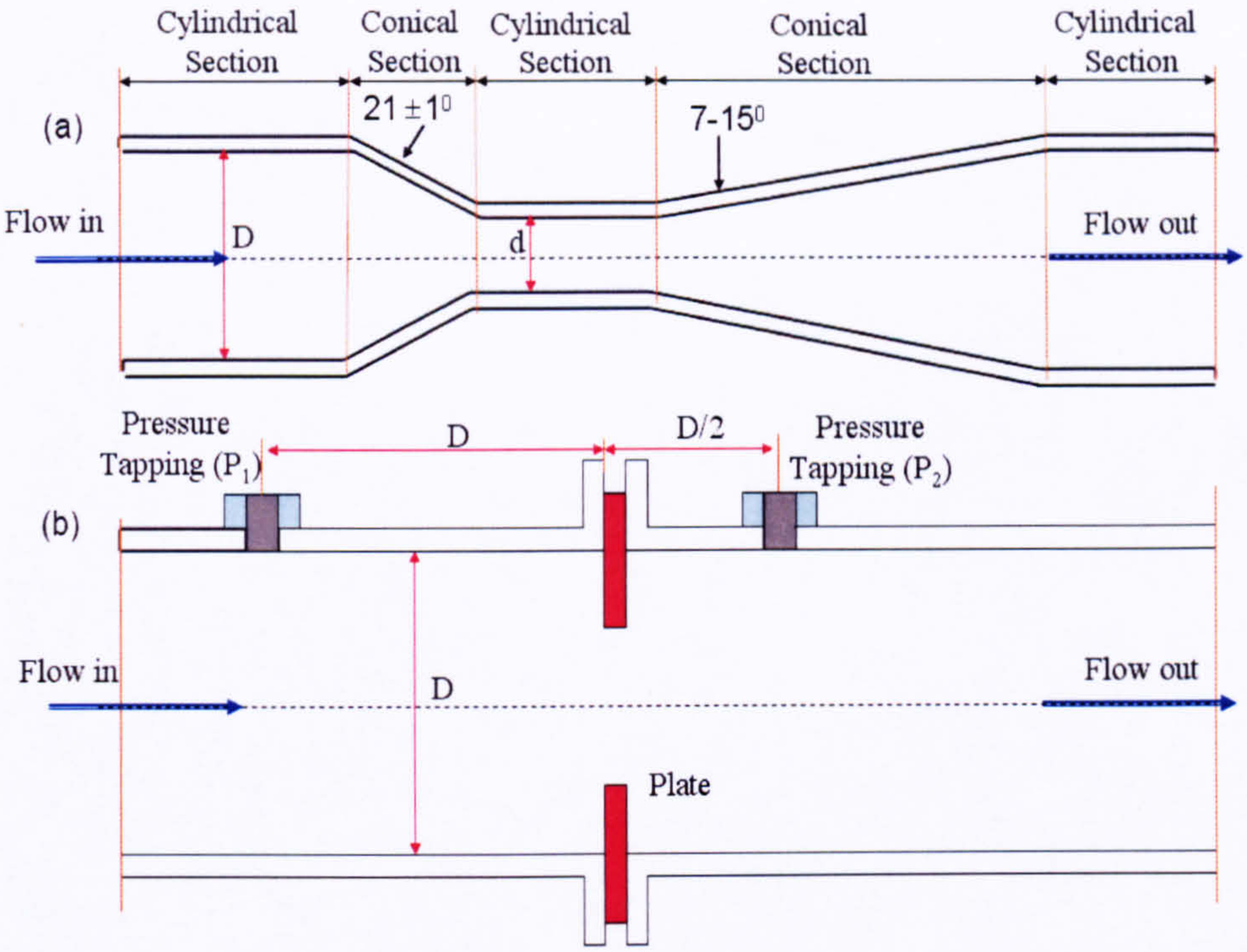

Figure 2-9: Differential Pressure Flowmeters Geometrical Designs

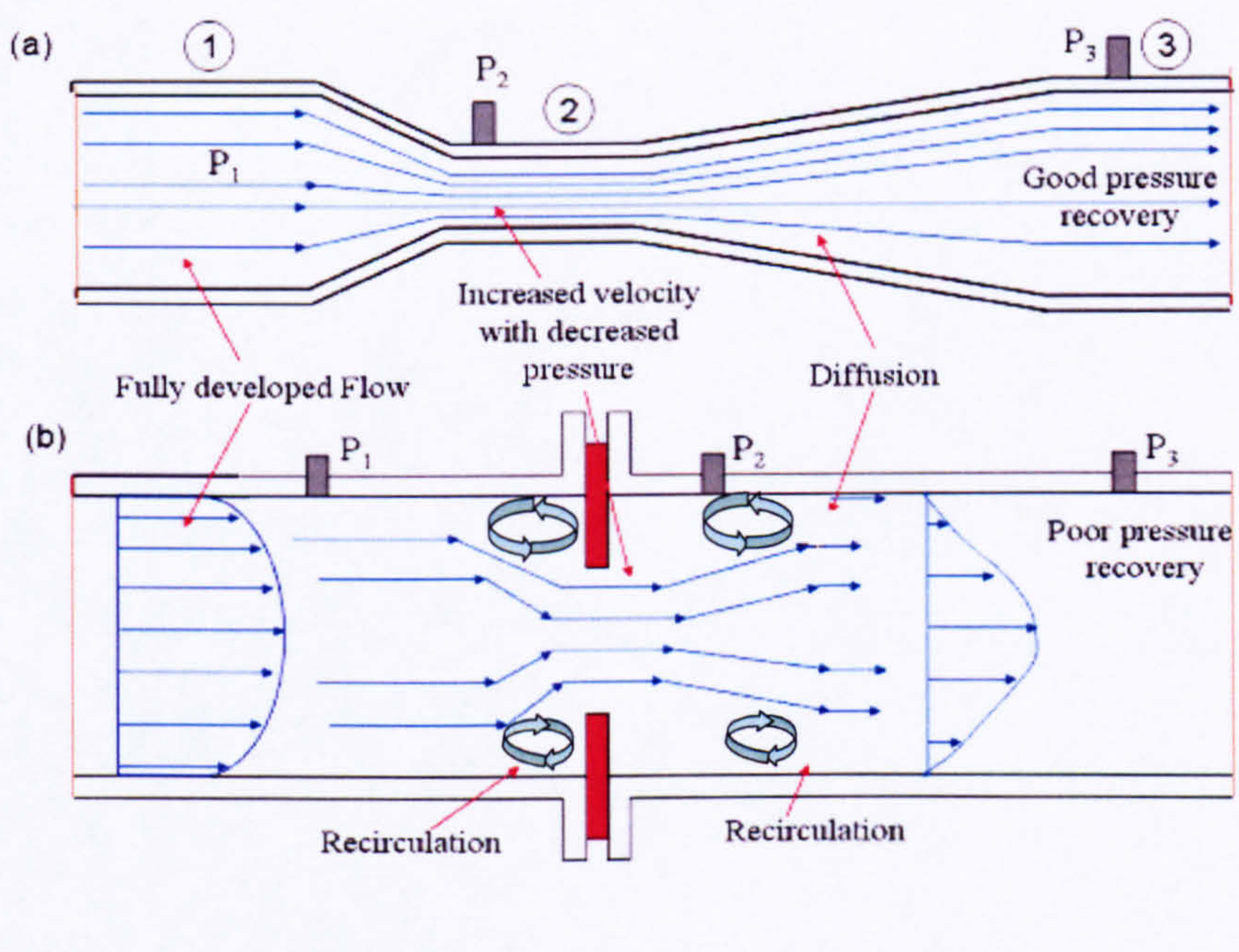

Figure 2-10: Flow Pattern through Differential Pressure Flowmeters

2.3.2.2 Positive Displacement

The measurement principle of positive displacement meters is based on the motion of the displaceable chamber in which fluid is passed and is metered by a precisely known volume. The total volume of flow will be the summation of the individual volumes that can be calculated by transmitting the motion of the chamber to a mechanical counter or an electronic counter (Tuss *et al.* 1996). Commercial multiphase flow systems using this technique are discussed by Tuss *et al.* (1996) and it was found that the positive displacement does not yield any information on the gas phase flowrate.

Positive displacement meters have been manufactured in various designs (multi-rotor meter, nutating disc meter, rotating valve meter, oval gear meter, oscillating circular piston meter, and reciprocating piston meter).

2.3.2.3 Cross-Correlation Technique

Cross correlation techniques are well-known and are becoming widely used in both laboratory and industry for pipeline flow velocity measurement. The presence of a second phase in a pipeline produces random disturbance signals which can be detected by various types of transducer, such as capacitance, microwave or gamma ray devices, and ultrasonic transducers, see Figure 2-11, (Yang and Beck. 1997).

To find the time delay of flow pattern, an up-stream transducer and down-stream transducer are installed axially along the flow stream in the pipeline with a known spacing L and the disturbance signals monitored by the two transducers are cross-correlated according to the following equation:

$$R_{XY} = \frac{1}{T}\int_0^T x(t-\tau)y(t)\,dt \qquad (2.13)$$

where $x(t-\tau)$ and $y(t)$ are the signals at the upstream and downstream sensors respectively with delay time of τ. The distance L between the upstream and downstream sensors being known, the velocity of the disturbance is determined by:

$$V = \frac{L}{\tau} \qquad (2.14)$$

The cross correlation technique has been used by several researchers to measure the slug translational velocity and bubble velocity (Reis and Goldstein 2005; Dong *et al.* 2005 and Cheng *et al.* 2005).

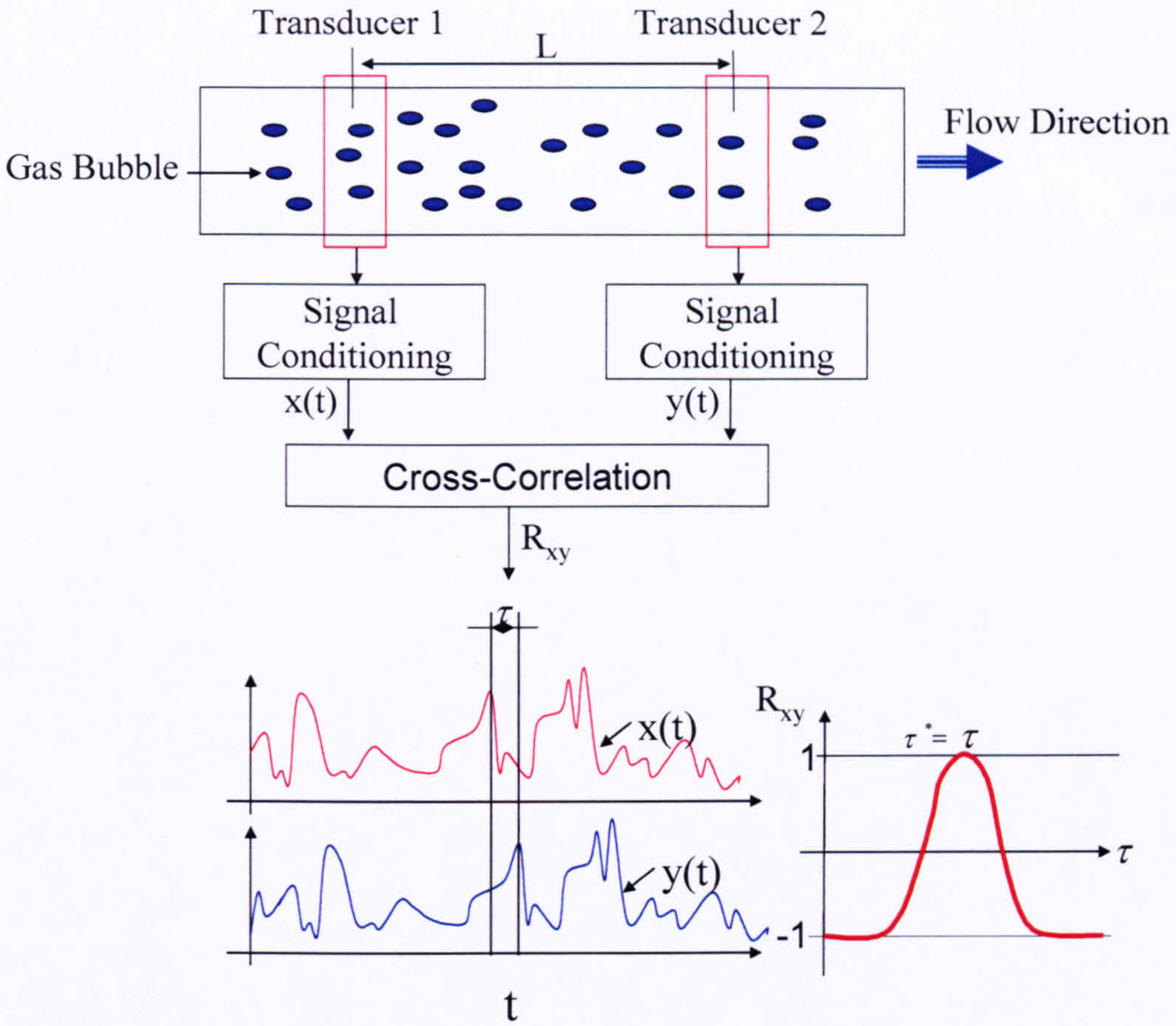

Figure 2-11: Cross-Correlation Technique

Reis and Goldstein (2005) developed a new technique for measuring the profile and mean velocity of elongated bubbles in horizontal air–water slug flows, by using the capacitance between two thin electrodes mounted on the external surface of a dielectric pipe. The elongated bubble mean velocity was determined by using a cross correlation technique applied to the signals coming from two identical capacitance probes, mounted 50 mm distant from each other. Tests were performed in an experimental facility with a 5 m long, 34 mm internal diameter Plexiglas pipeline. The results were compared with an empirical correlation from the literature and showed good agreement.

The accuracy of this method depends on the validity of the relationship used to connect the velocity inferred from the correlation function's peak position to the mean velocity of the flow. Some general procedures for obtaining good cross-correlation accuracy are outlined by Beck and Plaskowski. (1987),

1. B_S (sensor bandwidth) should be very large, to enhance the flow noise turbulence (cross-correlation of white noise leads to perfectly narrow correlation peak).

2. L (sensors separation) should be minimised, to reduce the possibility of flow evolution between sensors. However, this separation should not be over reduced, in order to avoid relative spacing uncertainty ($\Delta L/L$), signal quantisation errors, and signal crosstalk errors. However, for homogenous flow, Ong, (1975) suggested the optimum sensor separation is of the order of 3 to 4 pipe diameter.

2.3.3 Phase Density Measurement

As shown previously in Figure 2-4, to convert the phase volumetric flowrates into mass flowrates, the measurement of individual phase densities is required. However, the phase density measurement is well established and it is readily available from other parts of the production process, such as gamma densitometers, Coriolis flowmeter or simply from the PVT diagrams and by using the measured temperature and pressure.

2.4 Ultrasonic Measuring Techniques

Ultrasonic flowmeters have been successfully applied to measure single-phase liquid mean velocities in various industries. There have also been continuous efforts made to measure the characteristics of multiphase flow using ultrasonic flowmeters, since such meters do not introduce a pressure drop and can provide a fast response to changes in the flow. Thus, there are many potential applications for ultrasonic flowmeters in multiphase flow.

2.4.1 Measurement Principles of Ultrasonic Techniques

This section of the chapter describes the methods of measuring fluid flow ultrasonically including by transit time technique.

2.4.1.1 Transit Time Techniques

The transit-time method or time-of-flight is the most commonly used in ultrasonic flow metering and the most accurate and it is available as a spool piece meter for liquids and gases or as clamp-on design. The principle of this technique is based on the small difference in time taken for an ultrasound wave to travel upstream and downstream under flow condition.

In transit-time ultrasonic techniques, a pulse is transmitted from a transducer through the fluid to a second transducer positioned downstream in the pipeline, where the component of flow velocity along the path adds to, or subtracts from, the velocity of sound in the fluid in the downstream or upstream measurements respectively, as shown in Figure 2.12.

The propagation velocity of sound wave is the vector sum of the velocity of sound and the flow velocity in the direction of propagation. Therefore, the transit time of the upstream, t_1, and downstream, t_2, signals can be expressed as:

$$t_1 = \int_0^L \frac{dl}{c - V(l)\cos\theta} \tag{2.15}$$

$$t_2 = \int_0^L \frac{dl}{c + V(l)\cos\theta} \tag{2.16}$$

where
L is the acoustic path length,
c is the velocity of sound in the fluid,
V(l) is the axial flow velocity measured at point (dl) along the acoustic path and
θ is the angle of inclination of the acoustic propagation with respect to the axial direction of the flow.

It can be shown that equation (2.17) is found after arrangement between equation (2.15) and (2.16) the flow velocity across the acoustic path as given:

$$V_{Path} = \frac{L(t_1 - t_2)}{2t_1 t_2 \cos\theta} \tag{2.17}$$

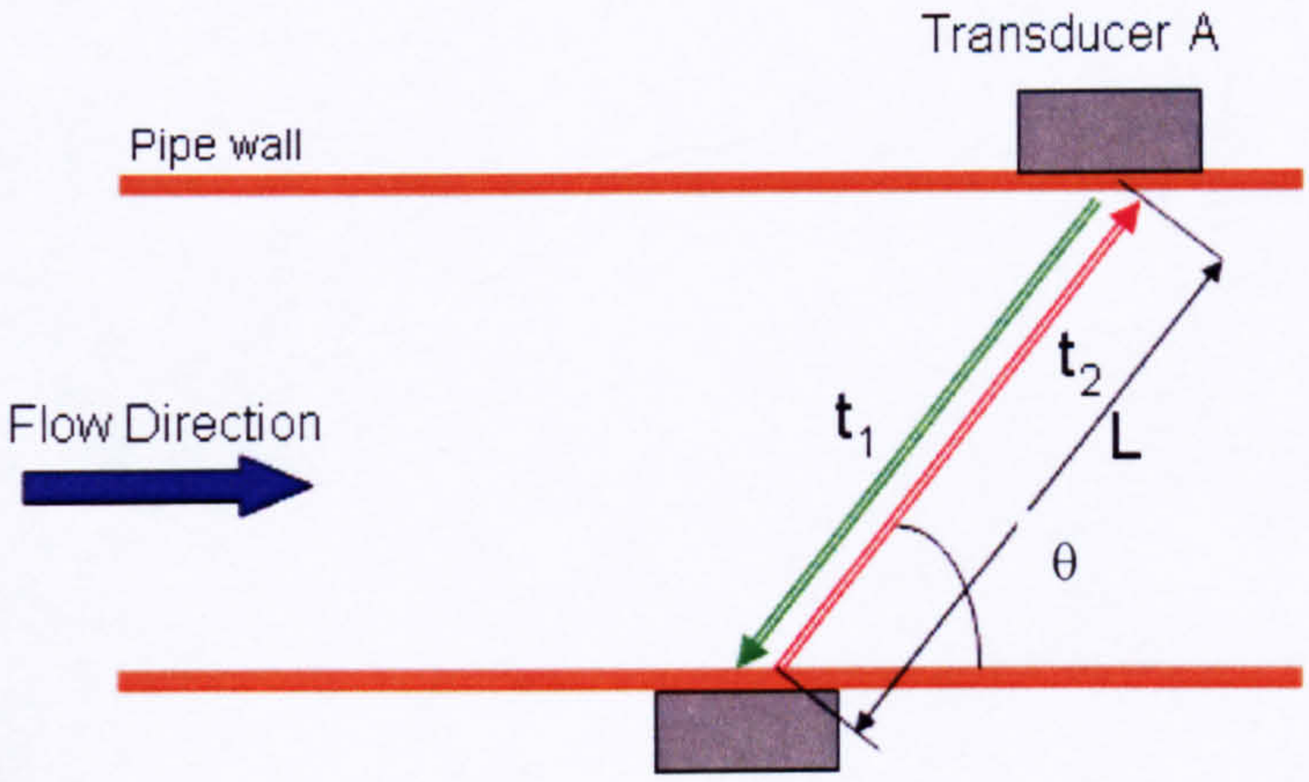

Figure 2-12: Schematic Diagram of Transit Time Ultrasonic Flowmeter

This is the basic measurement principle of the velocity profile along the acoustic path in a transit time ultrasonic flowmeter. To convert this path velocity to a velocity averaged over the entire-section of the flowing medium, the knowledge of the flow velocity

profile is essential (Gurevich, 2001). The averaged velocity is given by the following equation:

$$K = \frac{\overline{V_{Path}}}{\overline{V}} \tag{2.18}$$

where,
K is the flow profile correction factor;
$\overline{V_{Path}}$ is the flow velocity along the acoustic path (line average over the beam); and
$\overline{V}$ is the area-average velocity.

The single beam transit time ultrasonic flowmeter is affected by any distortions in the flow profile which often result in erroneous measurements. The velocity profile is the definition given to the distribution of velocities in the axial direction over the cross-section of the circular pipeline. This distribution can vary significantly depending on the fluid viscosity, the Reynolds number Re, the relative roughness and the shape of the conduit, upstream and down stream disturbances and whether the pipeline is fully charged (Moore, 2000).

There are three main types of transit time methods, namely direct transit time, phase difference, and sing-around. However, the focus of this work is on the direct transit time method.

Direct transit time ultrasonic flowmeters can be classified into two categories based on the form of transmission of acoustic signals, the single-path and multiple-path. Within these two types there are various configurations with equally weighted paths including, diametrical DIAM, orthogonal ORTH, three path THREE, double orthogonal DORTH, double triangle DTRI, five pointed star 5PTST and mid-radius MID.

The mid-radius, triangle and double triangle configurations are all variations of the mid-radius chordal position, where the chords are 0.5R from the centre of the pipeline. MID is a configuration that requires four transducers, one on each side of the two paths. TRI, although it has one more chordal path than MID, can be implemented with two transducers by utilising a bounce path (Moore, 2000).

Thompson (1978), used the mid-radius ultrasonic flow measurement and he found that the mid-radius chord is known to measure fully developed flow rate more accurately than a diametrical chord. Similarly, DTRI can be using four transducers by way of two bounce paths. This is advantageous to the reduction of cost. In a similar manner, the 5PTST configuration can be implemented by use of two transducers utilising one bounce path (Moore, 2000).

In the non-invasive single-path clamp-on transit time ultrasonic flowmeter, there are three configurations to mount the transducers (Sanderson and Yeung, 2002). The two main methods are direct transmission Z and single reflection V and multiple reflections W as illustrated in Figure 2-13.

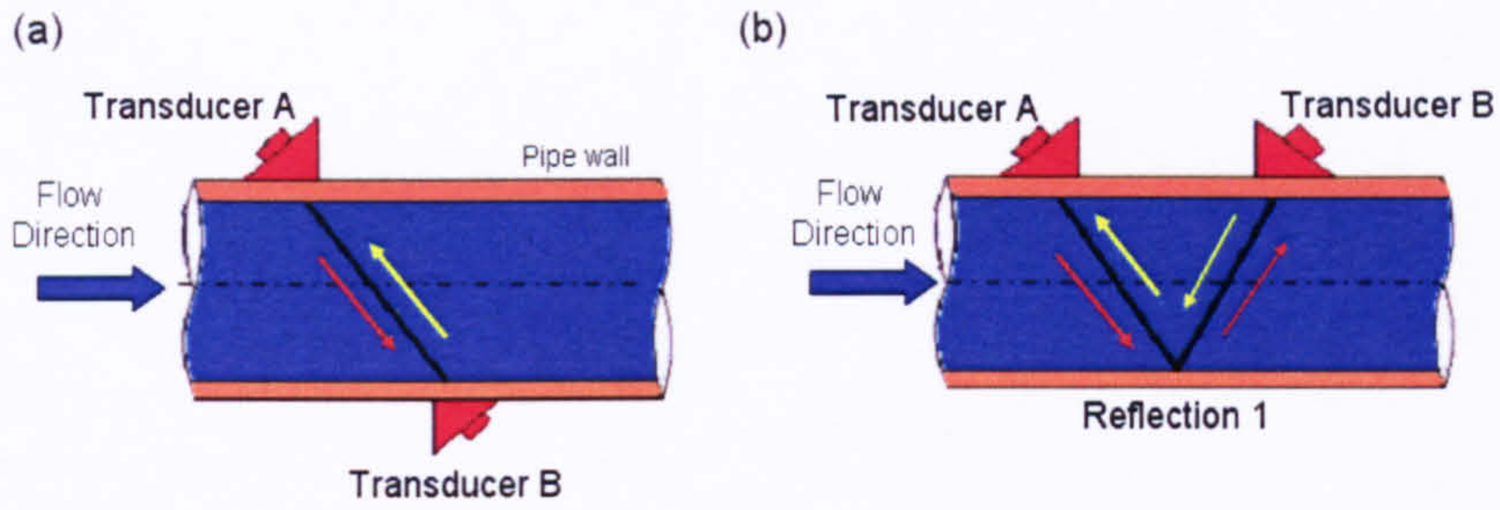

Figure 2-13: Clamp-on Ultrasonic Flowmeter Configuration (a) Z configuration, (b) V configuration, and (c) W configuration

2.4.2 Ultrasonic Metering Applications in Multiphase Flow

This section provides a literature review of the recent work on different ultrasonic measuring techniques applied in area of multiphase flow measurements. However, most of the ultrasonic measuring techniques recently developed and reviewed have the abilities to operate under two-phase gas/liquid flow in a form of wet gas flow in pipelines where the gas void fraction (GVF) is greater than 90%, and the liquid volume fraction $\leq$ 10%. The commonly observed flow patterns in a wet gas system are mist flow, which occurs at very low water content and very low gas velocities, annular- mist flow occurs at high gas velocities and stratified flow occurs at low gas velocities. In a wet gas annular-mist flow, the liquid film is very wavy and there is a change in the film height with time. However, in stratified flow the liquid film height is fairly constant.

2.4.2.1 Ultrasonic Multiphase Flowmeter Concept (Coull and Sattary, 2004)

A multiphase flow meter concept based on ultrasonic transit-time techniques was developed by Coull and Sattary (2004). The meter concept used non-intrusive multi-path (4-path) ultrasonic meters, one designed for gas flow measurement and the other for liquid, with horizontal path arrangements; these were supplemented by a pulse-echo interface level measurement system as shown in Figure 2-15. The concept was designed to operate ideally in the stratified flow regime, i.e. when gas and liquid are separate with gas running along the top of the pipe and liquid along the bottom. However, the meter limitations and its performance was tested in stratified wavy and slug flow conditions.

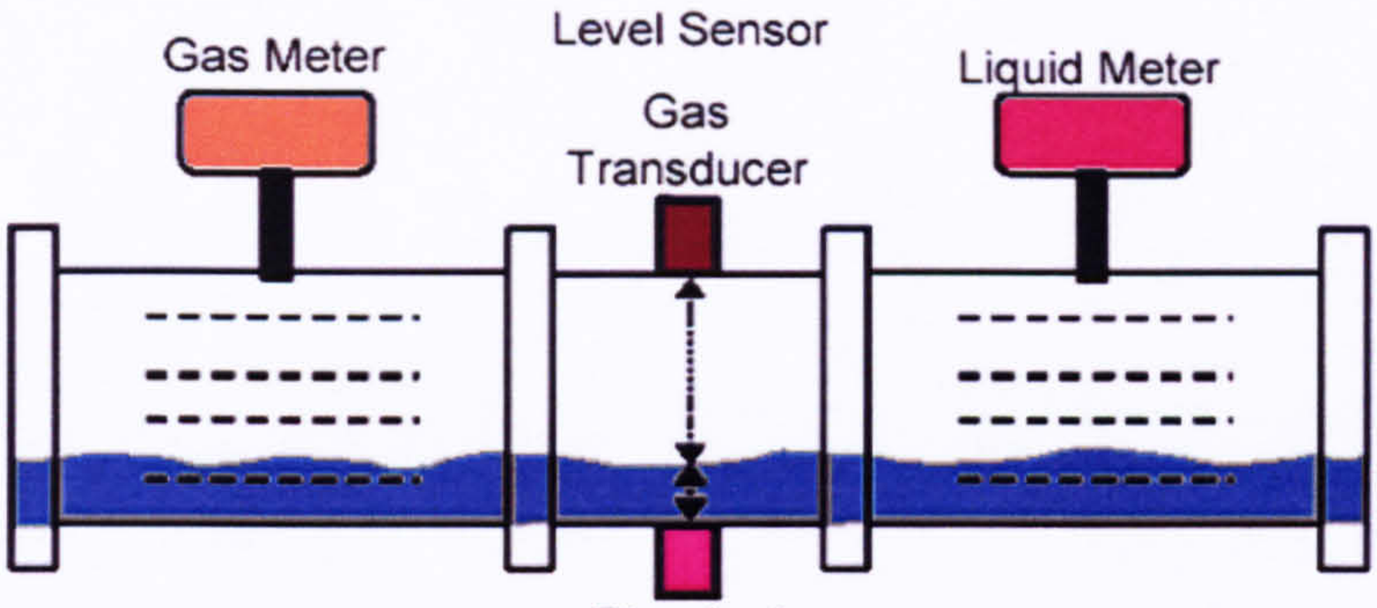

Figure 2-14: Multiphase Flowmeter Concept developed by Coull and Sattary (2004)

The experimental programme consisted of two sets of tests, one which tested crude oil with nitrogen and another which tested water with nitrogen. The tests were conducted under superficial gas velocities range from 0.5 to 4 ms^{-1} and superficial liquid velocities range from 0.03 to 0.23 ms^{-1}.

To calculate the gas and liquid volumetric flowrates, the path velocity for each path was calculated, and then the mean velocity calculated, using numerical integration techniques. Multiplying this mean velocity by the cross-sectional area returns the measured volumetric flowrate for gas and liquid as shown in Figure 2-15.

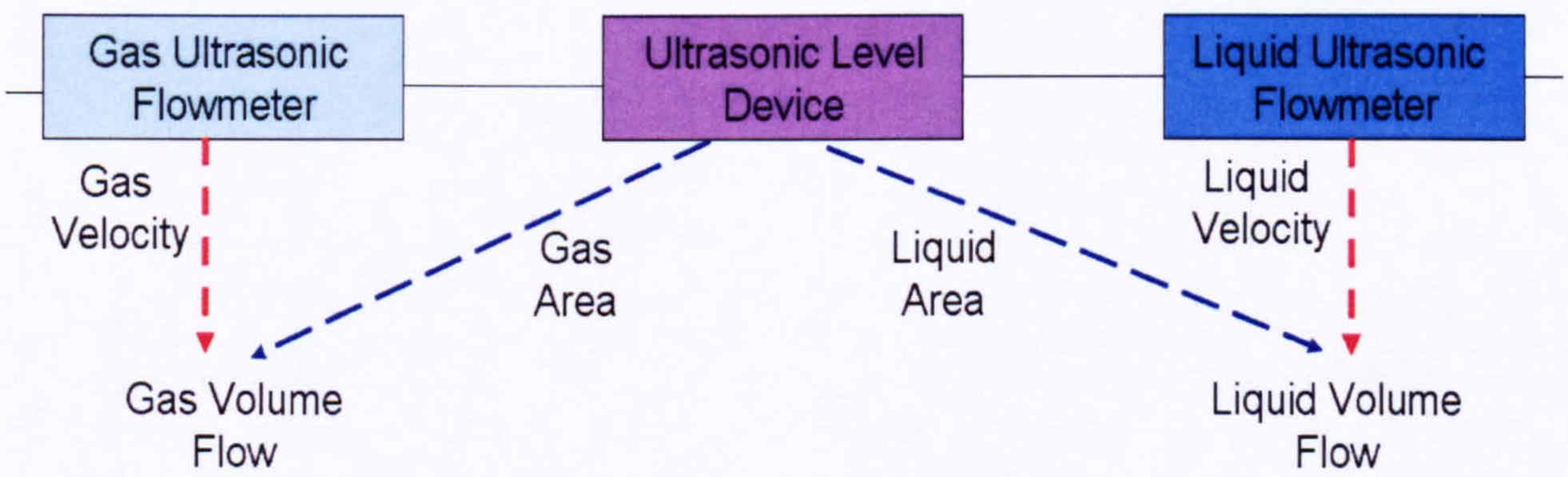

Figure 2-15: Schematic Diagram of Multiphase Flowmeter by Coull and Sattary (2004)

Liquid and gas cross-sectional areas were determined by measuring the interface level between the two phases. The pulse-echo interface-level system made two independent measurements of level, one through the gas phase, and the other via the liquid phase as shown in Figure 2-16.

The interface level was calculated using the following equations:

Based on the measurement of the gas transducer:

$$h_l = \frac{d - (c_g t_g)}{2} \tag{2.19}$$

For liquid transducer:

$$h_l = \frac{c_l (t_{std} - t_{per})}{2}; t_{per} = \frac{2x}{c_{per}} \tag{2.20}$$

where :

h_l is the interface level for stratified flow,
d is the internal pipe diameter,
c_g is the speed of sound in the gas, t_G is the transit time of the gas transducer signal from transmission to reception,
c_l is speed of sound in the liquid,
c_{per} is speed of sound in the perspex,
t_{Std} is transit time of the liquid standard transducer signal from transmission to reception,
t_{per} is the transit time in the Perspex outward and return,
x is the thickness of the Perspex wall at the point of transmission.

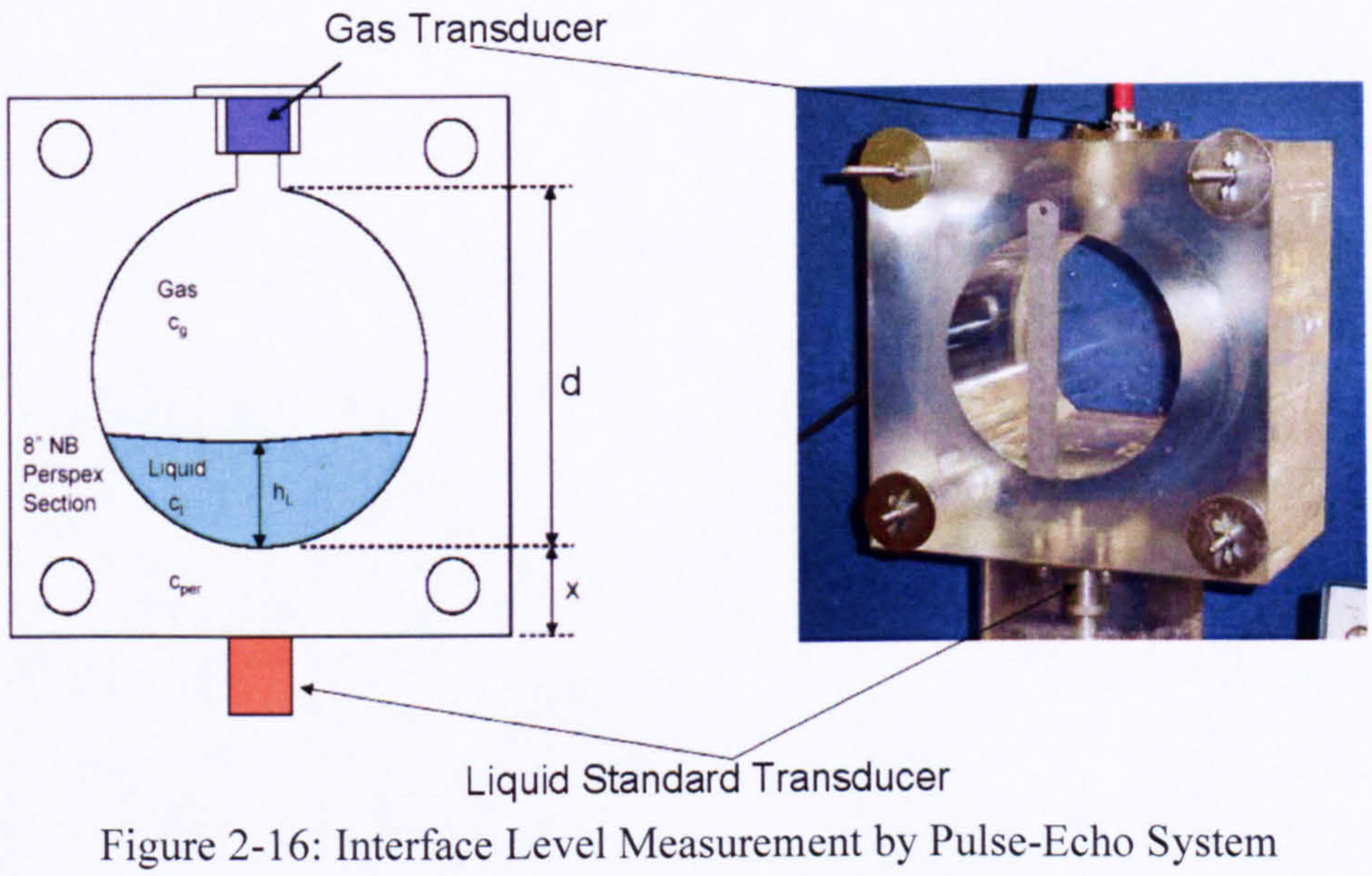

Figure 2-16: Interface Level Measurement by Pulse-Echo System

Lengths x and d were carefully measured using a digital micrometer. The sound speeds were determined during the commissioning of the system in the multiphase rig. The Perspex and gas sound speed were calculated by careful measurement of transit times in completely dry conditions, and the water and oil sounds were during full-immersed conditions.

The liquid A_{liquid} and gas A_{gas} areas are calculated using the following equations:

$$A_{liquid} = \frac{0.25\left(\pi - \cos^{-1}(2\times\left(\frac{h_l}{d}\right)-1) + (2\times\left(\frac{h_l}{d}\right)-1)\times\sqrt{1-(2\times\left(\frac{h_l}{d}\right)-1)^2}\right)}{\frac{\pi}{4}} \times A_{pipe} \quad (2.21)$$

$$A_{gas} = A_{pipe} - A_{liquid} \quad (2.22)$$

The liquid and gas velocities were calculated from the indicated velocities of the operating paths in the liquid and gas meters. The restriction of keeping the flow regime in the stratified region meant it was necessary to keep the actual liquid flow velocity very low, below 0.6 ms^{-1}. Gas velocities, however, ranged from 1 to 7 ms^{-1}. As a result, the flow profiles of the two phases were quite different as illustrated in the profile diagram in Figure 2-17.

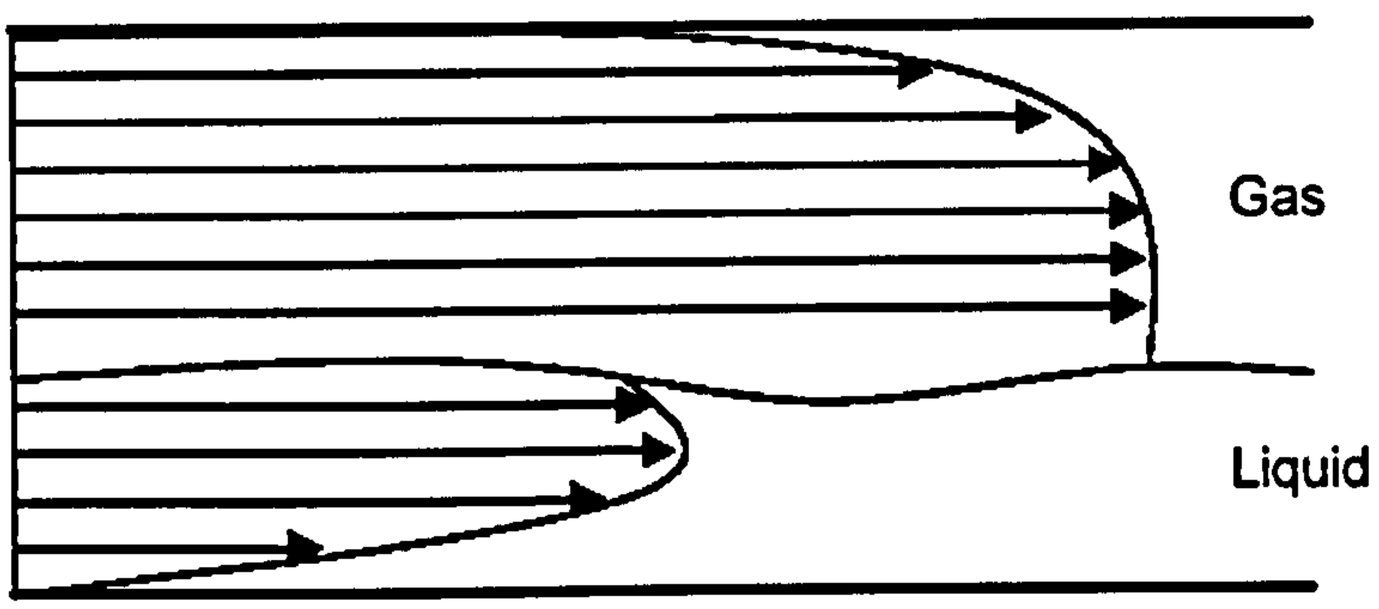

Figure 2-17: Velocity Profile of Stratified Flow

The gas flow in these tests was turbulent; hence its velocity profile was fairly flat. It was therefore considered reasonable to estimate the mean gas velocity as the average of the operating path velocities as given by the equation:

$$Q_{gas} = \frac{\sum_i v_i}{x} \times A_{gas} \quad (2.23)$$

where

i details the operating gas meter paths,

v_i is the path velocity of an operating path,

x is the number of operating gas meter paths,

A_{gas} is the gas area measured by pulse-echo system.

The pipe cross-section is divided into four sectors based on the liquid path locations as shown in Figure 2-18.

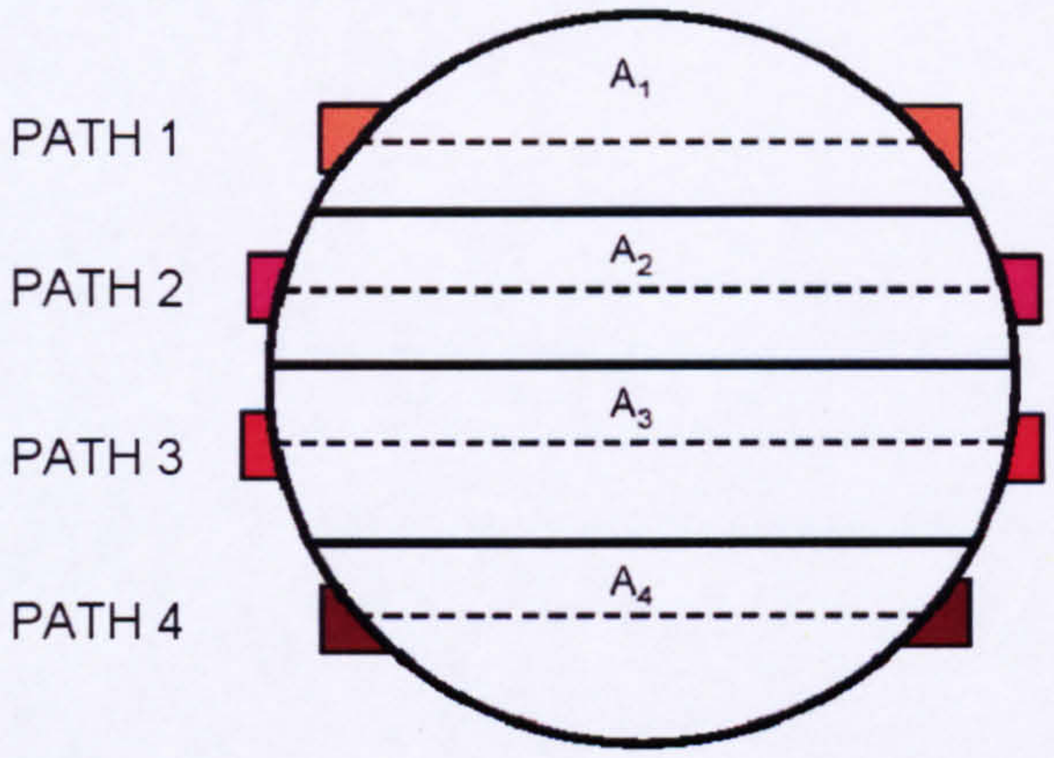

Figure 2-18: Liquid Flow Measurement Zones

The velocity measured by each path was assigned to its pipe sector. The area of the uppermost operational path sector was adjusted to the level measurement made by the pulse-echo interface level measurement system. For example, if path 3 and 4 were operational, the liquid flowrate would be calculated as follows:

$$Q_{liquid} = v_4 \times A_4 + v_3 \times A_3' \tag{2.24}$$

The area of the uppermost sector is adjusted so that the overall area matches that area calculated by the pulse-echo interface-level system. Hence, in this example, path velocity 3 v_3 would be multiplied by adjusted zone 3 area A_3`:

$$A_3' = A_{liquid} - A_4 \tag{2.25}$$

Multiphase flow meter concept can be summarised as follows:

- The ultrasonic meter technique proposed by Coull and Sattary (2004) demonstrated that transit-time ultrasonic flow measurement and pulse-echo level measurement methods can operate in two-phase liquid/gas flow under stratified and stratified wavy flow regime for superficial gas velocities ranging from 0.5 to 4 ms^{-1} and superficial liquid velocities ranging from 0.03 to 0.23 ms^{-1}.

- The gas flowrate measurements in stratified and stratified wavy flow regime were within 5% over substantial area of the flow matrix and almost all points within 15%. However, in non-operational area where the meter failed to operate at superficial liquid velocity V_{SL} of 0.23 $ms^{-1}$and superficial gas velocities V_{SG} range from 3 to 4 ms^{-1}, the error was 30%.

- Coull and Sattary (2004) reported that the liquid flow measurement was more challenging and the best performance achieved by the proposed ultrasonic technique was at superficial liquid velocity V_{SL} of the order of 0.23 ms^{-1} and at superficial gas velocity V_{SG} of 0.5 ms^{-1}. However, at higher superficial gas velocities the proposed meter performance has demonstrated to be within 60%.

- Water/oil mixture is likely to affect transit-time liquid-velocity measurement, and Doppler technology may be more suitable in these applications (Coull and Sattary, 2004).

- It can be concluded from the work by Coull and Sattary (2004) that the proposed method was not able to operate successfully under high superficial gas and liquid velocities. Therefore under intermittent slug flow conditions the proposed ultrasonic flowmeter by Coull and Sattary (2004) cannot operates satisfactorily due to the high superficial liquid and gas velocities.

The method of operation for the multiphase flowmeter concept proposed by Coull and Sattary (2004) for stratified flow is summarised and presented in Figure 2-19.

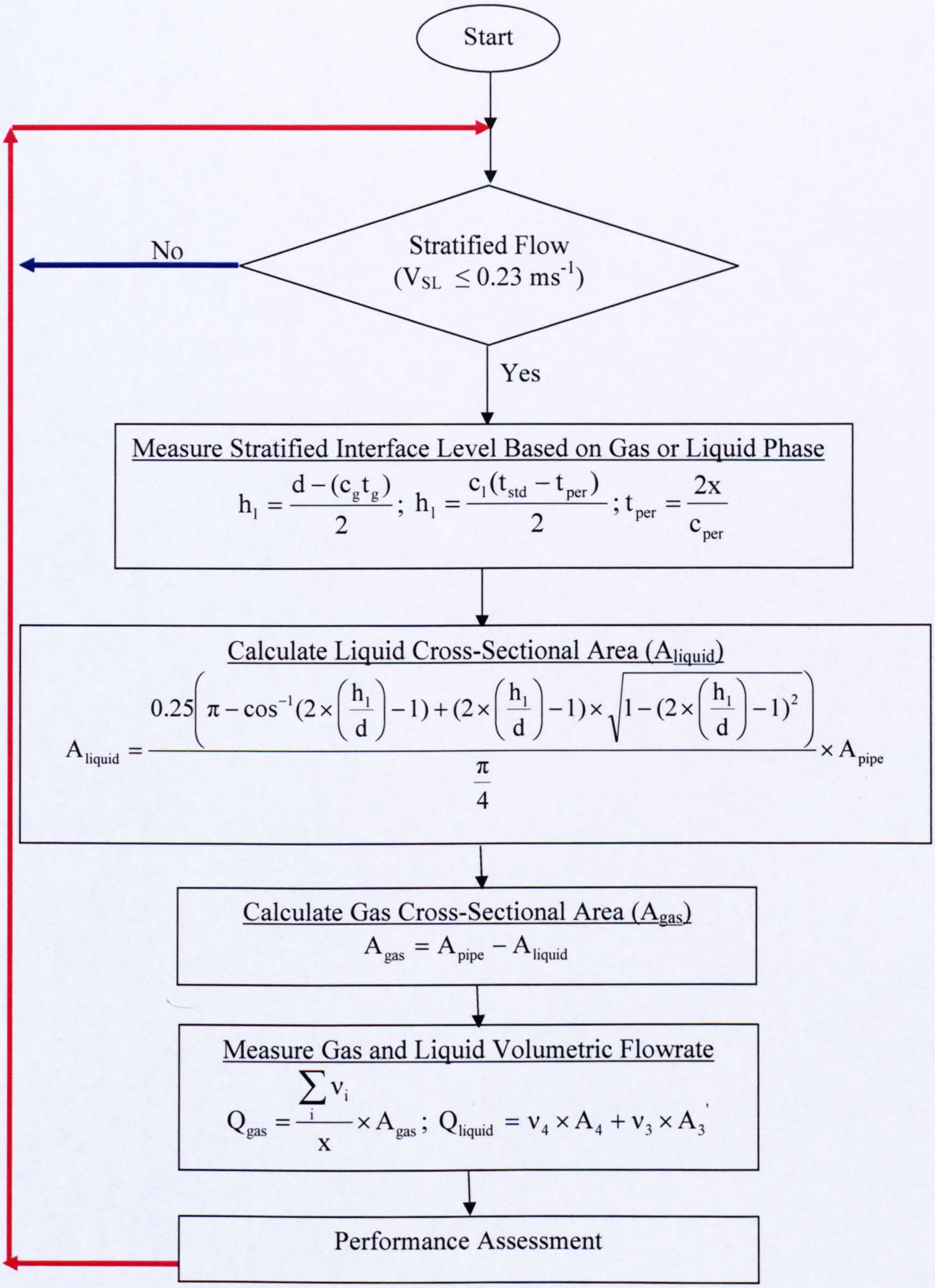

Figure 2-19: Flow Diagram for Ultrasonic Measuring and Operation Method

2.4.2.2 Ultrasonic Technique for Gas/Liquid Stratified Flow Measurement (Letton, 2003)

Non-intrusive multi-path ultrasonic flowmeter, suitable for two-phase flow measurements, having a gas flow or stratified flow regime in pipeline line were patented by Letton (2003).

In the multi-path ultrasonic system, there are three ultrasonic paths corresponding to three pairs of ultrasonic transducers. Transducers are ultrasonic transceivers, meaning that they generate and receive ultrasonic signals. Typically, these signals can be generated and received by a piezoelectric element in each transducer.

The first path travels wholly through one phase of the two-phase flow. A second path traverses through one phase of the two-phase flow, but reflects from the interface layer between gas and liquid flows. A third path traverses through the other phase of the two-phase flow, and also reflects from the interface between the gas and liquid flows as shown in Figure 2-20. Based on this configuration, an associated processor calculates flow velocity and speed of sound for each phase of the two-phase flow. The level of stratified flow for both gas height layer and liquid level can be also determined through the vertical path.

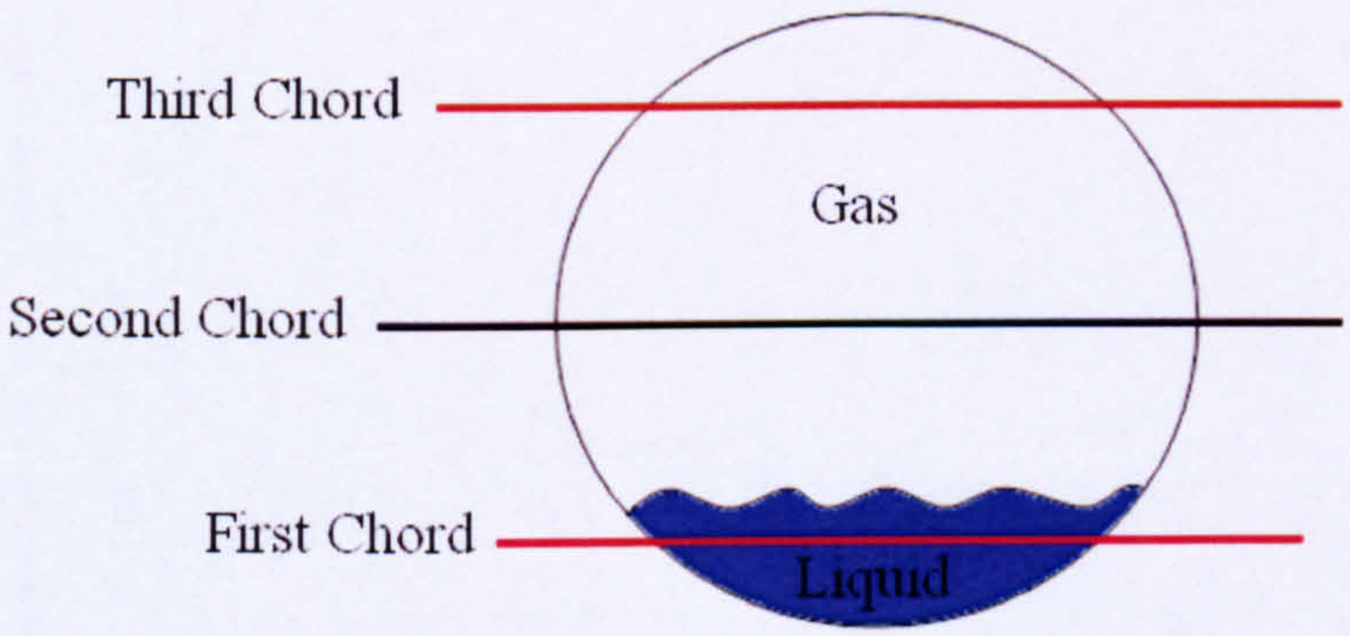

Figure 2-20: Multi-path Ultrasonic Flowmeter Configuration by Letton (2003)

To measure the average velocity of a selected phase, an ultrasonic signal is generated and detected within this phase layer. Figure 2-21, shows a cut-away top view of the ultrasonic flowmeter proposed. In this figure, a pair of ultrasonic transducers (M and N) is located along the pipeline.

A path (chord) exists between transducers at an angle θ to a centreline. The position of the transducers may be defined by this angle, or may be defined by a first length L measured between the transducers and a second length x corresponding to the axial distance.

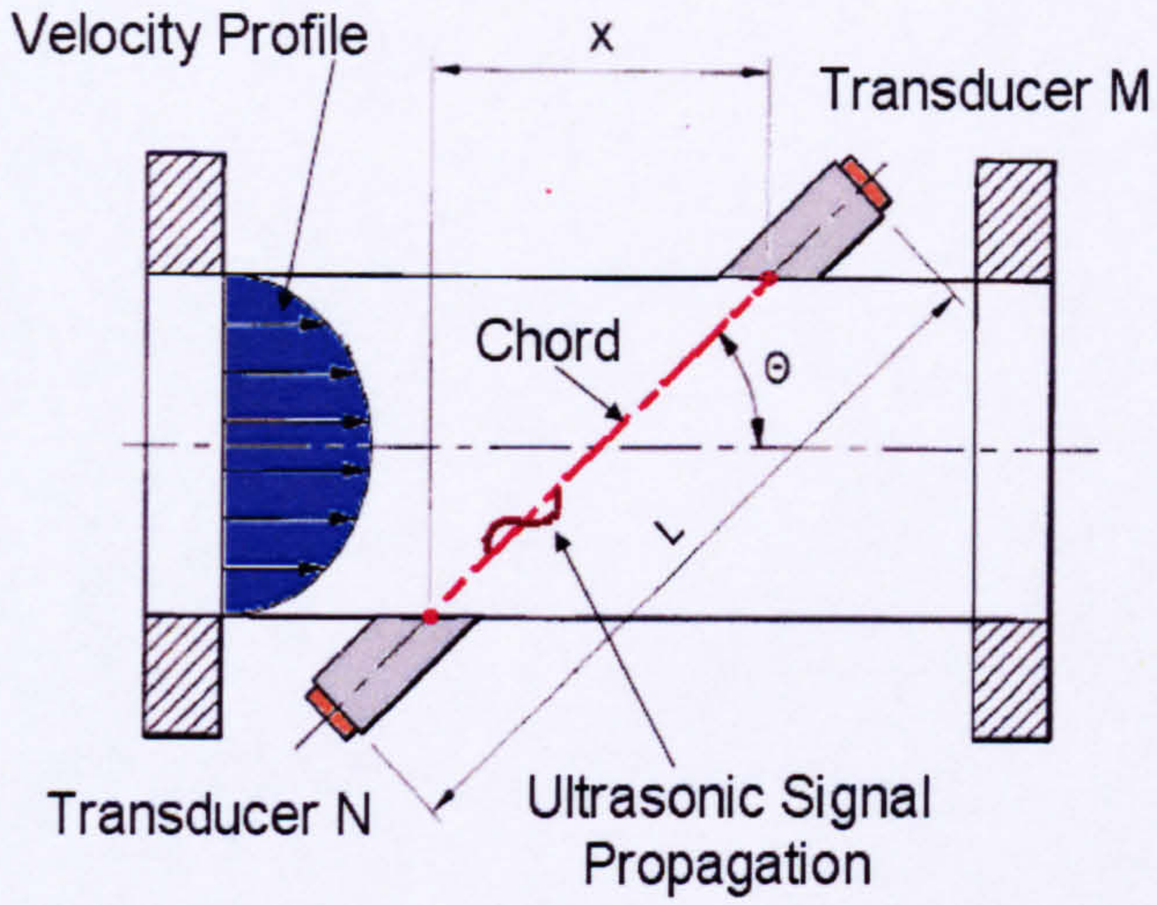

Figure 2-21: Cut-away Top View of Multi-path Ultrasonic Flowmeter

A simple equation gives the average velocity over the measurement path (chord) between transducers (M and N) as given:

$$V_M = \frac{L^2}{2x}\frac{t_{MN} - t_{NM}}{t_{MN}t_{NM}} \tag{2.26}$$

where
V_M is the mean chordal velocity of the phase measured,
L is the distance between transducers (M and N),
x is the axial distance between transducers (M and N),
t_{MN} is the transit-time from transducer M to transducer N and
t_{NM} is the transit-time from transducer N to transducer M.

Equation (2.26) may be applied to each chord A-C to obtain each chordal flow velocity. To obtain the average velocity over the entire pipeline, the chordal flow velocities are multiplied by a set of predetermined constants, known as weight factors. In the case of the ultrasonic flowmeter developed, the measured speed of sound of the fluid for any particular chord is:

$$c = \frac{L(t_{MN} + t_{NM})}{2t_{MN}t_{NM}} \tag{2.27}$$

where c is the speed of sound of fluid in still condition.

Figure 2-22 shows ultrasonic transducers designed for the measurement of the level of stratified flow. The ultrasonic transducers can be designed for gas operation and would only be capable of transmitting a signal if gas were present, as shown in Figure 2-22 (a). Ultrasonic transducer designed for liquid operation installed at the bottom of the pipe, as shown in Figure 2-22 (b).

In both the ultrasonic transducers designed, the transducer generates an ultrasonic signal that travels across the pipe, reflects off the surface (interface between the two phases), and returns to transducer. Thus the travel time of ultrasonic signal correspond to the depth of stratified flow.

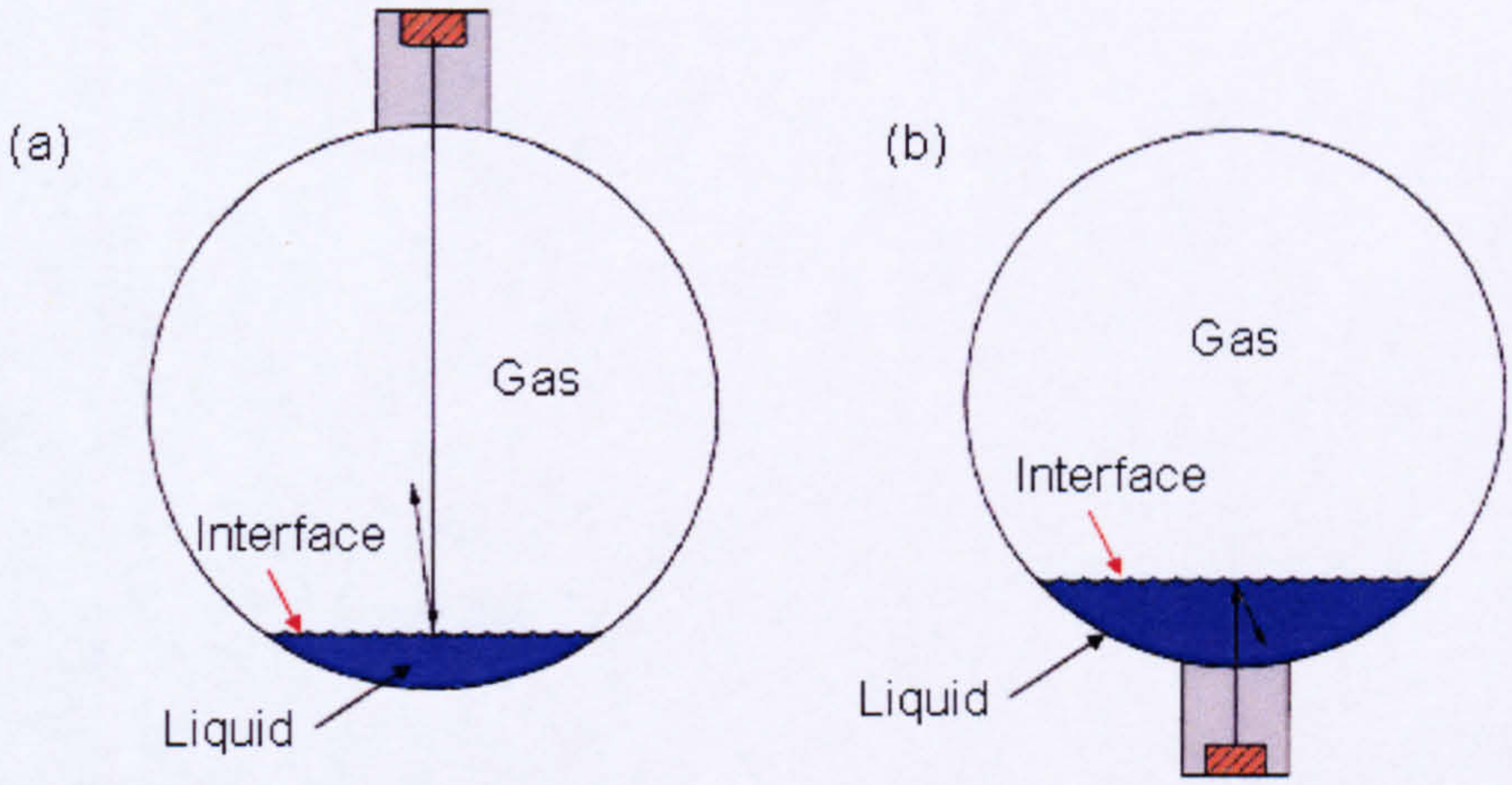

Figure 2-22: Stratified Liquid Level, (a) Ultrasonic Transducer designed for Gas Operation, (b) Ultrasonic Transducer designed for Liquid Operation

From the stratified liquid level h and the axial distance between transducers x, the distance X_1 can be determined based on the given equation:

$$X_1 = 2 \times \sqrt{h^2 + \left(\frac{x}{2}\right)^2} \tag{2.28}$$

Figure 2-24 shows a side view of the possibility of locating a pair of ultrasonic transducers below the surface of the stratified flow.

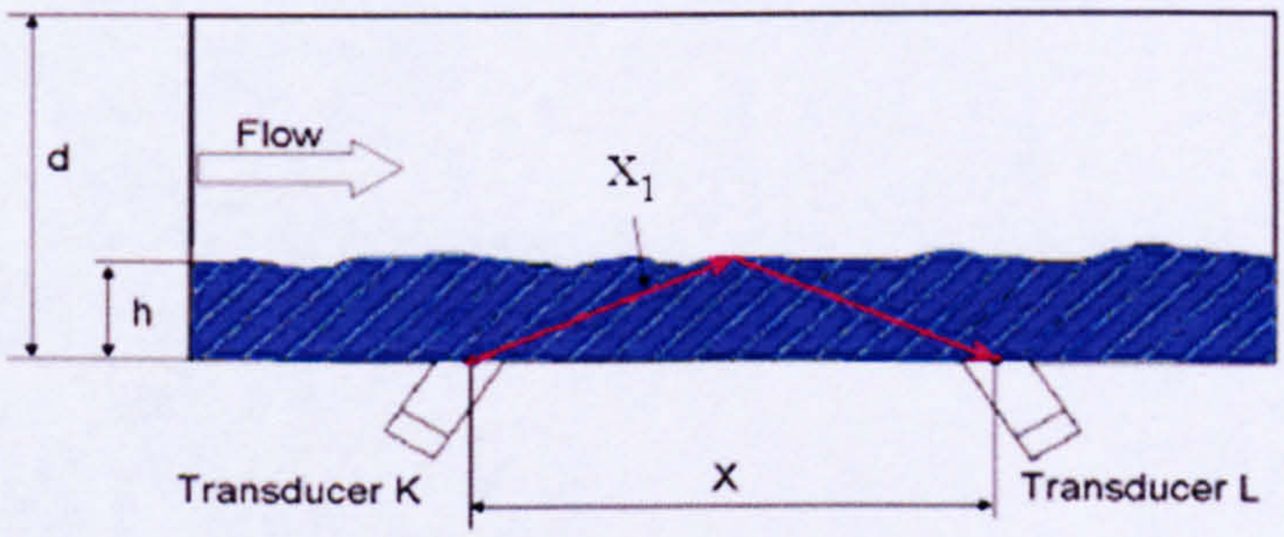

Figure 2-23: Side View of Multi-Transducer Stratified Level Detector

Transducers K and L are designed for liquid operation; therefore, they would provide an indication of liquid presence in multiphase flow system. As the height of the liquid in

the pipe, h, may be quite small, in this case the liquid volume acts as a wave guide between liquid transducers K and L.

The area of the pipeline occupied by a stratified flow is area that is not carrying gas. Knowledge of the depth of the stratified flow can be useful to adjust the measurement of the cross-sectional area being used to carry the flow of the gas.

If the velocity of the stratified flow can be established, knowledge of the cross-sectional area of the stratified flow can be used to calculate the volume of the stratified liquid flowing through the pipeline.

The multi-path ultrasonic operation method according to Letton, (2003) is summarised in the flow diagram (Figure 2-24). However, Letton, (2003) stated that the three-path ultrasonic flowmeter, designed for multiphase flow application, generally was not considered capable of measuring the flowrate or composition of stratified flow when the liquid fraction was above 5% of the total volume in the pipeline. Therefore, the multi-path ultrasonic technique cannot operate under intermittent flow conditions. It is important to highlight that Letton, (2003) multi-path ultrasonic operation method was neither tested under real flow conditions nor demonstrated by experimental data. Therefore the reliability of this technique is questionable.

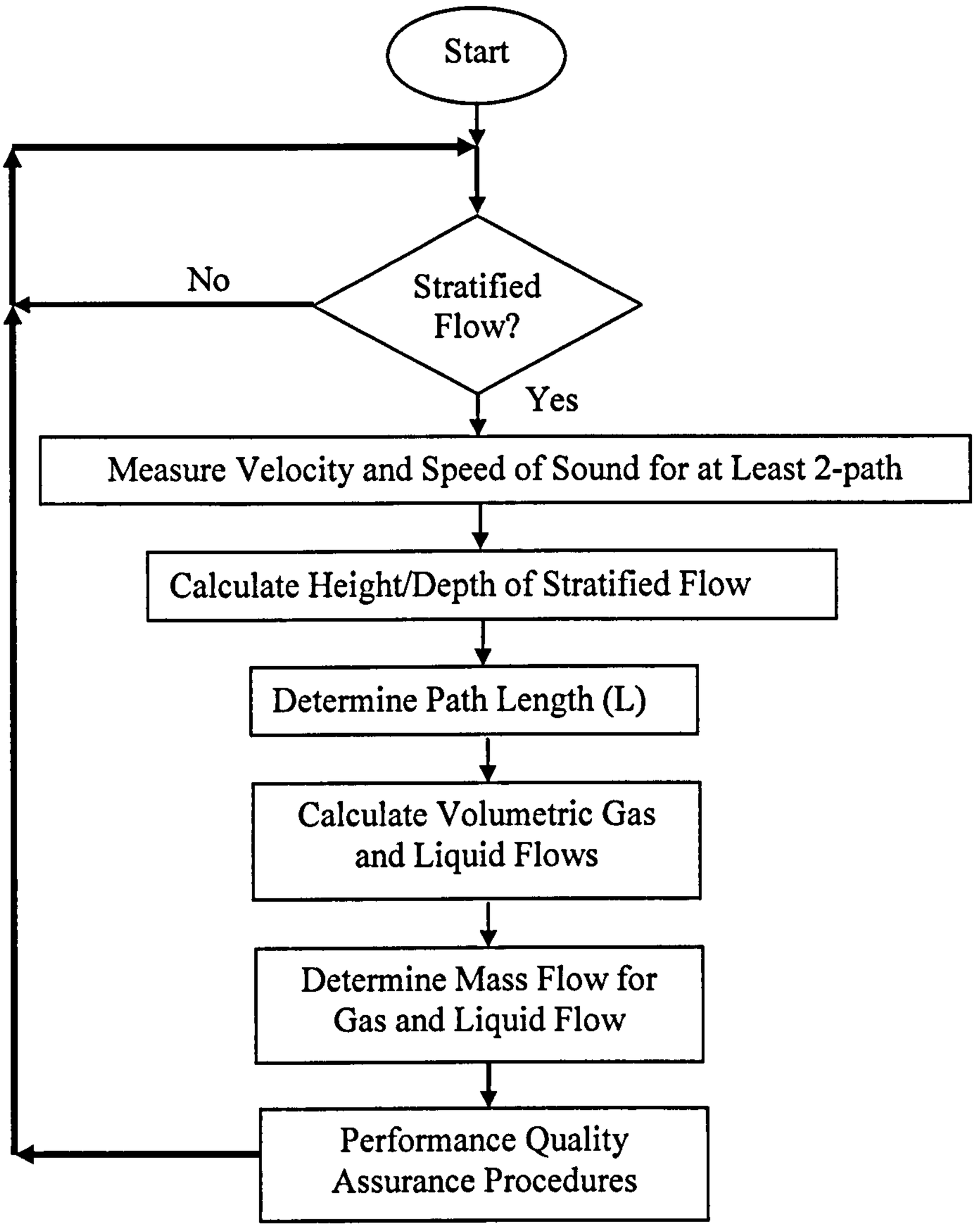

Figure 2-24: Flow Diagram illustrating Operation Method by Letton (2003)

2.4.2.3 Ultrasonic for Monitoring Gas and Liquid Flow in Multiphase Flow (Vedapuri and Gopal, 2003)

An ultrasonic technique to monitor and measure the liquid flowrate in wet gas pipeline lines for liquid volume fractions up to 10% in a 100 mm pipeline diameter was patented by Vedapuri and Gopal (2003).

The method utilises a set of gas phase upstream ultrasonic transducers G1, G3 and downstream transducers, G2, G4, positioned on opposite sides of the pipeline and a number of liquid phase ultrasonic transducers L1, L2, L3, and L4 positioned on the bottom and on one side of the pipe. In this manner, the ultrasonic gas and liquid

transducers are positioned to direct ultrasonic signals through the multi-phase flow system in pipeline, see Figure 2-25.

The gas and liquid ultrasonic transducers sets connect to a control system via ultrasonic data selection terminal, where the ultrasonic data selection terminal is controlled so as to establish a dwell time, during which data may be gathered from signals transmitted and received by a selected liquid or gas phase transducer set. Also an ultrasonic data selection terminal may be employed to switch analysis between different algorithms and sets of control parameters, in addition to switching analysis between stets of transducers, see Figure 2-25.

The control parameters are established for the gas phase transducers to define gas phase ultrasonic signals characterised by gas phase centre frequencies and gas phase bandwidth. The gas phase centre frequency is from 225 kHz-1MHz with bandwidth set at a value above about 225 kHz. The liquid phase control parameters will define the liquid phase ultrasonic signals to be generated by the corresponding set of liquid phase transducer. The liquid phase centre frequency is established at a value between 0.5MHz and 5MHz, with bandwidth set at a value that is about 30% to 80% of the value of the liquid phase centre frequency and is preferably above about 300 kHz.

A gas phase algorithm is established and is utilised to process the gas phase ultrasonic signals to enable determination of gas phase. The gas phase algorithm may comprise a gas phase transit time algorithm or a gas phase cross-correlation algorithm. However, the liquid phase algorithm typically comprises a liquid phase cross-correlation algorithm. To determine liquid flowrates under stratified and annular-mist flow regimes, the liquid film height is an important parameter in order to calculate the gas and liquid flowrate.

The conclusions for the clamp-on ultrasonic technique proposed to monitor liquid flowrate in natural gas pipeline lines can be summarised as follows:

- The design methodology for a clamp-on ultrasonic liquid flowrate monitor was presented where two parameters needed to be measured, the liquid film thickness and the liquid film velocity.
- The intensity of multiple reflections within the pipeline wall material is an order of magnitude higher than the reflection from the liquid-gas interface and hence masks the waveform of interest.
- Film thickness measurements were made for gas velocities up to 15 ms^{-1}. Film velocity measurements for gas velocities up to 5 ms^{-1} were made. However, for higher gas velocities, the required electronics needed to be modified.

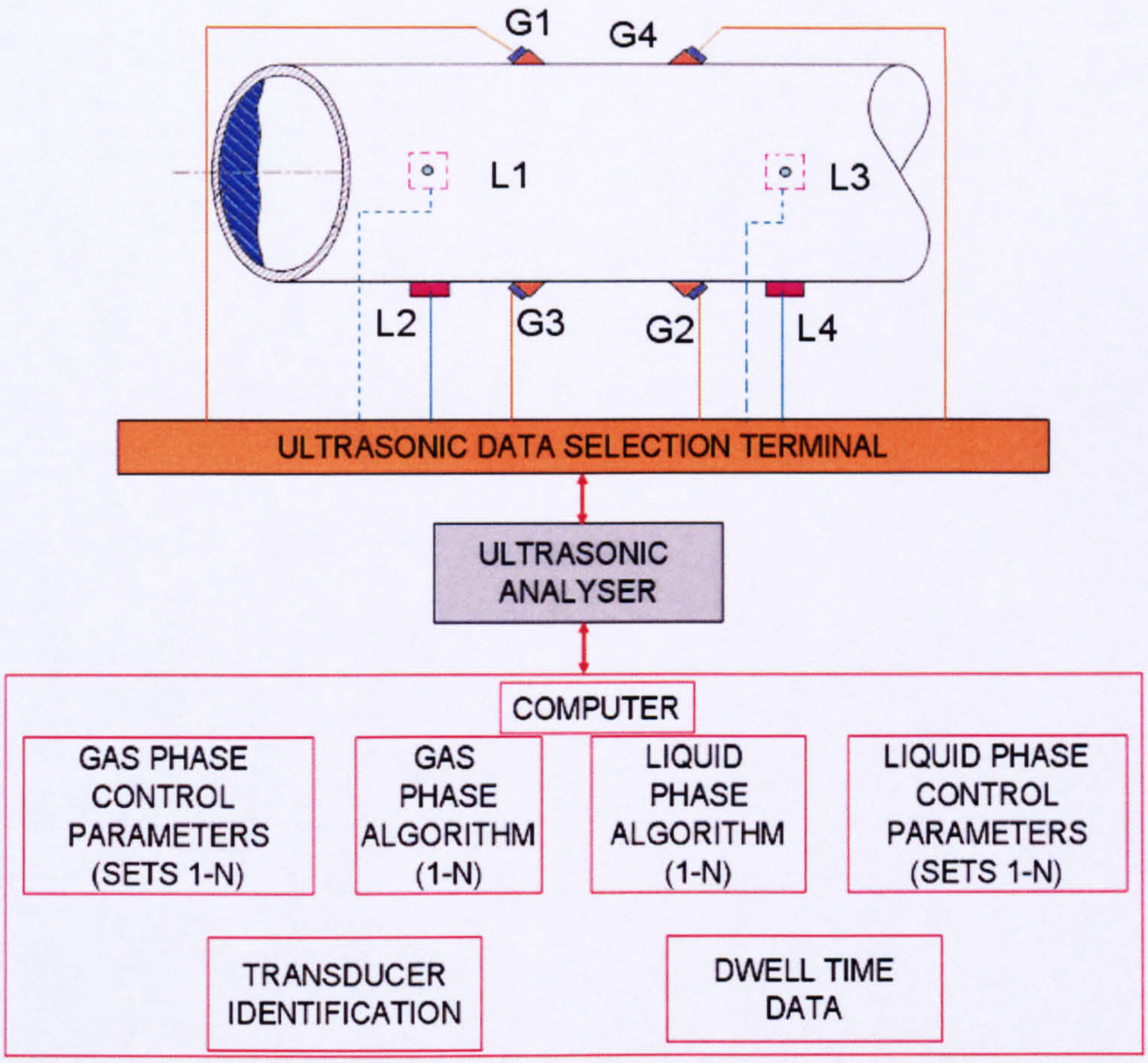

Figure 2-25: Ultrasonic Liquid/Gas Flowrates by Vedapuri and Gopal (2003)

2.4.2.4 Ultrasonic Measuring System and Operation (Jepson and Gopal, 1998)

Non-intrusive ultrasonic measuring technique to operate under two-phase flow system in pipeline line was patented by Jepson and Gopal (1998). In this patent, the two-phase flow measured using ultrasonic technique was a form of stratified flow regime or as liquid mist entrained in gas flow.

The system developed consists of a number of upstream and downstream ultrasonic transducers coupled non-intrusively to a multiphase flow pipeline line. The upstream and downstream ultrasonic transducers were coupled to a transducer control system, which used as a selective activation of ultrasonic transducers. The ultrasonic measuring system is utilised to determine a flow velocity of a selected phase by generating and detecting ultrasonic pulses in a selected single phase layer. In other words, the ultrasonic measuring system is utilised to determine film heights of the phases flowing within the pipeline. Figure 2.26 is a schematic illustration of an apparatus for the ultrasonic measuring system in two-phase gas/liquid stratified flow by Jepson and Gopal (1998).

The method of operating an ultrasonic measuring system comprises the following steps:

1. Determining a first absorption coefficient corresponding to a first phase occupying a first flow portion (i.e. water) related to its properties as follow;

$$\alpha = \frac{2\pi f \mu}{\rho c^3} \tag{2.29}$$

where
f is the frequency of the sound wave,
μ is the viscosity of the medium,
ρ is the density of the medium and
c is the velocity of sound in the medium.

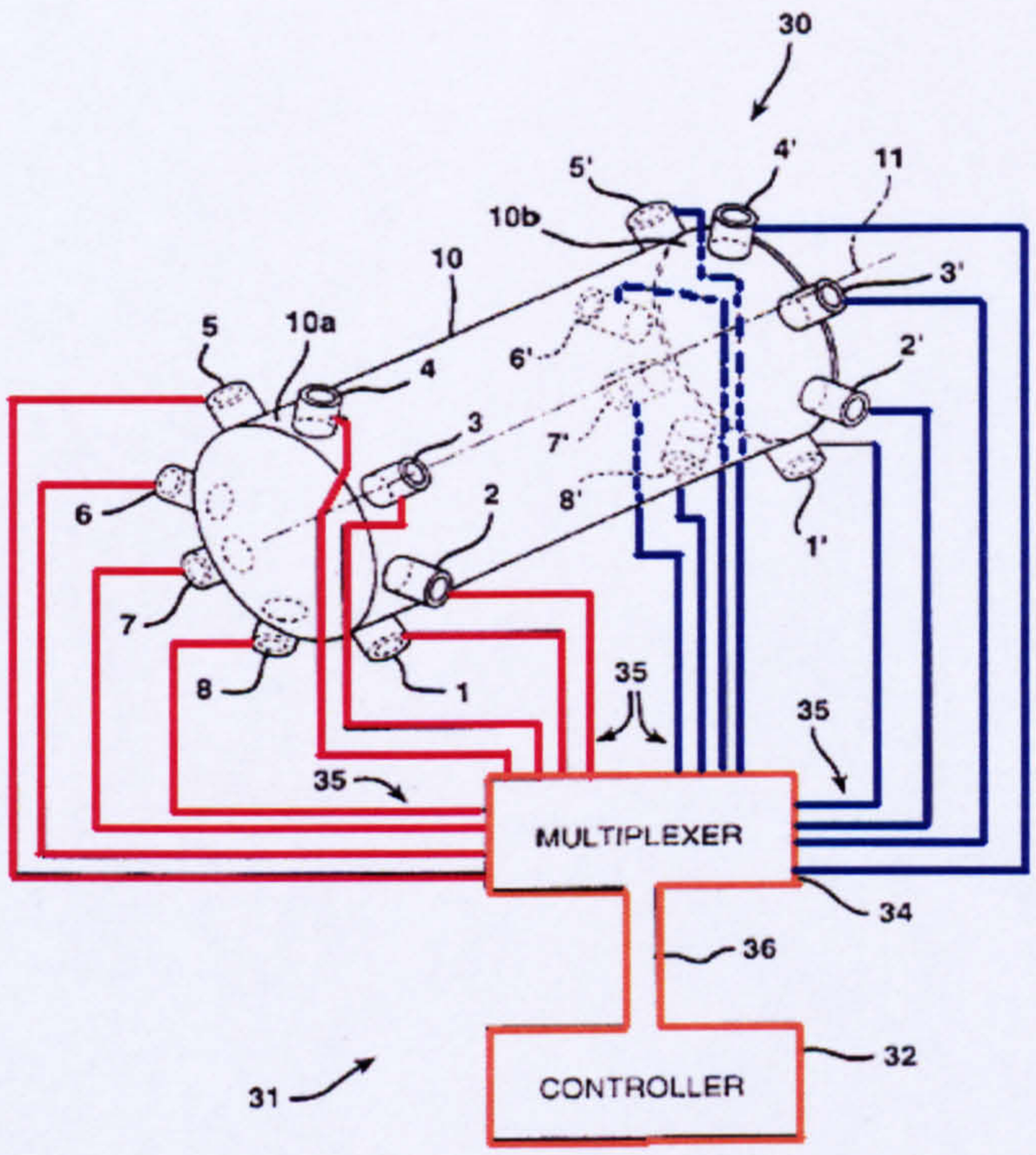

Figure 2-26: Ultrasonic Measuring System by Jepson and Gopal (1998).

2. Determining a first ultrasonic propagation factor corresponding to a first interface between the first flow portion (i.e. water) and a second phase occupying a second flow portion (i.e. gas);

An interface between two media may be characterised by a number of ultrasonic propagation factors including:

- A first reflection factor for an ultrasonic wave incident on the interface from a first side of the interface;

- A second reflection factor for an ultrasonic wave incident on the interface from a second side of the interface;

- A first transmission factor for an ultrasonic wave incident on the interface from a first side of the interface; and

- A second transmission factor for an ultrasonic wave incident on the interface from a second side of the interface.

The reflection factor, R and transmission factor T is defined in the following equations:

$$R = \frac{(\rho_1 c_1 - \rho_2 c_2)}{(\rho_1 c_1 + \rho_2 c_2)};\ T = \frac{2 \times \rho_2 c_2}{(\rho_1 c_1 + \rho_2 c_2)} \qquad (2.30)$$

where
ρ_1 is the density of the first phase,
c_1 is the velocity of sound in the first phase,
ρ_2 is the density of the second phase and
c_2 is the velocity of sound of the second phase.

3. Generating an ultrasonic pulse at a lowermost portion of a cross section of the pipeline line; detecting a first reflected ultrasonic pulse at the lowermost portion, the first reflected ultrasonic pulse being reflected from the interface between the two phases and then calculating the first phase film height based on the generated ultrasonic pulse, the first ultrasonic absorption coefficient, the first ultrasonic propagation factor, and the first reflected ultrasonic pulse.

As a sound wave signal passes through a medium, its amplitude, i.e., pressure, decreases is attenuated as follows:

$$P_x = P_o e^{-\alpha x} \qquad (2.31)$$

where
P_x is the pressure of the sound wave at a distance x from the source,
P_o is the pressure of the sound wave at the source,
α is the absorption of the medium is related to its properties as follow given in equation (2.29) and the quantity $e^{-\alpha x}$ corresponding to the attenuation of the sound wave by a medium and is identified as:

$$P_\alpha = e^{-\alpha x} \qquad (2.32)$$

In Figure 2-27 the pipeline line 10 has a known inside diameter d and includes the first phase layer 14 having a first film height (a) and a second phase layer 16 having a second film height b. The fluid interface 12 defines the mutual boundary between the

two phases 14 and 16. Ultrasonic transducer 1 is coupled to the bottom of a first cross section of the pipeline line 10. The ultrasonic transducer 1 is capable of generating and detecting an ultrasonic pulse. The film height (a) of the first phase 14 and the film height b of the second phase 16 may be determined by generating the ultrasonic signal at transducer 1 and detecting the ultrasonic signal reflected from the first interface (12).

The magnitude set by the transducer 1 is Pi, and the magnitude detected by the transducer 1 is Pr`. The difference between Pi and Pr` is equal to the sum of the pressure absorbed in the first phase 14 ($Pi`=A_1$), the pressure transmitted through the first interface 12 ($Pt=A_2$), and the pressure absorbed again in the first phase 14 between ($A_3$=Pr-Pr`):

$$Pi - Pr' = \sum (A_1 + A_2 + A_3) \tag{2.33}$$

The film height (a) of the first phase 14 is given as:

$$P_\alpha = \left[\frac{Pr'}{Pi(1-T)}\right]^{1/2} = e^{-\alpha x} \tag{2.34}$$

where
x is film thickness or film height (a) of the first phase 14,
α is calculated from equation (2.29),
Pr` is measured at transducer 1,
T is transmission factor determined using equation (2.30) and

Pi is proportional to the electrical volts applied to the transducer 1 and can be quantified by experimentally calibrating the transducer 1 using hydrophone within the pipeline to account for pressure lost in walls of the pipeline.

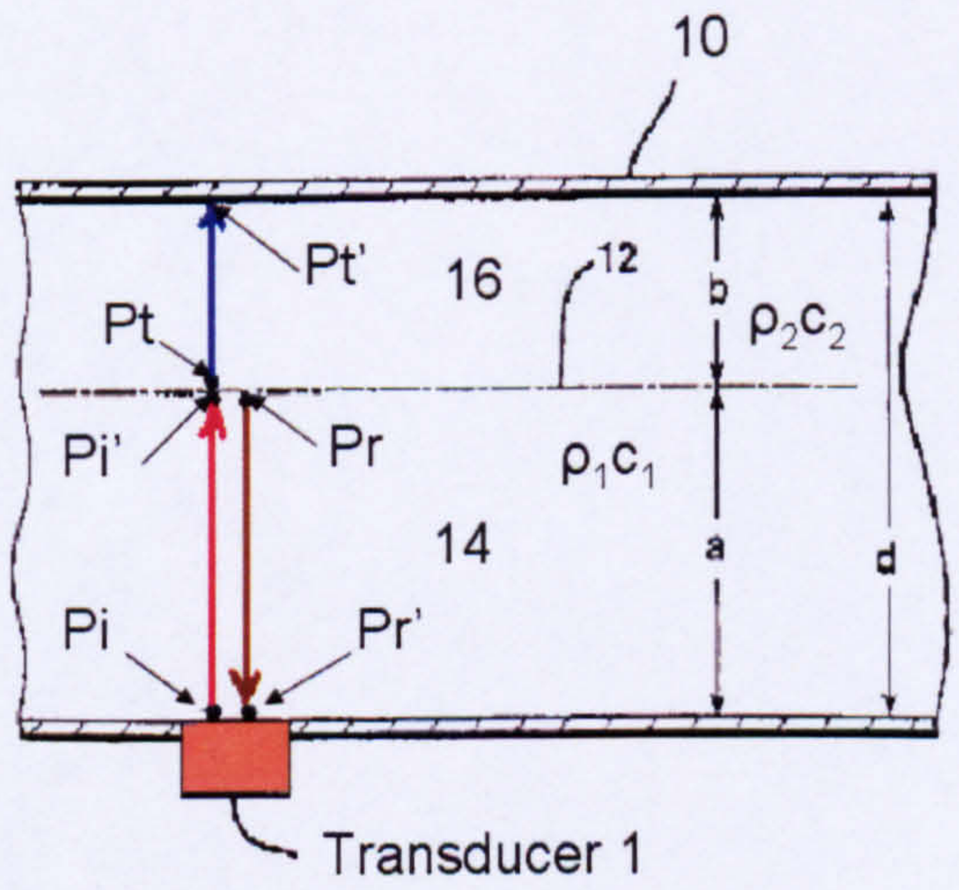

Figure 2-27: Stratified Liquid Level in Two-Phase Flow (Jepson and Gopal 1998)

The fluid film heights (b) can be obtained by subtracting the film height (a) from the inside pipe diameter d as (b=d-a).

The film height a measure based on derived equation (2.34) can be confirmed by comparison with film height determination derived from measuring the transit-time of a sound wave reflected from the first interface 12 and applying the given equation:

$$a = \frac{t\, c_{14}}{2} \tag{2.35}$$

where
t is defined as transit-time,
c_{14} is the velocity of sound in the phase 14, which can be measured experimentally or has been determined previously for the phase of interest.

In Figure 2-28, ultrasonic signals which are represented schematically by paths 24 are generated and detected within a selected layer 20 to obtain the selected layer velocity by measuring the change in transit time for a sound wave to travel with and in opposite directions between two points in a moving fluid.

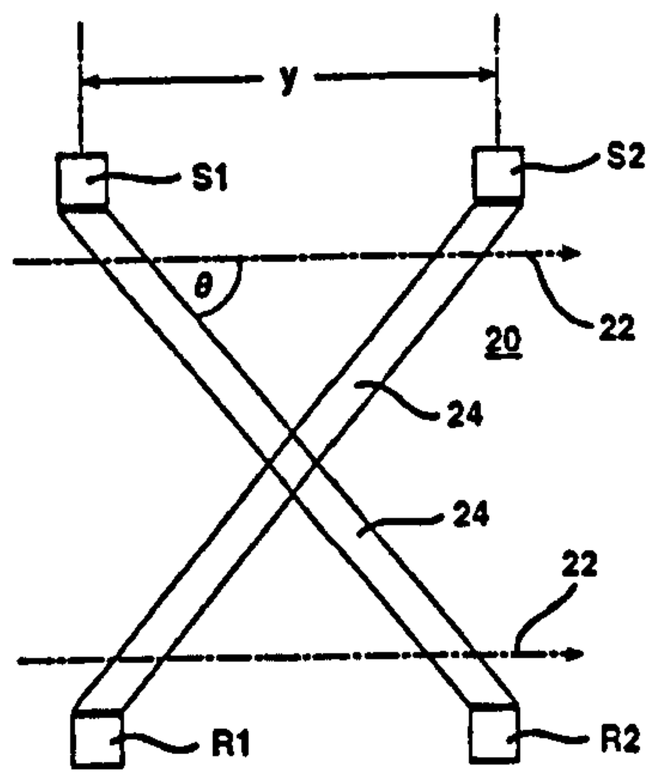

Figure 2-28: Process of Measuring Flow Velocity of Selected Fluid Layer

Specifically as illustrated in Figure 2-30, a first pair of transducers includes a transmitter S1 and a receiver R2 positioned within the selected phase and second pair of transducers includes a transmitter S2 and a receiver R1. The ultrasonic transducers S1, S2, R1, and R2 are positioned within the selected layer 20 and are separated by a known distance y.

The ultrasonic pulses are generated simultaneously at the first and second generating transducers S1, S2 and subsequently detected at the first and second detecting transducers R1, R2. The time interval t_1 is for the signal to travel in the upstream direction, i.e., from S2 to R1, and the time interval t_2 is for the ultrasonic signal to travel in the downstream direction, i.e., from S1 to R2, The difference Δt between t_1 and t_2 can be related to moving fluid as follows:

$$\Delta t = \frac{2V_{fy}\cos\theta}{c^2} \tag{2.36}$$

where
V_f is the phase velocity,
y is the distance between the upstream and downstream ultrasonic transducers,
θ is the angle of inclination with respect to the fluid flow direction, of the paths defined between the generating and detecting transducers,
c is the velocity of sound in the medium of interests.

V_f is the only unknown, the equation is solved to determine the phase velocity within the selected layer.

The ultrasonic measuring system patented by Jepson and Gopal (1998) has not been tested and is schematically illustrated in Figure 2-29.

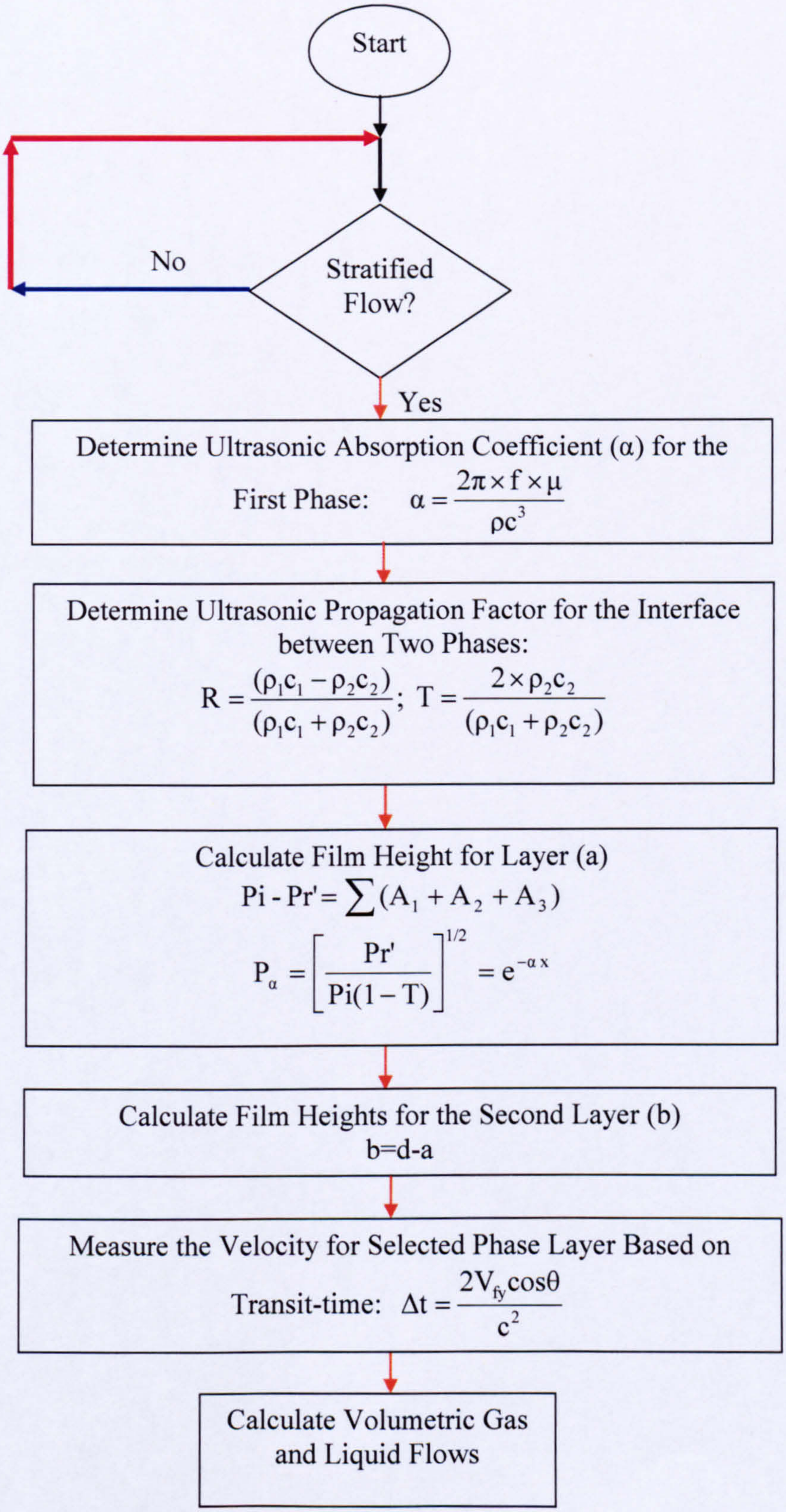

Figure 2-29: Flow Diagram for Ultrasonic Measuring System (Jepson and Gopal 1998)

2.5 Summary

In this chapter a literature review is presented which covers most of the currently available techniques implemented in the area of multiphase flow measurement including the ultrasonic technique and the following points are concluded:

- Currently, most multiphase flow meters (MPFM) are bulky, complex and intrusive and non-invasive metering techniques are still the preferred technique.

- Ultrasonic techniques have significant potential benefits over the traditional mechanical flow measurement with higher reliability, greater rangeability and lower maintenance requirements and non-invasive and non-intrusive measurement techniques have the advantage of minimising flow disturbance and providing no additional pressure loss. Moreover, instruments for pipes of various sizes tend to use identical transducers and electronics giving proportionately lower costs for larger size meters.

- The advantages of ultrasonic techniques in flow measurements appear promising for multiphase flow measurement applications. However, the successful implementations of this technique in multi-phase flow systems are varied and depend on gas/liquid flow regime presented in pipeline and gas /liquid phase distributions within the cross-sectional area of the pipe (GVF and liquid holdup).

- The works reported in the literature to investigate the applications of ultrasonic techniques in two-phase gas/liquid flow measurements in pipeline mention the following points:

    1. Transit-time ultrasonic technique is the most promising for further development in the implementations of this technique in two-phase gas/liquid flow measurements.

    2. Most of the previous experimental works undertaken in ultrasonic two-phase gas/liquid flow measurements were limited to stratified, and annular-mist flow, where the liquid volume fraction was $\leq 10\%$ and gas void fraction $\geq 90\%$.

    3. The ultrasonic measuring systems developed or proposed by different researchers were unable to continue their functionality when the liquid volume fraction is above 5% of the total flow volume. Further research and experimental studies to improve ultrasonic measuring technique in two-phase gas/liquid wet gas flow at higher liquid volume fraction is still a challenge and requires further investigations.

    4. The implementation of the ultrasonic measuring techniques under slug flow condition is still difficult to be achieved as the slug flow occurs over a wide range of gas and liquid flowrates in pipelines, and also due to the unpredictable and complicated natures of the slug flow.

Chapter 3

Slug Closure Model and Ultrasonic Metering Concept

In this chapter, the slug closure model and the ultrasonic metering concept for measuring the gas and liquid phases volumetric flowrates are presented.

After the introduction Section 3.1, this chapter is divided into five sections. Section 3.2, concentrates on the description of the process of slug initiation, growth and decay, which in turn provides details of the initial conditions necessary for the better understanding of the slug flow characteristics.

The development of the slug closure model based on "slug unit" is presented in Section 3.3. Review of the empirical correlations developed previously for slug characteristics is presented in Section 3.4.

The review also includes closure relationships for slug body velocities. An ultrasonic metering concept developed based on the combinations of the non-invasive/non-intrusive ultrasonic devices and the slug closure model to obtain the phase volumetric flowrates is presented in Section 3.5. Finally, the summary of this chapter is described in section 3.6.

3.1 Introduction

Slug flow in pipes exists for the whole range of pipe with upward inclinations and over a wide range of gas and liquid flowrates. It is characterised by a complex dynamic structure, which consists of aerated slugs of liquid that travel down the pipeline approximately at the local gas velocity. These slugs are separated from one another by a stratified configuration of gas and liquid phases.

A slug closure model approach has been developed in the present work to obtain the gas/liquid phase volumetric flowrates from the measurement of slug flow parameters. The slug closure model developed is based on the "slug unit" model which gives a simplified representation the complex structure of slug flow. The slug closure model proposed is a function of slug flow characteristics, including slug translational velocity, V_T, the slug body liquid fractions, E_{LS}, and the film zone liquid fraction, E_{LF}, and the slug body length, L_S, and the film length, L_F, within each "slug unit".

3.2 Slug Flow Initiation and Dissipation

In order to achieve accurate measurement of the volumentric flowrates of slug flows,the hydrodynamic slugs have to be reasonably developed. Thus it is important to understand the slug development and dissipation process. The prediction of the flow conditions at which slug initiation and dissipation occur has received considerable attention in the last two decades (Woods and Hanratty, 1996).

One approach of predicting slug initiation is based on studying and analysing the stability of a stratified flow as investigated by several researchers. Kordyban and Ranov (1970) suggested that the transition from stratified flow to a slug flow might be described through a classical linear stability analysis. Graham *et al.* (1973) examined the growth of linearly unstable long wavelength disturbances on a flowing liquid. Taitel and Dukler (1976), Mishima and Ishii (1980) and Fan *et al.* (1993a) considered the evolution of a slug from a finite amplitude wave, with a wavelength in a range that would be stable by the Kelvin Helmholtz mechanism.

Another approach is to examine the stability of slugs travelling over a liquid layer as was investigated by Dukelr and Hubbard (1975) and Ruder *et al.* (1989). These authors investigated the initiation of a slug using visual observations in two-phase gas/liquid flow in horizontal pipe.

In their slug phenomena description, Dukler and Hubbard (1975) and Taitel and Dukler (1976) presented the development of gas and liquid flow in a pipeline. Near the entrance, the gas tends to flow above a moving stratified liquid layer. However, because of the shear forces created at the pipe wall, the liquid layer tends to decelerate as it moves along the pipe and its height changes gradually towards an equilibrium height which is governed by the pressure force, shear and gravitational forces.

As this occurs, small perturbations on the stratified layer could develop into growing waves. Due to the suction effect caused by an increased gas velocity over these disturbances as shown in Figure 3-1 (a) and (b), until eventually one of the waves grows to a sufficient size to momentarily bridge the pipe. This process blocks the flow of gas, see Figure 3-1 (c), and so the upstream pressure builds causing the blockage to be accelerated to the gas velocity.

During this stage, the fluid blockage appears to be accelerated uniformly across its cross-section, thereby acting as a scoop, picking up all the slow moving liquid in the film ahead of it (pick-up process) and beginning to grow in volume to become a slug as shown in Figure 3-1 (d).

Gas may also be entrained in the form of small bubbles, which are deformed by the combined effect of buoyancy forces and the turbulent shear forces created by velocity differences between the slug front and the liquid film. As a result, a dispersion of small bubbles is often produced which may be transported through the body of the liquid slug.

Meanwhile, at the slug tail, liquid and previously entrained gas are released (shedding process) from the slug body. The "shed" liquid decelerates to a velocity determined by the shear stresses at the wall and the interface and becomes a stratified layer as illustrated in Figure 3-1 (e). The "shed" gas mainly passes into the elongated bubble region above this layer, although a fraction may remain entrained within the liquid film.

As long as the volumetric "pick-up" rate is larger than the "shedding" rate, the slug continues to grow. However, eventually the "pick-up" rate becomes equal to the "shedding" rate and the slug becomes fully developed so that the slug length stabilises. Nydal *et al.* (1992) experimentally investigated the length of the pipe required to reach quasi-stable flow conditions (slug development distance) and found that it is between 300 and 600 pipe diameters. Once the quasi-stable conditions are reached, the slug length has a mean value between 12 to 15 pipe diameters.

Based on the shedding and pick-up processes, slug flow might be classified into three main states. When the pick-up rate is greater than the shedding rate; the slug in this case continues to grow. The "pick-up" rate equals to the "shedding" rate, the slug becomes fully developed so that the slug length stabilises. Finally, when the "pick-up" rate is less than the "shedding" rate, the slug under this condition dissipates.

The slug dissipation process occurs as the gas flowrate and consequently the slug velocity and the degree of aeration of the slug increases. Ultimately the gas forms a continuous phase through the slug body. When this occurs the slug begins bypassing some of the gas. At this point the slug no longer maintains a competent bridge to block the gas flow so the characteristics of the flow changes. This point is the beginning of "blow-though" and the start of the annular flow regime.

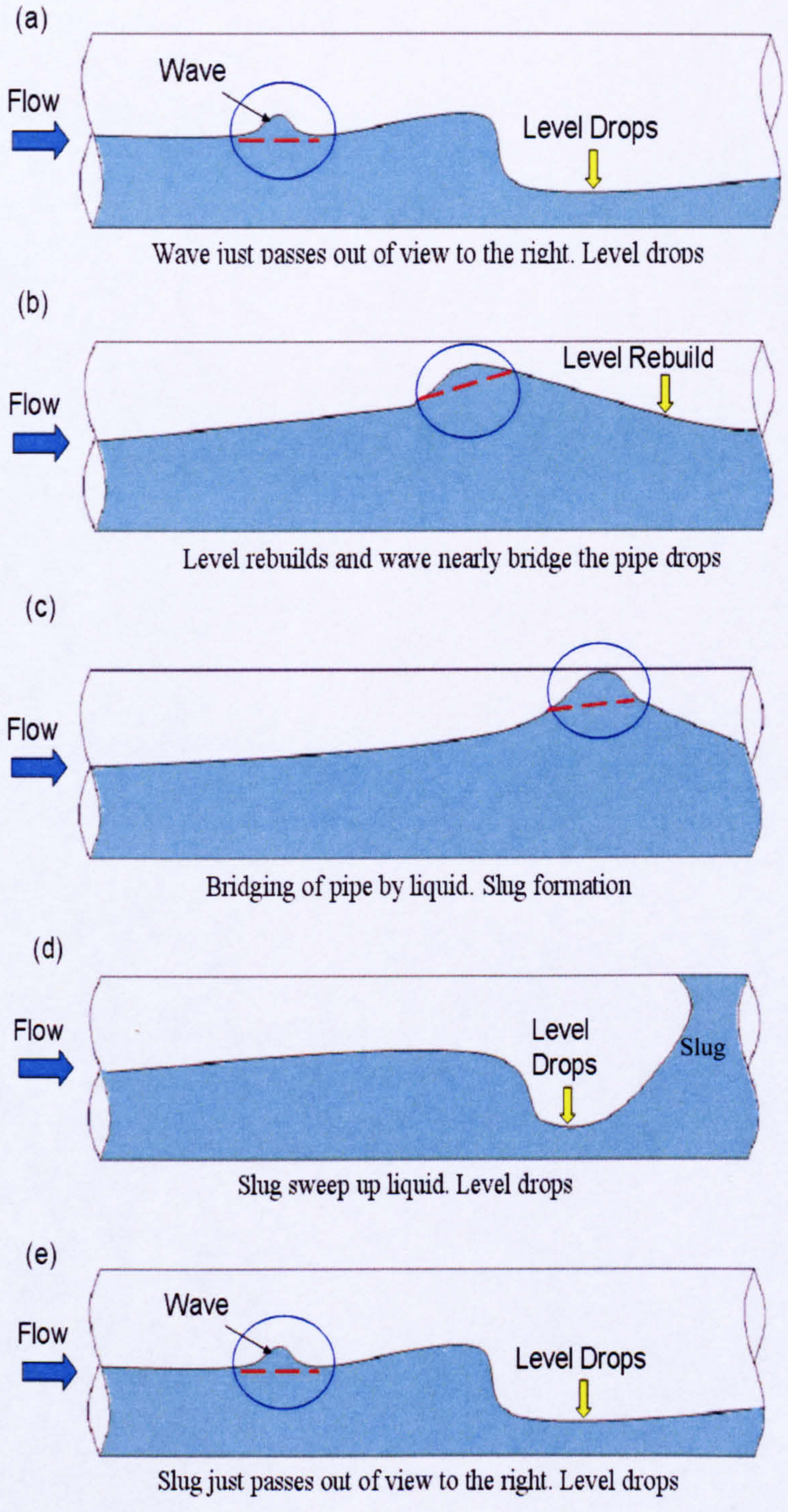

Figure 3-1 : The Process of Slug Formation by Dukler and Hubbard (1975)

3.3 Development of a Slug Closure Model

3.3.1 Slug Unit "Steady-State" Model

The "slug unit or unit cell" model of slug flow firstly was proposed by Kordyban (1961) who modelled the liquid slug as "skating" over a slow-moving liquid film of uniform thickness. However, a more seminal model was proposed by Dukler and Hubbard (1975) who were the first workers to treat the flow in the film region, and process of liquid pickup at the slug front in mechanistic fashion.

In the "slug unit" model, the slug flow is assumed to be fully developed where slugs have identical structure. In other words, the growth, shrinking, generation and disappearance of slugs as they propagate along the pipe are not considered and therefore, the pickup rates and shedding rates for each successive slug unit must be balanced. The "slug unit" consists of two regions; see Figure 3-2, namely, the slug region and the film region. The slug region has a length of length, L_S, and liquid height, H_{LS}. The average liquid velocity in the liquid slug body is V_{LS} and the average axial velocity of the dispersed bubbles in this section is V_{GS}.

The film region consists of liquid film and an elongated gas bubble and has a length of L_F. For the case of horizontal and inclined pipes the bubble is in the upper part of the pipe. It moves downstream at a translational velocity V_T. The liquid film velocity is V_{LF} at the front of the slug zone and the gas velocity in film zone is V_{GF}. The liquid film velocity in the film zone varies along the pipe, $V_{LF(X)}$, due to change of the film height, $E_{LF(X)}$. However, the film height rapidly decreases with increasing distance from the tail of the slug until it reaches an equilibrium level.

By moving the system at the translational velocity of the elongated bubble, V_T, the slug unit appears to be stationary. This enables the "steady-state" mass balances across the slug unit to be obtained. The slug unit approach was subsequently used and adapted by Nicholson *et al.* (1978); Stanislav *et al.* (1986); Bendiksen *et al.* (1996) and Taitel and Barnea (1990).

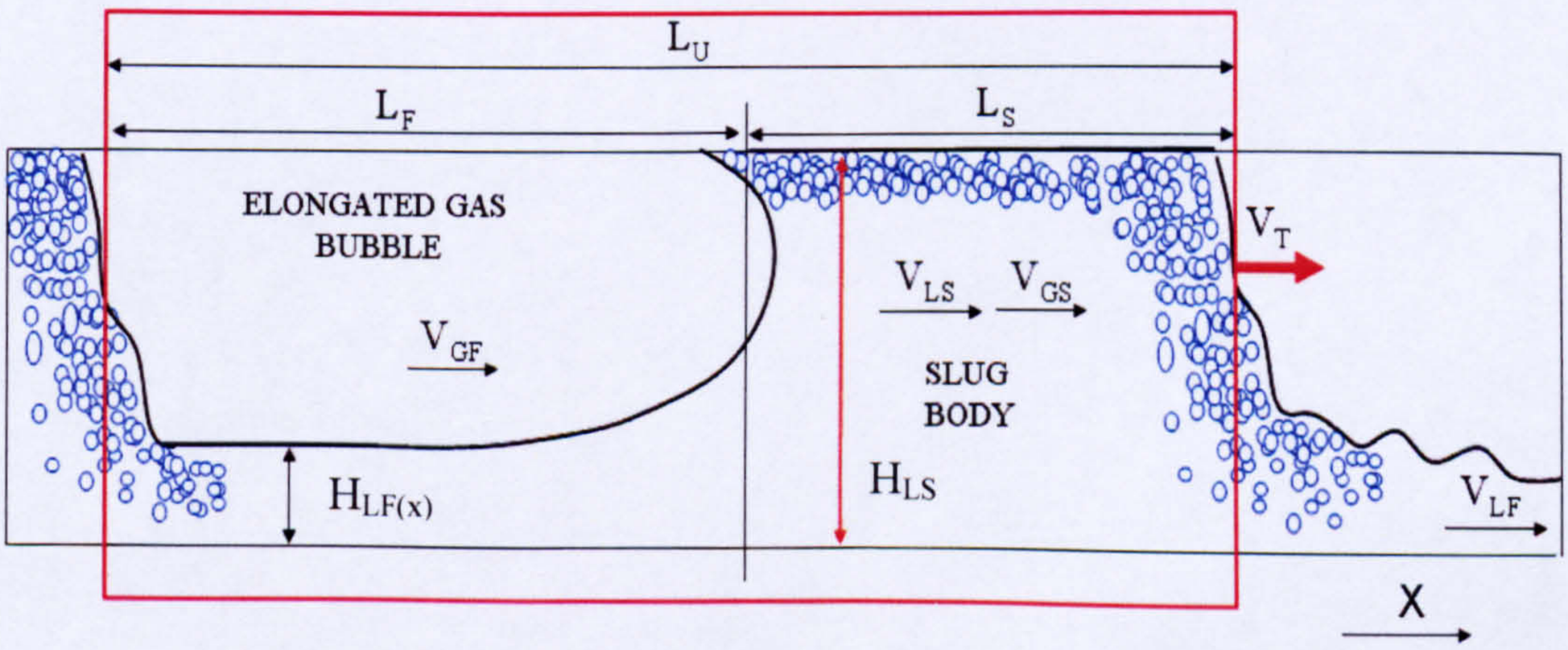

Figure 3-2 : Slug Unit used for the Slug Closure Model

In the present work, to achieve the measurement of the volumetric flowrates of the gas and liquid phases under slug flow conditions, a slug closure model was developed. The slug closure model was derived based on the "slug unit" model concept.

In this model, the superficial velocities for each slug unit are a weighted sum of fluxes from the passing slug and film zones, allowing slip between the gas and liquid in slug body and as given by Dukler and Hubbard (1975) following equations:

$$V_{SL} = \frac{1}{L_U} \int_0^{L_F} E_{LF(x)} V_{LF(x)} \, dx + V_{LS} E_{LS} \frac{L_S}{L_U} \qquad (3.1)$$

$$V_{SG} = \frac{1}{L_U} \int_0^{L_F} (1 - E_{LF(x)}) V_{GF(x)} \, dx + V_{GS} (1 - E_{LS}) \frac{L_S}{L_U} \qquad (3.2)$$

It is obvious from the above equations (3.1) and (3.1), that the superficial velocities for liquid and gas are functions of slug body and film zone characteristics. However, the film zone velocities are difficult to be measured; therefore these equations need simplifications.

In fully developed slug flow the pickup rates and shedding rates for each successive slug unit must be balanced. As a result, the volumetric flowrate balance can be applied across the slug body between boundaries (1) and (2) of the control volume as shown in Figure 3-3, resulting in the extra relations:

$$(V_T - V_{LS}) \times E_{LS} = (V_T - V_{LF}) \times E_{LF} \qquad (3.3)$$

$$(V_T - V_{GS}) \times (1 - E_{LS}) = (V_T - V_{GF}) \times (1 - E_{LF}) \qquad (3.4)$$

From equations (3.3) and (3.4), the liquid film and gas elongated bubble velocities can be obtained as given:

$$V_{LF} \times E_{LF} = V_T \times (E_{LF} - E_{LS}) + V_{LS} \times E_{LS} \qquad (3.5)$$

$$V_{GF} \times (1 - E_{LF}) = V_T \times (E_{LS} - E_{LF}) + V_{GS} \times (1 - E_{LF}) \qquad (3.6)$$

By Substituting equations (3.5) and (3.6) into equations (3.1) and (3.2) respectively, the following equations are obtained:

$$V_{SL} = V_{LS} \times E_{LS} + \frac{L_F}{L_U} \times V_T \times (E_{LF} - E_{LS}) \qquad (3.7)$$

$$V_{SG} = V_{GS} \times (1 - E_{LS}) + \frac{L_F}{L_U} \times V_T \times (E_{LF} - E_{LS}) \qquad (3.8)$$

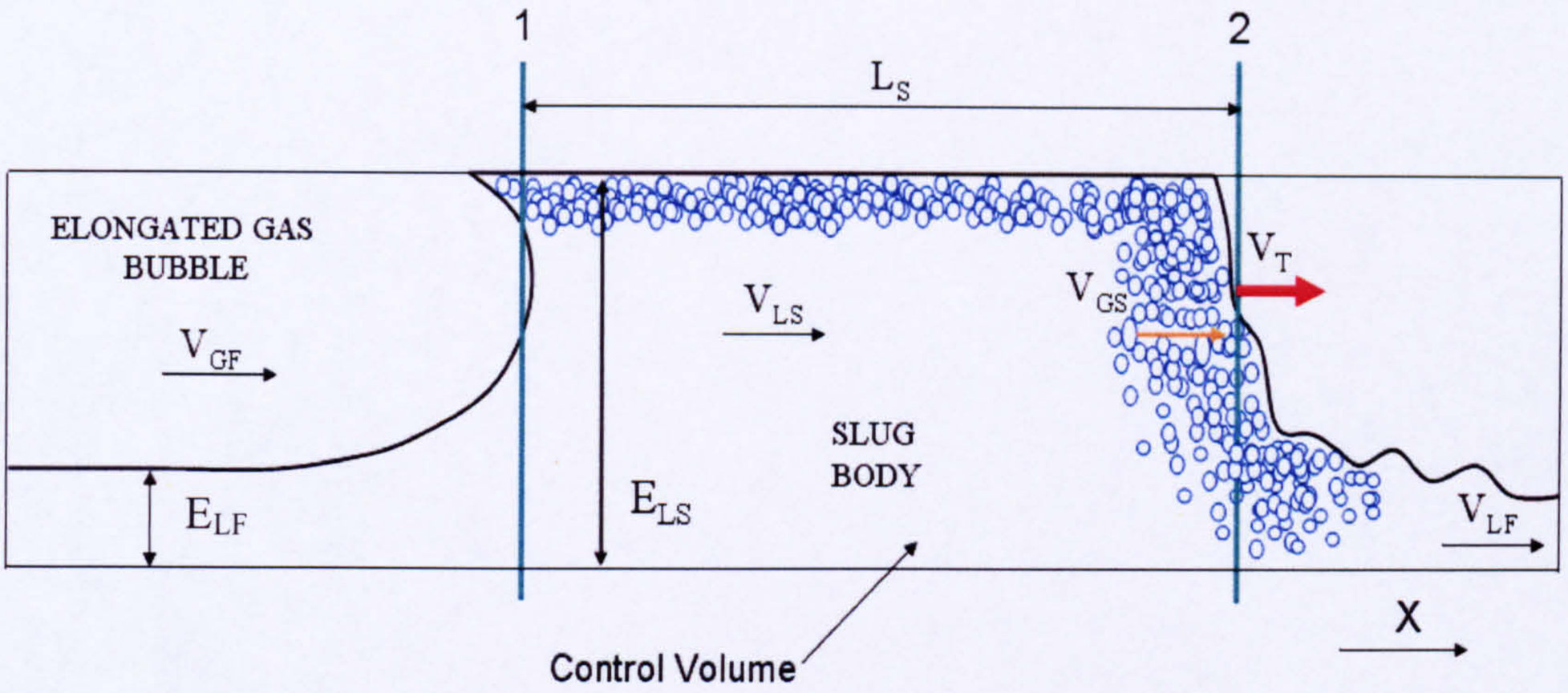

Figure 3-3 : Control Volume used for Mass Balance

The superficial velocities are converted into volumetric flowrates using the following relationships:

$$V_{SL} = \frac{q_L}{A_{Pipe}} \tag{3.9}$$

$$V_{SG} = \frac{q_G}{A_{Pipe}} \tag{3.10}$$

The slug body equations V_{LS} and V_{GS} are given as:

$$V_{LS} = \frac{V_{mix}}{E_{LS} + (1 - E_{LS}) \times s} \tag{3.11}$$

$$V_{GS} = \frac{s \times V_{mix}}{E_{LS} + (1 - E_{LS}) \times s} \tag{3.12}$$

where slip ratio, s, and mixture velocity, $V_{mix,}$ are given by the equation:

$$s = \frac{V_{GS}}{V_{LS}} \quad , \quad V_{mix} = \frac{V_T - V_d}{C_o} \tag{3.13}$$

where the coefficient C_o is explained in detail in the the following 3.4 section

By substituting equations (3.9) to (3.13) in equations (3.7) and (3.8) for liquid and gas phase superficial velocities respectively the following expressions for liquid and gas volumetric flowrates can be obtained (Figure 3-4):

$$q_{L(\text{Closure Model})} = (V_T - V_d) \times A_{pipe} \times K_{1(\text{Liquid})} + V_T \times A_{pipe} \times K_{2(\text{Liquid})} \qquad (3.14)$$

$$q_{G(\text{Closure Model})} = (V_T - V_d) \times A_{pipe} \times K_{3(\text{Gas})} - V_T \times A_{pipe} \times K_{4(\text{Gas})} \qquad (3.15)$$

where :

$$K_{1(\text{Liquid})} = \frac{E_{LS}}{C_o \times [E_{LS} + (1 - E_{LS}) \times s]} \quad \text{and} \quad K_{2(\text{Liquid})} = \frac{(E_{LF} - E_{LS}) \times L_F}{L_U} \qquad (3.16)$$

$$K_{3(\text{Gas})} = \frac{(1 - E_{LS}) \times s}{C_o \times [E_{LS} + (1 - E_{LS}) \times s]} \quad \text{and} \quad K_{4(\text{Gas})} = \frac{(E_{LF} - E_{LS}) \times L_F}{L_U} \qquad (3.17)$$

where coefficients C_o and V_d can be extracted form the experimental data.

Slug Closure Model

Superficial Velocities (Taitel and Barnea, 1990)

$$V_{SL} = \frac{1}{L_U} \int_0^{L_F} E_{LF(x)}\, V_{LF(x)}\, dx + V_{LS}\, E_{LS} \frac{L_S}{L_U}$$

$$V_{SG} = \frac{1}{L_U} \int_0^{L_F} (1 - E_{LF(x)})\, V_{GF(x)}\, dx + V_{GS}\, (1 - E_{LS}) \frac{L_S}{L_U}$$

1

2

Mass Balance across the Slug Body

$$V_{LF} E_{LF} = V_T (E_{LF} - E_{LS}) + V_{LS} E_{LS}$$

$$V_{GF} (1 - E_{LF}) = V_T (E_{LS} - E_{LF}) + V_{GS} (1 - E_{LF})$$

Total Superficial Velocities

$$V_{SL} = V_{LS} \times E_{LS} + \frac{L_F}{L_U} \times V_T \times (E_{LF} - E_{LS})$$

$$V_{SG} = V_{GS}\,(1 - E_{LS}) + \frac{L_F}{L_U}\, V_T (E_{LF} - E_{LS})$$

$$V_{LS} = \frac{V_{mix}}{E_{LS} + (1 - E_{LS})s}$$

$$V_{GS} = \frac{s V_{mix}}{E_{LS} + (1 - E_{LS})s}$$

$$V_{mix} = \frac{V_T - V_d}{C_o}$$

Slug Closure Model Correlations for Liquid/Gas Flowrates

$$q_{L(\text{Closure Model})} = (V_T - V_d) A_{Pipe} K_{1(\text{Liquid})} + V_T\, A_{Pipe} K_{2(\text{Liquid})}$$

$$q_{G(\text{Closure Model})} = (V_T - V_d) A_{Pipe} K_{3(\text{Gas})} - V_T\, A_{Pipe} K_{4(\text{Gas})}$$

Figure 3-4 : Schematic Diagram of Slug Closure Model

3.4 Empirical Correlations for Slug Flow Characteristics

3.4.1.1 Slug Body Velocities

Local liquid slug velocity V_{LS} may be measured indirectly from the pressure drop profile as developed by the theoretical model of Dukler and Hubbard (1975). The pressure drop over the slug unit ΔP_U is given by:

$$\Delta P_U = \Delta P_S + \Delta P_{Film} = (\Delta P_{mix} + \Delta P_f) + \Delta P_{Film} \approx \Delta P_{acc} + \Delta P_f \qquad (3.18)$$

where
ΔP_U is the slug unit pressure drop;
ΔP_S is slug region pressure drop;
ΔP_{Film} is the film region pressure drop
ΔP_{acc} is accelerating pressure drop

In the liquid slug region the overall pressure drop, ΔP_S, is assumed to be composed of a frictional component, ΔP_f, due to the motion of the homogenous mixture, and a component, ΔP_{mix}, resulting purely from accelerating the slow moving liquid film to the slug velocity so that $\Delta P_{mix} = \Delta P_{acc}$. Compared to slug zone, the gas phase pressure drop above the liquid film in the film region is negligible. Based on the assumption of a homogenous mixture within the liquid slug section yields:

$$V_{LS} = V_{GS} = V_{mix} = V_{SL} + V_{SG} \qquad (3.19)$$

To obtain the local slug velocity, V_{LS}, the measurement of frictional pressure drop ΔP_f is required as given by:

$$V_{LS} = \left(\frac{2 \times \Delta P_f \times d}{f \times \rho_{mix} \times L_S} \right)^{1/2} \qquad (3.20)$$

where
d is the pipe inner diameter,
ρ_{mix} is the mixture,
L_S is the slug body length and
f is the friction factor.

However, in order to obtain the local slug body velocities using the pressure drop measurements the following difficulties were discussed by Stewart (2001):

- In order to measure the passing slugs, the pressure transducers require a high measurement precision and a wide measurement range. Differential pressure transducers offer a high precision, but not a wide range. Conversely, absolute pressure transducers offer a wide range, but not high precision.

- Extracting the "ideal" pressure drops ΔP_{mix}, ΔP_f and ΔP_{Film} from the real pressure profile is difficult, particularly as the gas flowrate becomes high (Fan *et al.* 1993b)

As a result, in the absence of any reliable technique for measuring local slug body velocities it is more convenient to use closure relationships. Review of the previous work on the relationship between the slug translational velocity V_T, and the local slug body velocities V_{LS} and V_{GS} is presented in the following subsections

3.4.1.1.1 Dukler and Hubbard (1975) Model

The relationship between the slug translational velocity, V_T, and liquid slug body velocity, V_{LS}, was established by the theoretical model developed by Dukler and Hubbard (1975). In this model, the phases (gas and liquid) in the slug body were assumed to be homogenous mixture ($V_{LS}=V_{GS}$) with a velocity profile identical to single-phase fully developed pipe flow.

According to the Dukler and Hubbard (1975) model, the average velocity of the liquid in the slug is distributed radially from a value of zero at the wall to a value above V_{LS} at the centre. Therefore, in the region close to the wall the fluid moves slower than the average fluid in the slug so that it is eventually shed from the rear of the slug.

However, There is one specific radial location where the local velocity, U, equals the average velocity, V_{LS} and that at radial position as (r_P). If r_p is the radial position at which the local velocity (u) equals the mean velocity (V_{LS}) then the shedding rate is given by:

$$X = V_{LS} \times E_{LS} - E_{LS} \times \int_{r=0}^{r_P} \frac{2 \times \pi \times r \times u(r) dr}{A} \qquad (3.21)$$

where X is the shedding rate, u(r) is a standard single phase velocity profile for turbulent flow, and $u(r_P)=V_{LS}$ defines the boundary of the shedding zone as (1) $r < r_P$, the fluid moves faster than V_{LS}, thus it advances in the direction of flow with respect to the motion of the slug, (2) $r > r_P$ the fluid moves slower than the average fluid in the slug body, thus eventually is shed from the rear of the slug.

Based on the Dukler and Hubbard (1975) model, the translational velocity, V_T must satisfy the following relationship:

$$V_T = V_{LS} + \frac{X}{E_{LS}} = V_{LS} \times (1 + C) \equiv V_{LS} \times C_o \qquad (3.22)$$

where
C is the ratio of the rate of shedding X to the rate of flow in the slug:

$$C = \frac{X}{E_{LS} \times V_{LS}} \tag{3.23}$$

In their analysis, Dukler & Hubbard evaluated a range of conditions and suggested that for $30000 \leq Re_S \leq 400000$, the C-ratio is well approximated by:

$$C = \frac{V_T}{V_{mix}} - 1; \text{ or } C = 0.021 \times \ln(Re_S) + 0.022$$
$$Re_S = \frac{\left[\rho_l \times E_{LS} + \rho_g \times (1 - E_{LS})\right] \times d \times V_{LS}}{\mu_l \times E_{LS} + \mu_g \times (1 - E_{LS})} \tag{3.24}$$

where
Re_S is the slug Reynolds number,
ρ_l is the liquid density,
ρ_g is the gas density,
μ_l is the liquid dynamic viscosity and
μ_g is the gas dynamic viscosity.

Dukler and Hubbard (1975) compared their theoretical model developed against experimental data from a 0.0375 m air-water horizontal pipe. The slug translational velocity, V_T, was measured by using two pairs of electrical contact probes which introduced into the top of the pipe. The values of V_{LS} were measured by removing the end of the tube and allowing the slugs to flow out the end and then undergo a free fall onto a measured surface. The standard deviations associated with these measurements are as follow: V_T=8% and V_{LS}=5%. The agreement between experiment and theory was reported to be excellent.

3.4.1.1.2 Bendiksen (1984)

Bendiksen (1984), performed an experimental investigation of the propagation of air bubbles in slug flow in pipes, with diameters 0.019 m to 0.05 m, and inclinations (φ) ranging from - 30° to 90° with the horizontal. In a specially designed experiment, large bubble were injected into the flowing liquid, and the translational velocity, V_T, was carefully measured at four locations using an array of emitter and detector diodes.

Bendiksen (1984) suggested that there is a critical Froude number (Fr) at which the values of C_o and the drift velocity, V_d, change. As no aeration was presented within the liquid plug body during experiments, liquid superficial velocity, V_{SL}, was equal to the local slug body velocity V_{LS}. This fact allowed data to be fitted by the correlation:

$$V_T = (1 + C) \times V_{LS} + V_d \equiv C_o \times V_{LS} + V_d \tag{3.25}$$

The set of coefficient values (C_o and V_d) summarised by Bendiksen for all positive inclinations with the horizontal (φ) as:

$$\left\{C_o = 1.05 + 0.15 \times \sin^2\varphi \quad V_d = \sqrt{gd} \times (0.35 \times \sin\varphi + 0.54 \times \cos\varphi), \qquad Fr = \frac{V_{LS}}{\sqrt{gd}} < 3.5\right\}$$
$$\left\{C_o = 1.2 \qquad\qquad V_d = \sqrt{gd} \times (0.35 \times \sin\varphi), \qquad\qquad Fr = \frac{V_{LS}}{\sqrt{gd}} > 3.5\right\} \tag{3.26}$$

Based on equation (3.26) the following points were observed by Bendiksen (1984):

1. The coefficient C_o is seen to be a function of pipe geometry, liquid velocity and inclination angle (Figure 3-5). However, Figure 3-6 shows the influence of Reynolds number on the distribution of the coefficient C_o.

2. For low liquid velocities (Fr < 3.5), the slug bubble nose is located close to the top of the pipe. The bubble has a clearly defined tail and behaves like a Benjamin bubble, yielding the coefficient C_o tends to unity. The fluid pickup and shedding process in the slug body cease to operate; therefore, V_T tends to equal V_{LS}.

3. For horizontal flows at low liquid velocities, Bendiksen (1984) observed a dimensionless non-zero drift-velocity of around $V_d = 0.54(gd)^{1/2}$. However, as the liquid velocity increased (Fr >3.5), the tip of the bubble nose moves down towards the centre of the pipe, yielding a value of $C_o \approx 1.2$. As a result, the gravity forces become lower, resulting in a reduced value of V_d, approaching zero.

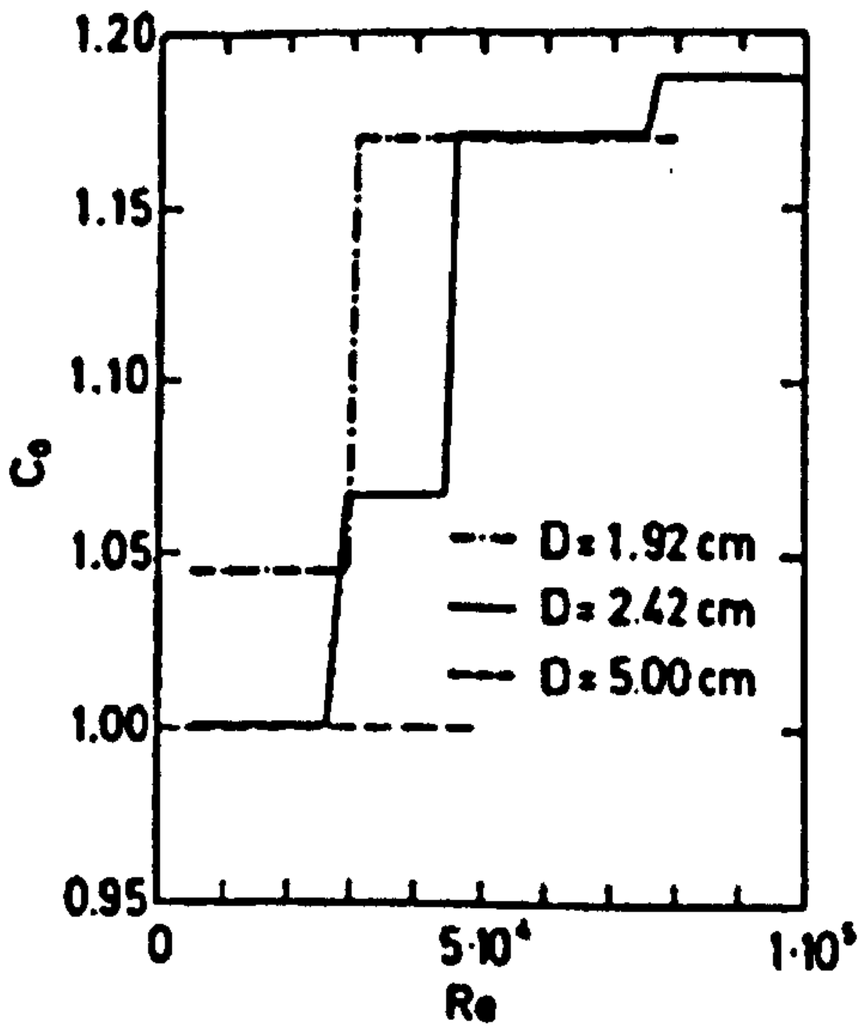

Figure 3-5 : The Coefficient C_o vs Reynolds Number for Different Pipe Diameters (φ=0)

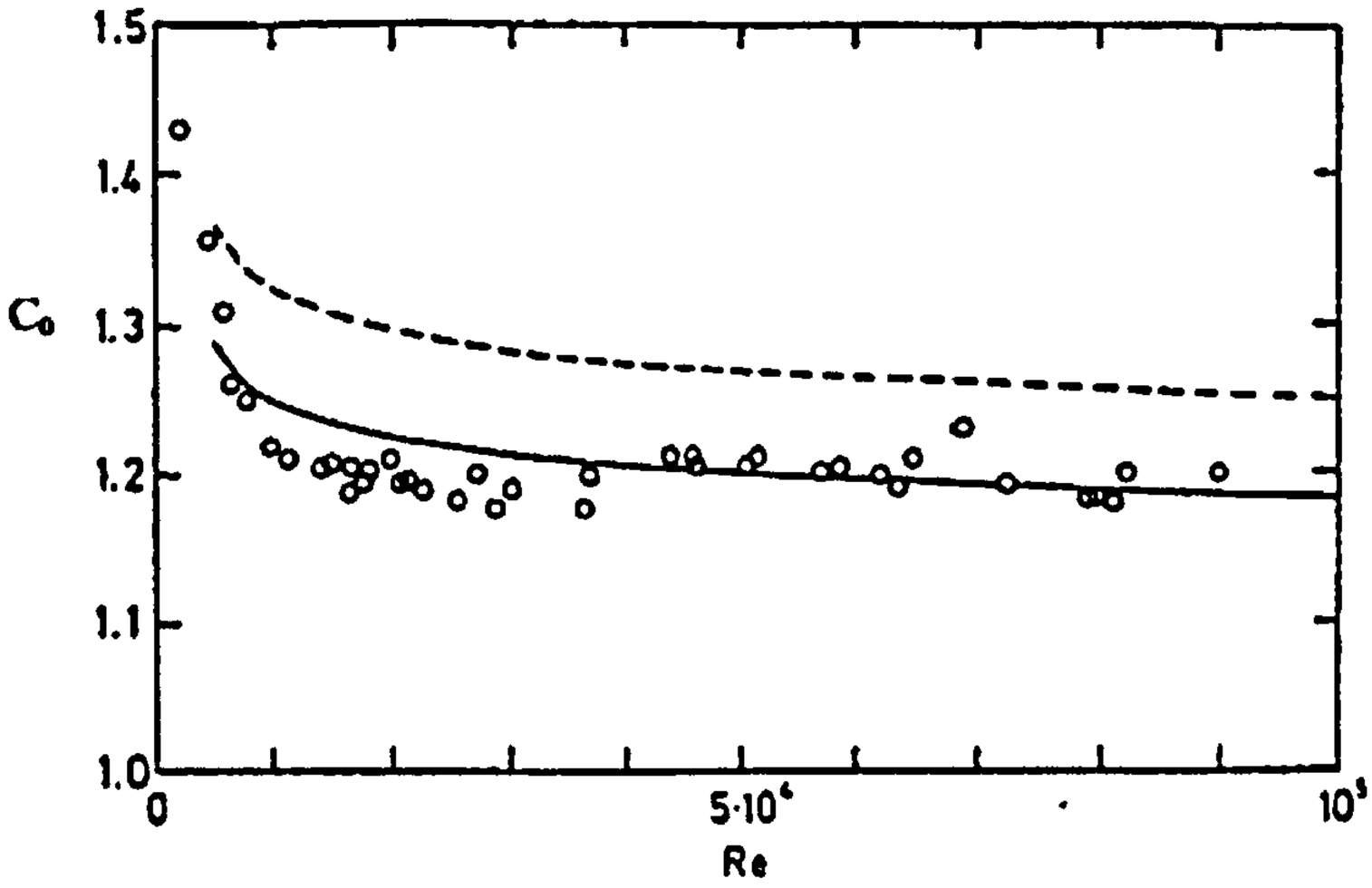

Figure 3-6 : Influence of Reynolds Number on the Distribution of C_o

An approach to modelling transient slug flow was presented by Bendiksen *et al.* (1996). In this model further investigations were performed to study the motion of the gas elongated bubble and the gas and liquid velocities V_{GS}, V_{LS} respectively in the slug body. Starting from a total volume flow balance in the slug gives:

$$V_{SG} + V_{SL} = V_{LS} \times E_{LS} + V_{GS} \times (1 - E_{LS}) \qquad (3.27)$$

Davies (1992) and Manolis (1995) conducted experiments to study the translational velocity of the slug for the case of an unaerated liquid slug. In their experiments, gas was injected at a predetermined rate into one end of a pipe which was initially full of liquid. The translation velocity V_T, was measured using electrical conductivity probes spaced a known distance apart. Manolis (1995) correlated these data and obtained an expression in the same form as that of Bendiksen (1984):

$$\begin{cases} C_o = 1.033 & V_d = 0.477 \times \sqrt{gd}, & Fr = \dfrac{V_{LS}}{\sqrt{gd}} < 2.86 \end{cases}$$
$$\begin{cases} C_o = 1.216 & V_d = 0, & Fr = \dfrac{V_{LS}}{\sqrt{gd}} \geq 2.86 \end{cases} \qquad (3.28)$$

3.4.1.1.3 Woods and Hanratty (1996)

Bendiksen *et al.* (1984) conducted experimental studies on the bubble motion measurements were extended by Woods and Hanratty (1996) to superficial velocities in the range of V_{SL}= 0.5 to 2 ms^{-1} and V_{SG}=0.2 to10 ms^{-1} for horizontal gas-water flow in a 0.0953 m pipe at atmospheric condition.

Conductance profiles were used to determine the liquid holdup at several locations along the pipeline. These conductance measurements establish the profiles of the liquid layer and the tail of the slug and the degree of aeration in a slug. By using a translating control volume attached to the back of the slug, conservation of liquid volume is used to calculate shedding flux velocity (X/A_{pipe}), given as:

$$\frac{X}{A_{pipe}} = \left(V_T - \frac{V_{mix}}{1+(s-1)\times E_{LS}} \right) \times (1-E_{LS}) \qquad (3.29)$$

where
s is the slip parameter and is equal to the ratio of the slug body velocities (V_{GS}/V_{LS}).

The slip parameter s is obtained by achieving the measurements of V_T and E_{LS} combined with an approximate estimate for the shedding flux velocity (X/A_{pipe}). The slip ratio data summarised as following:

$$s = \begin{bmatrix} 1 & V_{mix} < 3\,ms^{-1} \\ 1+0.125\times(V_{mix}-3) & 3 < V_{mix} < 7\,ms^{-1} \\ 1.5 & V_{mix} > 7\,ms^{-1} \end{bmatrix} \qquad (3.30)$$

The slip ratio s is increased from unity at low V_{mix} (homogenous flow) to 1.5 for $V_{mix}>7ms^{-1}$ (blow-through).

The coefficient C_o and drift velocity V_d concluded as following:

$$\begin{Bmatrix} C_o = 1.10 & V_d = 0.54\times\sqrt{gd} & Fr = \frac{V_{mix}}{\sqrt{gd}} < 3.5 \end{Bmatrix}$$
$$\begin{Bmatrix} C_o = 1.2 & V_d = 0 & Fr = \frac{V_{mix}}{\sqrt{gd}} > 3.5 \end{Bmatrix} \qquad (3.31)$$

The parameters C_o and V_d are in close agreement with the horizontal flow data of (Bendiksen *et al.* 1984).

3.4.1.1.4 Stewart (2001)

Stewart (2001) developed a correlation for the motion of the elongated gas bubble based on a linear fit to experimental data extracted from 0.1 m horizontal pipeline, given by the following equation:

$$V_T = 1.29\times V_{mix} + V_d \qquad (3.32)$$

where
C_o=1.29 and
V_d=1.09 (ms^{-1}).

Stewart (2001) implemented this correlation in the predictive model developed for the measurement of mass flowrates of gas-water slug flow using non-intrusive conductivity sensors, and to calculate the local slug body velocities V_{LS} and V_{GS} for liquid and gas respectively as a function of mixture velocity V_{mix} and slip ratio (s) from the basic mass balance across the slug unit as given by the following equations:

$$V_{GS} = \frac{s \times V_{mix}}{E_{LS} + s \times (1 - E_{LS})} \quad \text{and} \quad V_{LS} = \frac{V_{mix}}{E_{LS} + s \times (1 - E_{LS})}$$

$$s = \frac{V_{GS}}{V_{LS}} \;, s = \begin{cases} 1 & V_{mix} < 3 ms^{-1} \\ 1 + 0.125 \times (V_{mix} - 3) & 3 < V_{mix} < 7 ms^{-1} \\ 1.5 & V_{mix} > 7 ms^{-1} \end{cases} \tag{3.33}$$

3.4.1.1.5 King et al. (1997)

King *et al.* (1997) compared the experimental data for different researchers (Davies, 1992; Manolis, 1995; Dukler and Hubbard (1975); Ruder *et al.* (1989); Bendiksen, 1984) as shown in Figure 3-7. He concluded that, the relationships proposed by Dukler and Hubbard (1975) do not fit the experimental data at all well.

The model by Ruder *et al.* (1989) shows a good agreement with the data at low value of the Froude number but significantly underpredicts the C_o at higher mixture velocity.

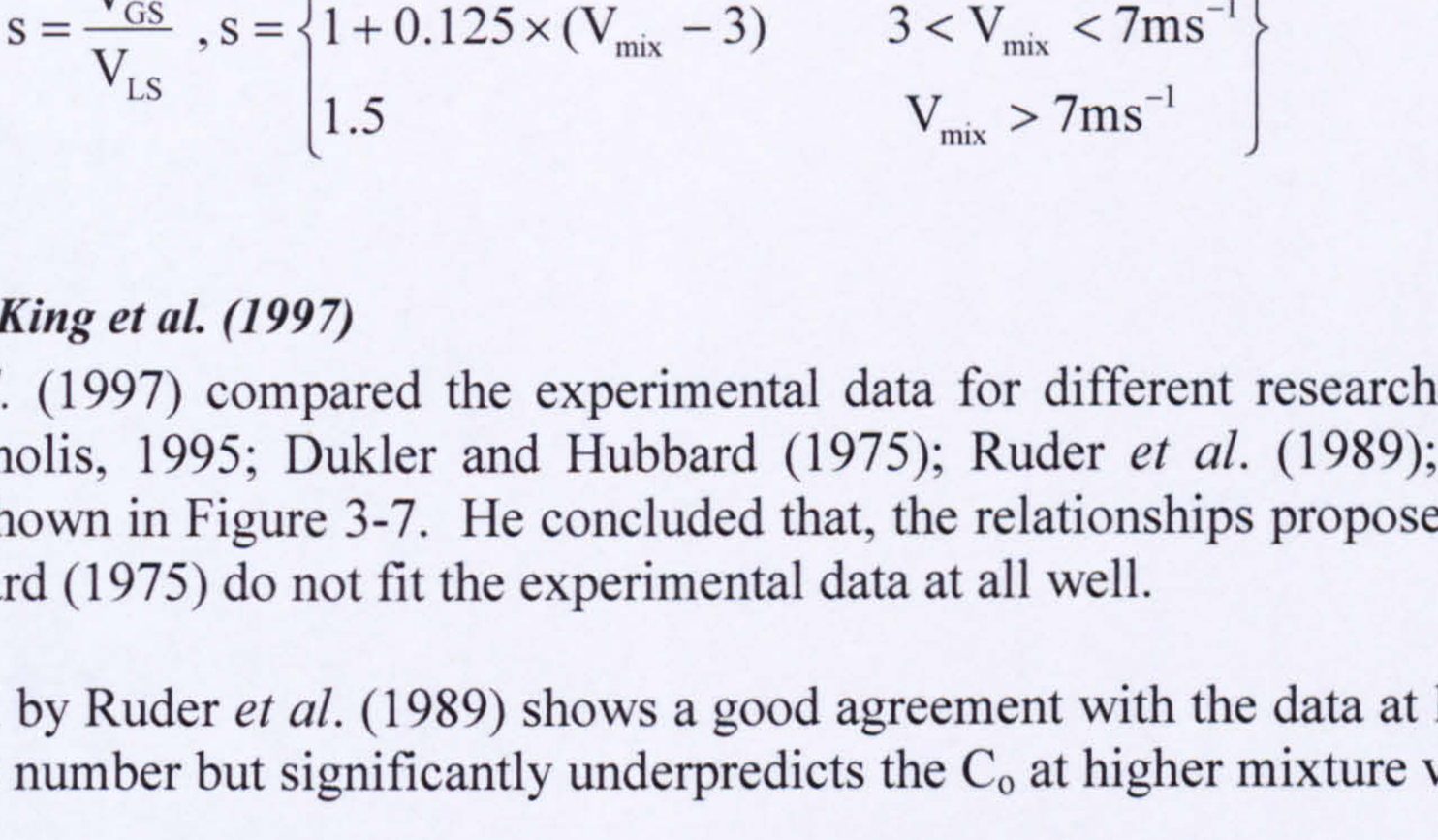

Figure 3-7: Performance of C-ratio Correlations by King *et al.* (1997)

3.4.1.1.6 Hale (2000)

Based on different previous investigators, Hale (2000) stated that the large spread values of both C_o (0.95 to 1.54) and V_d (0 to 0.6) for horizontal flow is less clear. And this may be partly due to the fact that the plot of translational velocity (V_T) versus mixture velocity (V_{mix}) is not perfectly linear, but instead bends very slightly upwards.

Table 3-1 listed the values of the coefficients C_o and C_1 which was calculated based on a line of best fit to their experimental data, however, Table 3-2 listed the values of the coefficients C_o and C_1 based on theoretical and analytical studies.

Table 3-1 : Values of C_o and the mean drift velocity C_1 for horizontal flow (Adopting best fit to data approach).

Reference	System	C_o (Re> 8000)	$C_1=V_d/(gd)^{1/2}$
Manolis (1995)	Air-Water d = 0.075 m, Slug Flow	1.033 Fr < 2.86	0.477 Fr < 2.86
Manolis (1995)	Air-Water d = 0.075 m, Slug Flow	1.216 Fr > 2.86	0.0 Fr >2.86
Lunde and Asheim (1989)	Air-Water d = 0.0678 m	1.107	0.260
Singh and Griffith (1970)	Air-Water d = 0.05-0.15 inch Pressure = 1atm	0.95	0.15

Table 3-2 : Values of C_o and the mean drift velocity C_1 for horizontal flow.

Reference	C_o (Re> 8000)	$C_1=V_d/(gd)^{1/2}$
Gregory and Scott (1969)	1.35	0.0 (Assumed)
Dukler and Hubbard (1975)	1.25-1.28 (theory) (30000 < Re < 400000)	0.0 (Assumed)
Andreussi *et al.* (1989)	1.2	0.0 (Assumed)
Nicholson *et al.*, (1978)	1.196 (d=0.0258 m) 1.128 (d=0.0512 m)	0.538 (d=0.0258 m) 0.396 (0.0512m)
Nydal *et al.*, (1992)	1.2-1.3	0.0
Bendiksen (1984)	1.0-1.05 (Fr < 3.5) 1.2 (Fr > 3.5)	0.54 (Fr < 3.5) 0.0 (Fr > 3.5)

3.4.1.2 Others Correlations

3.4.1.2.1 Slug Body Liquid Holdup

The liquid holdup in the slug body is an important parameter for the design of multiphase pipelines and associated separation equipment. It is also of importance for the slug predictive model in order to measure the phase mass flowrates. Few theoretical methods are available for the prediction of the average liquid holdup (E_{LS}) within the slug body. However, the extensively-used correlation by Gregory *et al.* (1978) was obtained from the measurements of liquid holdup, using electrical capacitance probes, in air-water and oil-water flow in horizontal pipes with diameter of 0.0258 m and 0.0512 m. The correlation gives slug body holdup as a function of the mixture velocity only:

$$E_{LS} = \frac{1}{1 + \left(\frac{V_{mix}}{\alpha_{1G}} \right)^{\alpha_{2G}}} \tag{3.34}$$

where
$\alpha_{1G} = 8.66$ and
$\alpha_{2G}=1.39$.

Based on the same data (Malnes, 1979) proposed an alternative form of correlation, given by:

$$E_{LS} = 1 - \frac{V_{mix}}{C_M + V_{mix}} \tag{3.35}$$

where the coefficient C_M is a function of physical properties given by:

$$C_M = 83 \times \left(\frac{g \times \sigma}{\rho_L} \right)^{1/4} \tag{3.36}$$

Ferschneider (1983) developed a more complex correlation for slug body holdup E_{LS} using data obtained from natural gas and a light hydrocarbon oil facility. The facility loop comprised a 0.15 m diameter with 120 m long test section loop and operated at elevated pressure of between 10 and 50 bar. Correlation proposed by Ferschneider (1983) took account for surface tension of the fluids:

$$E_{LS} = \frac{1}{\left\{1+\left[\left(\frac{V_{mix}}{\sqrt{\left(1-\rho_g/\rho_l\right)gd}}\right)\times\left(\frac{Bo^{\alpha_{2F}}}{\alpha_{1F}}\right)\right]^2\right\}^2} \qquad (3.37)$$

where
α_{1F}=25 and
α_{2F} =0.1
Bo is Bond number and is given by:

$$Bo = \frac{(\rho_l - \rho_g)\times g\times d^2}{\sigma} \qquad (3.38)$$

Andreussi *et al.* (1989) developed correlation based on the experimental data obtained from air-water flow in 0.05m and 0.09 m horizontal pipes with different pipe inclinations. The correlation is given by the expressions:

$$\begin{aligned} &\{E_{LS} = 1 && V_{mix} < 2.5ms^{-1}\} \\ &\{E_{LS} = 1.242 - 0.263\times\ln(V_{mix}) && V_{mix} \geq 2.5ms^{-1}\} \end{aligned} \qquad (3.39)$$

Ghassan and Majeed (1999) developed a new empirical equation for estimating liquid slug holdup in horizontal and slightly inclined two-phase slug flow. The empirical correlation was developed as a function of mixture velocity, liquid viscosity and inclination angle and is given as:

$$E_{LS} = (1.009 - N\times V_{mix})\times A\,;\, N = 0.006 + 1.3377\times\frac{\mu_g}{\mu_l} \qquad (3.40)$$

In this correlation the parameter A is included to account for the effect of inclination angle. The following equations are suggested for estimating the parameter A:

$$\begin{aligned} &\varphi \leq 0 \quad \text{(downward flows)} && A = 1.0 \\ &\varphi > 0 \quad \text{(upward flows)} && A = 1.0 - \sin\varphi \end{aligned} \qquad (3.41)$$

3.4.1.2.2 Slug Frequency

Slug frequency, ν, is defined as the average number of slug units passing a fixed point in the system, per unit time Gregory *et al.* (1978). Many authors have reported slug frequency data and many correlations have been proposed. Several of these are given below:

Based on measured values for the carbon dioxide-water system in a 0.019 m diameter pipe, Gregory *et al.* (1978) suggest that the slug frequency may be given by:

$$\nu = 0.0226 \times \left[\frac{V_{SL}}{g \times d} \times \left(\frac{19.75}{V_{mix}} + V_{mix} \right) \right]^{1.2} \qquad (3.42)$$

Using a similar approach to Gregory and Scott (1969), Manolis (1995) performed experiments for both air-water and air-oil data at various system pressure. Their correlation based on modified Froude number and the slug frequency correlation proposed given as:

$$\nu = 0.0037 \times \left[\frac{V_{SL}}{g \times d} . \frac{25 + V_{mix}^{\ 2}}{V_{mix}} \right]^{1.8} \qquad (3.43)$$

3.4.1.2.3 Slug Body Length

The mean slug length has been discussed by many researchers based on both experimental studies by Brill *et al.* (1981) and Nydal *et al.* (1992) and theoretical models by Dukler and Hubbard (1975) and Barnea and Taitel (1993) as listed in Table 3-3. In Table3-3, the slug boy length obtained experimental and theoretical by different researchers ranged from 12d to 30d. Although a large statistical variation around the mean value of the slug zone length, L_S, exists. However, the observed experimental mean slug length values are independent of gas and liquid flow rates and range between 12-30 times the diameters for slug flow.

Table 3-3 : Mean Slug Lengths in Horizontal Pipe.

Reference	System	Mean Slug Length
Dukler and Hubbard (1975)	Air-water d = 0.075 m	12d – 30d
Nicholsen *et al.* (1978)	Air-light oil d = 0.026 m, 0.05 m	30d
Gregory *et al.* (1978)	Air-light oil d = 0.026 m, 0.05 m	30d and 37d
Barnea *et al.* (1993)	Theory	32d
Andreussi *et al.* (1989)	Air-water d = 0.05 m	22d

Brill *et al.* (1981) developed a correlation to predict liquid slug length for larger diameter pipes, based on their data from 305 mm and 406 mm diameter test lines and on data from 102 mm and 178 mm diameters pipes and is given by:

$$\ln(3.2808\times L_S) = -2.663 + 5.441\times\left[\ln(39.37d)\right]^{0.5} + 0.059\times\ln(3.2808V_{mix}) \quad (3.44)$$

In large pipes diameter pipes, Scott *et al.* (1986) proposed the following correlation to calculate slug length:

$$\ln(3.2808\times L_S) = -25.4134 + 28.4948\times\left[\ln(39.37\times d)\right]^{0.1} \quad (3.45)$$

Nydal *et al.* (1992) used horizontal pipes (0.053 m and 0.090 m) to measure the length of the slug. The range of the liquid and gas superficial velocities was 0.6 to 3.5 ms^{-1} and 0.5 to 20 ms^{-1} respectively. They came up with an equation after distinguishing between the developing and developed slug and neglecting the former one:

$$L_S \approx 15\times d \quad (3.46)$$

3.5 Ultrasonic Metering Concept Approach

The ultrasonic metering concept approach for the measurement of the phase volumetric flowrates of the gas-water under slug flow conditions was based on the slug closure model developed in the previous section and summarised schematically in the Figure3-8 and given in the following equations:

$$q_{L(\text{Closure Model})} = (V_T - V_d)\times A_{pipe}\times K_{1(\text{Liquid})} + V_T\times A_{pipe}\times K_{2(\text{Liquid})} \quad (3.47)$$

$$q_{G(\text{Closure Model})} = (V_T - V_d)\times A_{pipe}\times K_{3(\text{Gas})} - V_T\times A_{pipe}\times K_{4(\text{Gas})} \quad (3.48)$$

In order to obtain the gas and liquid phase volumetric flowrates, the slug closure model factors $K_{1\ (\text{Liquid})}$, $K_{2\ (\text{Liquid})}$, $K_{3\ (\text{Gas})}$ and $K_{4\ (\text{Gas})}$ must be calculated after measuring the following parameters by non-invasive or non-intrusive ultrasonic methods

- The slug body holdup E_{LS} and the liquid film holdup E_{LF} can be obtained after measuring the liquid height in the slug body H_{LS} and film zone H_{LF} then using the following equation:

$$E_{LS} = \frac{1}{\pi}\times\left(\pi - \cos^{-1}\left[2\times\left(\frac{H_{LS}}{d}\right)-1\right] + \left[2\times\left(\frac{H_{LS}}{d}\right)-1\right]\times\sqrt{1-\left[2\times\left(\frac{H_{LS}}{d}\right)-1\right]^2}\right) \quad (3.49)$$

$$E_{LF} = \frac{1}{\pi}\left(\pi - \cos^{-1}\left[2\left(\frac{H_{LF}}{d}\right)-1\right] + \left[2\times\left(\frac{H_{LF}}{d}\right)-1\right]\times\sqrt{1-\left[2\times\left(\frac{H_{LF}}{d}\right)-1\right]^2}\right) \qquad (3.50)$$

- Slug translational velocity V_T can be measured using cross correlation technique for the conditioning ultrasonic signals;

- The film zone and slug zone duration, t_{Film} and t_{Slug} ;

- The film length L_F and slug length L_S obtained from the following equations after measuring V_T , t_{Film} and t_{Slug} :

$$L_S = V_T \times t_{Slug} \quad \text{and} \quad L_F = V_T \times t_{Film} \qquad (3.51)$$

- The assumption of no slip in the slug model (homogenous mixture flow) is adopted to the slug closure model.

- Compute the coefficient C_o and V_o based on a linear fit to mixture velocity V_{mix} versus the slug translational velocity V_T experimental data and given by the equation:

$$V_T = mV_{mix} + n \qquad (3.52)$$

where :
m is representing C_o and
n is representing the drift velocity V_d

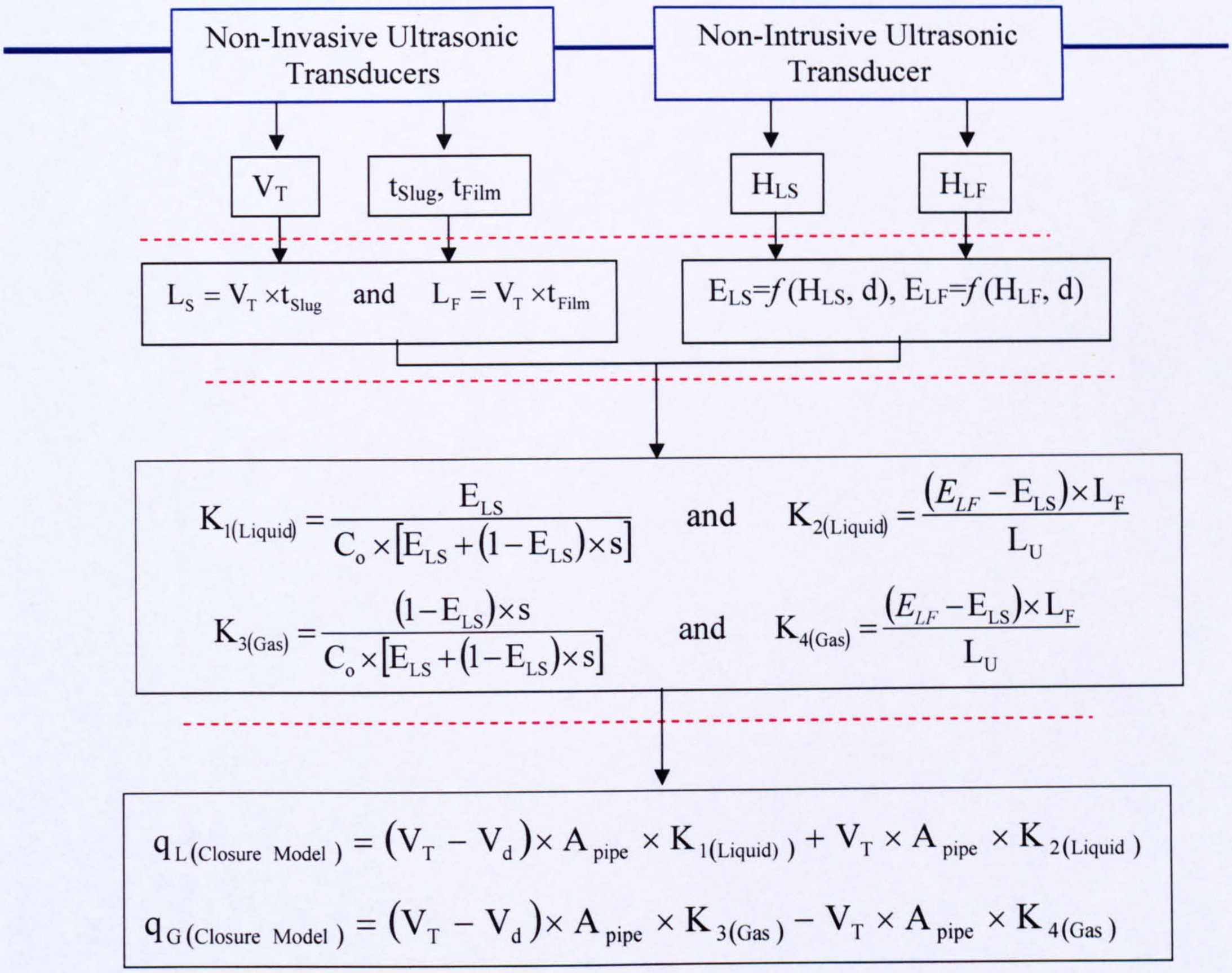

Figure 3-8: Schematic Diagram for the Ultrasonic Metering Concept

3.6 Summary

The process initiation and development of slug flow in horizontal pipe were described. Review of empirical correlations for slug flow characteristics was presented. The review included correlations for the slug body velocities, slug translational velocity, the mean slug frequency, the mean slug body holdup, and the mean slug length.

Slug closure model to infer the gas and liquid phase volumetric flowrates was developed based on the "slug unit" model. Ultrasonic metering concept was developed based on the combinations of the non-invasive and non-intrusive ultrasonic sensors and the slug closure model to obtain the phase volumetric flowrates.

Chapter 4

Experimental Set-up

A two-phase (water and air) facility for testing the ultrasonic metering concept presented in previous chapters was designed and constructed in the Department of Process and Systems Engineering, Cranfield University.

In section 4.1.1, the fluid supplies (water and air) and the measuring instrumentations are described. The measuring section is presented in details in section 4.1.2. This section includes the design aspects of the conductivity probes and their calibration process, the non-invasive ultrasonic technique and its signal conditioning unit, and the non-intrusive ultrasonic (pulse-echo) technique and its associated electronic circuit.

The experimental measurement methods used to determine the slug characteristics are presented in section 4.1.3.

Section 4.1.4 presents the data acquisition system (DAS) which is used to collect the data from the two-phase facility. Finally, the chapter summary is presented in section 4.2.

4.1 The Two-Phase Facility

The two-phase (water and air) facility was designed and constructed in the Department of Process and Systems Engineering, Cranfield University as illustrated in Figure 4-1. The test section is a 22 m long plastic ABS (class E) horizontal pipe of 50 mm inner diameter. The pipeline length was enough to allow the formation of fully developed slugs.

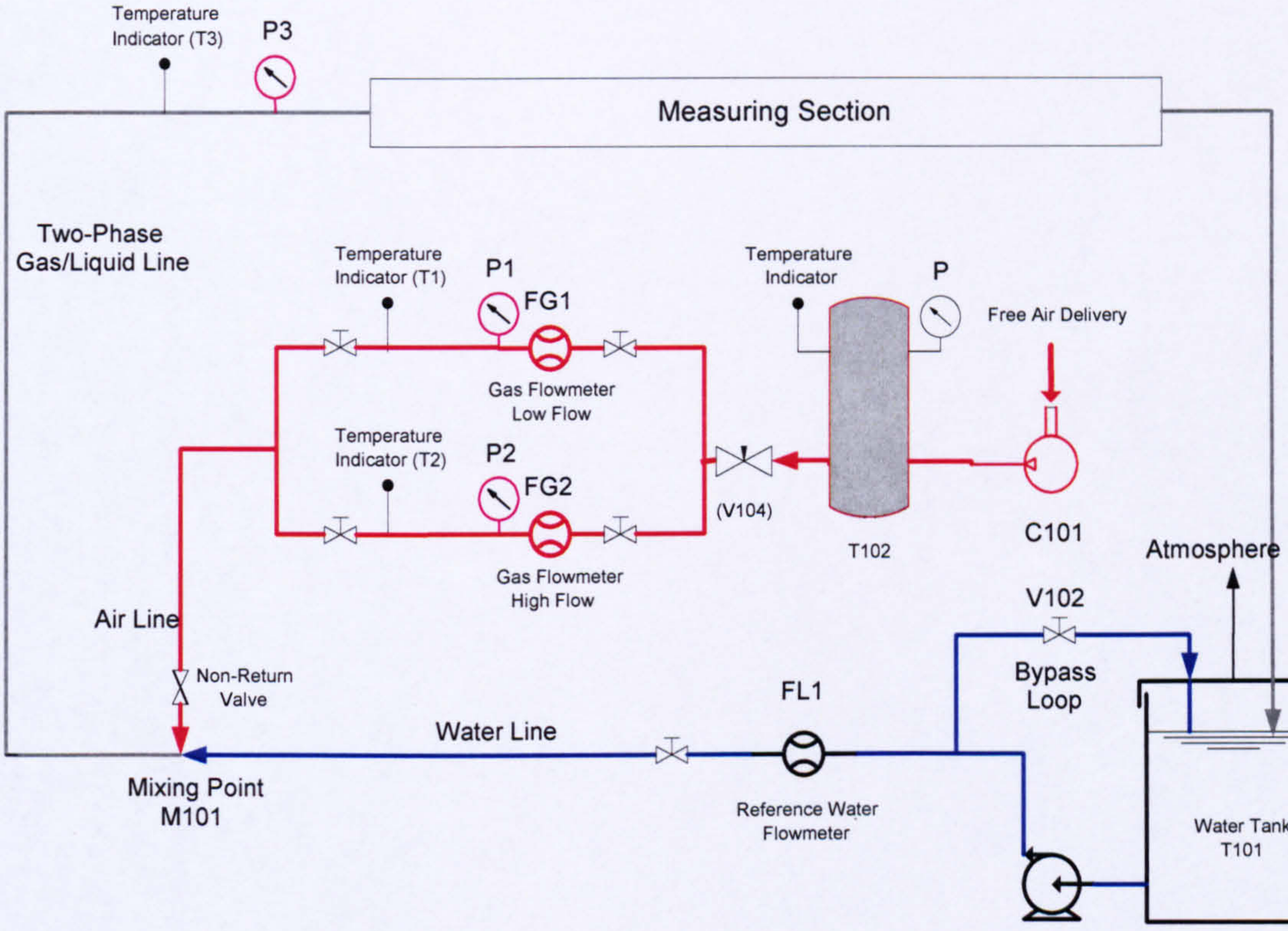

Figure 4-1: Two-Phase (water and air) Facility

4.1.1 Fluid Supplies

4.1.1.1 Water Supply

Water is stored in a tank T101 of 4.408 m^3 capacity, Figure 4-2(a). The water is pumped to the test section using a centrifugal pump. The water pump (P101) is a Worthington Simpson centrifugal pump, which has a maximum capacity of 40 m^3/hr and a maximum discharge pressure of 5 bar(g). The water flow from the pump is controlled by means of a by-pass line in which a portion of the fluid from the pump outlet is recycled back to the water tank via a valve V102. The water passes through the metering system and then it is taken to the mixing point M101, where it is combined with the gas flow before passed to the measuring section.

4.1.1.2 Air Supply

Gas is supplied by a Screw Engineering compressor C101, Figure 4-2(b). This compressor has a maximum supply capacity of 400 m^3/ hr Free Air Delivery (FAD) and a maximum discharge pressure of 10 bar (g). From the compressor outlet, the gas is passed to a 2.5 m^3 air tank receiver, T102. The arrangement of the air tank receiver before the test section stabilises the gas supply from the compressor. From the receiver, air flow goes to the gas metering station via a needle valve, V104. This valve controls the flow to the metering station, maintaining a constant mass flow for a given receiver pressure, and further acts to stabilise the flow entering the test section. From the gas metering station, the gas passes to the mixing point M101, where it combines with the water flow and enters the measuring section (Figure 4-1).

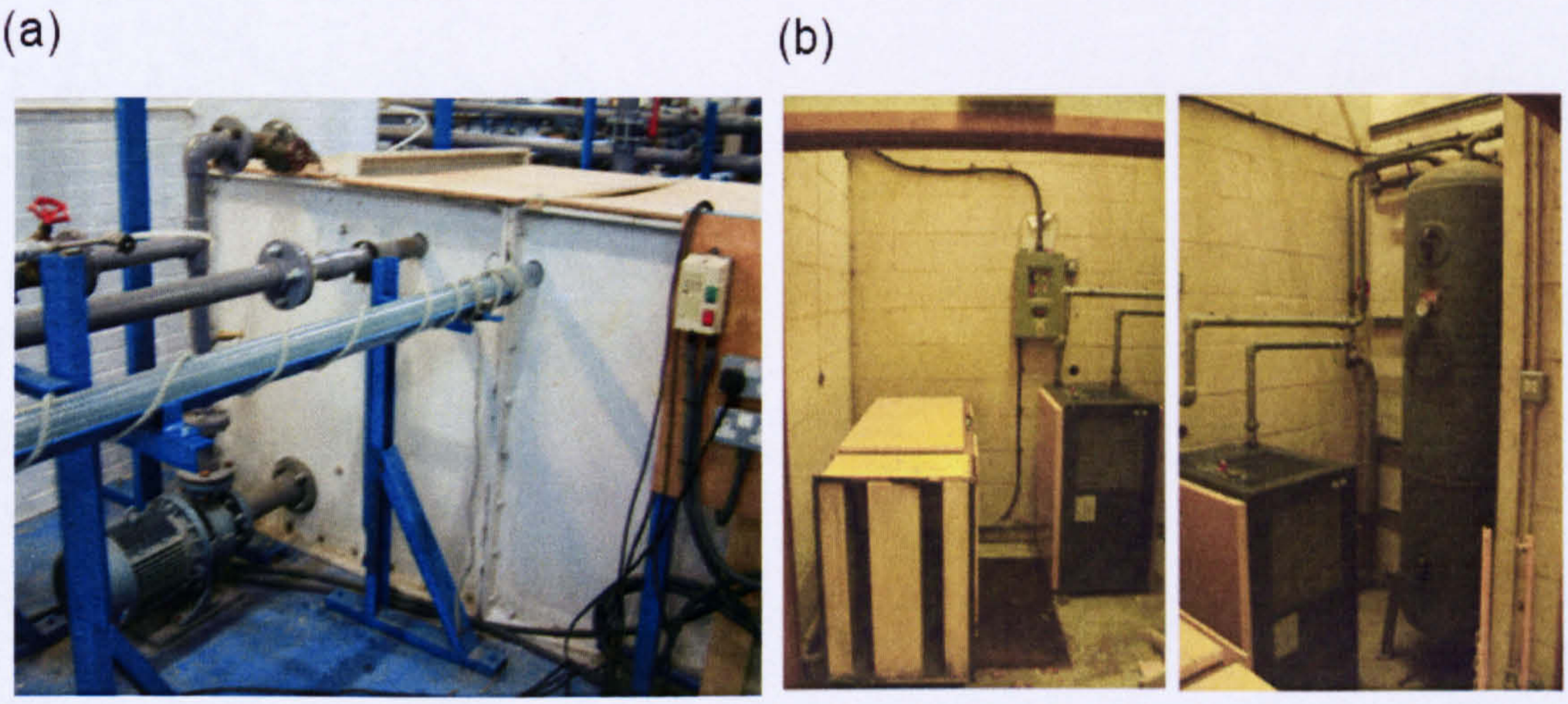

Figure 4-2: (a) Water Supply Tank, (b) Air Supply Station

4.1.1.3 Fluids Instrumentation

Details of the instrumentation for the two-phase air\water facility fluid metering systems are provided in Table 4-1.

The water flow is metered using Khrone Altoflux Series electromagnetic K280/0 AS model with 0 - 4.524 m^3/hr range as shown in Figure 4-3(a). Air flow is metered using a pair of Quadrina gas turbine flowmeters, see Figure 4-3(b), the first, designation QFG/13B/EP1, has a range of 1-8 m^3/hr and second, designation QFG/25B/EP1 has a range of 6-60 m^3/hr. At the gas metering point, temperature and pressure are measured to calculate the volumetric flowrate of the gas entering to the test section. All data from the two-phase water/air facility instrumentation is recorded by the Data Acquisition System (DAS) see Section 4.14.

Table 4-1: Two-Phase Water-Air Facility Fluids Instrumentation

Designation	Description	Details	Range
FL_1	Inlet Liquid Flowmeter (Reference meter)	Khrone Altoflux Elecotromagnetic Flowmeter Model K280/0 AS	0-4.524 m^3/hr
FG_1	Inlet Gas Flowmeter (Low Flow)	Quadrina Turbine Meter, Model QFG/13B/EP1	1-8 m^3/hr
FG_2	Inlet Gas Flowmeter (High Flow)	Quadrina Turbine Meter, Model QFG/25B/EP1	6-60 m^3/hr
P_1	FG1 Reference Pressure Sensor	Pressure Gauge Transducer RS 286-671	0-5 bar(g)
P_2	FG2 Reference Pressure Sensor	Pressure Gauge Transducer RS 286-671	0-5 bar(g)
P_3	In-Line Pressure Sensor	Gauge Style RS 286-671	0-5 bar(g)
T_1	FG1 Reference Temperature Sensor	RS Thermocouple	0-100 ° C
T_2	FG2 Reference Temperature Sensor	RS Thermocouple	0-100 ° C
T_3	In-Line Temperature Sensor	RS Thermocouple	0-100 ° C

(a)

(b)

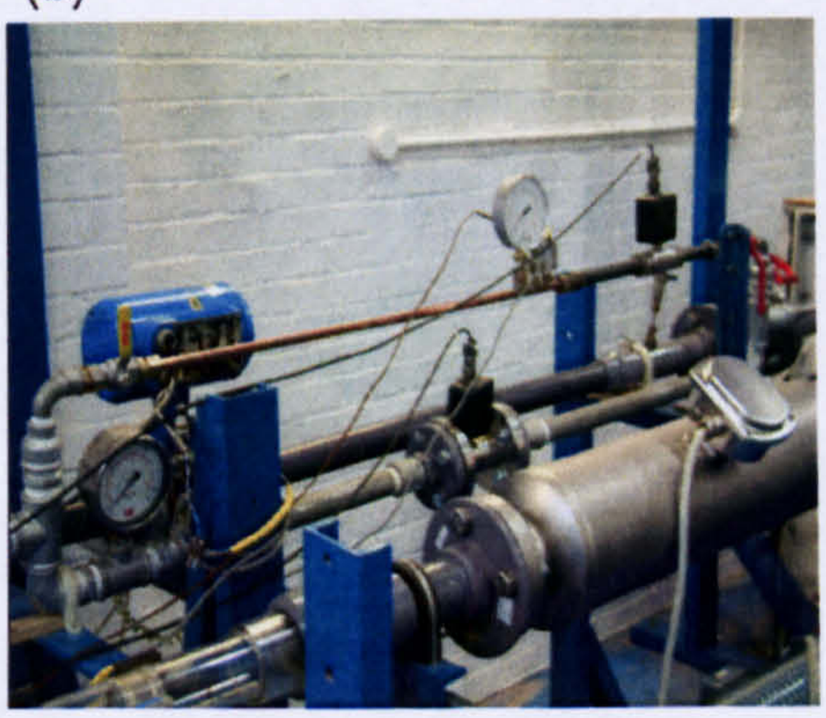

(a) Water Electromagnetic Flowmeter (b) Air Metering Station

Figure 4-3: Air and Water Metering Stations

4.1.2 Measuring Test Section

The measuring working section is 0.875 m long Perspex pipe of 50 mm inner diameter. The measuring working section consists of four pairs of flush-mounted "O" ring conductivity probes ($C_{(A)}$, $C_{(B)}$, $C_{(C)}$ and $C_{(D)}$) , two pairs of 1 MHz non-invasive mounted ultrasonic transducers and non-intrusive pulse-echo mode level measurement ultrasonic transducer with 2.25 MHz operating frequency, see Figures 4-4 and 4-5 respectively. The measuring section and its instrumentations are illustrated in Figure 4-6.

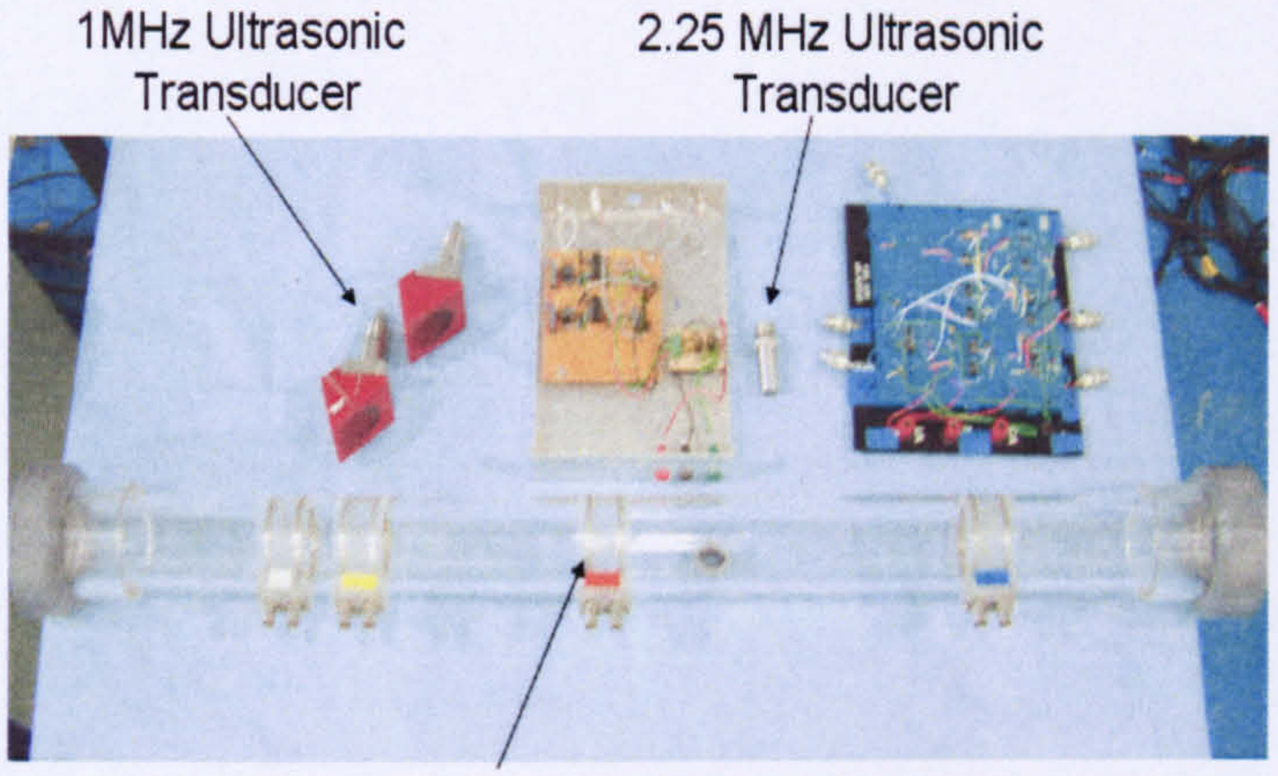

Figure 4-4: Components of Measuring Section

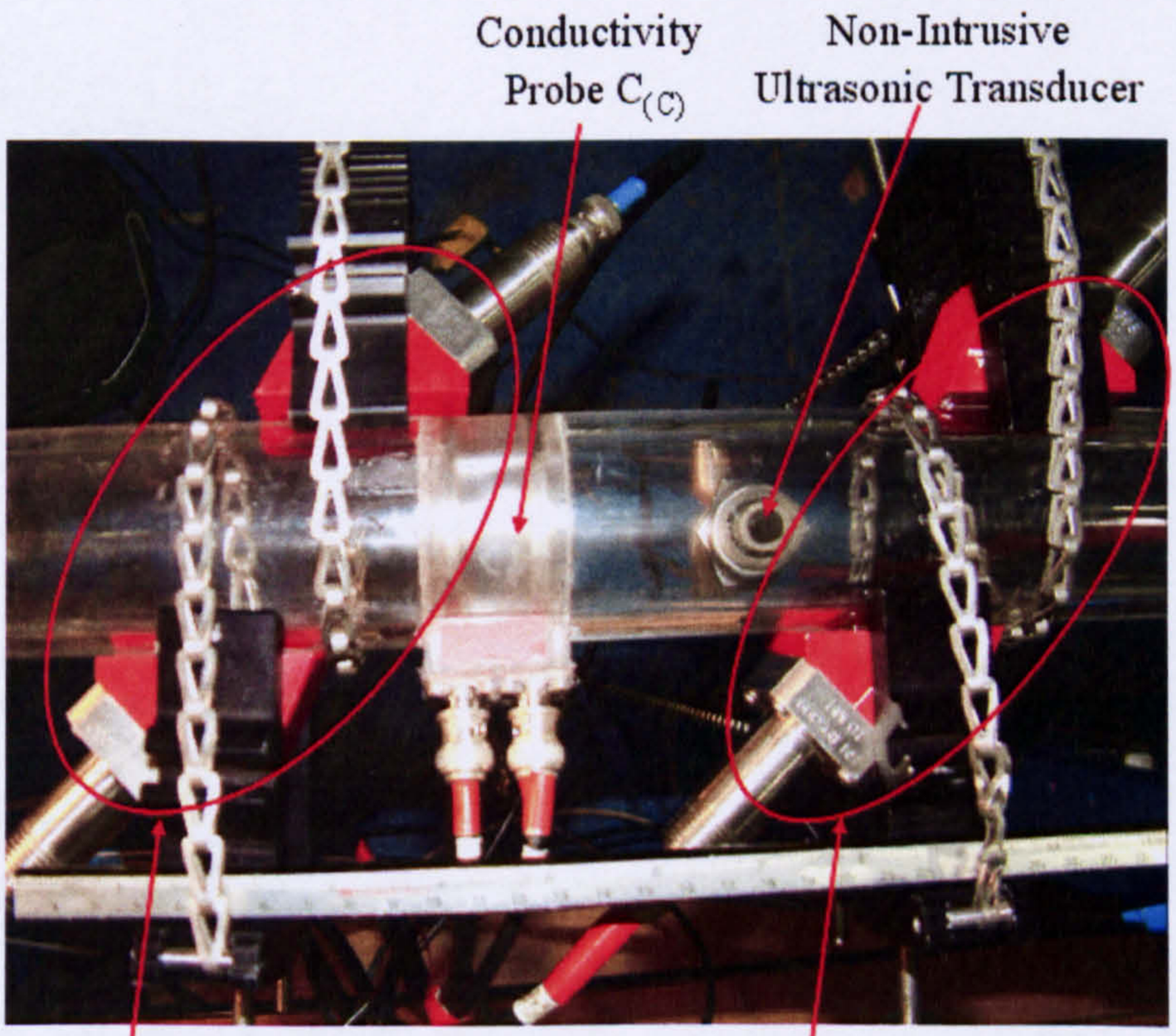

Figure 4-5: Top View of Measuring Section Showing the Ultrasonic Sensors

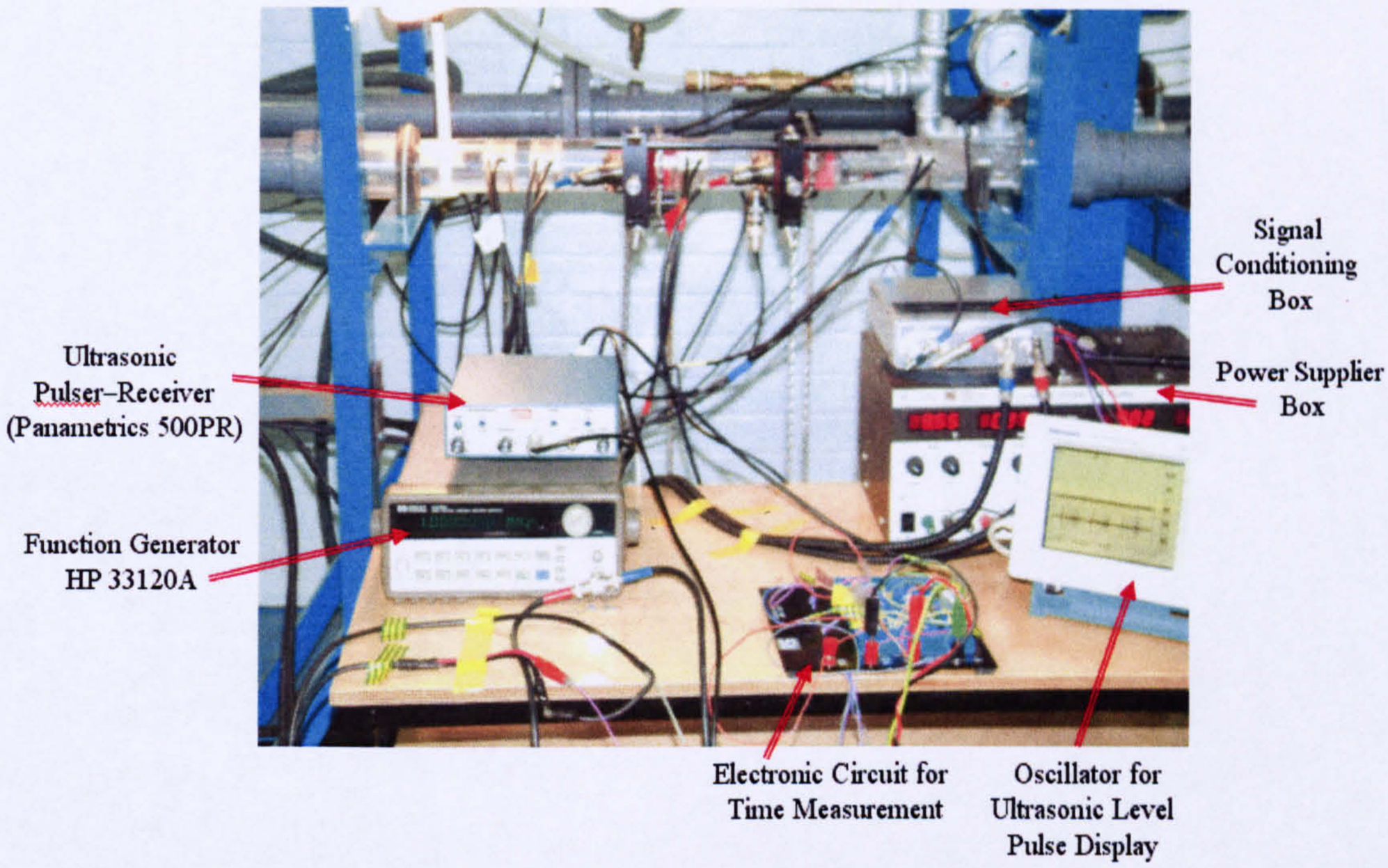

Figure 4-6: Test Section and Instrumentations

4.1.2.1 Conductivity Probes

Conductivity probes provide a continuous measure of liquid holdup and with some statistical analysis; they can be used to determine the slug characteristics (Fossa *et al.* 2003). The probes discussed here are of twin-ring electrodes type . They consist of two stainless steel rings electrodes with a width of (S_p=3.7 mm) and spaced at (D_e=17 mm) apart as shown in Figure 4-7.

An electronic circuit is used to measure the electrical impedance between the electrodes. Probes based on this technique have been used by Coney *et al.* (1971), Brown *et al.* (1978), Andristsos *et al.* (1987), Fore (1993) and Fossa *et al.* (2003). Such probes can be operated either in the conductance (lower AC frequency) or in capacitance (very high AC frequency) mode.

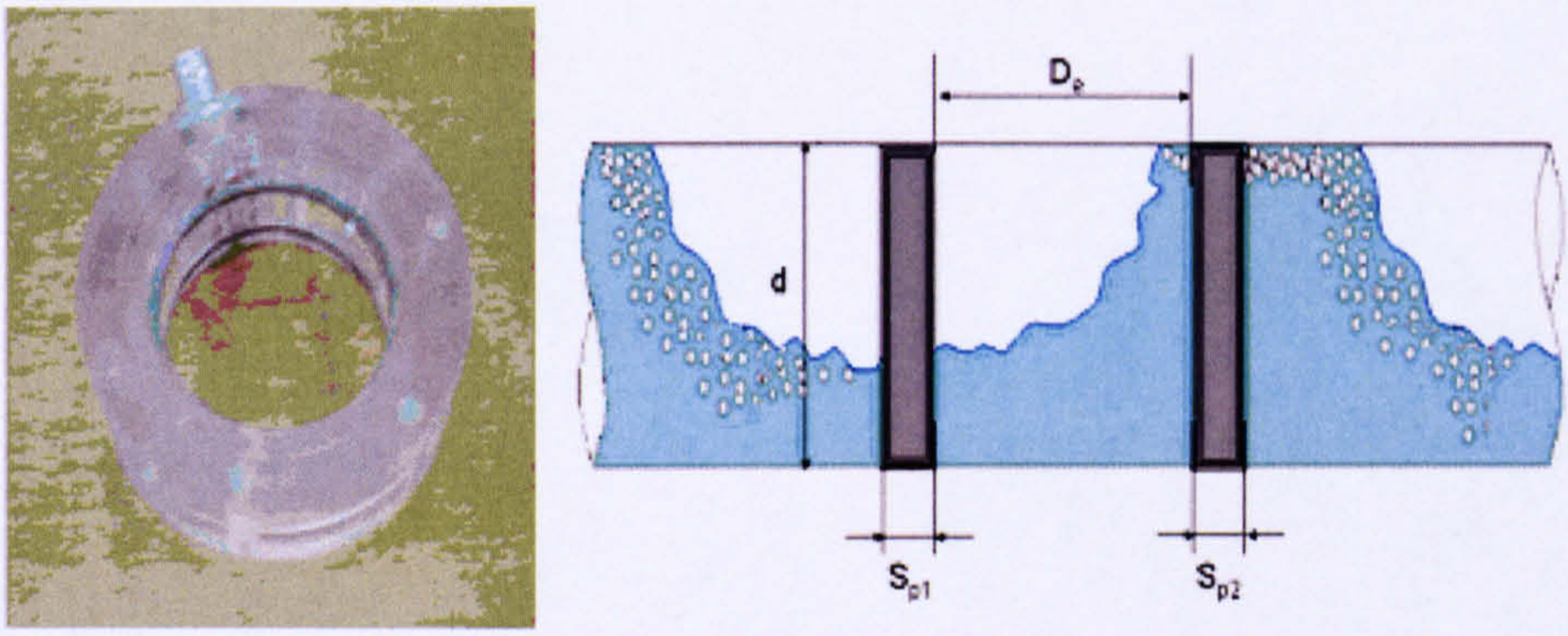

Figure 4-7: Scheme of Flush Mounted Stainless Steel Conductivity Ring Electrodes

4.1.2.1.1 Design & Construction Aspect of Conductivity Probe

In order to perform the measurements of the phase fraction under slug flow conditions using conductivity probes, the slug flow regime was assumed to be constituted of stratified regions separated by liquid regions where dispersed bubble may be present (Fossa *et al*. 2000).

Fossa *et al*. (2003) stated, based on theoretical and experimental investigations, that the conductivity probe response is affected by the probe geometry and even more by the flow pattern. As a consequence, at the same mean void fraction, the mixture impedance changes with the phase distribution. Therefore, in order to overcome this problem, the conductivity probe geometry was chosen to produce a probe response that is relatively insensitive to the changes between the uniformly dispersed (bubble) regime and the stratified regime.

Based on preliminary tests, Fossa *et al*. (2003) suggested that the probe geometry aspect ratios (D_e/d) and (S_p/d) should be equal to 0.34~0.4 and 0.071~0.08 respectively. The selection of the proper electrode aspect ratios also resulted in small measuring volumes as compared with holdup spatial fluctuations.

The assumption adopted concerns the possibility to describe the structure of intermittent horizontal flows as if they were constituted of stratified regions separated by liquid regions where a few gas bubbles might be present.

In the present work, the conductivity probes geometry aspect ratios (D_e/d=0.34) and (S_p/d=0.074) were chosen based on the design recommendations by Fossa *et al*. (1998).

These probes were joined together using "Tensol 12" cement. The probes were distributed along the Perspex pipe with separation distance L_{AB} = 54 mm, L_{BC} = 175 mm, L_{CD} = 275 mm and L_{AD}=504 mm respectively, see Figure 4-8.

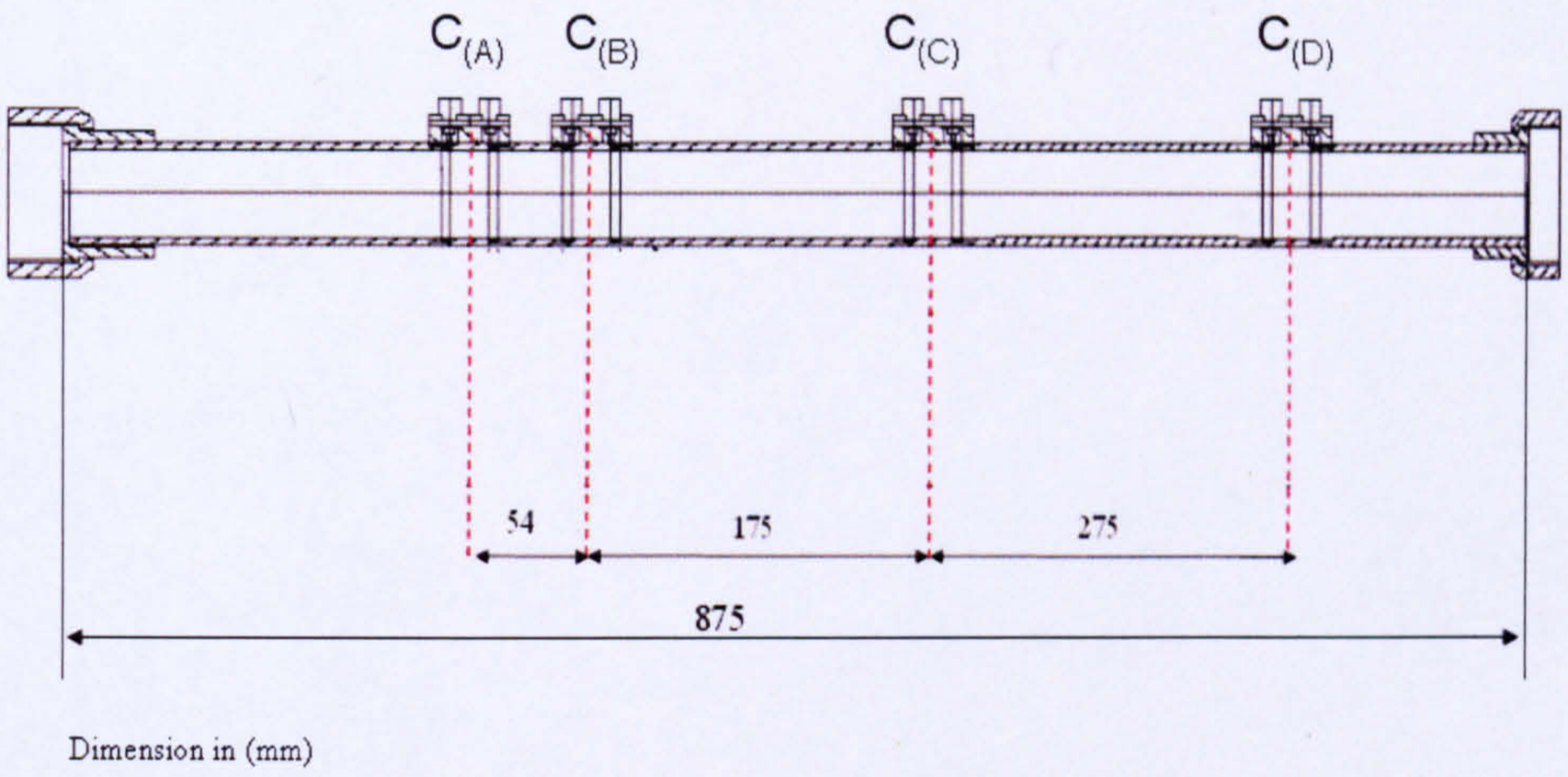

Figure 4-8: Measuring Section with the Distribution of Conductivity Probes

The design of the electronic circuit for each probe was based on the classical scheme design by Fossa *et al* (2003) with the carrier frequency of 3 kHz, 5 kHz, 7 kHz and 13 kHz for conductivity probes $C_{(A)}$, $C_{(B)}$, $C_{(C)}$ and $C_{(D)}$ respectively.

4.1.2.1.2 Calibration of Conductivity Probes

The aim of the calibration was to characterise a set of rings probes $C_{(A)}$, $C_{(B)}$, $C_{(C)}$ and $C_{(D)}$ for film height measurement during intermittent flow. The calibration of the probes was performed by connecting the electrode pairs to the Conductivity Electronic Box device. The device supplies 3 kHz, 5 kHz, 7 kHz, and 13 kHz of a.c. carrier signal.

The gas-liquid phase distribution has been achieved by introducing known liquid volumes into the horizontal positioned test pipes. Tap water was used and great care was taken to check the inclination of the pipe at each measurement.

A total of 4 probes were calibrated. Their aspect ratios are $D_e/d=0.34$, $S_p/d=0.074$ and d is equal to 0.05 m. For each probe, 48 measurements were performed in order to cover the liquid fraction range 0~1.

At each measurement, both the weight of the water exclusive the weight of the conductivity ring and the corresponding value in volt was recorded. As a result, a calibration curve for each probe was obtained as shown in Figure 4-9.

The correlated liquid holdup as a function of the normalised output voltage with 1 when the pipe is full and 0 when the pipe is empty for conductivity probes $C_{(A)}$, $C_{(B)}$, $C_{(C)}$ and $C_{(D)}$ are given as following:

$$E_{L(A)} = -1.2713 \times (G^*)^4 + 1.2518 \times (G^*)^3 + 0.4108 \times (G^*)^2 + 0.6007 \times (G^*) \qquad (4.1)$$

$$E_{L(B)} = -1.4613 \times (G^*)^4 + 1.9962 \times (G^*)^3 - 0.3178 \times (G^*)^2 + 0.7763 \times (G^*) \quad (4.2)$$

$$E_{L(C)} = -1.1236 \times (G^*)^4 + 1.086 \times (G^*)^3 + 0.4182 \times (G^*)^2 + 0.6069 \times (G^*) \quad (4.3)$$

$$E_{L(D)} = -1.4267 \times (G^*)^4 + 1.4225 \times (G^*)^3 + 0.499 \times (G^*)^2 + 0.4984 \times (G^*) \quad (4.4)$$

The relationship between the normalised output voltage (G*) and the liquid holdup and gas void fraction shown in Figure 4-9. As expected, the conductivity decreases with the gas phase fraction while it increases as the liquid phase fraction in the control volume increases.

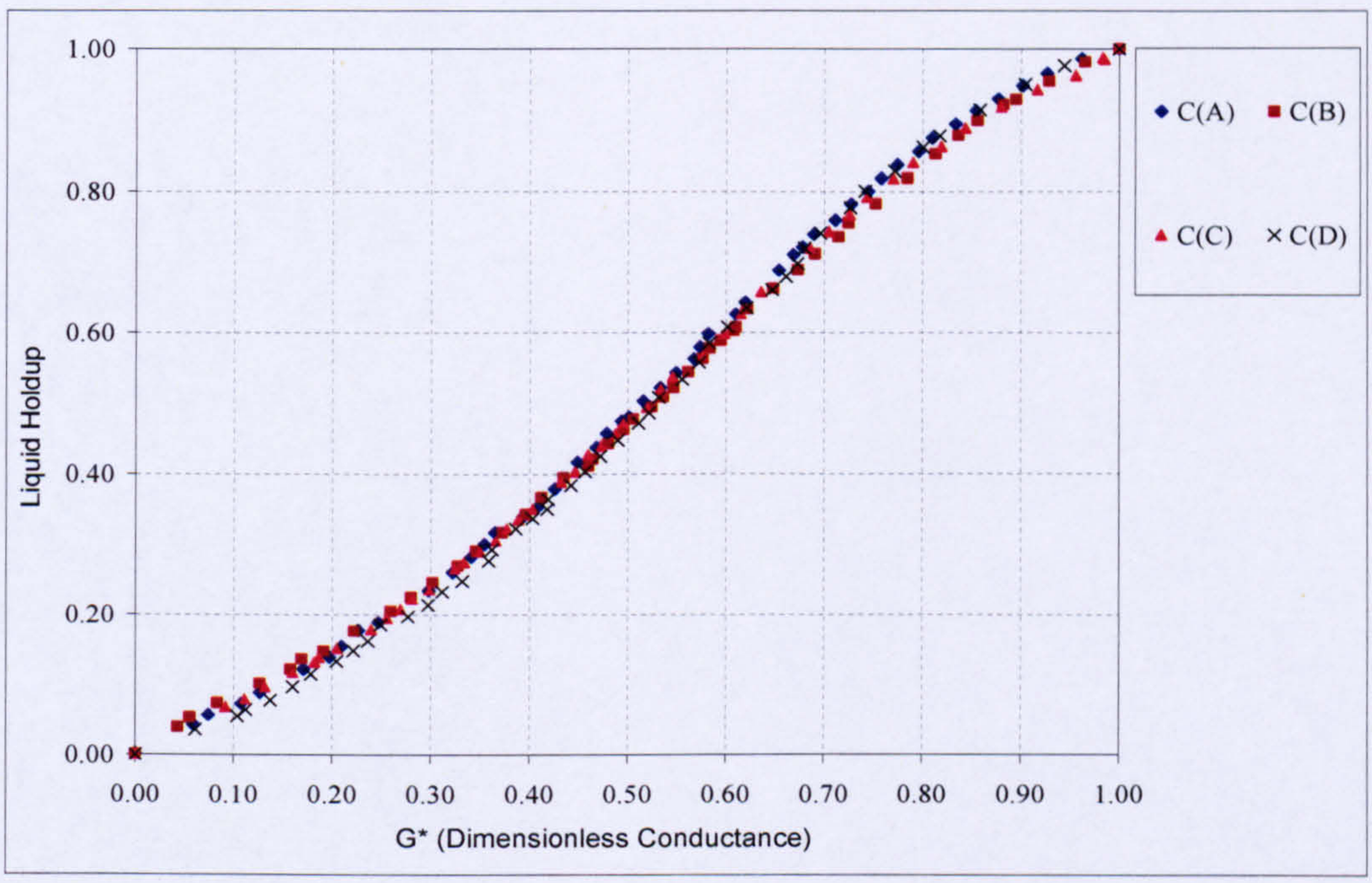

Figure 4-9: Calibration of Conductivity Ring Probes (A, B, C and D)

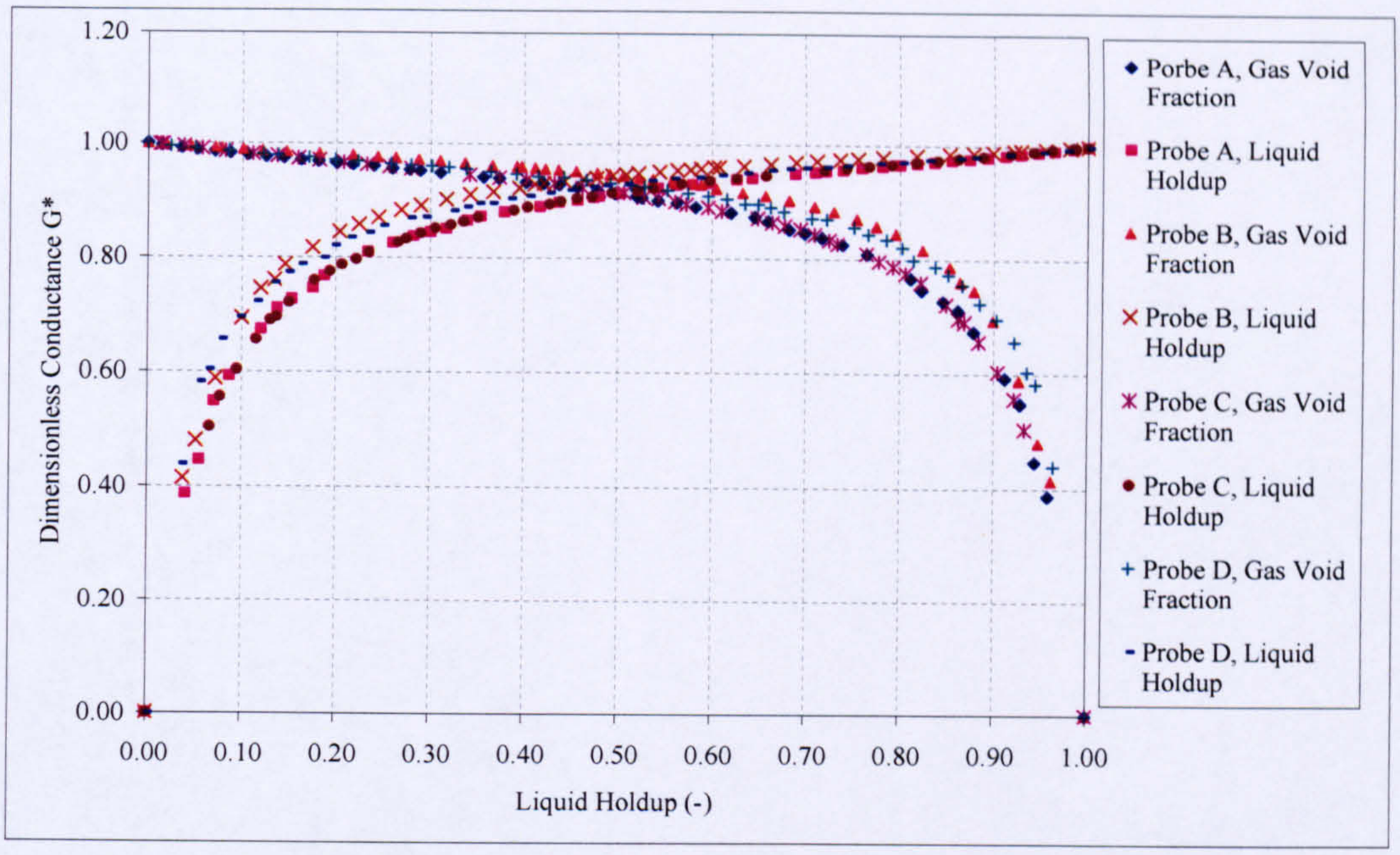

Figure 4-10: Phase Fraction vs. Normalised Voltage Output

A sample trace collected from the conductivity probes $C_{(C)}$ and $C_{(D)}$ under slug flow conditions is presented in Figure 4-11.

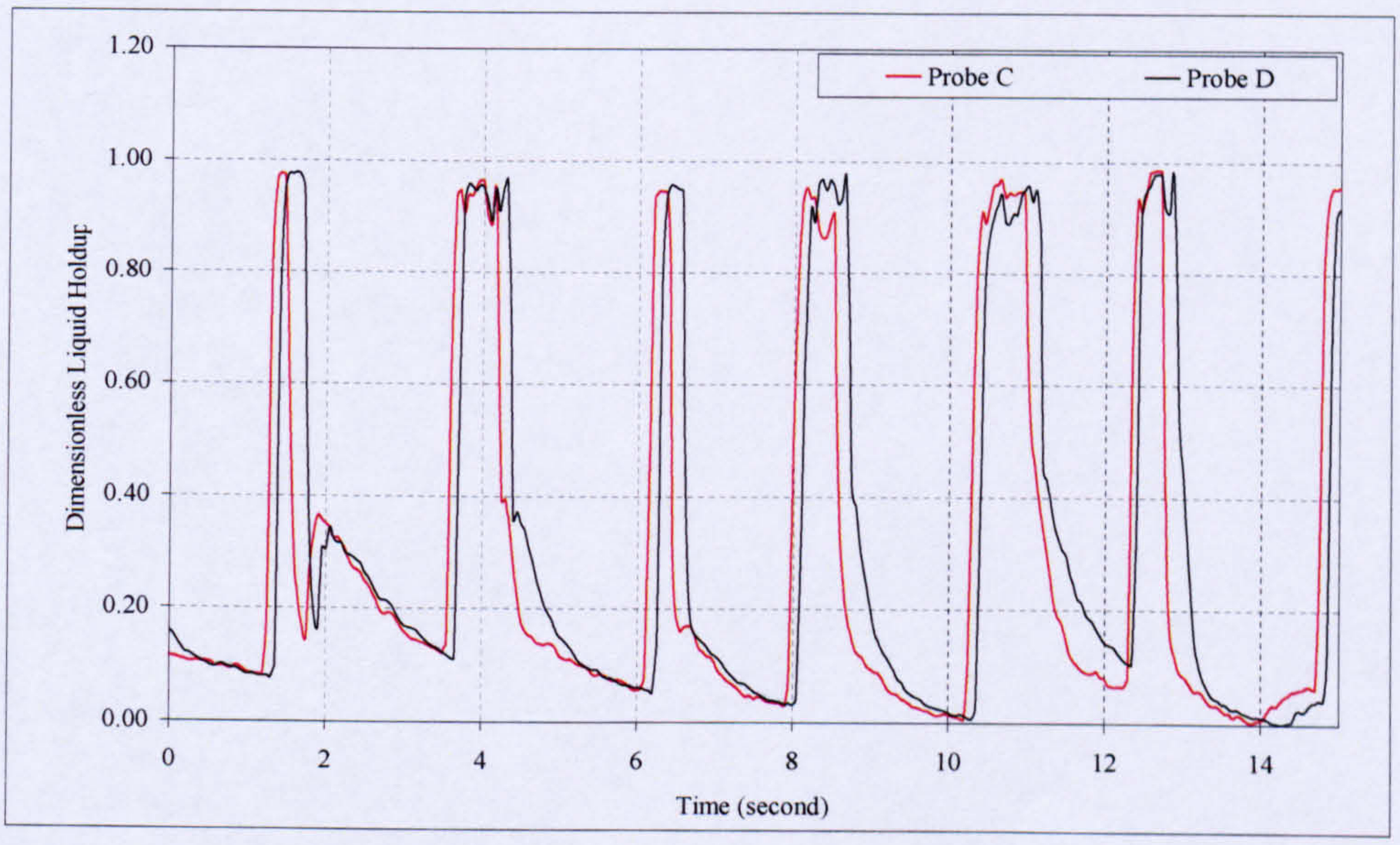

Figure 4-11: Slugs Trace by Conductivity Probes $C_{(C)}$ and $C_{(D)}$

4.1.2.2 Non-invasive Ultrasonic System

The non-invasive ultrasonic technique is based on continuous ultrasonic waves which propagated through the liquid phase, where the successive passing slug unit modulates the received ultrasonic signal.

Non-invasive ultrasonic system consists of two pairs of ultrasonic angle beam transducers (SN 1195399) with a frequency of 1MHz as illustrated in Figure 4-12, signal function generator (HP 33120 A), signal conditioning box, data acquisition system (DAS) and LabView software which is used to collect the conditioned modulated ultrasonic signals as shown in Figure 4-13.

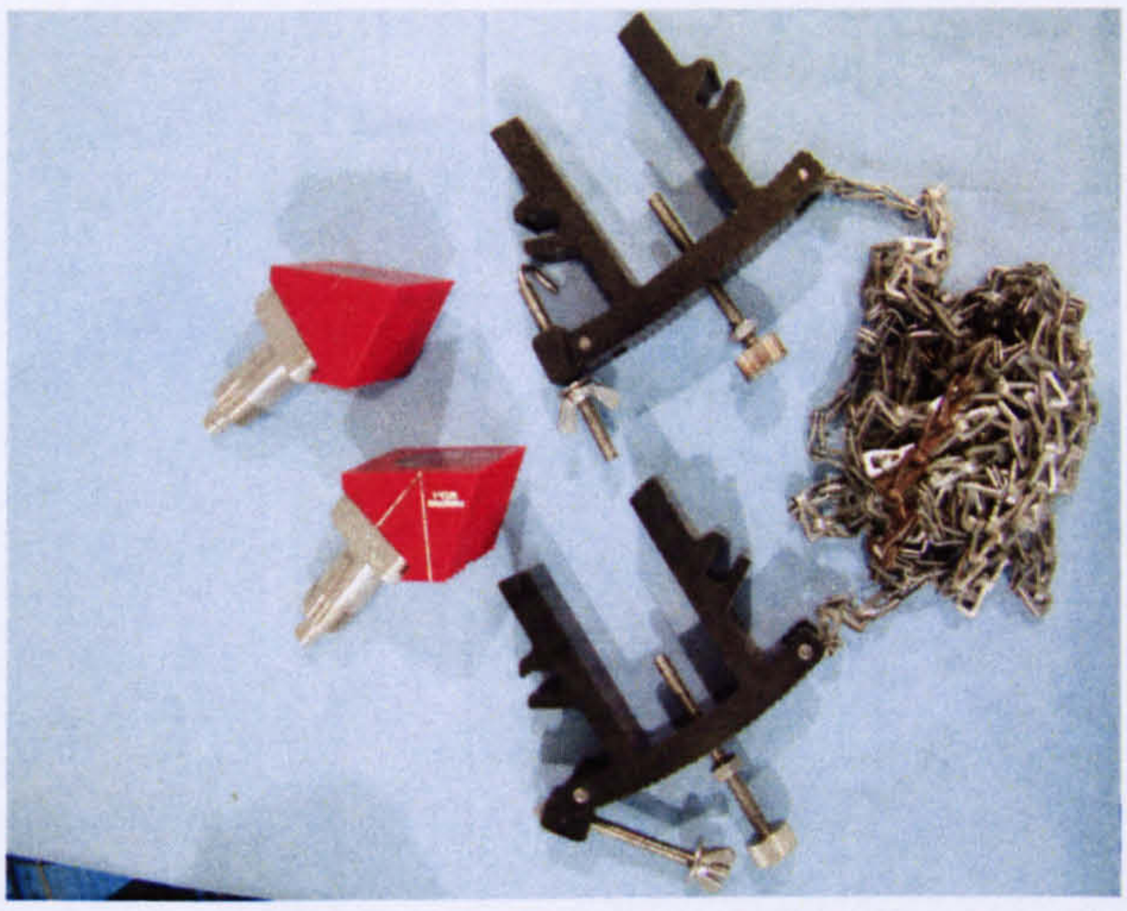

Figure 4-12: 1 MHz Ultrasonic Transducers and their Clamps

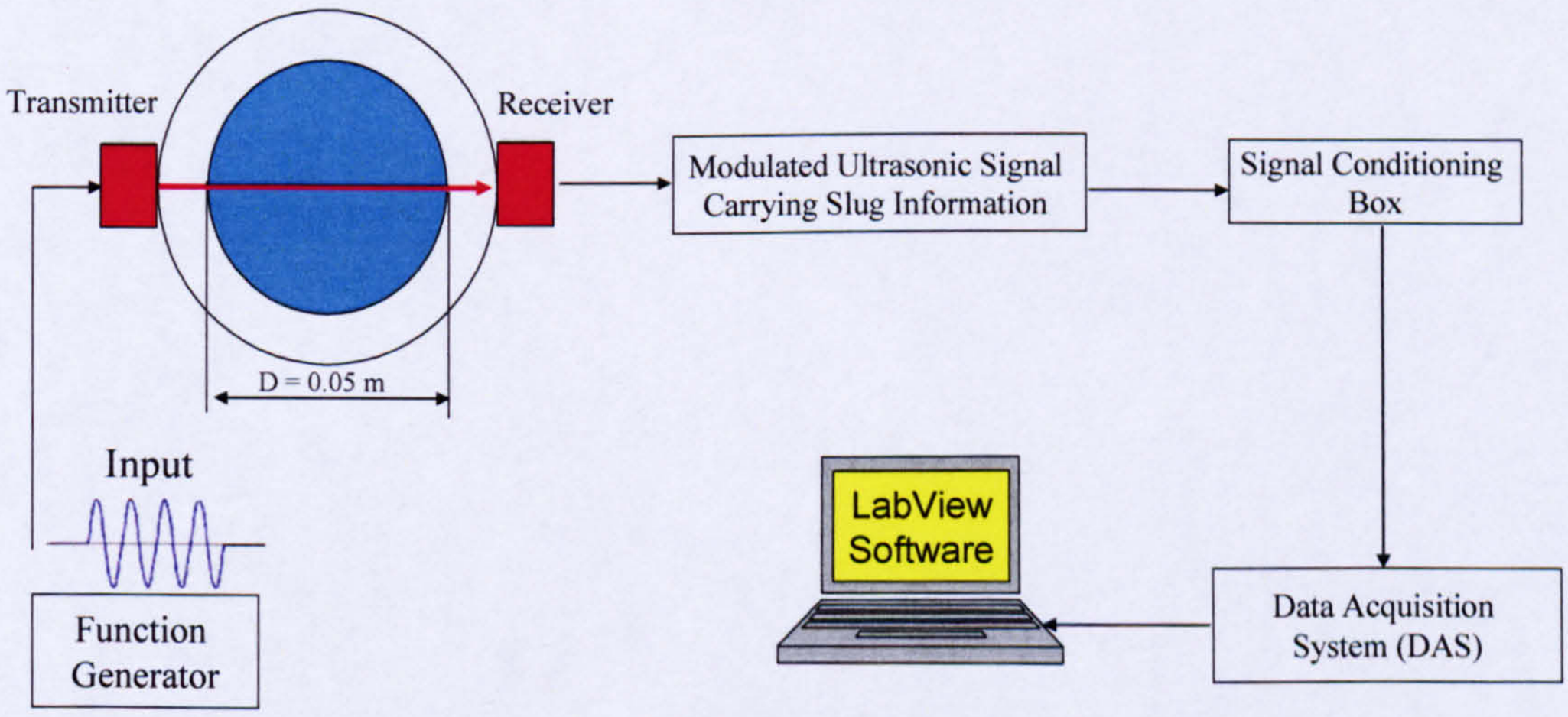

Figure 4-13: Schematic Diagram of Non-invasive Ultrasonic System

4.1.2.2.1 Function Generator/Arbitrary Waveform Generator

The HP (33120A) function generator was used to generate a 1MHz sine wave signal to ultrasonic piezoelectric transducer (transmitter). The received signal is modulated by the passing of the slugs as illustrated in Figure 4-14.

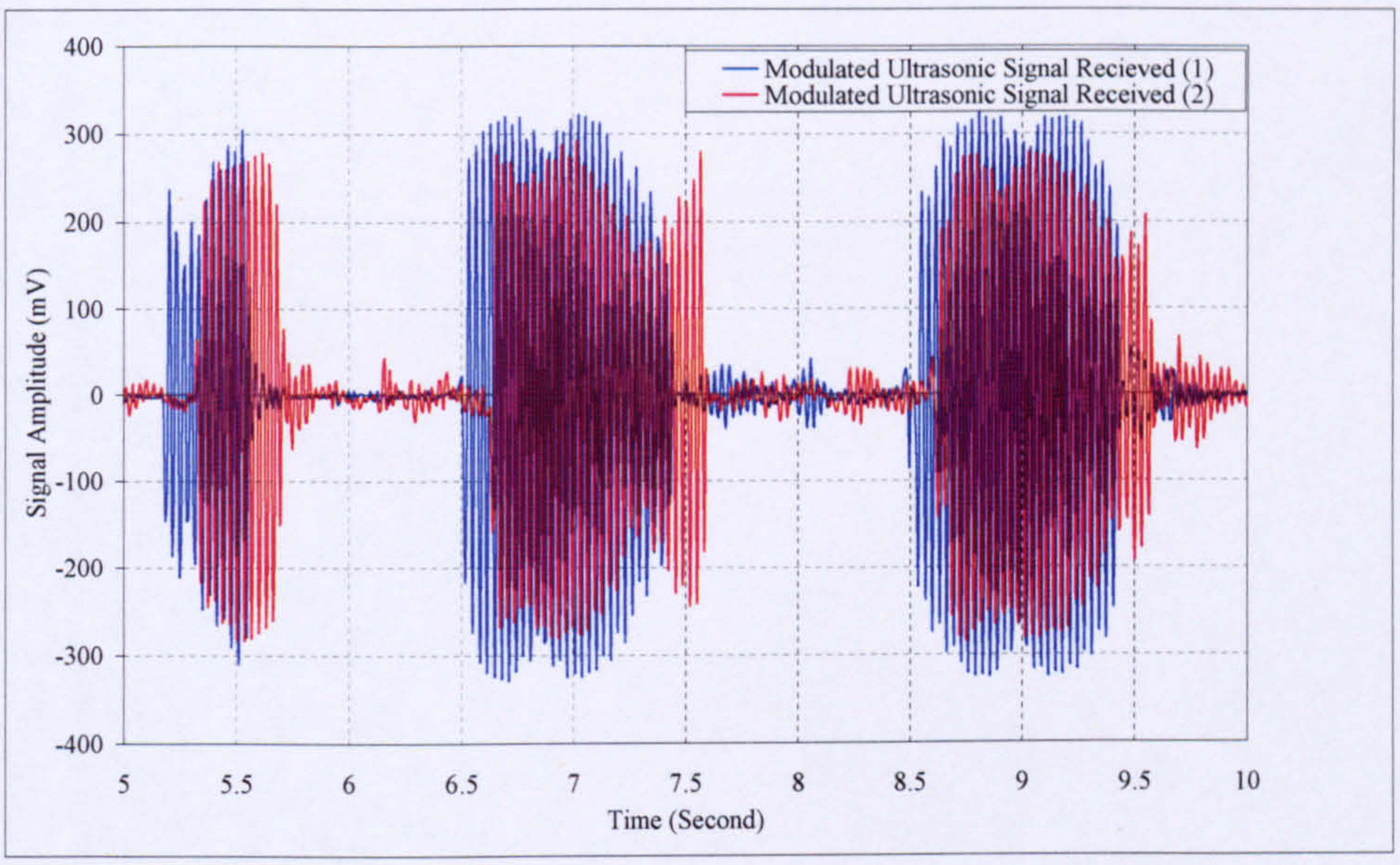

Figure 4-14: Sample Ultrasonic Traces under Slug Flow Conditions

4.1.2.2.2 Signal Conditioning Unit

To extract the envelope of the amplitude modulated received ultrasonic signal, a signal conditioning unit was designed and built at Cranfield University. The signal conditioning unit consists of a non-inverting amplifier, the active full wave rectifier and low pass filter as shown in Figure 4-15.

The performance of the signal conditioning unit compared with the conductivity probe is shown in Figure 4-16.

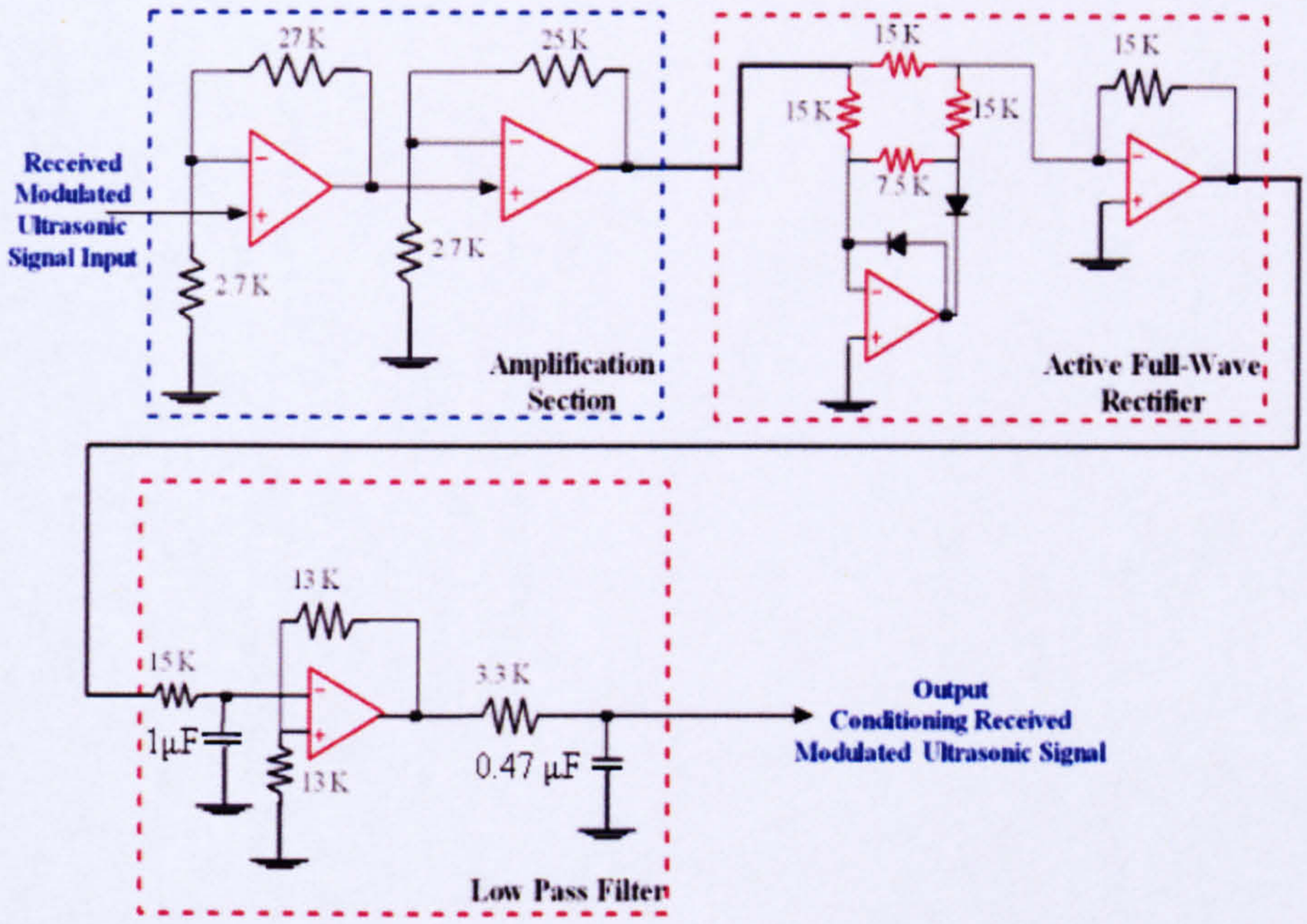

Figure 4-15: Electronic Circuit of the Signal Conditioning Unit

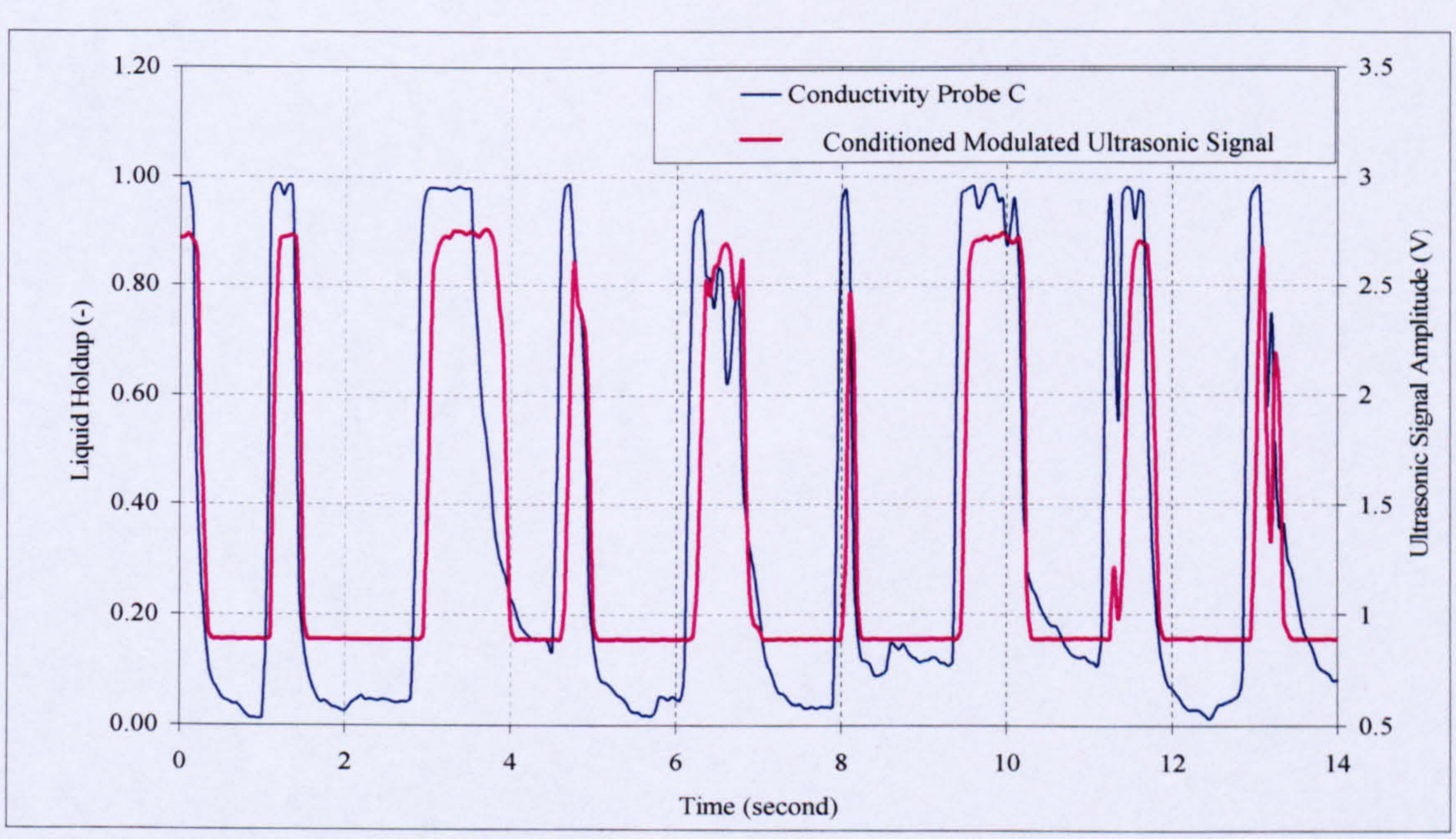

Figure 4-16: Slug Tracing by Conductivity Probe and Conditioned Modulated Ultrasonic Signal

4.1.2.3 Non-intrusive Ultrasonic Pulse-Echo Mode System

A non-intrusive ultrasonic pulse-echo mode system was designed to measure the liquid holdup in slug body and film region. The system consists of an ultrasonic pulser–receiver (Panametrics Model 500PR) which was used to excite the ultrasonic transducer, to receive and amplify the reflected signals.

The ultrasonic pulse-echo technique is based on measuring the liquid level in the pipe and by using appropriate equation the liquid holdup can be obtained.

A focused longitudinal wave piezoelectric ultrasonic transducer (immersion type) acted as both an emitter and a receiver (pulse-echo mode) at a centre frequency of 2.25 MHz with an active diameter of 16.86 mm, and an electronic circuit to measure the time of transmitted and reflected ultrasound wave in liquid phase as shown in Figure 4-17.

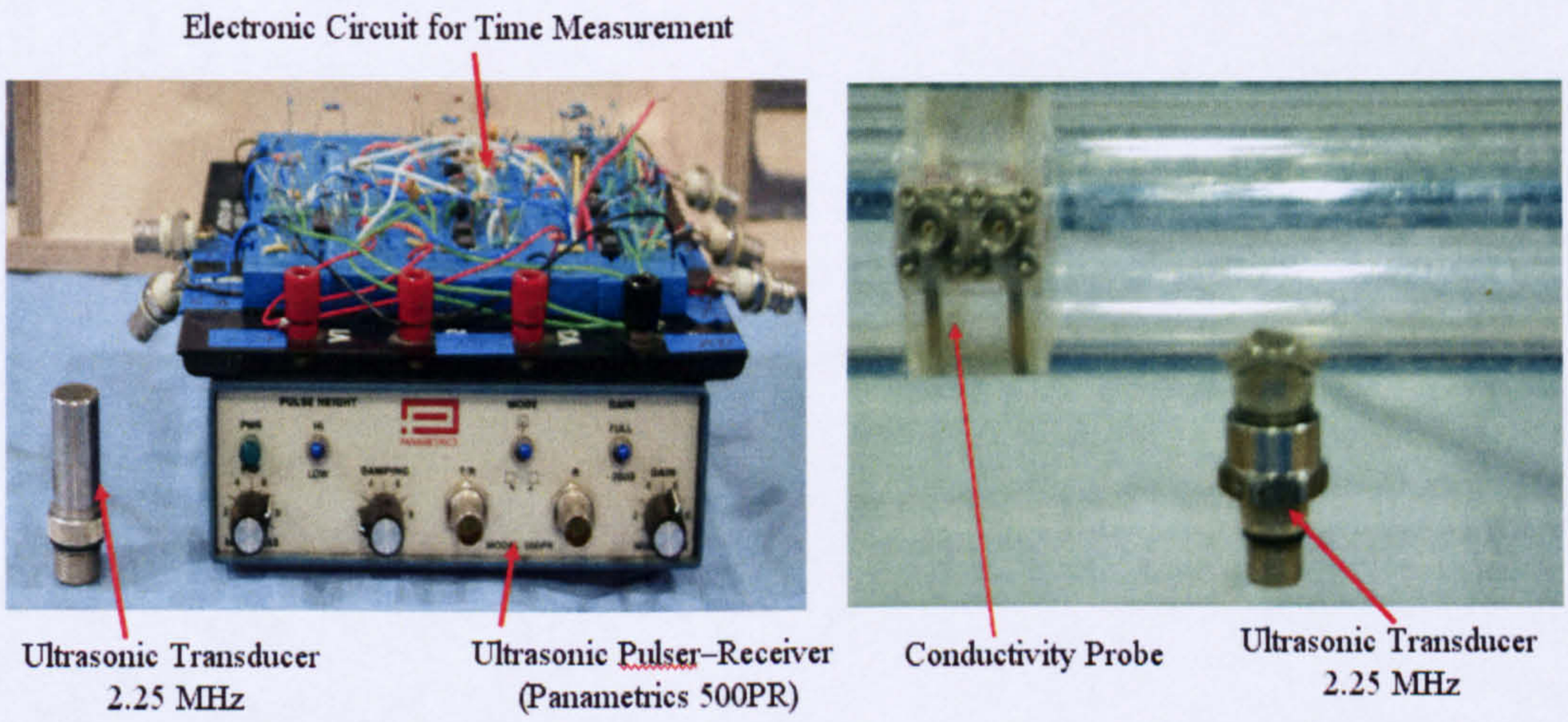

Figure 4-17: Non-Intrusive Ultrasonic Pulse-Echo Mode System and Components

The schematic diagram of the non-intrusive ultrasonic system used to measure the liquid holdup is illustrated in Figure 4-18.

The concept of liquid height measurement using non-intrusive ultrasonic (pulse-echo mode) is illustrated in Figures 4-19 and 4-20.

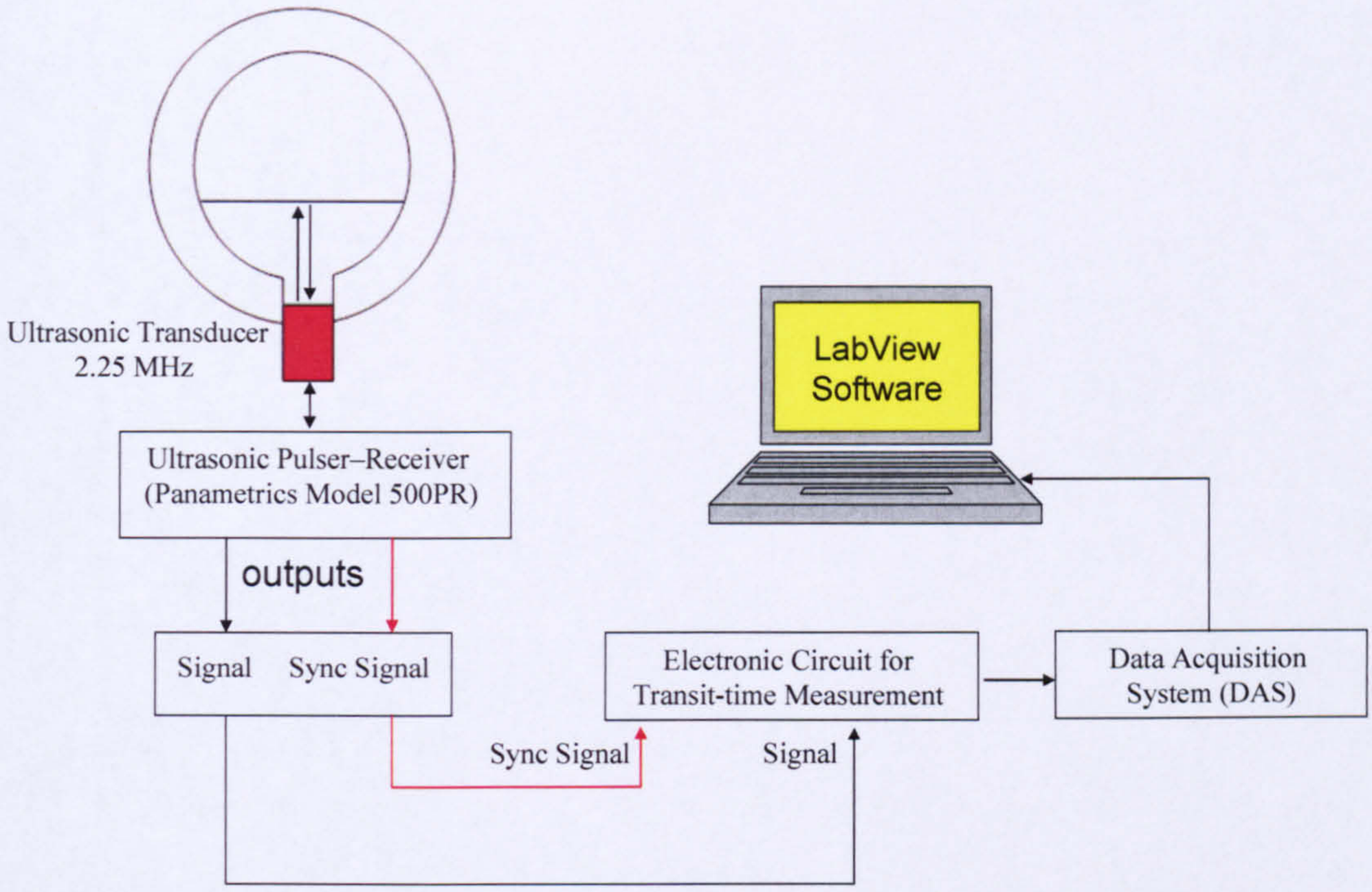

Figure 4-18: Schematic Diagram of Non-Intrusive Ultrasonic Pulse-Echo Mode System

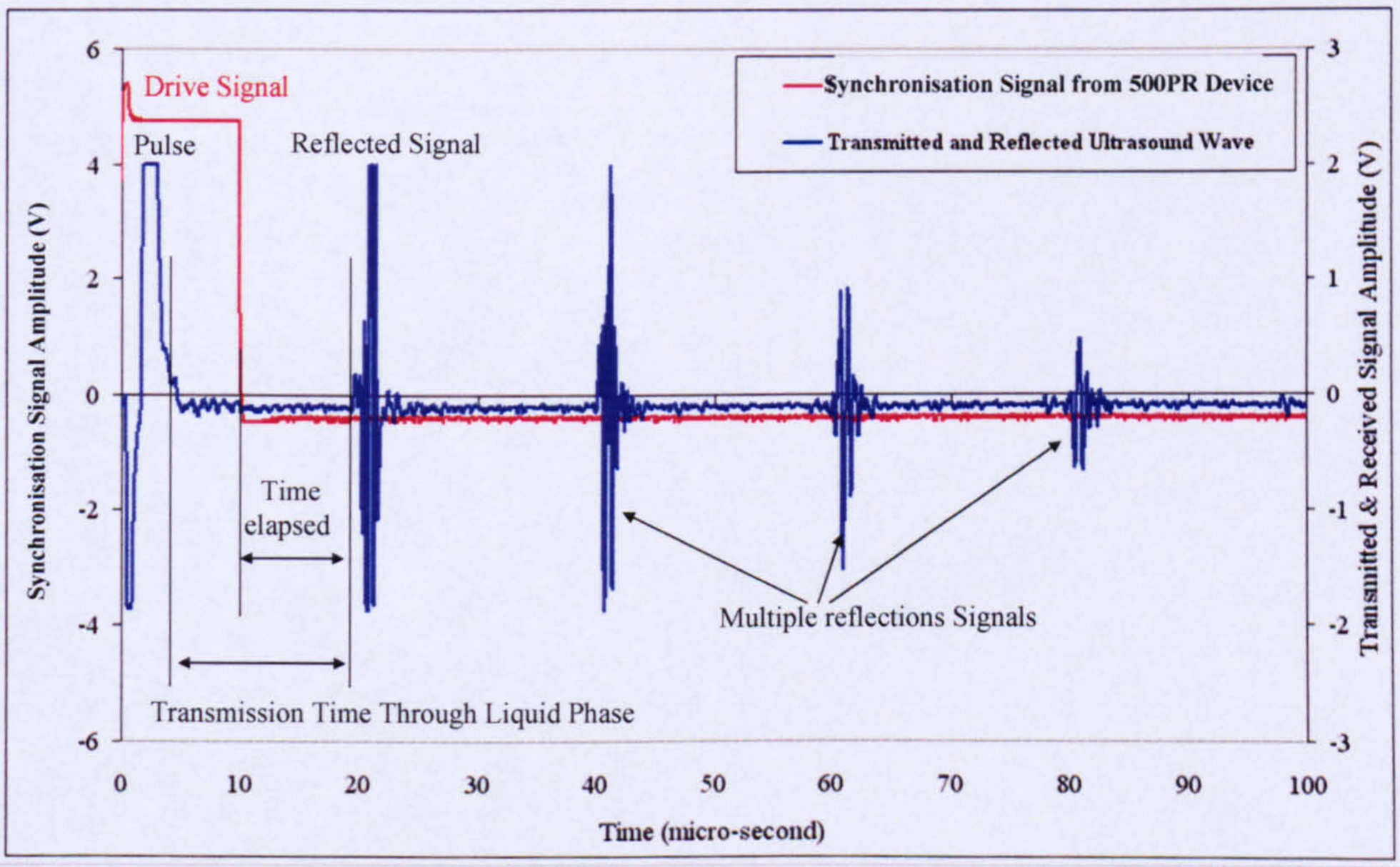

Figure 4-19: Ultrasonic Pulse-Echo Mode for Liquid Height Measurements

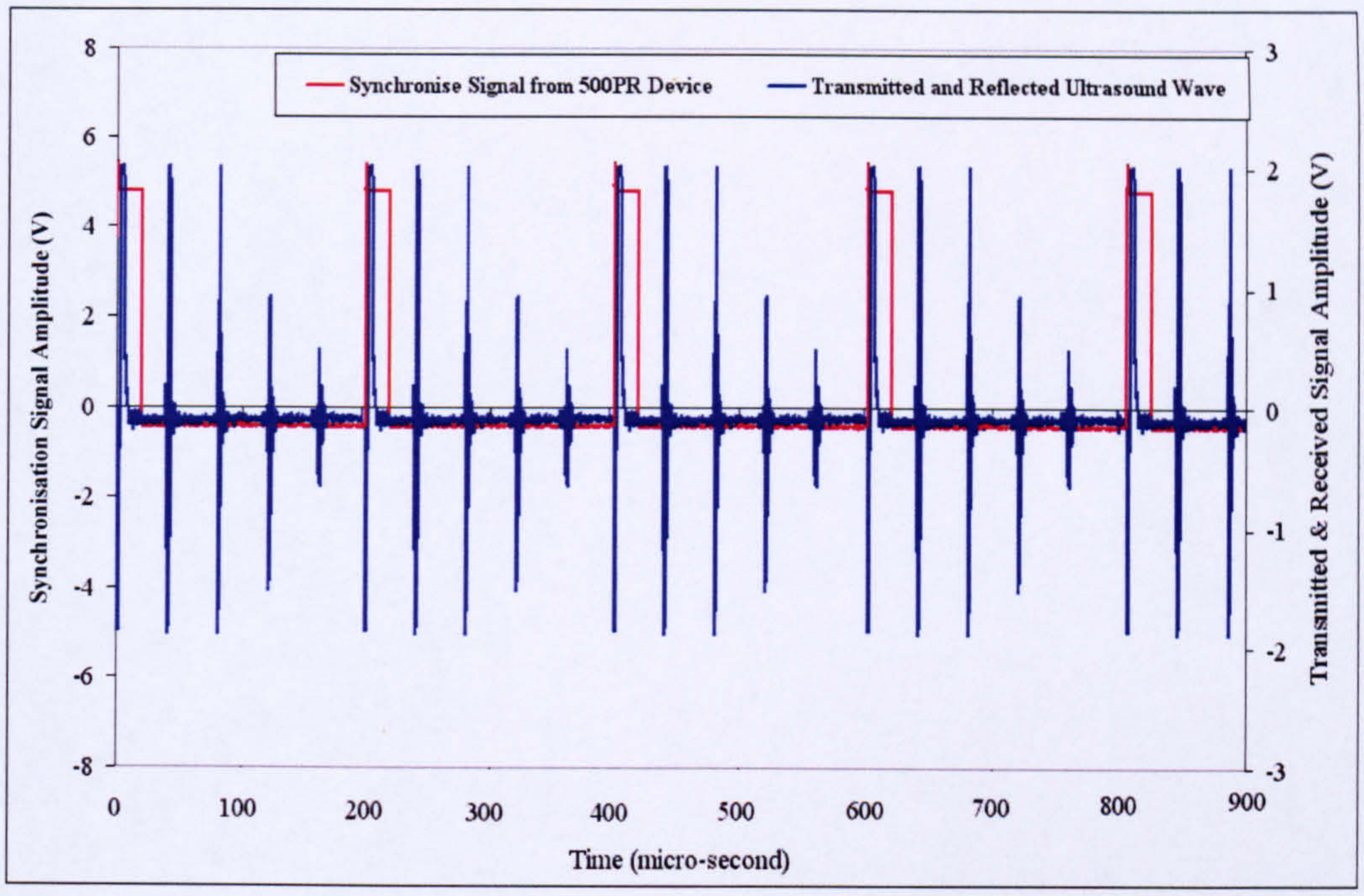

Figure 4-20: Transit Time and Repetition Time in Ultrasonic Pulse-Echo Mode

As shown in Figures 4-23 and 4-24, the pulse was generated by the 500PR device (blue line) and transmitted through the liquid phase until it reached the liquid surface, then it was reflected back.

The time taken for the ultrasound wave to travel through the liquid phase and to reflect back at each triggering is the time elapsed T_1, T_2, $T_{3...}$ and T_i. The 500PR device was set at a repetition rate of 5000Hz; therefore, the repetition time $T_{repetition}$ was 200 μs.

4.1.2.3.1 Calibration of Ultrasonic Level Measurement Transducer

The non-intrusive liquid based ultrasonic transducer was calibrated at the static conditions. The aim of the calibration was to derive a correlation between the measured liquid height ,h_L, in the pipe using a ruler and the corresponding voltages ,$V_{(U)}$, from the 2.25 MHz ultrasonic transducer as shown in Figure 4-21. As a result of the calibration, a linear correlation was obtained and given as:

$$h_L = 0.0302 \times (V_{(U)}) + 5.307 \qquad (4.5)$$

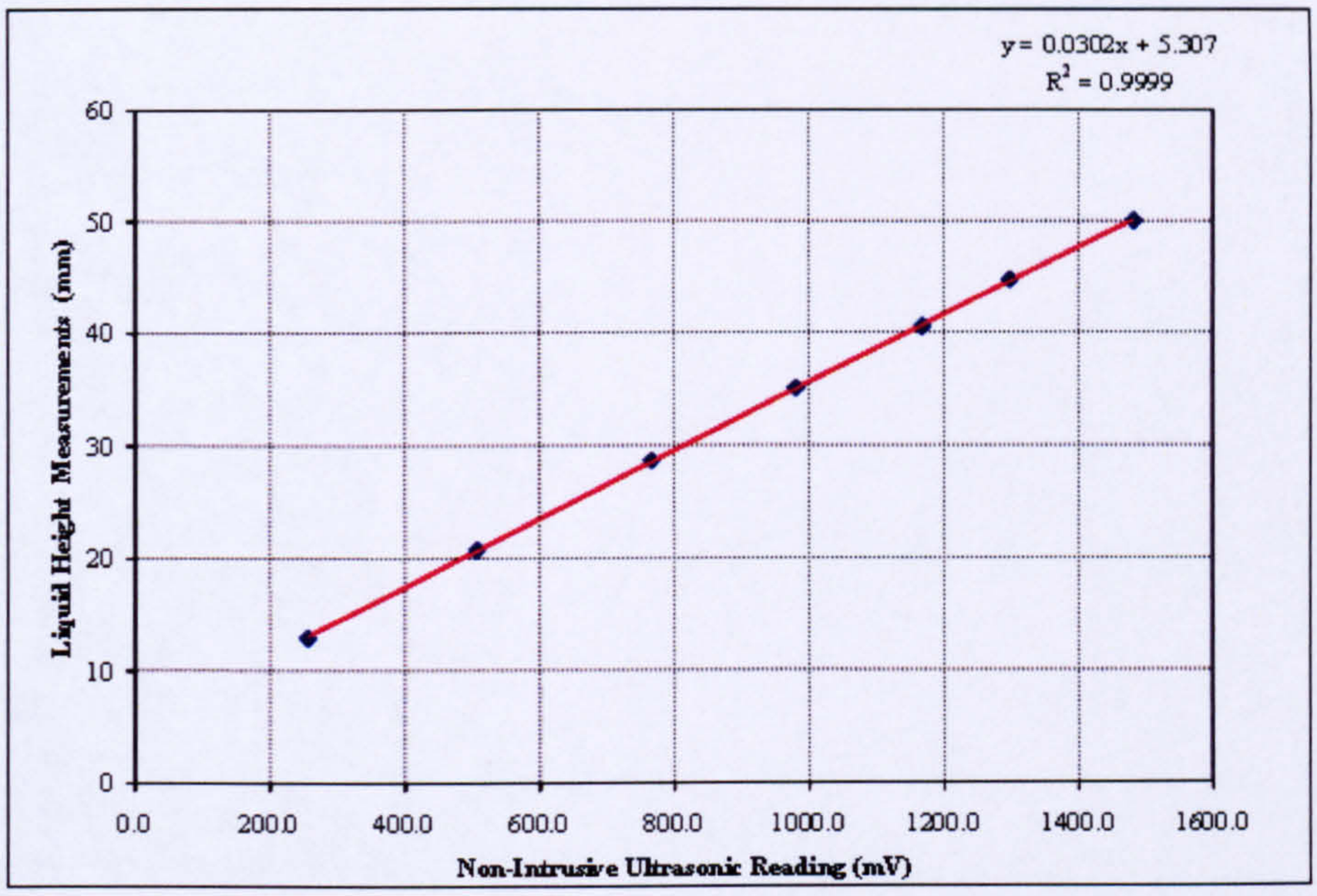

Figure 4-21: Output Voltages of Ultrasonic Transducer vs. Liquid Height Measurements

From the ratio of the liquid height measurement to the output voltage in equation (4.5) and by introducing the $V^*_{(U)}$, the liquid height $h_{L\ (U)}$ can be measured using ultrasonic technique and is given by the following equation:

$$h_{L(U)} = \frac{V_{(U)} - V_{(U)(min)}}{V_{(U)(max)} - V_{(U)(min)}} \times d = V^*_{(U)} \times d \qquad (4.6)$$

where $V^*_{(U)}$ is the normalised value for the voltage value

To calculate the liquid holdup using ultrasonic technique ($E_{L\ (U)}$) the following equation must be used:

$$E_{L(U)} = \frac{1}{\pi} \times \left(\pi - \cos^{-1}\left[2 \times \left(\frac{h_{L(U)}}{d} \right) - 1 \right] + \left[2 \times \left(\frac{h_{L(U)}}{d} \right) - 1 \right] \times \sqrt{1 - \left[2 \times \left(\frac{h_{L(U)}}{d} \right) - 1 \right]^2} \right) \qquad (4.7)$$

However, to achieve the measurements of the liquid holdup by the non-intrusive ultrasonic technique under slug flow conditions, the corresponding output voltage which are proportional to the transit time elapsed must be measured. Accordingly, an electronic circuit was designed and built at Cranfield University workshop for this purpose.

4.1.2.3.2 Electronic Circuit Design

The purposes of the electronic circuit was to measure the time elapsed between the transmitted and first reflected signal and to give an analogue output voltage proportional to the time elapsed measured. The electronic circuit consists of the following components as shown in Figure 4-22:

1. Inverter IC1,
2. Monostable 555 timer IC3, IC4, and IC5,
3. AND Gate IC6,
4. Analog digital device IC2 and
5. Low-pass filter.

The operating principle of the electronic circuit is given as follows:

1. Inverter IC1, deployed to invert the drive signal before it is passed to the timer from H, L to L, H status.

2. Timer IC3, used to stop false triggering within the ultrasonic transducer and that by increasing the drive signal width from 10 μs to 12 μs, obtained by the given equation:

$$T_{(IC3)} = 1.1 \times 10^{3} \times 0.1 \times 10^{-6} = 12 \ \mu s \tag{4.8}$$

3. Analog device IC2 used to setup the threshold level of the reflected signal at 1V.

4. The output signal from the IC2 and the output signal from the timer IC3 after being inverted by IC1 were used as inputs signals to AND Gate IC6. The AND Gate IC6 combines both signals and select the points at which both signals are at H condition. The output signal from the AND Gate IC6 was used to reset the timer IC5. However, a reflected signal received earlier than 1.1 μs was too short to reset the timer IC5 therefore the interval was increased by 1.1 μs using timer IC4.

$$T_{(IC4)} = 1.1 \times 10^{3} \times 0.01 \times 10^{-6} = 11 \ \mu s \tag{4.9}$$

5. Timer IC5 triggers from the drive signal, however, the output of this timer remains high till it is reset by AND Gate IC6 signal. As a result of the reset, the time elapsed between the transmitted and received signal was measured.

6. A low pass filter gives an analogue output proportional to the time elapsed. Therefore the output voltages from the electronic circuit depend and proportional on the time elapsed.

7. From Figure 4-23, the relationship between the time elapsed T_i and repetition time $T_{repetition}$ can be written as:

$$T_i \times V_{(U)} = T_{repetition} \times V_{(U)(average)i} \quad (4.10)$$

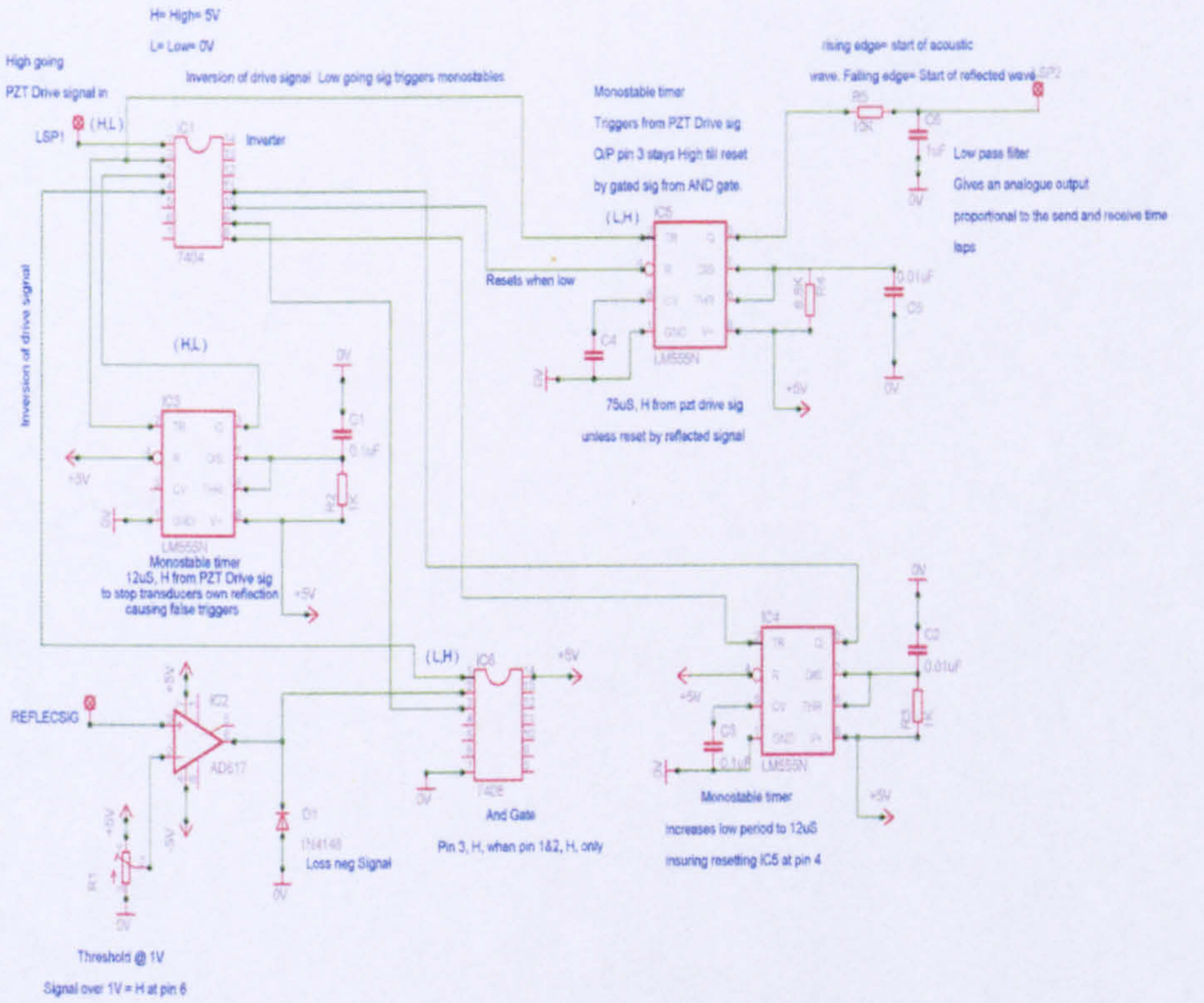

Figure 4-22: Electronic Circuit of the Ultrasound Pulse-Echo Mode

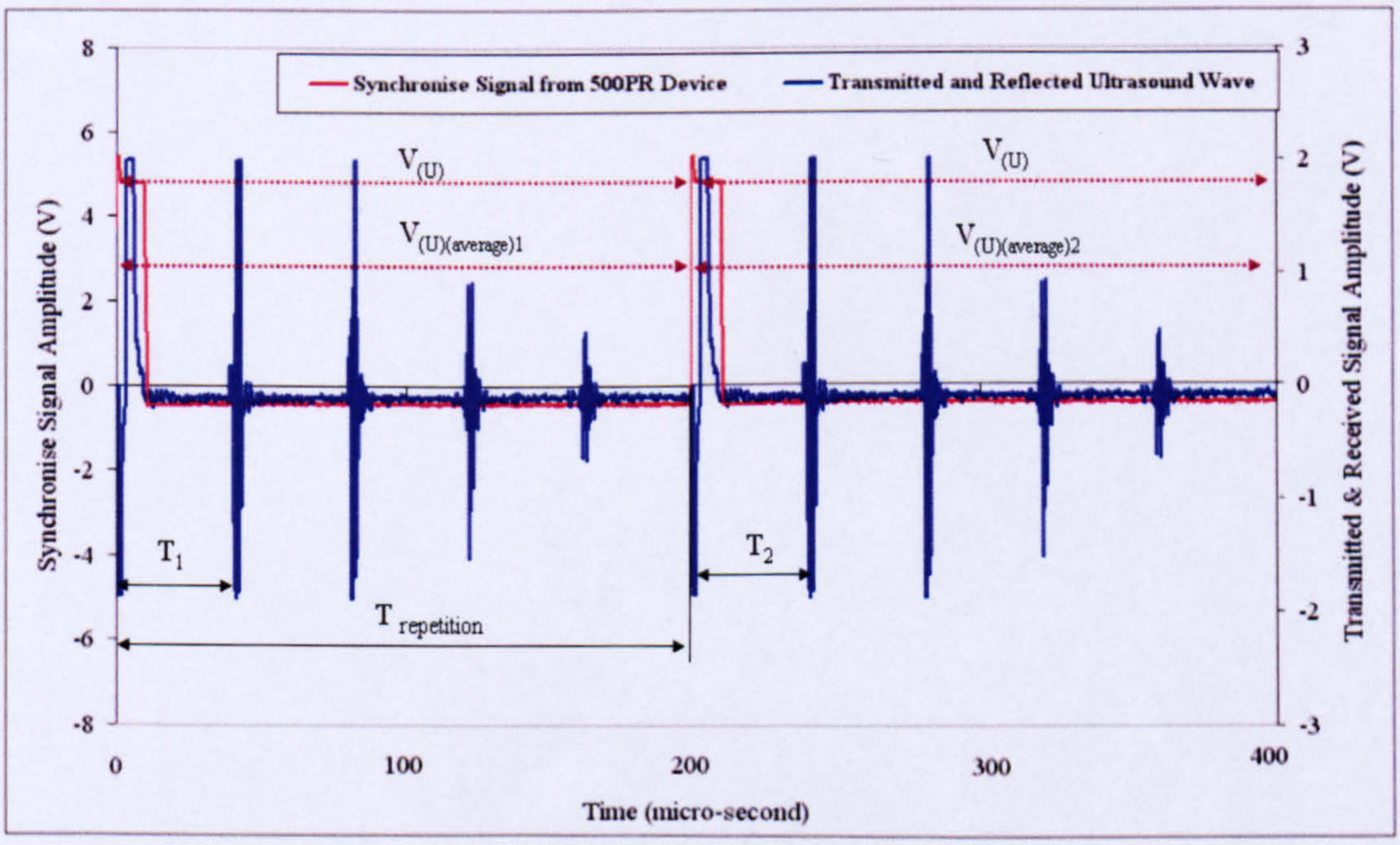

Figure 4-23: Relationship between Ultrasonic Signal Amplitude and Liquid Height

8. From the basic equation for liquid height measurement using the ultrasonic sensor (pulse-echo mode), the relationship between the time elapsed T_i and the liquid height at triggering i is given as:

$$h_{L(U)i} = \frac{C_L \times T_i}{2} \tag{4.11}$$

By substituting equation (4.11) in equation (4.10), the relationship between the ultrasonic signal amplitude and liquid height using pulse-echo mode is given as:

$$h_{L(U)i} = \frac{T_{repetition} \times V_{(U)(average)i} \times C_L}{2 \times V_{(U)}} \tag{4.12}$$

where
$h_{L(U)i}$ is liquid height at i triggering,
$T_{repetiton}$ is repetition time,
C_L is the speed of sound in the water,
$V_{(U)}$ is the drive signal amplitude and
$V_{(U)(average)i}$ is the average reflected signal amplitude over (i) triggering.

9. Typical output voltage of the electronic circuit designed for the measurement of the liquid height under slug flow conditions is shown in Figures 4-24 and 4-25.

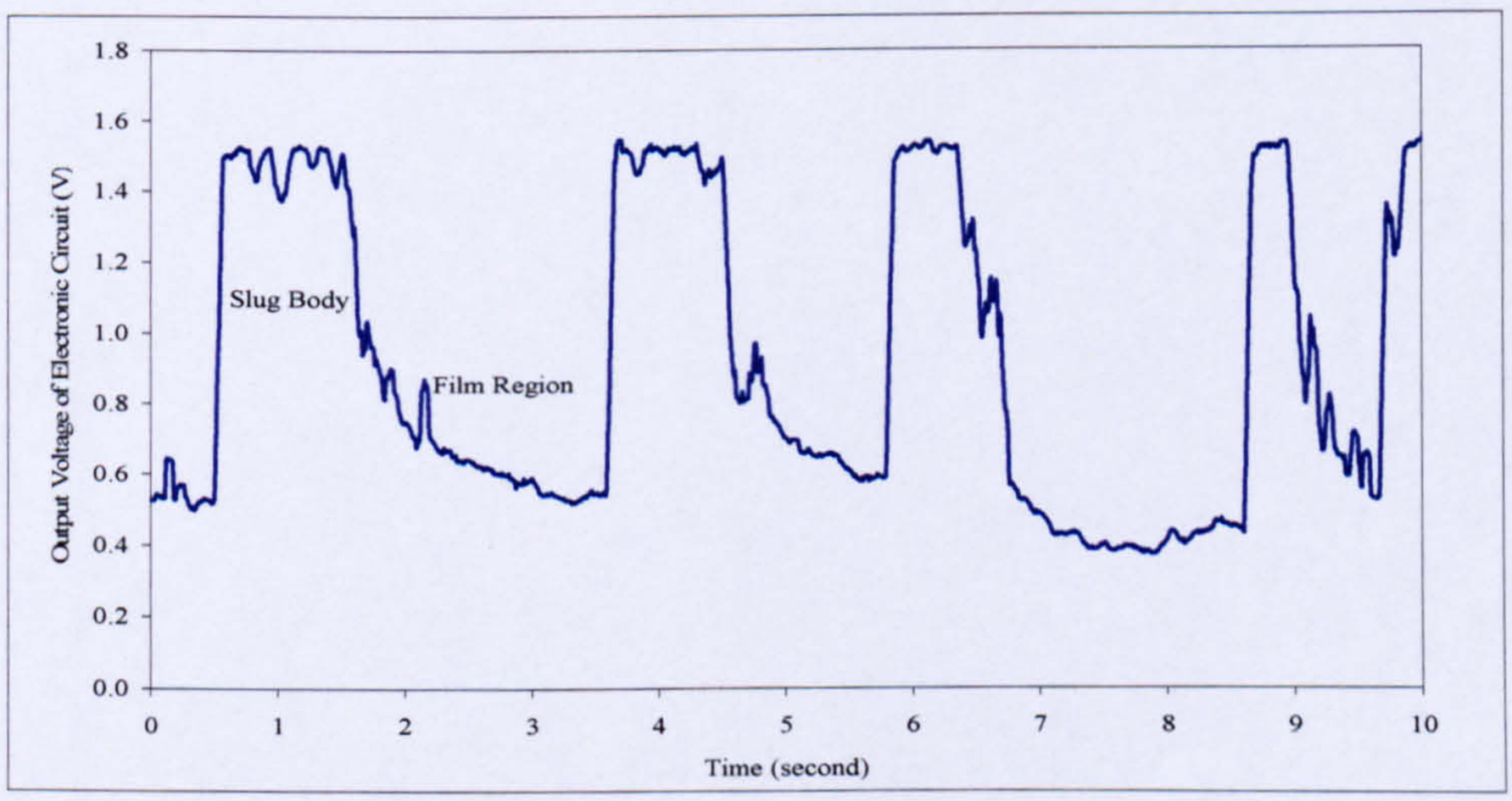

Figure 4-24: Slug Tracing by Non-Intrusive Ultrasonic (V_{SL}=0.5 ms^{-1}, V_{SG}=1.01 ms^{-1})

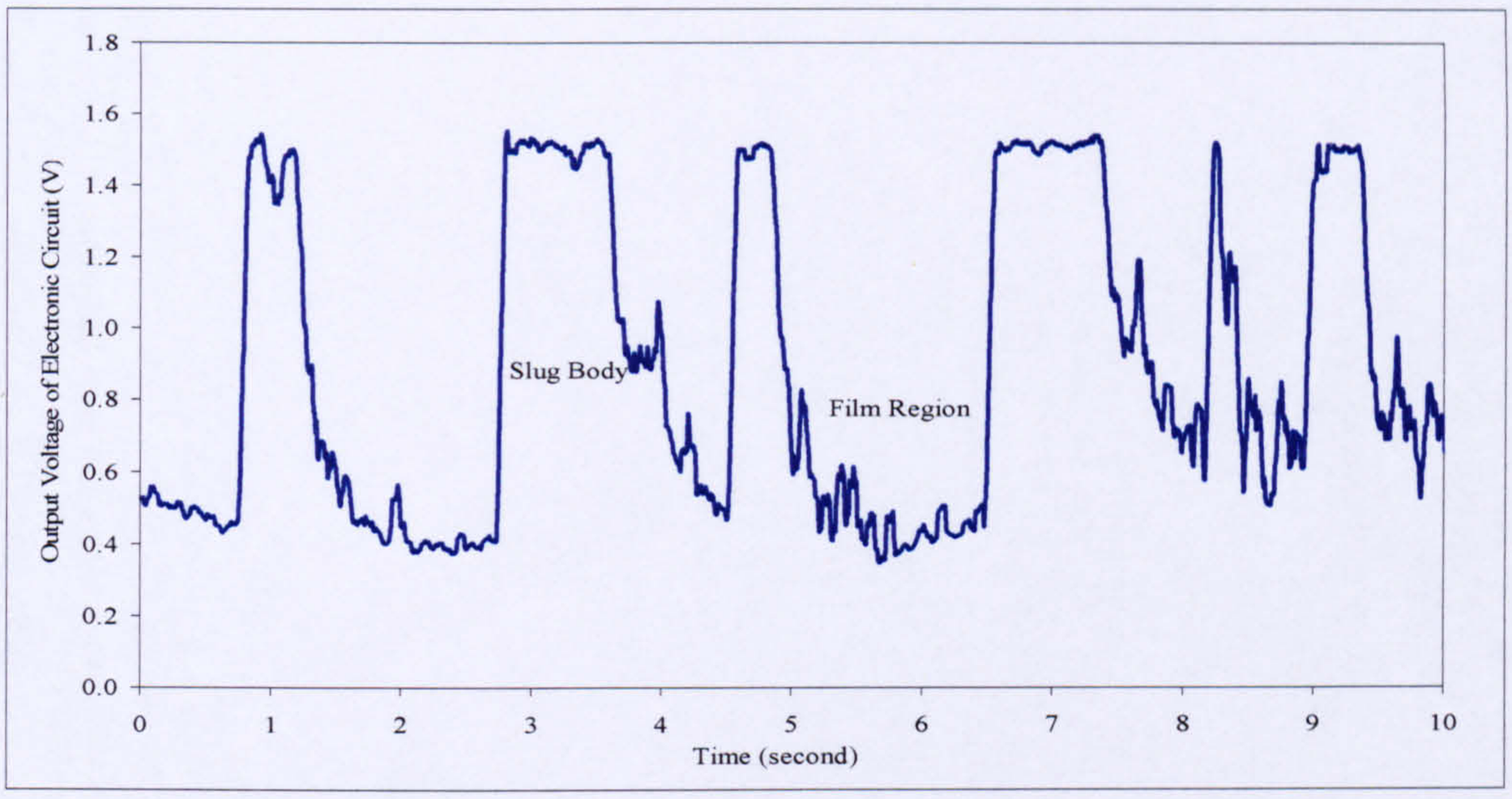

Figure 4-25: Slug Tracing by Non-Intrusive Ultrasonic (V_{SL}=0.7 ms^{-1}, V_{SG}=1.25 ms^{-1})

4.1.3 Experimental Measurement Method

In this work, all experiments reported were conducted on the two-phase water/air facility at atmospheric pressure. The experimental method was based on the measurements of the slug parameters by using the non-invasive ultrasonic system to measure the slug translational velocity, slug body passage time, film region passage time, slug body and film length. The non-intrusive ultrasonic system was used to measure the liquid holdup in both the slug body and film region.

Conductivity probes $C_{(C)}$ and $C_{(D)}$ measured the slug parameters and these measurements were used to validate the ultrasonic measurement. Table 4-3 summarises the experimental measurement method.

Table 4-2: Experimental Measurement Method

Measurement System	V_T	t_{Slug}	t_{Film}	L_S	L_F	L_U	E_{LS}	E_{LF}
Non-invasive Ultrasonic	X	X	X	X	X	X		
Non-intrusive Ultrasonic							X	X
Conductivity Probes	X	X	X	X	X	X	X	X

4.1.3.1 Description of the Experimental Campaigns

A series of experimental campaigns was conducted to study the behaviour of the proposed ultrasonic metering system to measure the two-phase water-air under slug flow conditions. The experimental campaigns cover a range of superficial gas and liquid velocities as shown in Figure 4-26.

In Figure 4-27, the experimental campaigns plot in three dimensions in order to show the initial distribution of the gas void fractions. The gas initial gas void fraction is calculated by $GVF = V_{SG}/(V_{SG} + V_{SL})$ and it ranged from 0% up to 80%.

The experimental campaigns strategy was based on the fixing of the value of the superficial liquid velocity and increasing gradually the gas superficial velocity. All campaigns were conducted at atmospheric pressure. Table 4-4 listed the experimental campaigns conducted on the two-phase water/air facility.

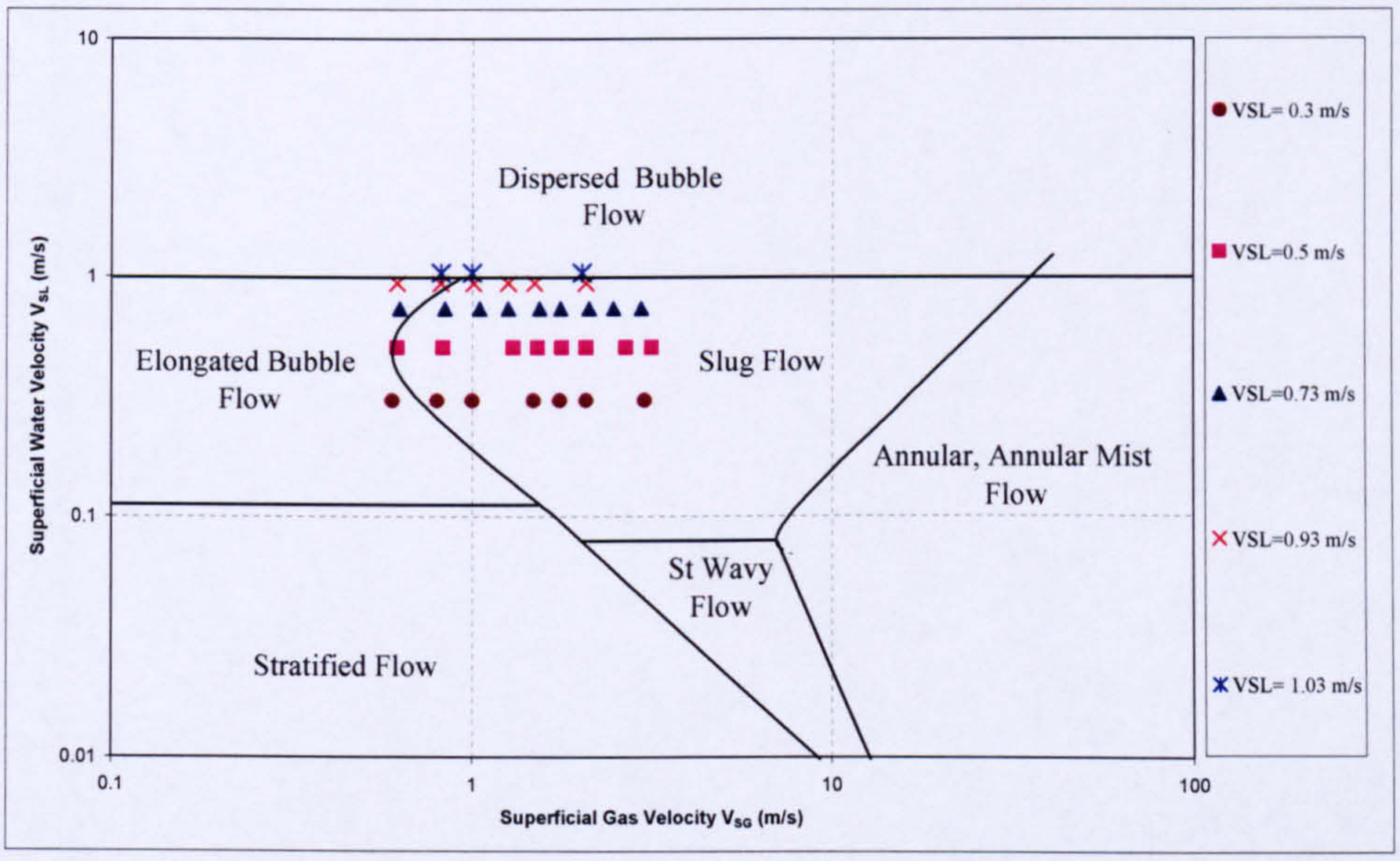

Figure 4-26: Two-Phase Water/Air Experimental Campaigns Flow Map

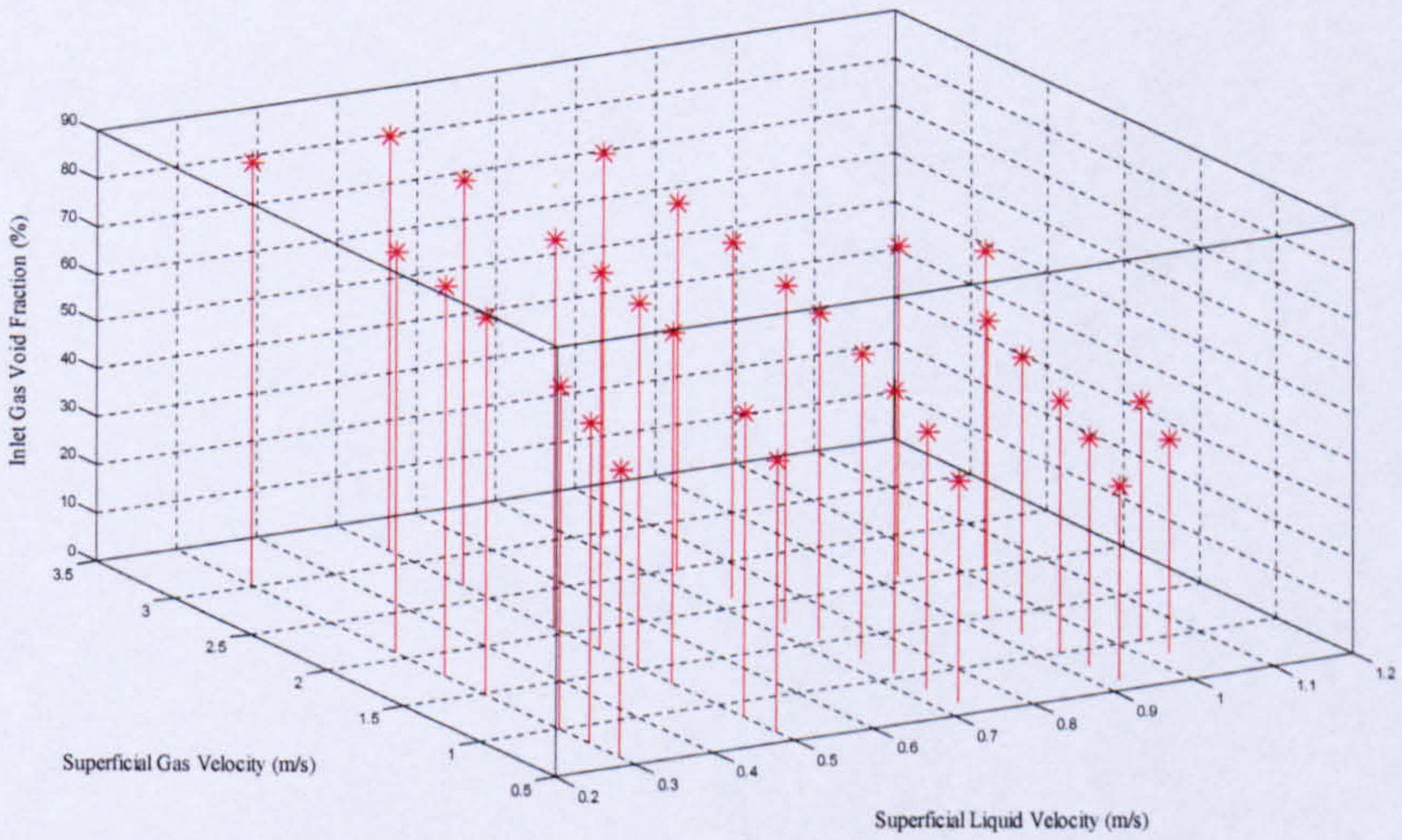

Figure 4-27: Initial GVF distributions

Table 4-3: Experimental Campaigns Range of Liquid and Gas Superficial Velocities

Experimental Campaigns	V_{SL} (ms^{-1})	V_{SG} (ms^{-1})
Campaign #1	0.3	0.6, 0.8, 1, 1.48, 1.75, 2.07, 3.01
Campaign #2	0.5	0.62, 0.83, 1.30, 1.52, 1.77, 2.07,2.67, 3.15
Campaign #3	0.73	0.63, 0.84, 1.05, 1.26, 1.54, 1.76, 2.11, 2.47, 2.95
Campaign #4	0.93	0.62, 0.82, 1.01, 1.26, 1.49, 2.07,
Campaign #5	1.03	0.82, 1.0, 2.02

4.1.4 Data Acquisition System

Data from the two-phase air/water facility was acquired by a dedicated PC-based Data Acquisition System (DAS). This System consisted of a series of custom-built signal conditioning units. Data was collected from the signal conditioning units, with a range of 0 to 10 V d.c, and then transferred to the PC via the parallel port multiplexer (SCB-68).

Digital Data from (SCB-68) was sent to the PC system (100 MHz Dell PC) with 10 GB (AMD Athlon) hard disk, running the Windows 2000 operating system. A runtime version of Labview 'Virtual Instrument' 6.2 Version was used to gather data in real time from DAS hardware and display the results to the computer screen for control and operation purpose.

The Data Acquisition System (DAS) software took information on the raw voltage information entering the computer from the DAS hardware and converted this information to engineering units for the corresponding instruments. To do this, the following equation was used:

$$EU = K \times (V - V_0) \tag{4.13}$$

where
EU is the required engineering unit (the measured variable),
K is the gain, V is the voltage signal and
V_O is the voltage at zero signal reading where the measured variable is zero.

The DAS for the 17 channels is presented in Table 4-4.

Table 4-4: Data Acquisition System Channels

Name	Zero	Gain	Engineering Units	A/D Channel
FL_1	0.5	6.27	l/s	1
FG_1	0.0	26.88	l/min	2
FG_2	0.0	60	l/min	3
P_1	0.0	0.679	bar	4
P_2	-0.001	1.336	bar	5
P_3	0.0	0.859	bar	6
dp	0.2	4.0	mbar	7
T_1	0.091	9.98	°C	8
T_2	0.5	10.02	°C	9
T_3	0.5	10.02	°C	10
$C_{(A)}$	0	1	Vdc	11
$C_{(B)}$	0	1	Vdc	12
$C_{(C)}$	0	1	Vdc	13
$C_{(D)}$	0	1	Vdc	14
Ultrasonic 1	0	1	Vdc	15
Ultrasonic 2	0	1	Vdc	16
Ultrasonic 3	0	1	Vdc	17

4.2 Summary

In this chapter, the experimental set up for the two-phase air-water facility was described in detail.

- Section 4.1.1 described the supply for air and water to the two-phase air-water facility, and the instrumentation specification for air and water flowrate measurements,

- Section 4.1.2 described the measuring section. In this section the design aspects of the conductivity probe and the calibration process were presented. The schematic diagram of the non-invasive ultrasonic transducers and the signal conditioning unit were described in detail. Also the non-intrusive ultrasonic (pulse-echo) mode transducer which was used to measure the phase fraction was described with its electronic circuit,

- Section 4.1.3 described the experimental measurement methods used to achieve the measurements of the slug characteristics. In this section, the two

ultrasonic techniques, namely the non-invasive ultrasonic technique and the non-intrusive ultrasonic technique were combined to achieve the measurements of the slug characteristics.

- Section 4.1.4 presented the data acquisition system (DAS) deployed to extract the experimental data from the tests which were conducted at atmospheric pressure and with different air and water flowrates.

Chapter 5

Slug Characteristics Measurements by Ultrasonic Techniques

In order to obtain the gas and liquid volumetric flowrates under slug flow conditions from the slug closure model proposed in Chapter 3, the slug flow characteristics were measured using non-invasive/non-intrusive ultrasonic techniques.

The slug frequency measurements by non-invasive ultrasonic technique were validated by conductivity measurements is described in Section 5.2.

Slug translational velocity measurements by a non-invasive ultrasonic method were also validated by conductivity measurements, as described in Section 5.3.

Slug length and film length measurements by a non-invasive ultrasonic method and validation of the data with conductivity measurements are given Section 5.4.

The slug body and film liquid holdup measurements by a non-intrusive ultrasonic method and validation with conductivity are described in Section 5.5.

The coefficients C_o, and drift velocity V_d obtained based on experimental data are derived in section 5.6. Then the chapter summary is presented in section 5.7.

5.1 Slug Regions Classifications

In order to measure the slug characteristics using ultrasonic techniques, slug regions have to be idealised to identifiable regions so that signals from non-invasive ultrasonic techniques can be objectively analysed. A possible definition of a slug is a liquid mass travelling in a pipe being driven by the difference in the dynamic pressure (the driving force) between the gas in front and of behind it. This liquid mass covers the whole cross-section of the pipe. The shape of the slug constitutes a front (Region 1-2), body (Region 2-3), and a tail (Region 3-4), as shown in Figure 5-1. The arrangement of the non-invasive ultrasonic sensors is presented in Figure 5-2.

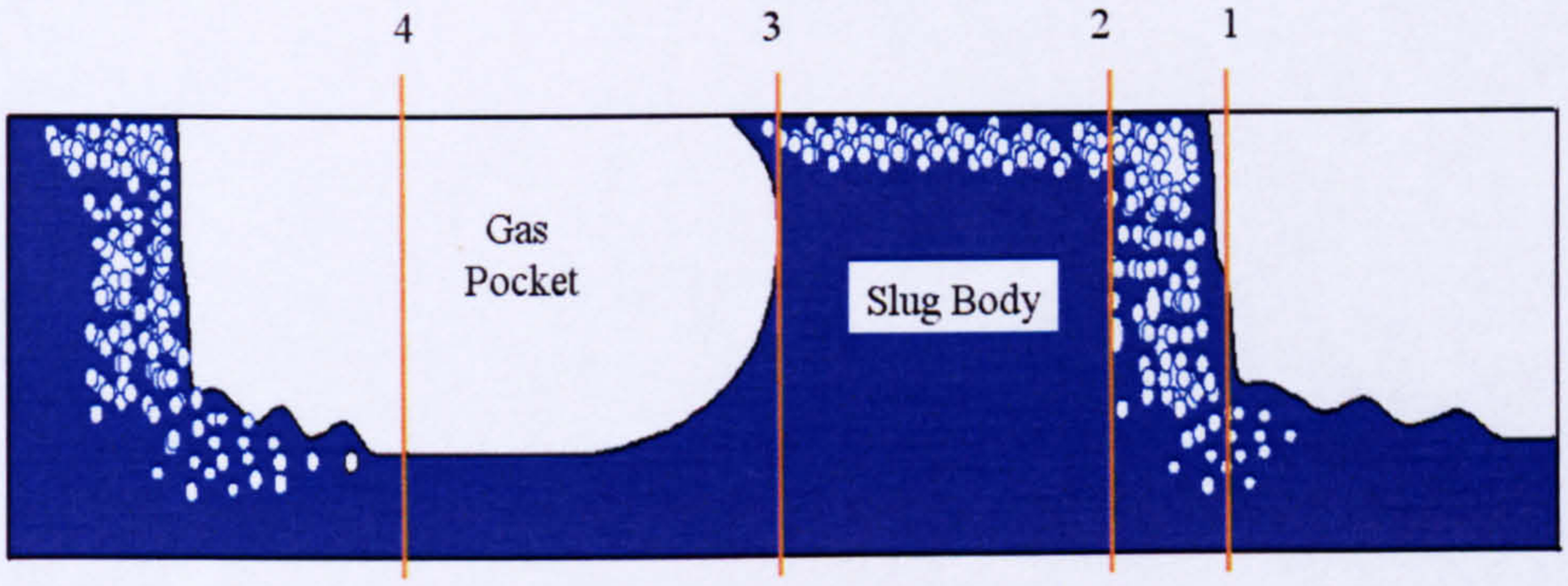

Figure 5-1: Slug Regions

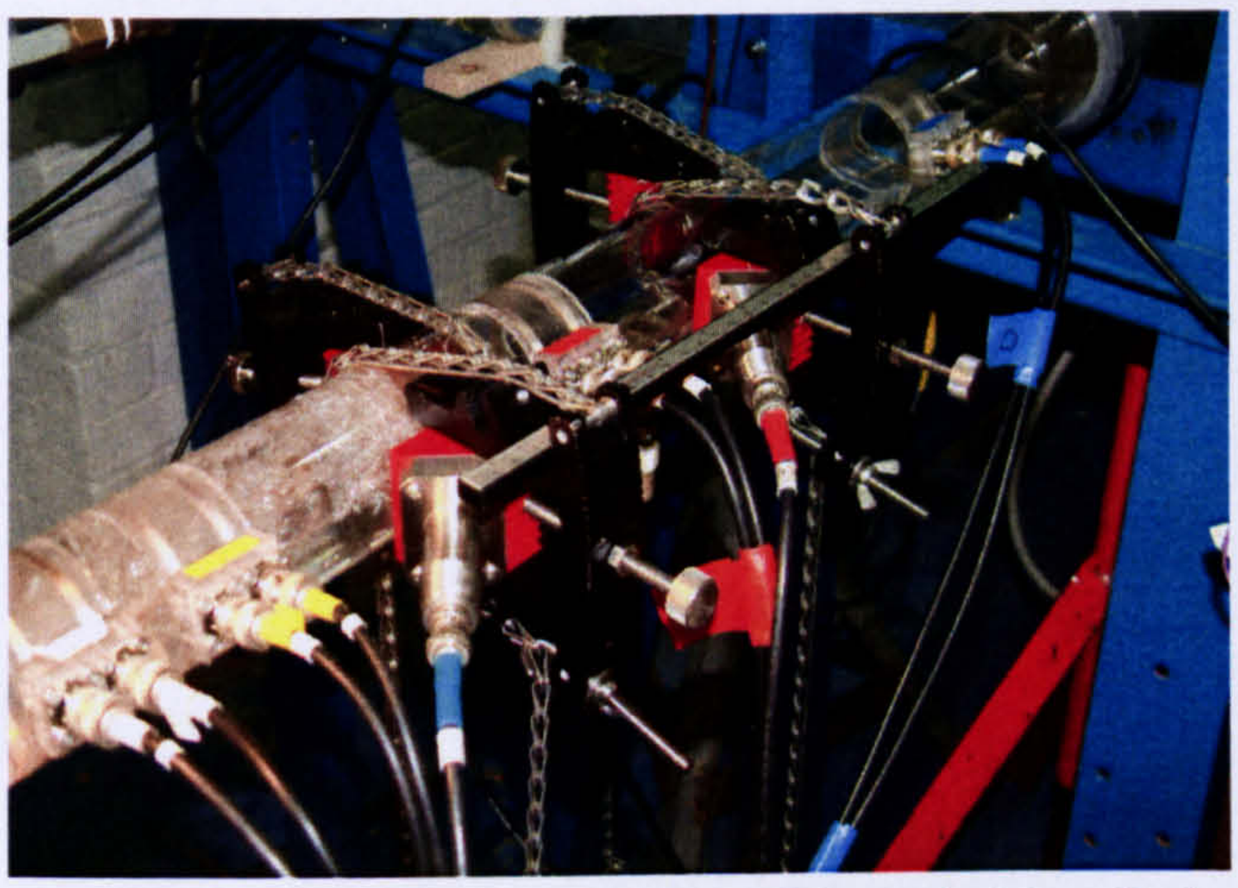

Diametrical Installation of Non-invasive Ultrasonic Sensors Pair 1

Diametrical Installation of Non-invasive Ultrasonic Sensors Pair 2

Figure 5-2: Measuring Section with Ultrasonic Transducers and Conductivity Probes

Installing the ultrasonic transducers diametrically ensures that the slug body is captured and discriminated from the film region. Typical signals through the body and film zones are as shown in Figures 5-3.

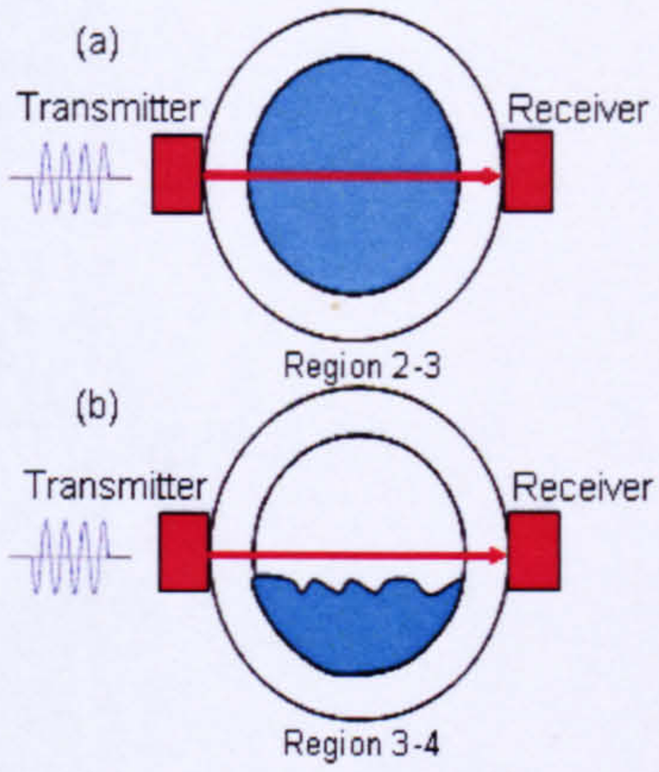

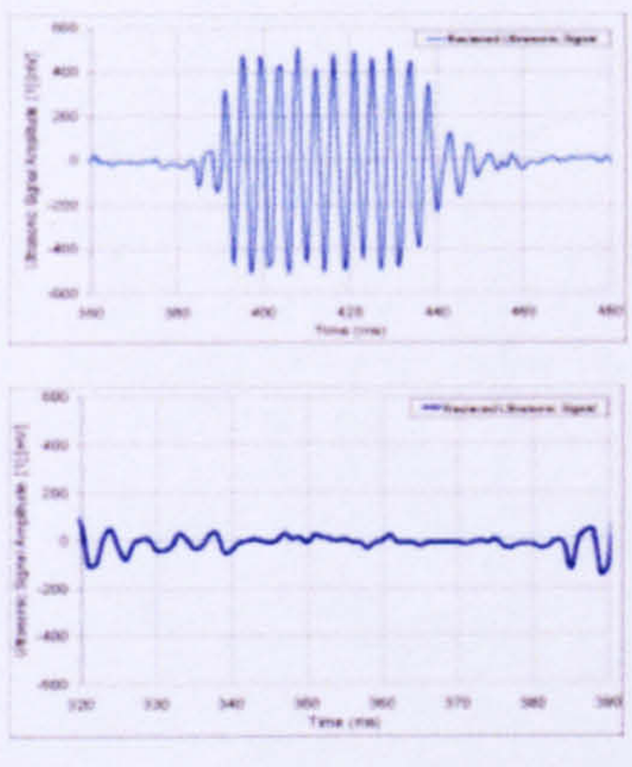

Body of the Slug

Film Zone

Figure 5-3: Non-Invasive Ultrasonic Discriminations for Slug Regions

5.2 Slug Frequency Measurements

In this work, the slug frequency (υ) was measured by non-invasive ultrasonic techniques and the measured values of frequency were validated against the conductivity probe $C_{(C)}$ measurements and compared with the correlations from Gregory and Scott (1969), Azzopardi (1997) and Fossa *et al*. (2003).

The practical method of measuring the slug frequency is by obtaining the number of slugs counted in a given time interval. When the threshold value of the liquid holdup is above a given value, a slug is considered to be established.

The threshold was setup in order to discriminate between the wave passing and slug passing. From statistical analysis applied on the conductivity probe signals under slug flow, Nydal *et al*. (1992) reported threshold liquid holdup values ranged from 0.42 to 0.7.

For the ultrasonic signals, the geometrical threshold value was setup based on the ultrasonic transducers positioned on the outside diameter of the pipe. In this work, the sensors were installed diametrically; therefore the geometrical threshold was setup at 0.5. However, the threshold was setup at 0.7 for the conditioning modulated ultrasonic signals and conductivity signals during the slug body and film zone length analysis.

The slug frequency measurements by both non-invasive ultrasonic technique and conductivity probe $C_{(C)}$ were collected at L /d = 255 downstream from the mixing point. Several tests were performed at various superficial liquid velocities keeping superficial gas velocity constant as listed in Table 5-1.

Table 5-1: Slug Frequency Test Conditions

Tests Conducted	V_{SG} (ms^{-1})	V_{SL} (ms^{-1})
Test 1	0.8	0.3
Test 2	0.8	0.5
Test 3	0.8	0.8
Test 4	0.8	0.9
Test 5	0.8	1.0

The aim of this chosen set of tests was to study the effect of the changes of the superficial liquid velocities on the measured values of slug frequency at a constant superficial gas velocity as shown in Figures 5-4, 5-5, 5-6, 5-7, and 5-8. Also the measured values of slug frequency were investigated at a fixed value of superficial liquid velocity and at various values of superficial gas velocities as listed in Table 5-2 and presented in Figures 5-9, 5-10, and 5-11.

Table 5-2: Slug Frequency Measured at Fixed Superficial Liquid Velocity

Tests Conducted	V_{SL} (ms^{-1})	V_{SG} (ms^{-1})
Test 1	0.5	0.6
Test 2	0.5	0.8
Test 3	0.5	1.25

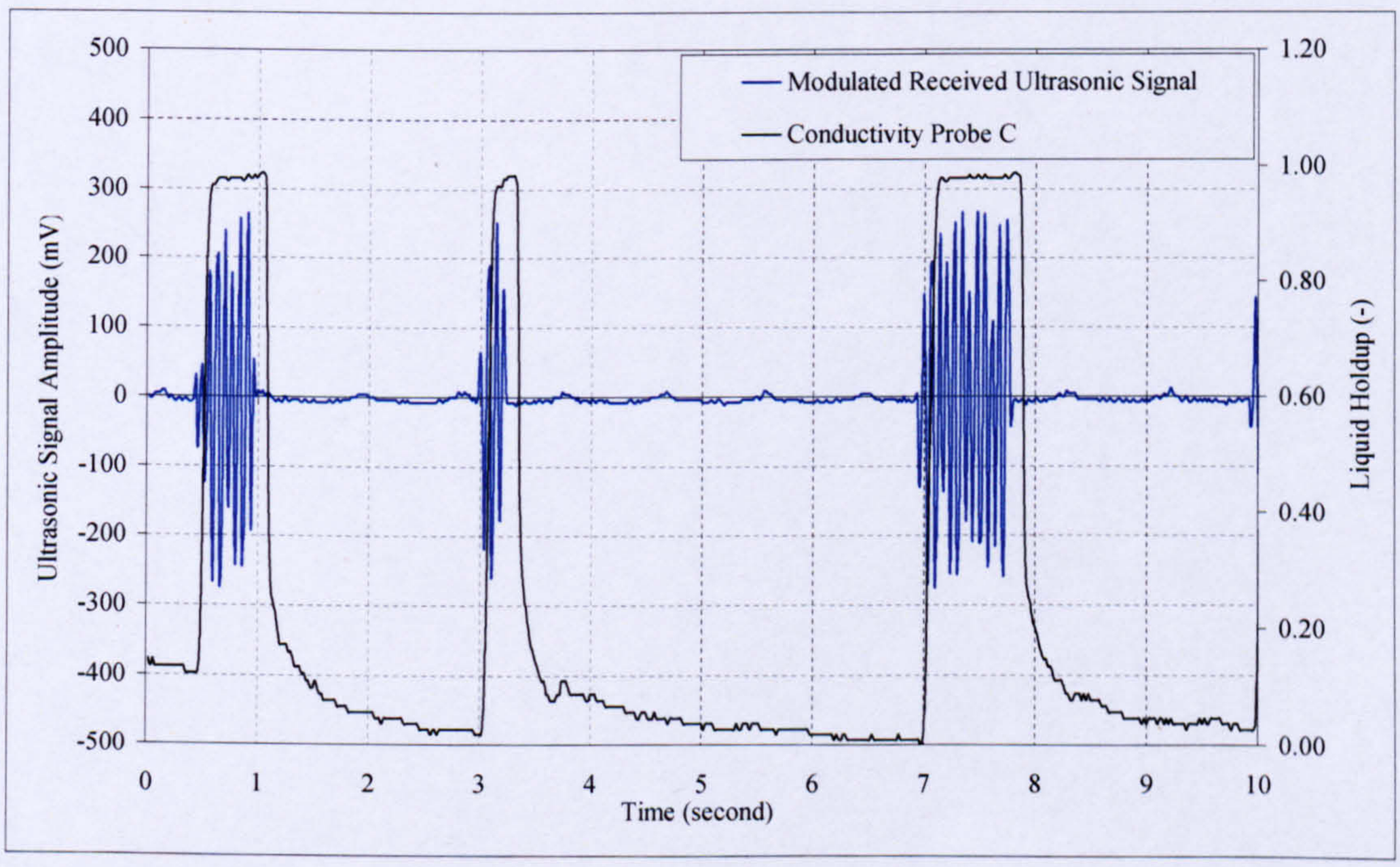

Figure 5-4: Slug Detection at (V_{SG}= 0.8 ms^{-1} and V_{SL}=0.3 ms^{-1})

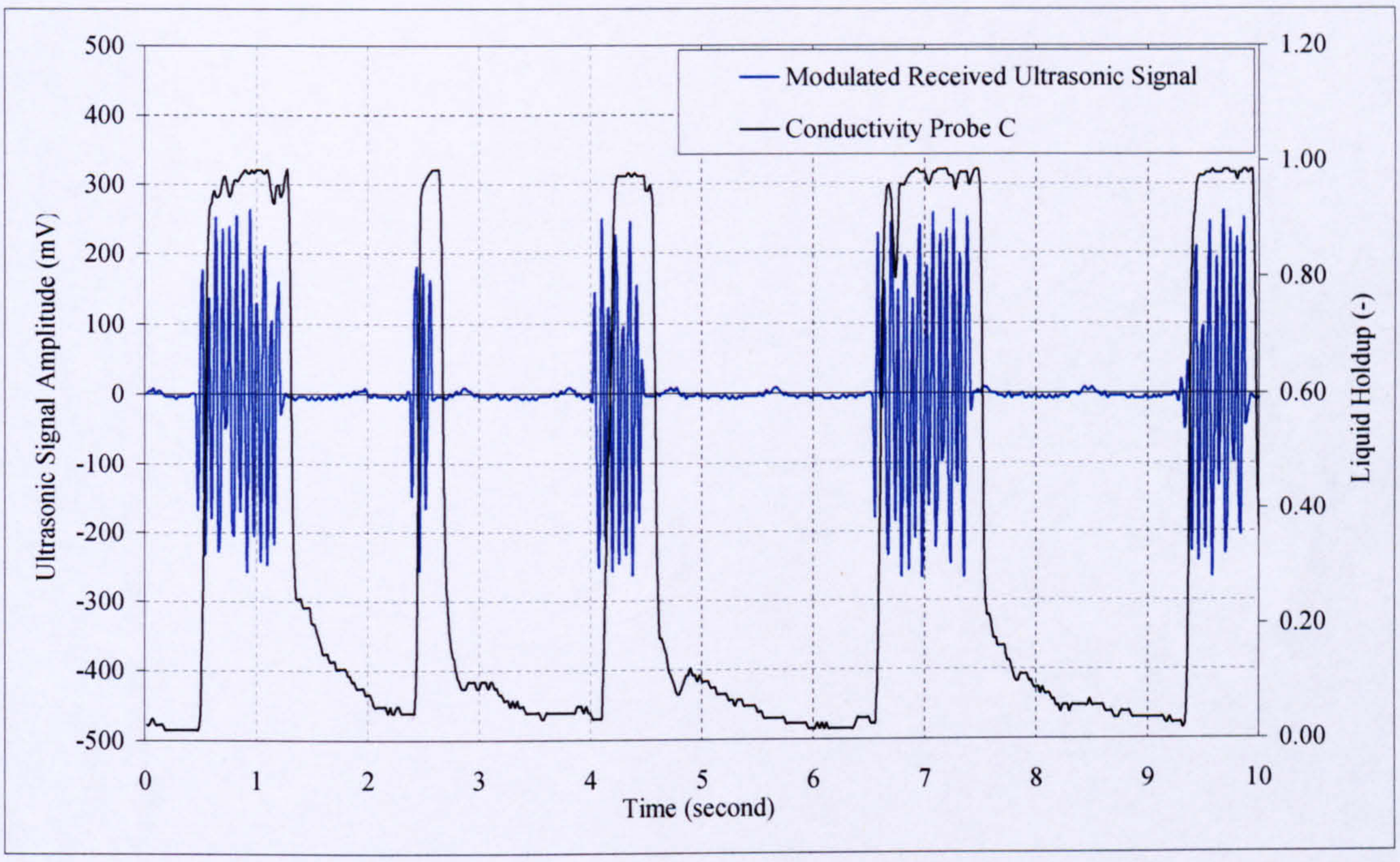

Figure 5-5: Slugs Detection at (V_{SG}= 0.8 ms^{-1} and V_{SL}=0.477 ms^{-1})

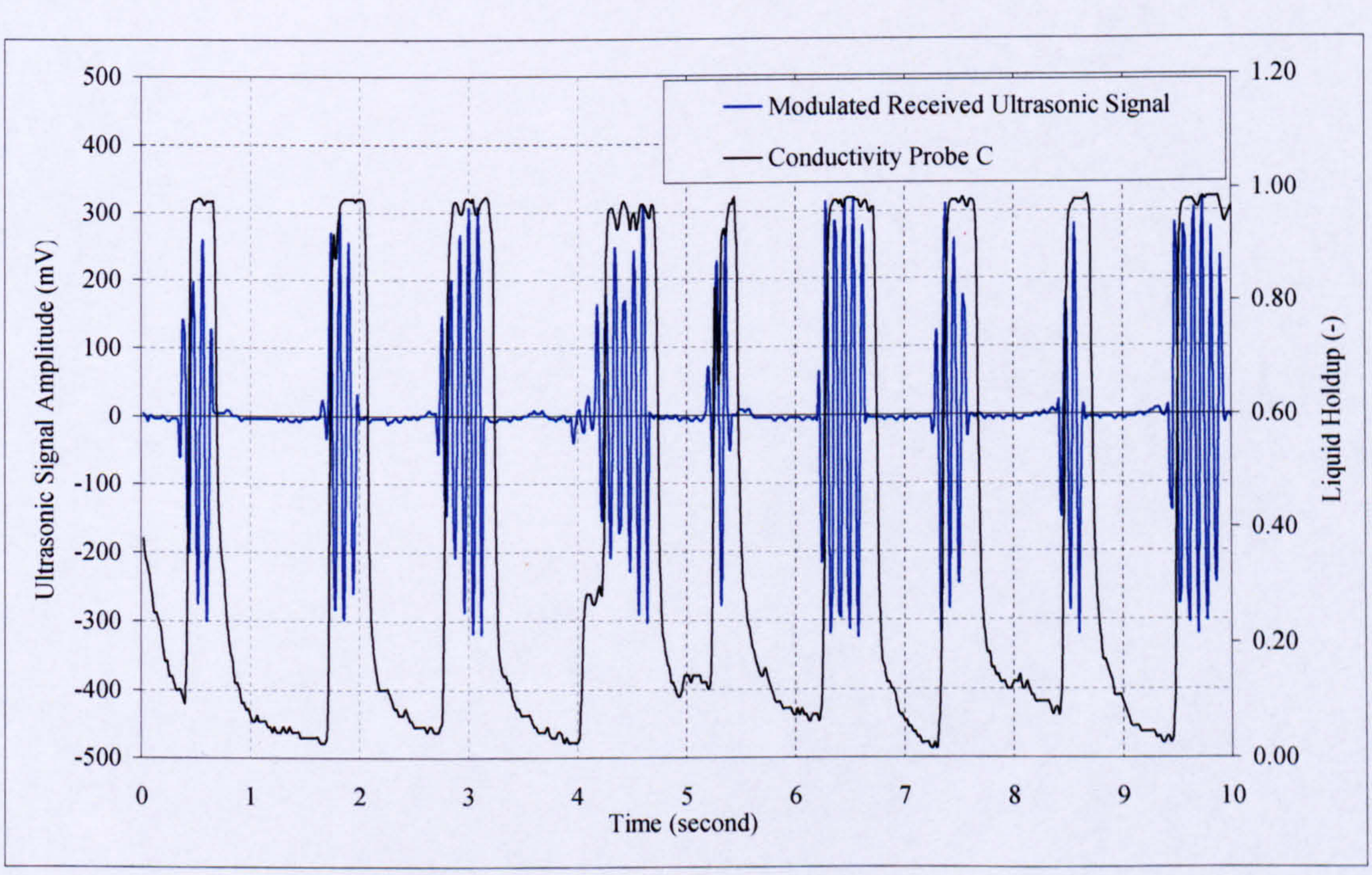

Figure 5-6: Slug Detection at (V_{SG}= 0.8 ms^{-1}, and V_{SL}=0.73 ms^{-1})

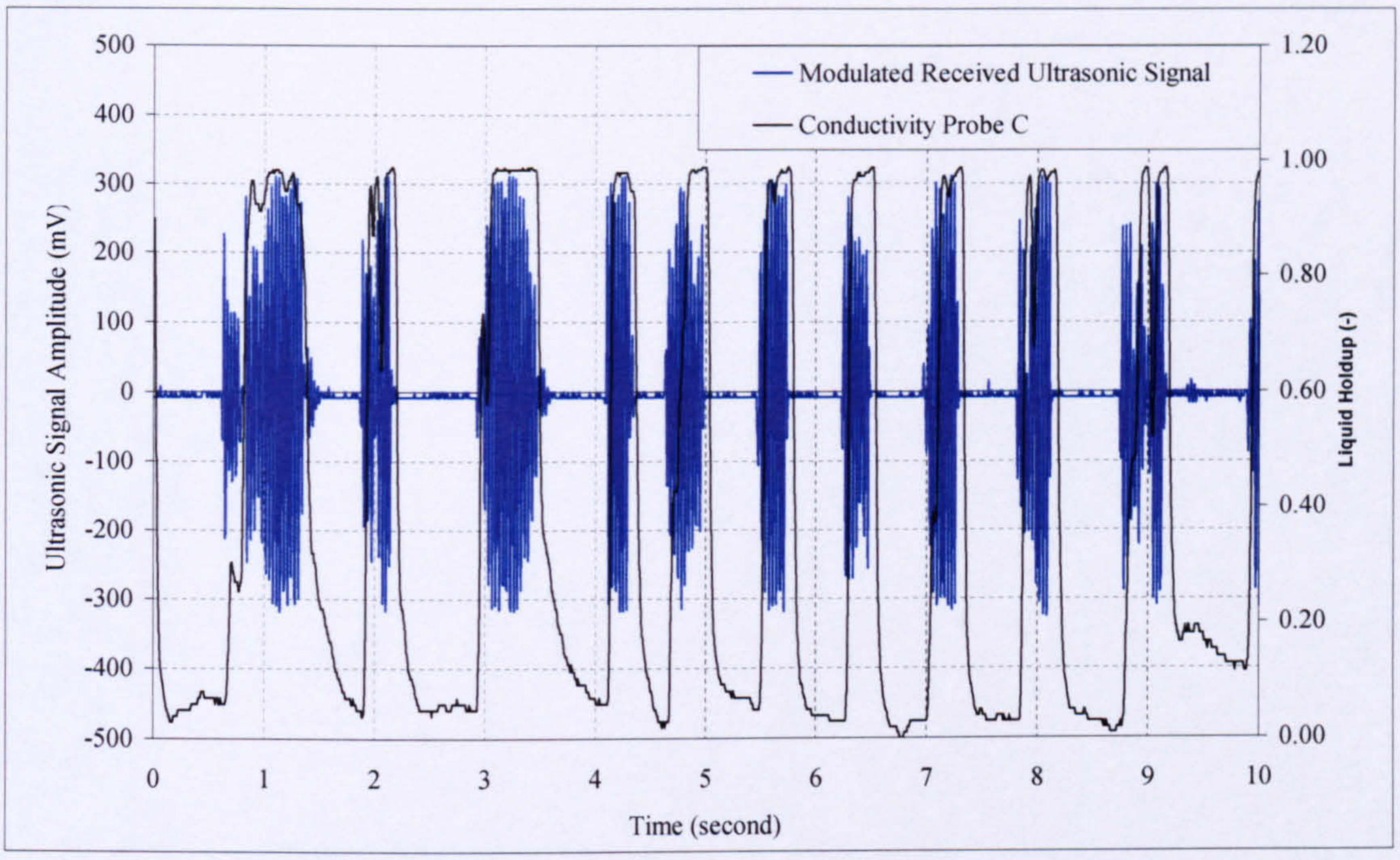

Figure 5-7: Slug Detection at (V_{SG}= 0.8 ms^{-1}, and V_{SL}=0.9 ms^{-1})

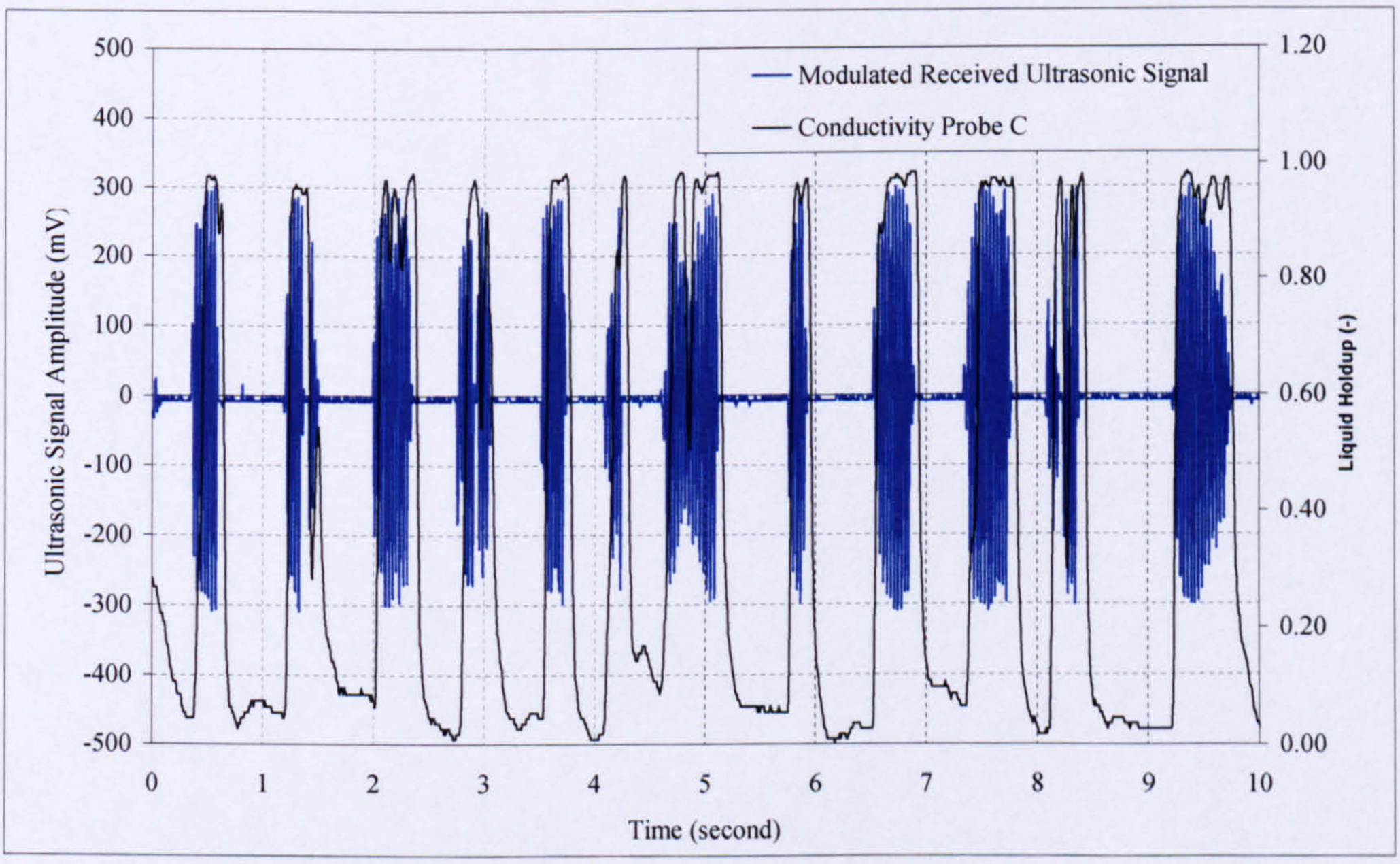

Figure 5-8: Slug Detection at (V_{SG}= 0.8 ms^{-1}, and V_{SL}=1.03 ms^{-1})

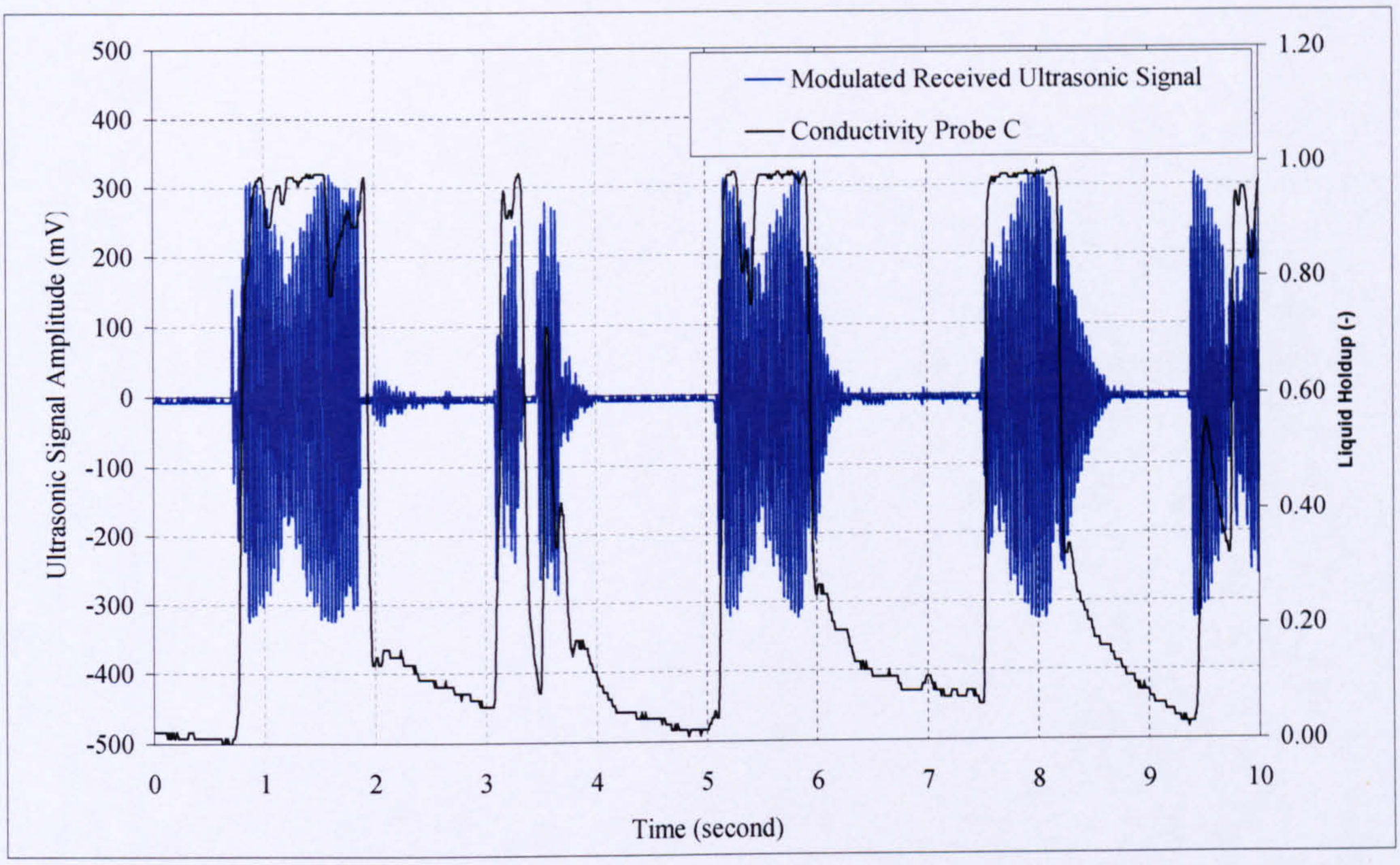

Figure 5-9: Slug Detection at (V_{SL}=0.5 ms^{-1} and V_{SG}= 0.6 ms^{-1})

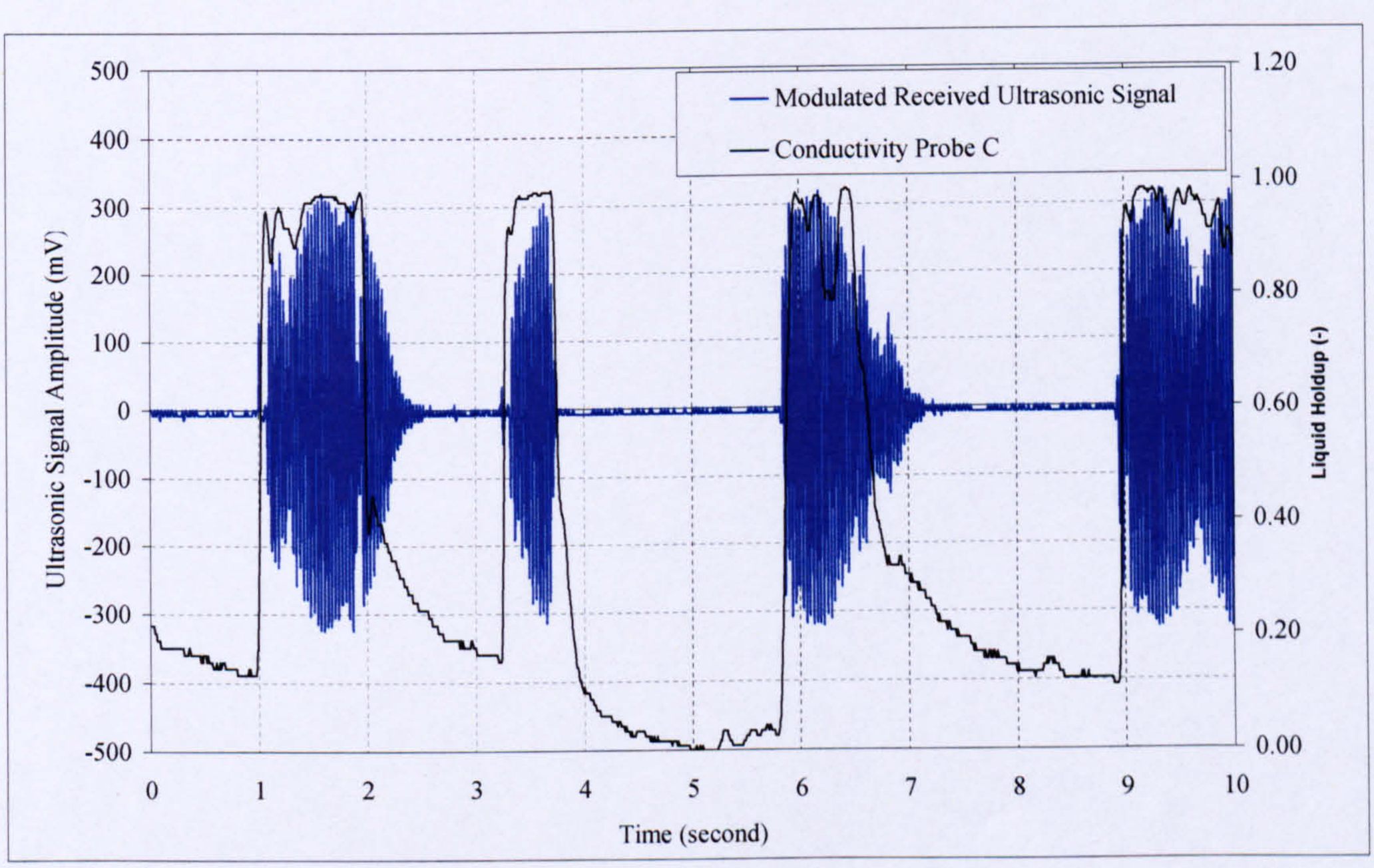

Figure 5-10: Slug Detection at (V_{SL}=0.5 ms^{-1} and V_{SG}= 0.8 ms^{-1})

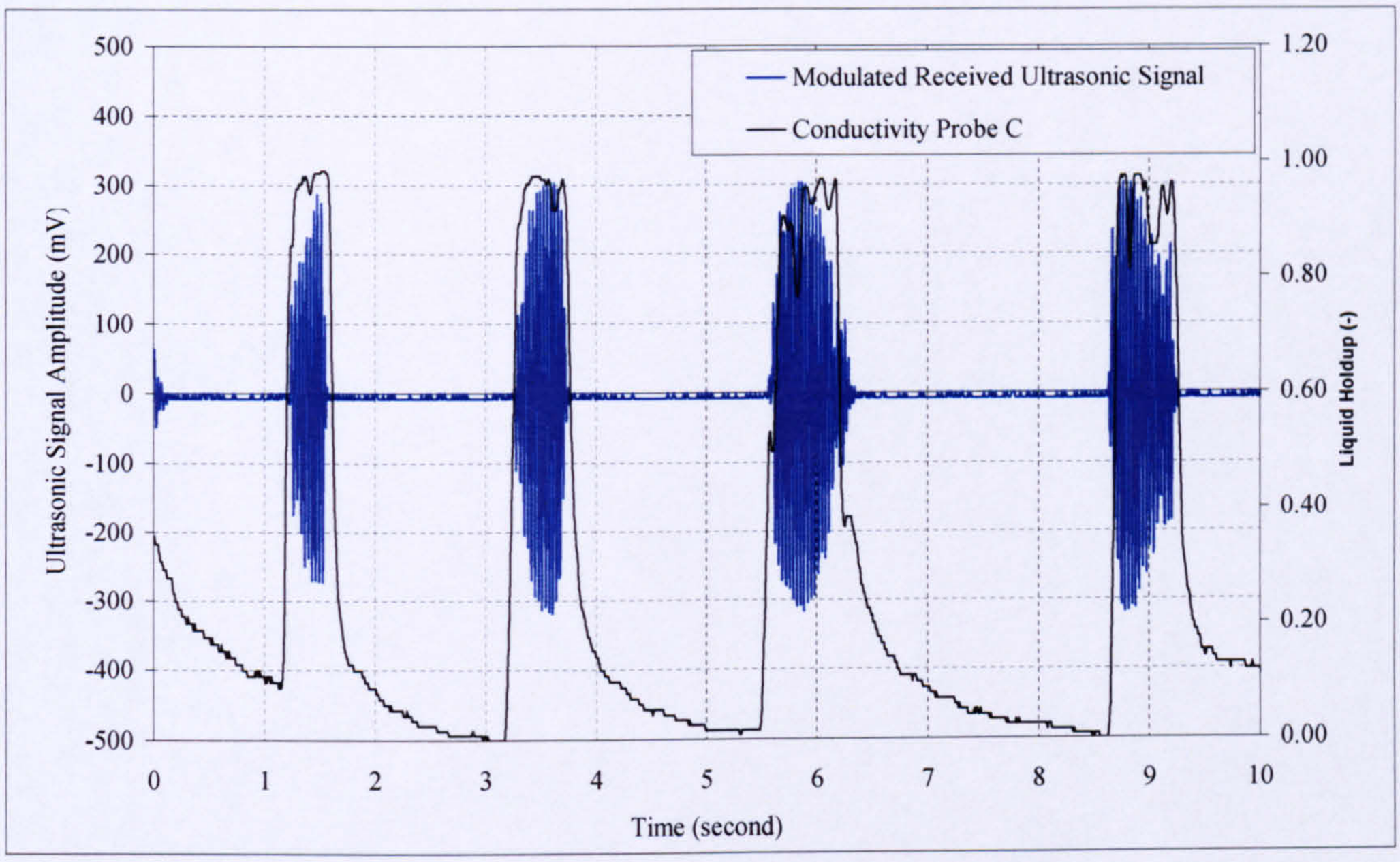

Figure 5-11: Slug Detection at (V_{SL}=0.5 ms^{-1} and V_{SG}= 1.25 ms^{-1})

Based on the range of tests performed under different flow conditions, it was found from the results of the slug frequency presented from Figure 5-5 to Figure 5-8 that the slug frequency shows a very strong dependence on superficial liquid velocity. However from Figure 5-9 to Figure 5-11, the slug frequency increases only slightly with the increase of the superficial gas velocity.

In this work, the slug frequency measure by a non-invasive ultrasonic method was compared with the slug frequency correlation developed by Azzopardi, (1997) and Fossa *et al.* (2003) and was validated against the conductivity probe measurements.

This method is based on validating the slug frequency in term of the Strouhal number:

$$St = \frac{v \times D}{V_{SG}} \qquad (5.1)$$

In this case the slug frequencies measured were plotted in terms of the Strouhal number against the liquid volumetric fraction X_L.

Fossa *et al.* (2003) developed an empirical correlation for Strouhal number based on experimental investigations. The study refers to air-water horizontal flows in 60 and 40 mm inner-diameter pipes. The operating tests conditions range from (0.3–4.0 ms^{-1}, and 0.6–3.0 ms^{-1}) for gas and liquid superficial velocity respectively. Intermittent flows

(plug and slug) were observed. The slug frequency equation was developed by Fossa *et al.* (2003) is given as:

$$St_{(Fossa)} = \frac{\nu \times D}{V_{SG}} = \frac{A \times X_L}{1 + B \times X_L + C \times (X_L)^2} \tag{5.2}$$

where
A= 0.044 , B= -1.71, and C = 0.70 and
X_L is the liquid volumetric fraction and is given as $X_L = V_{SL}/V_{mix}$.

The slug frequency equation was developed by Gregory and Scott (1969) is given as:

$$\nu_{Gregory} = 0.0226 \times \left[\frac{V_{SL}}{gd} \times \left(\frac{19.75}{V_{mix}} + V_{mix} \right) \right]^{1.2} \tag{5.3}$$

Figure 5-12 presents the comparison of Strouhal number obtained in the present work with that obtained from the empirical correlations developed by Fossa *et al.* (2003), and Gregory and Scott (1969) and the following conclusions were made:

- The slug frequency expressed in terms of Strouhal number in this work exhibits the same trends as that obtained by Fossa *et al.* (2003) and Gregory and Scott (1969).

- From this data it is clear that slug frequency values increases by increasing the superficial liquid velocity.

- The correlation of Gregory and Scott (1969) shows good agreement with the data obtained in this work.

- The correlation of Fossa *et al.* (2003) provides a good match to the present work data, however, beyond 0.57 liquid volumetric fractions, the difference increases marginally. This probably because the constants (A, B and C) in Fossa *et al.* (2003) correlation were based on his own experimental data.

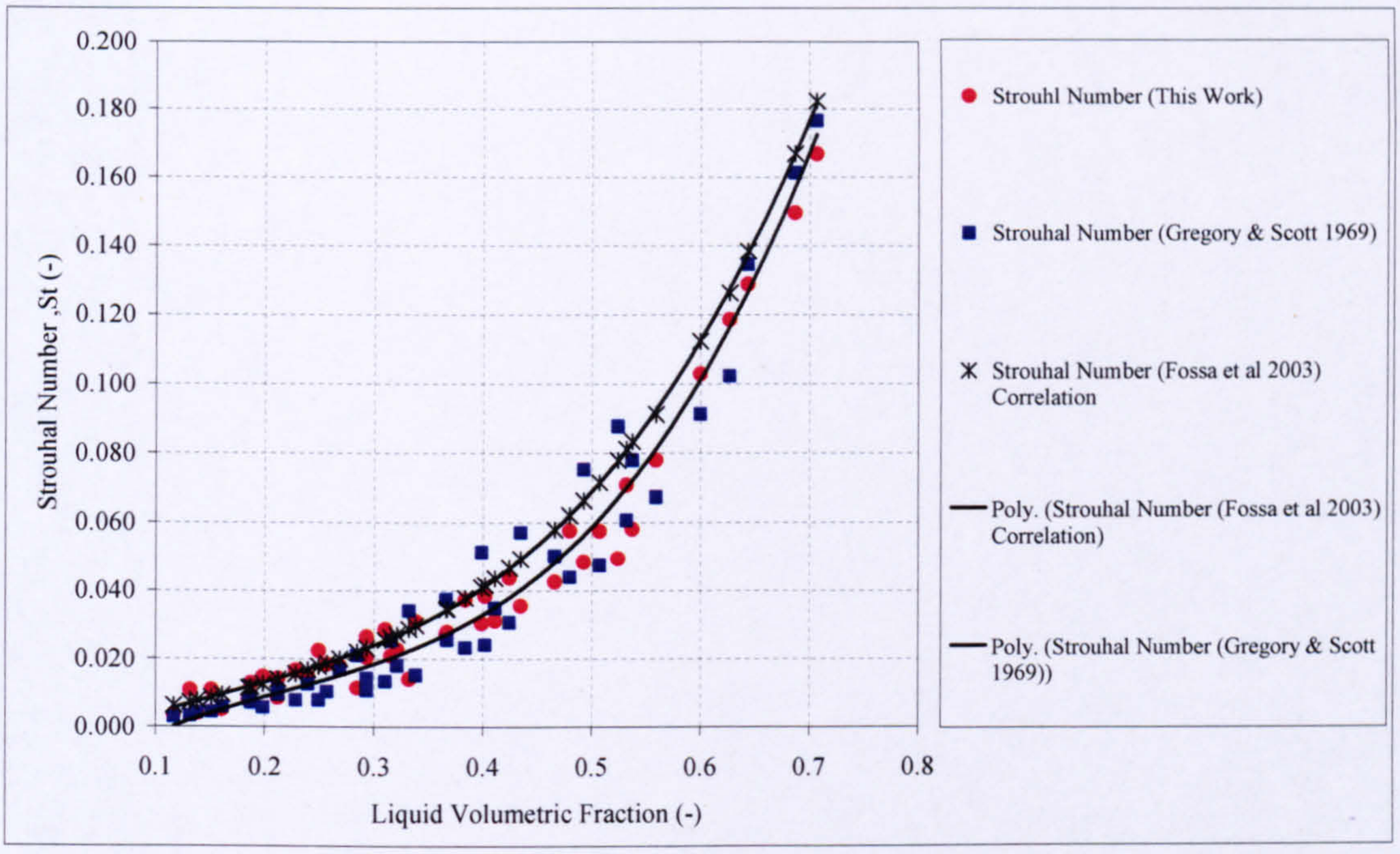

Figure 5-12: Strouhal Number vs. Liquid Volumetric Fraction

5.3 Slug Translational Velocity Measurements

The ultrasonic cross-correlation technique is an attractive approach to measure the slug translational velocity because it can be non-intrusive or non-invasive and does not require information of the speed of sound of the fluid. Cross-correlation technique was applied to the signals from two pairs of ultrasonic transducer installed apart to calculate the slug translational velocity, V_T.

To validate the slug translational velocity determined by ultrasonic technique, the cross-correlation technique was also applied to the signals from the two conductivity probes $C_{(C)}$ and $C_{(D)}$ as shown in Figure 5-13.

. Two upstream and two downstream ultrasonic transducers with 1MHz frequency were installed in the pipeline with a known spacing $L_{(U)} = 0.18$ m. The two conditioned modulated received ultrasonic signals were cross-correlated according to the following equation:

$$R_{xy} = \frac{1}{T}\int_0^T x(t-\tau)y(t)\,dt \qquad (5.4)$$

where
R_{xy} is the cross correlation function,
T is extraction duration and

x(t-τ) and y(t) are the two ultrasonic signals at time (t-τ) and (t)respectively. The time delay $\tau_{(u)}$ are when the value of Rxy was at maximum. The slug translational velocity is determined by:

$$V_{T(U)} = \frac{L_{(U)}}{\tau_{(U)}} \tag{5.5}$$

where

$V_{T(U)}$ is the slug translational velocity measured by ultrasonic technique,

$L_{(U)}$ is the known separation distance between the two-pair of ultrasonic transducer and $\tau_{(U)}$ is the time delay obtained by cross-correlation technique between the two ultrasonic signals.

For validation purpose, the slug translational velocity was also obtained by correlating the signals of conductivity probes $C_{(C)}$ and $C_{(D)}$ as given by:

$$V_{T(C\text{-}D)} = \frac{L_{(C\text{-}D)}}{\tau_{(C\text{-}D)}} \tag{5.6}$$

where

$V_{T(C\text{-}D)}$ is the slug translational velocity determined from the conductivity probes $C_{(C)}$ and $C_{(D)}$,

$L_{(C\text{-}D)}$ is the known separation distance between the two conductivity probes $C_{(C)}$ and $C_{(D)}$ and

$\tau_{(U)}$ is the time delay obtained by cross-correlation technique between two conductivity probes $C_{(C)}$ and $C_{(D)}$.

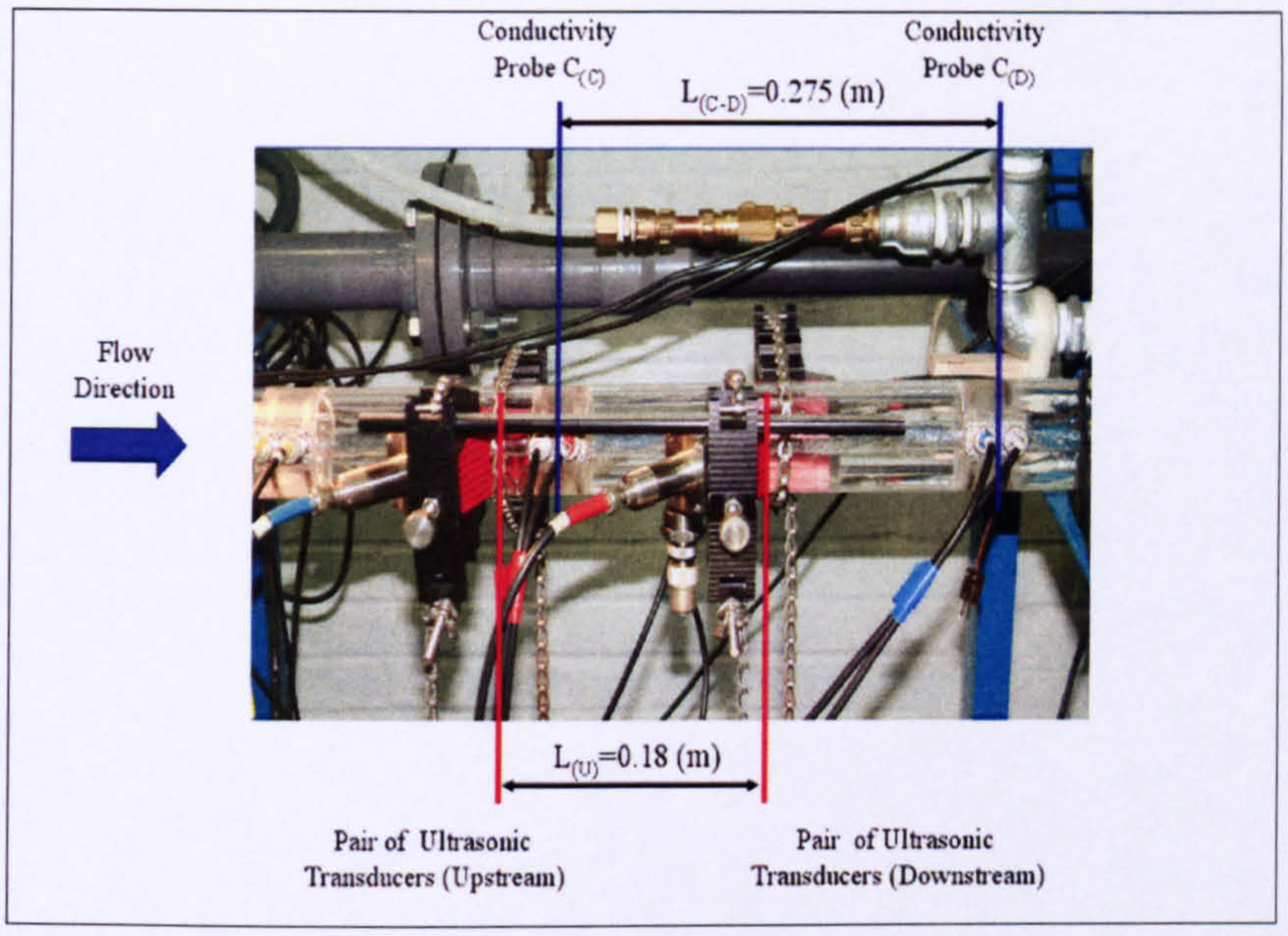

Figure 5-13: Arrangement of the Ultrasonic Transducers and Conductivity Probes

Figures 5-14, 5-15 and 5-16 show the upstream and downstream modulated received ultrasonic signals at different flow conditions. The ultrasonic signals follow the same pattern which duplicated the slugs shape.

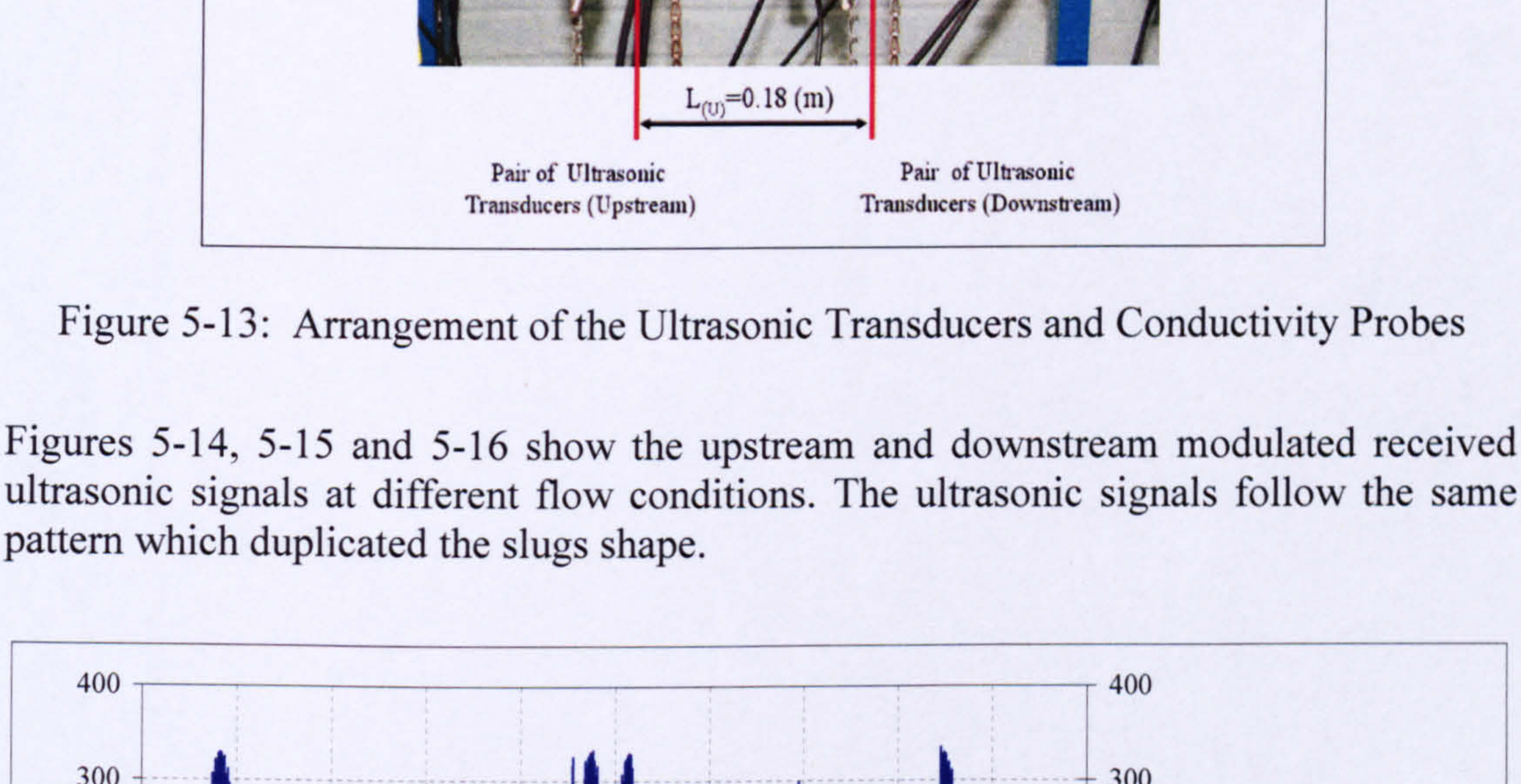

Figure 5-14: Modulated received Ultrasonic Signals at V_{SL}=0.3 ms^{-1}, V_{SG}= 1.06 ms^{-1}

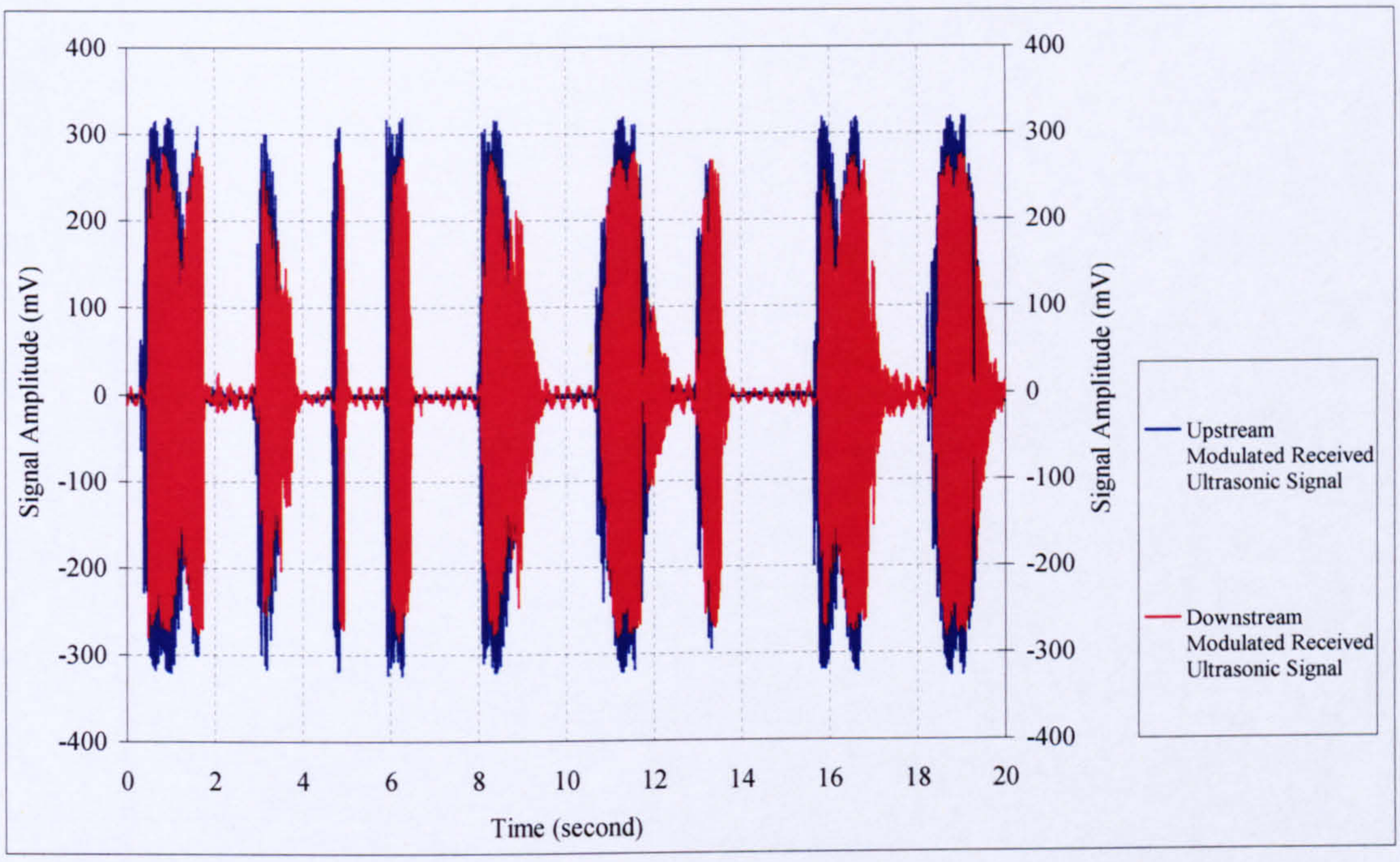

Figure 5-15: Modulated received Ultrasonic Signals at V_{SL}=0.5 ms^{-1}, V_{SG}= 0.8 ms^{-1}

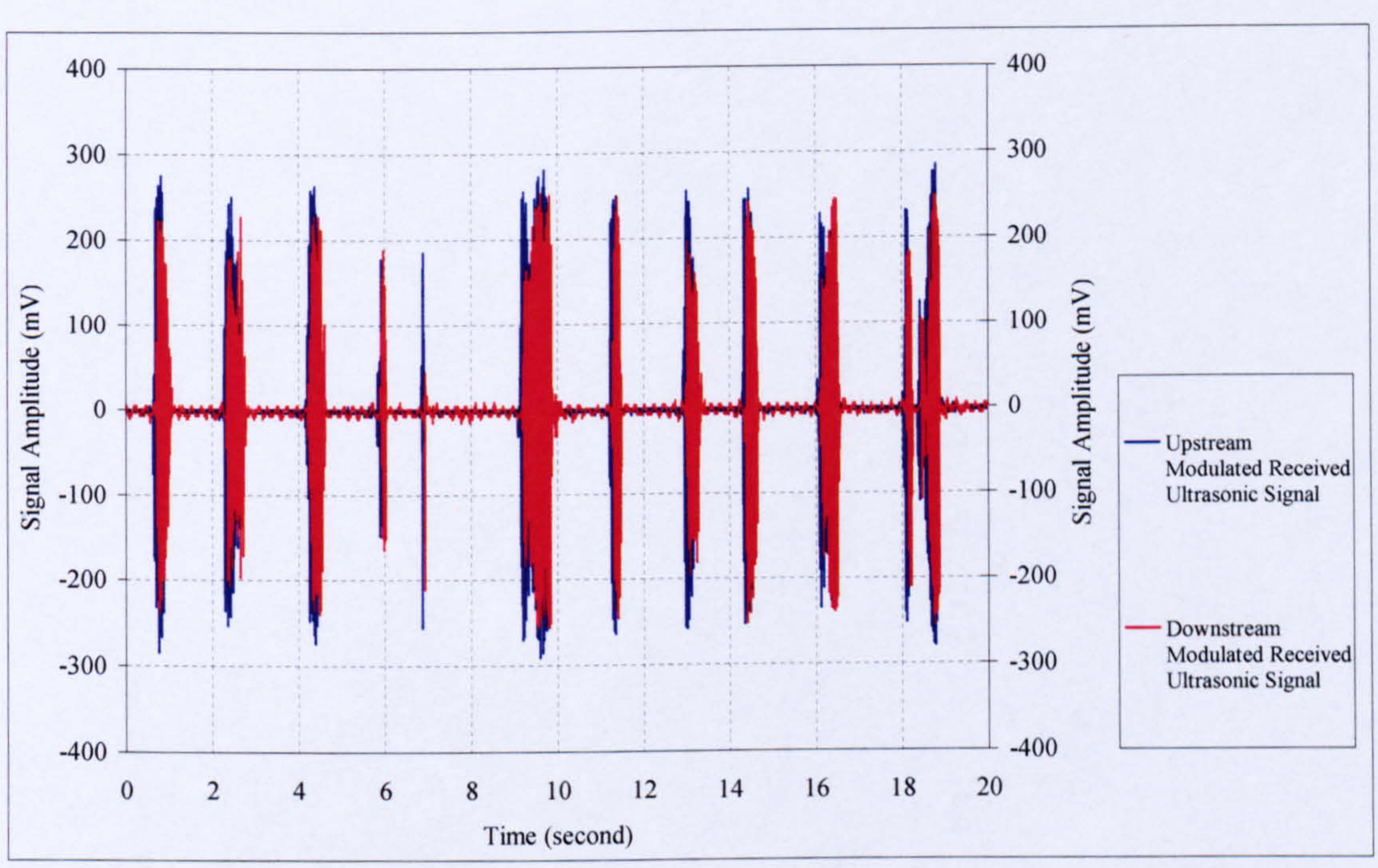

Figure 5-16: Modulated received Ultrasonic Signals at V_{SL}=0.7 ms^{-1}, V_{SG}= 1.51 ms^{-1}

To cross correlate the upstream and downstream modulated ultrasonic signals the ultrasonic signals envelope must be extracted as shown in Figures 5-17 and 5-18. The subroutine "xcorrel" was written using Matlab version 7.1 for the analysis.

The ultrasonic signals envelop was obtained using the signal conditioning unit as described in Section 4.1.2.2.2. By extracting the ultrasonic signal envelop the edge in the signal for each slug becomes clearer and then the cross-correlation technique can be accurately applied.

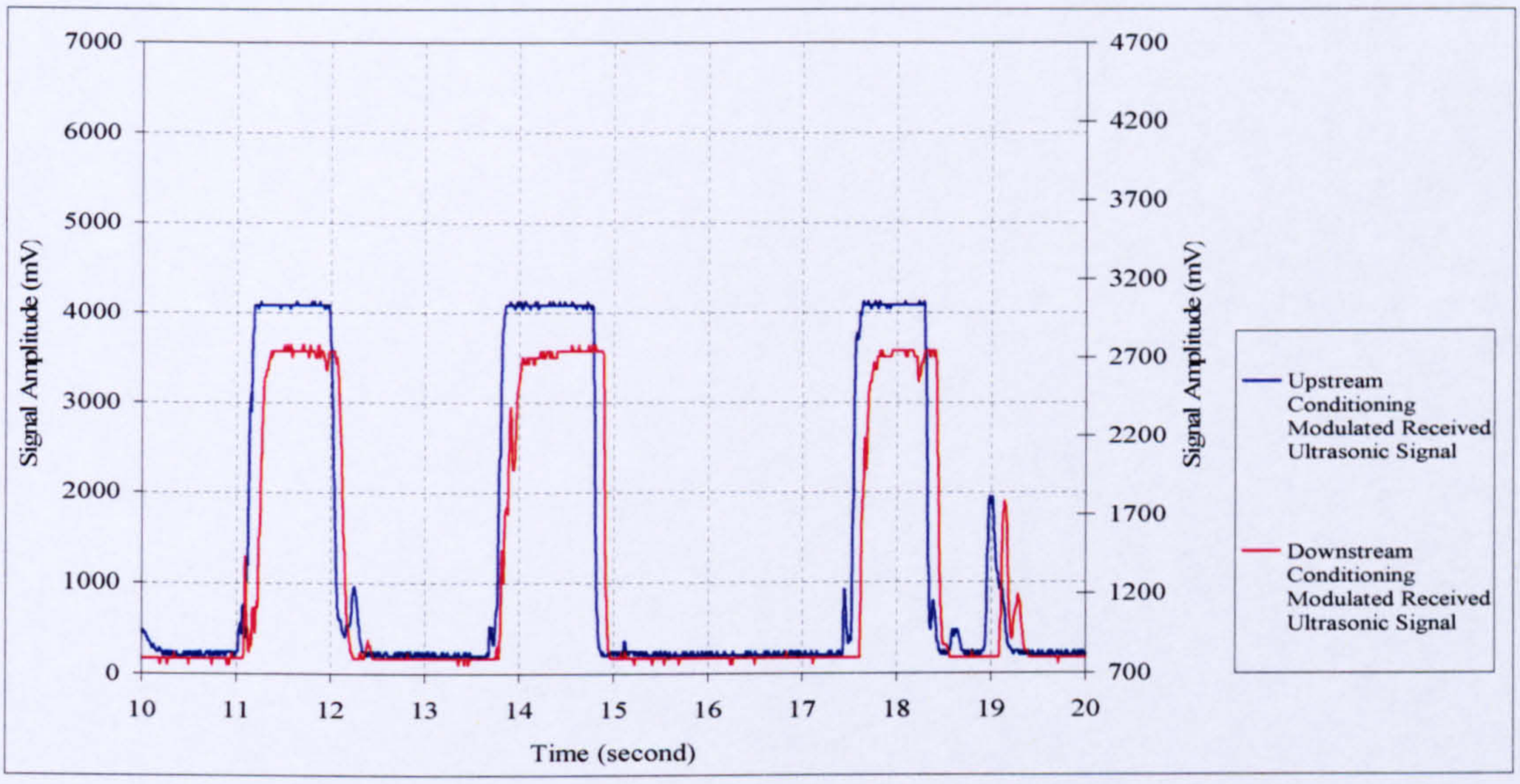

Figure 5-17: Ultrasonic Signals Envelop at V_{SL}=0.5 ms^{-1}, V_{SG}= 1.01 ms^{-1}

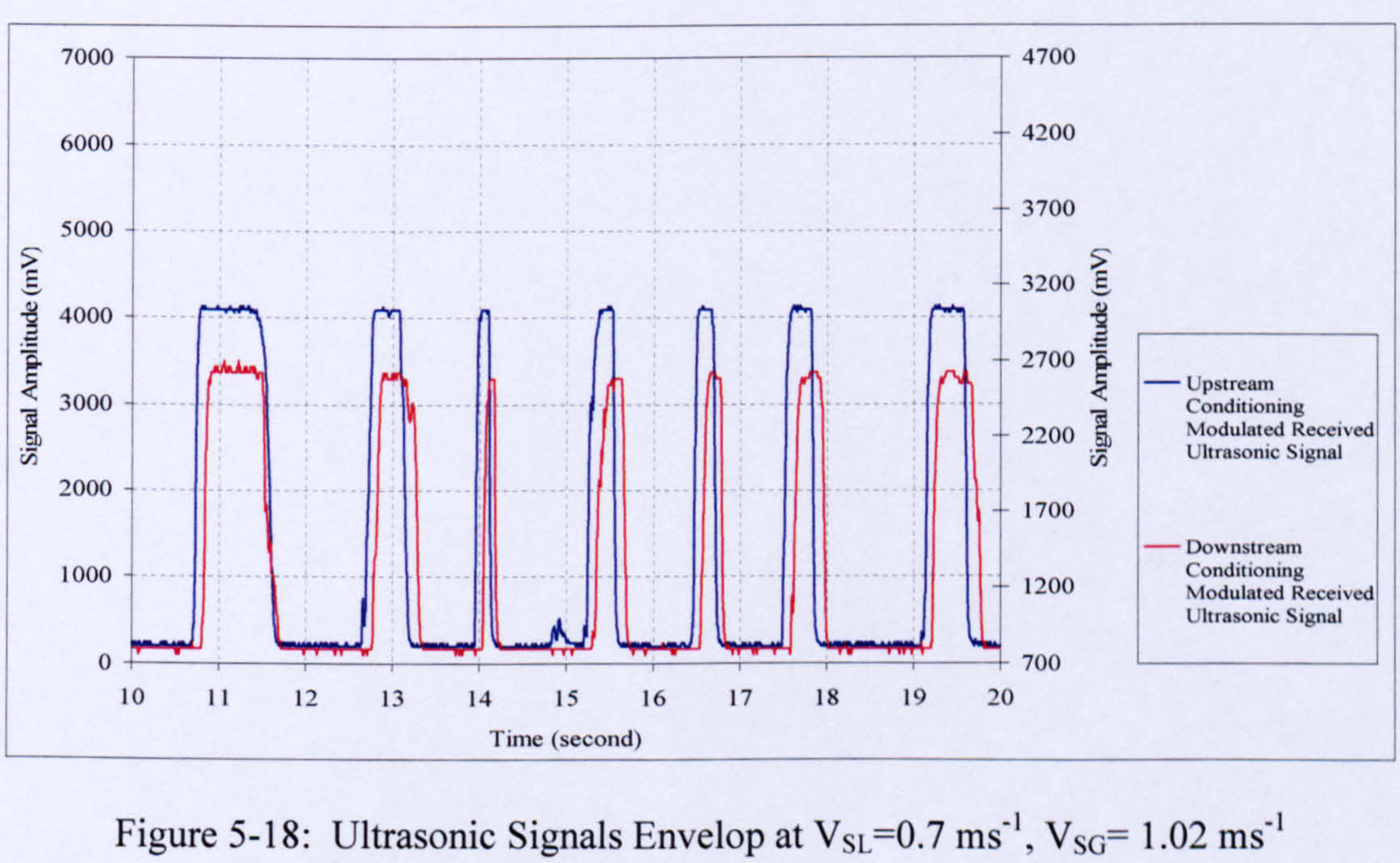

Figure 5-18: Ultrasonic Signals Envelop at V_{SL}=0.7 ms^{-1}, V_{SG}= 1.02 ms^{-1}

To validate the slug translational velocity measured by non-invasive ultrasonic technique, cross-correlation technique was also applied on the conductivity probes $C_{(C)}$ and $C_{(D)}$ signals as shown in Figure 5-19.

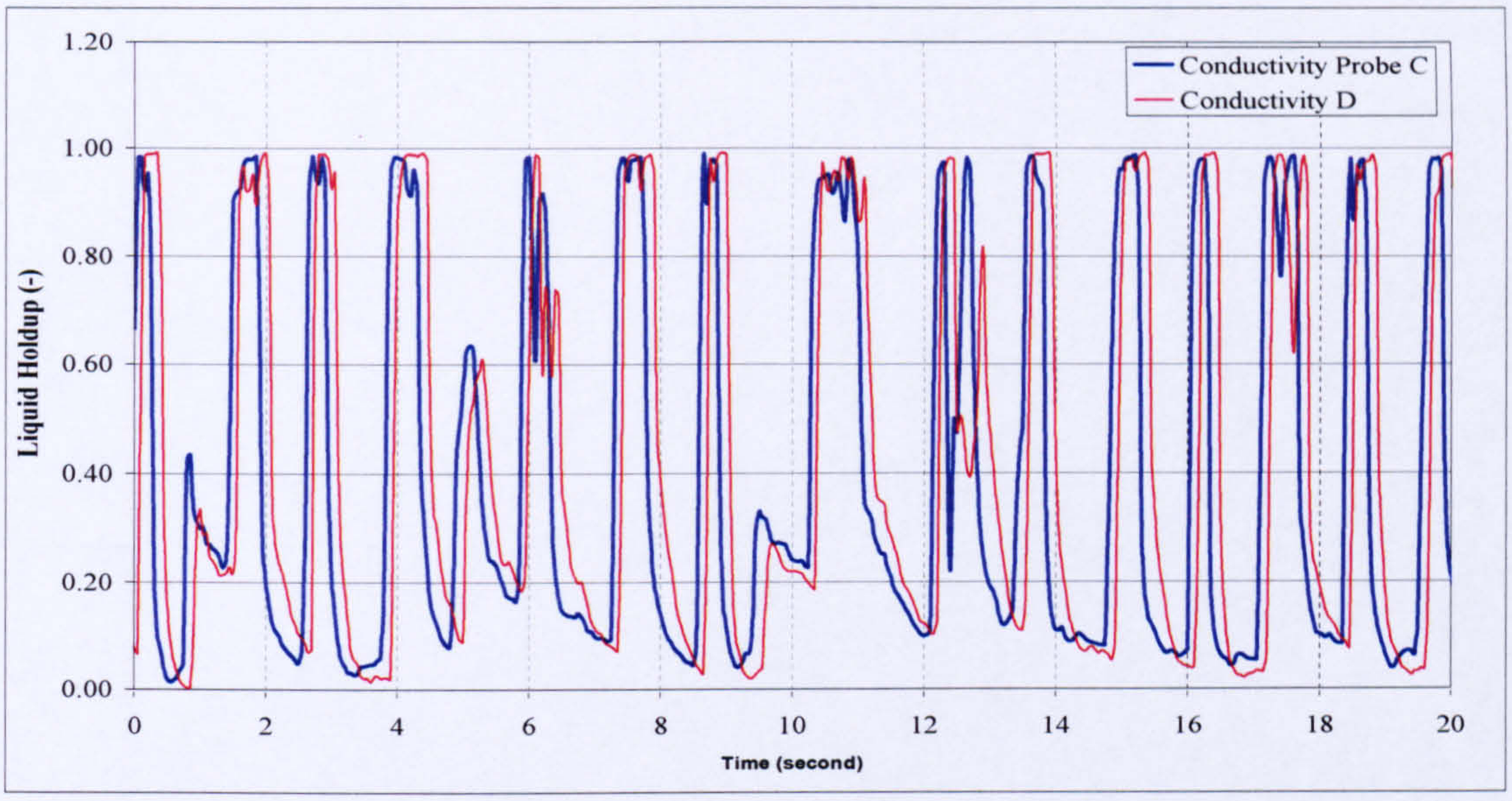

Figure 5-19: Conductivity Probes $C_{(C)}$ and $C_{(D)}$ V_{SL}=0.7 ms^{-1}, V_{SG}= 1.02 ms^{-1}

The standard deviation (95.4% confidence (±2σ)) of the slug translational velocities measured by ultrasonic techniques was ±2.939., see Appendix A Figure 5-20 represents the validation of slug translational velocity $V_{T(U)}$ measured by ultrasonic technique with the conductivity measurements technique $V_{T(C-D)}$.

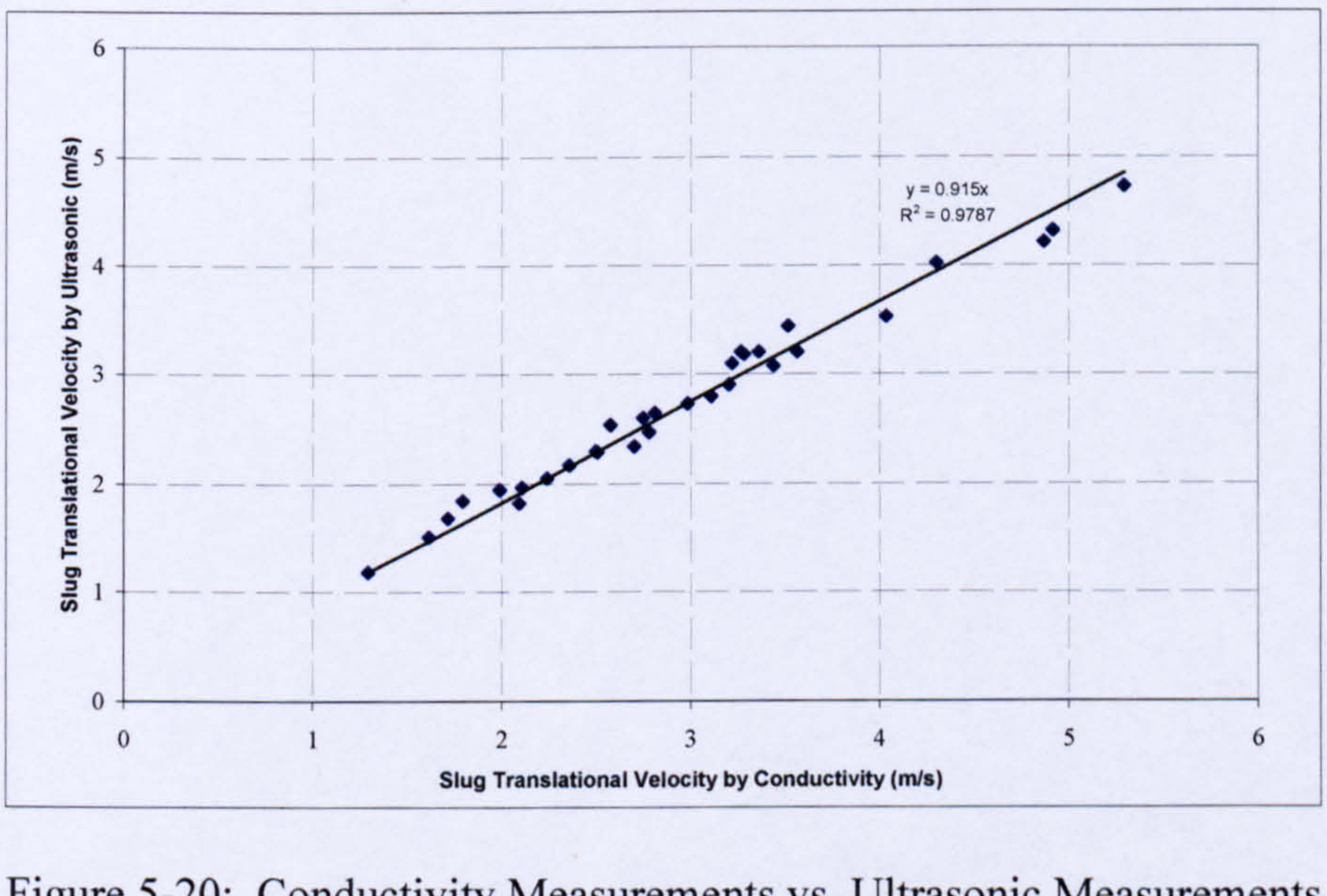

Figure 5-20: Conductivity Measurements vs. Ultrasonic Measurements

From the comparison between the non-invasive ultrasonic and conductivity techniques, it was found that the relative percentage error range from 2.9% up to 13.6%.

5.4 Slug Body Length and Film Region Length Measurements

To obtain the slug length distributions, the time of the slug passing must be measured. The width of the conditioning modulated ultrasonic signal gives the time of the slug body passage t_{Slug}.

The slug body passing time t_{Slug} and the film region time t_{Film} were measured by means of applying the threshold level processing on the conditioned modulated ultrasonic signals using Matlab 7.1. The operating principle of the threshold level processing method is summarised as follows:

- First of all, the ultrasonic signal is normalised.
- The normalised ultrasonic signal data was scanned point-by-point, and the positions at which the threshold level processing was crossed were stored. Threshold level, θ, was obtained based on the following factors as recommended by Stewart (2001) and Nydal *et al.* (1992):

    1. The threshold level, θ, should be as high as possible to ensure that only the slug body is identified and not the rising or falling edges (0.7).

    2. The threshold level, θ, should not be too high; otherwise the slug body is not identified at all.

    3. As results, the best way to optimise θ is by a trial and error process in order to obtain good results for both conductivity signal and conditioned modulated ultrasonic signals.

    4. Based on their experimental analysis on the slug body holdup obtained from the conductivity measurements, Stewart (2001) and Fossa *et al.* (2003) suggested the value of θ to be between 0.42 and 0.8. However, the authors recommended that the value of θ should be reduced at large gas superficial velocities since the slug body liquid holdup E_{LS} decreases.

- The difference in time between successive crossings (falling edge of the first successive passing slug and rising edge of second successive passing slug) is considered to be the time duration of the film region passing $t_{(Film)}$ as shown in Figure 5-21.

In the Figure 5-21 at test conditions of V_{SL}=0.4 ms^{-1} and V_{SG}=0.8 ms^{-1}, the slug body passing time ($t_{Slug(U)}$) and the film region passing time $t_{Film(U)}$ were computed using threshold level analysis.

It is clear from this figure, the successful discrimination within the slug unit between the slug body and film region, also between the slug passing and wave passing.

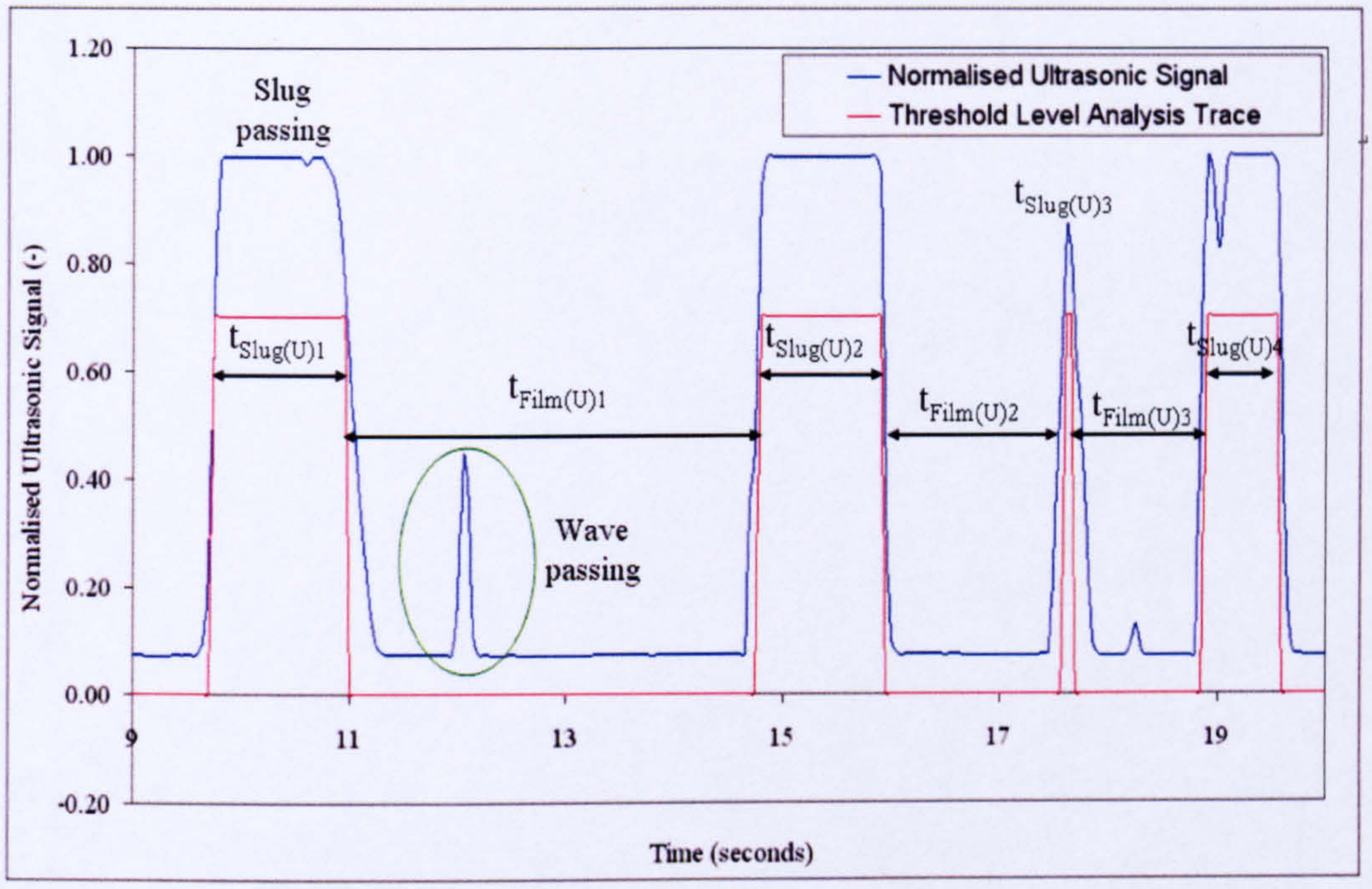

Figure 5-21: Threshold Level Analysis applied on the Normalised Ultrasonic Signal

- The average slug length then calculated from the given equation:

$$\overline{L_{(SU)}} = \overline{t_{Slug(U)}} \times \overline{V_{T(U)}} \quad \text{and} \quad \overline{L_{(FU)}} = \overline{t_{Film\,(U)}} \times \overline{V_{T(U)}} \tag{5.7}$$

where

$\overline{L_{(SU)}}$ is the average slug length ,

$\overline{t_{Slug(U)}}$ is the average slug body passing time,

$\overline{L_{(FU)}}$ is the average film region length,

$\overline{t_{Film\,(U)}}$ is the average film region passing time and

$\overline{V_{T(U)}}$ is the average slug translational velocity determined by non-invasive ultrasonic technique

The total average length of the slug unit is given as:

$$\overline{L(U)_{(U)}} = \overline{L_{(SU)}} + \overline{L_{(FU)}} \tag{5.8}$$

At V_{SL}=0.5 ms^{-1} and V_{SG}=0.8 ms^{-1} test, the time of the passing of the slug body $t_{Slug\,(U)}$ measured by non-invasive ultrasonic is presented in Figure 5-22.

At the same test condition, the time of the passing of the film region $t_{Film\,(U)}$ is shown in Figure 5-23.

The lengths of slug body and film region obtained from equation (5.7) are illustrated in Figures 5-24 and 5-25.

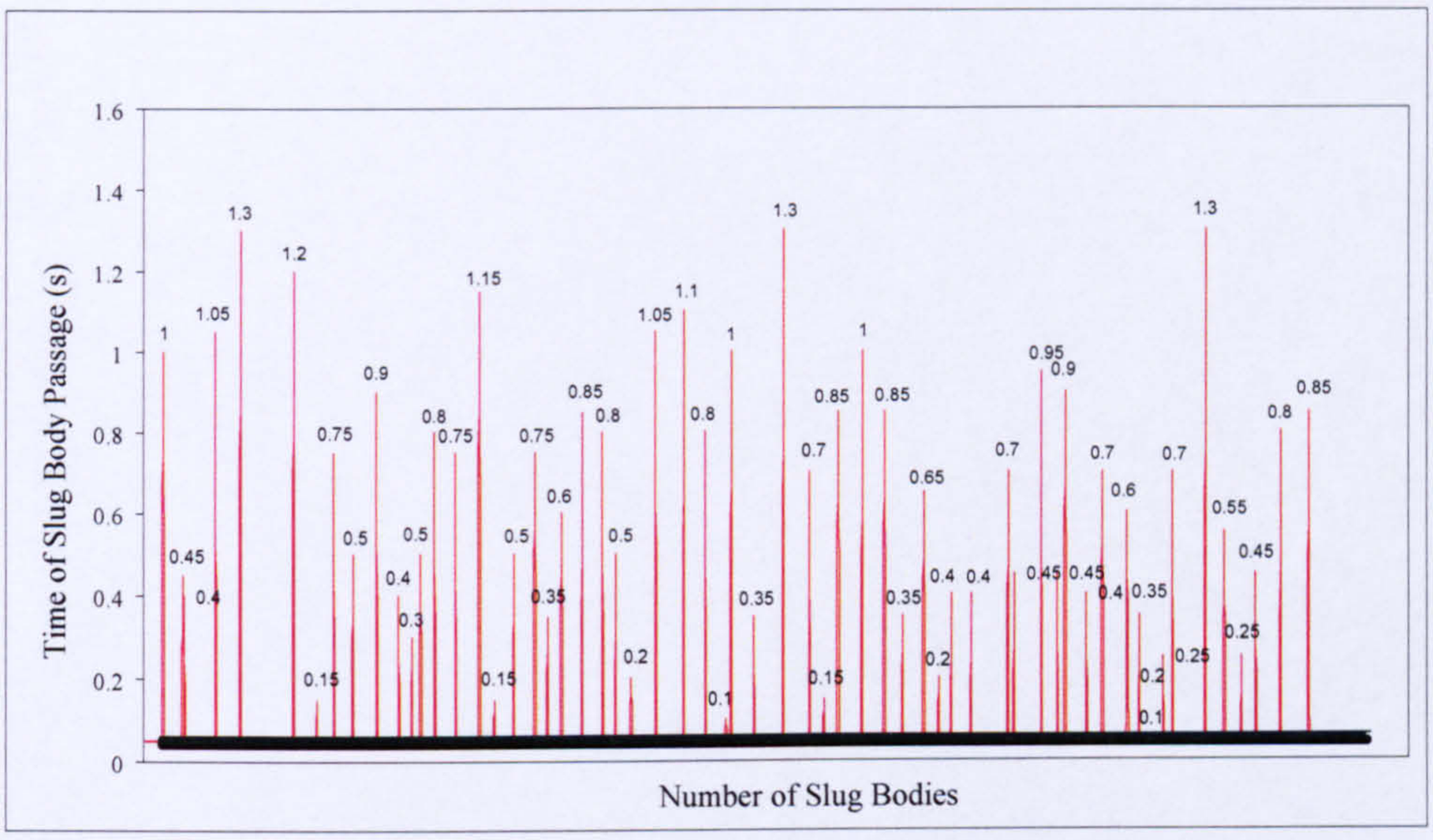

Figure 5-22: Slug body Passing Time Measurements Ultrasonically

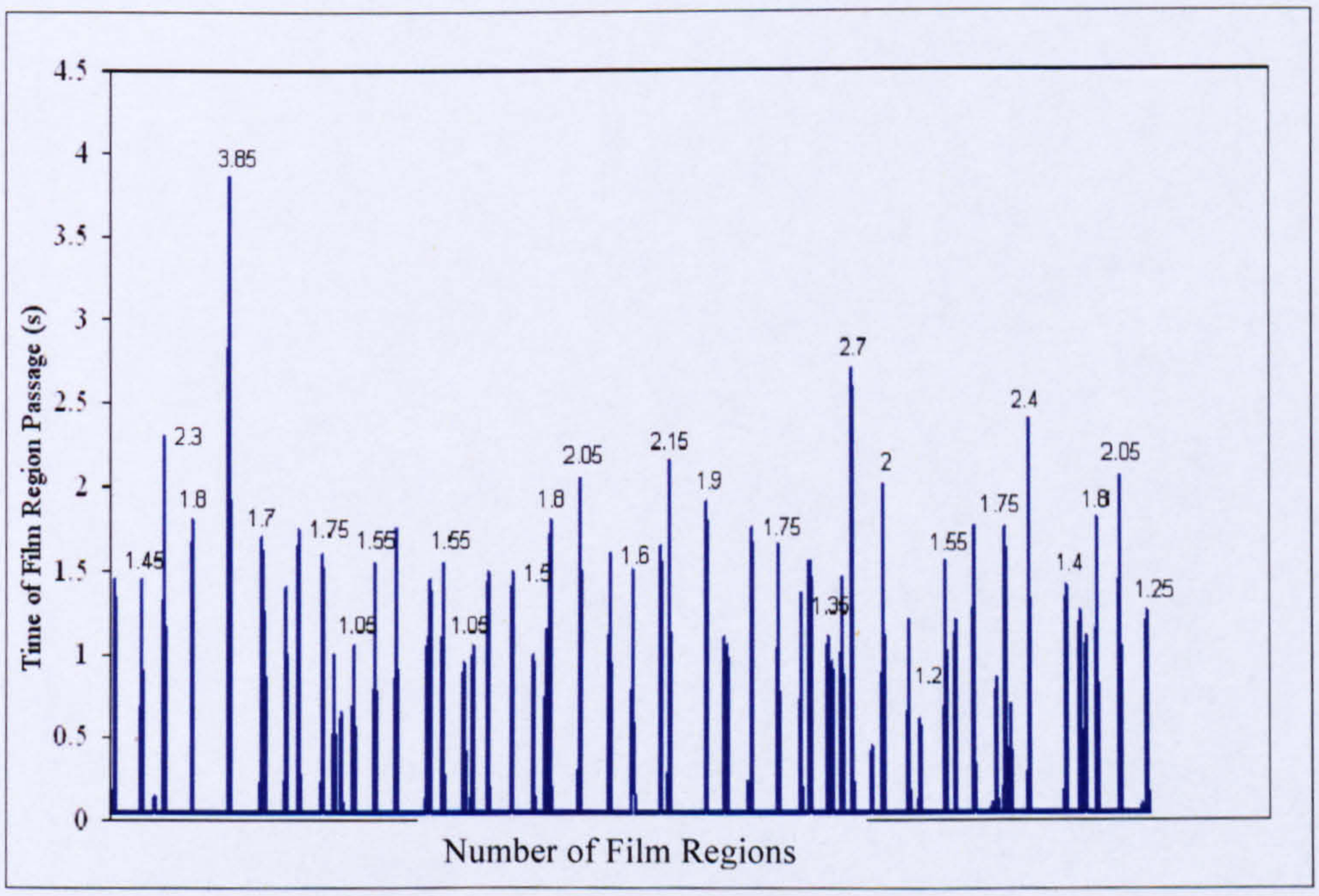

Figure 5-23: Film Regions Passing Time by Ultrasonic Technique

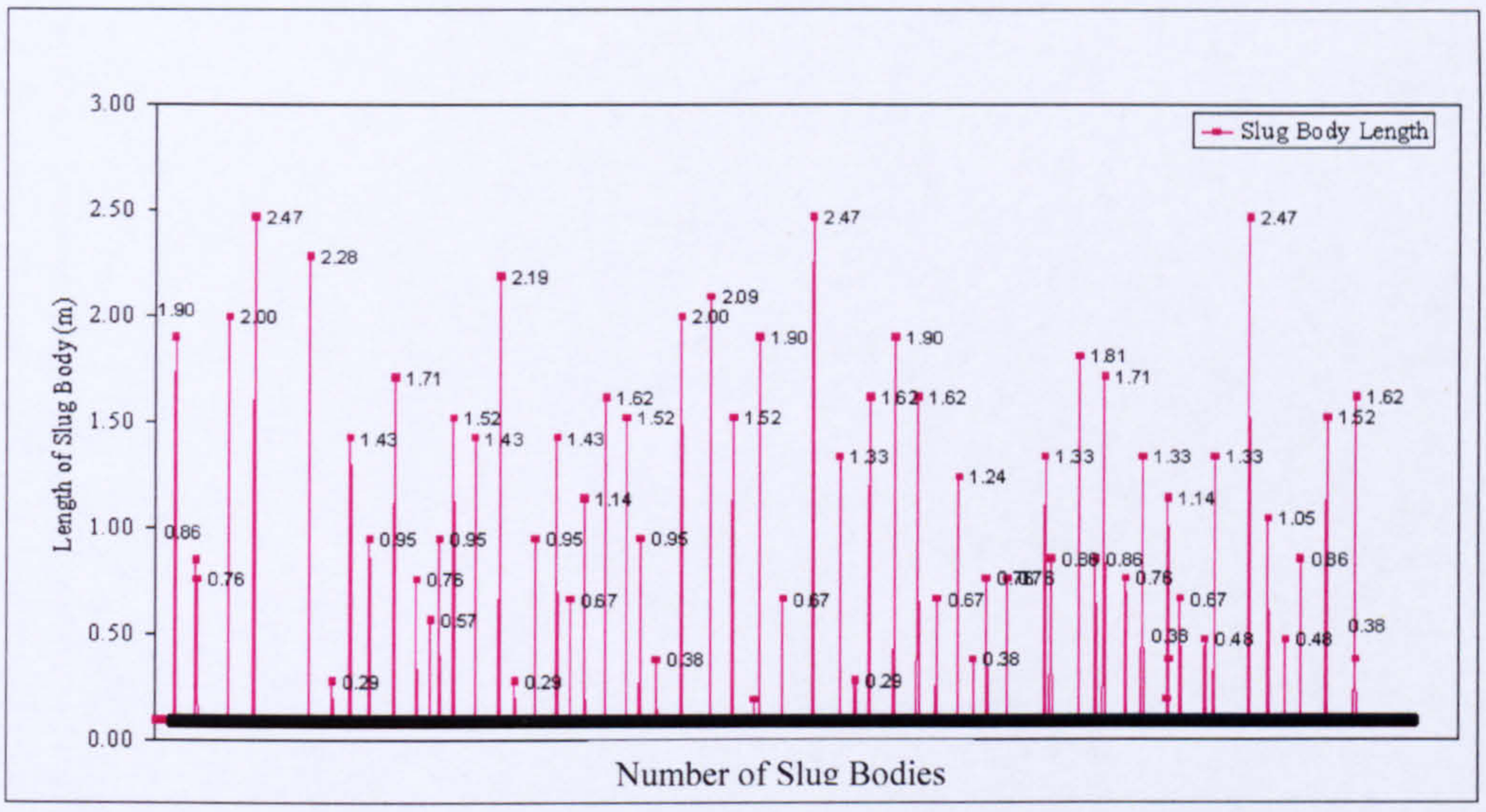

Figure 5-24: Slug body Lengths Measurements by Ultrasonic Technique for V_{SL}=0.5 ms^{-1} and V_{SG}=0.8 ms^{-1}

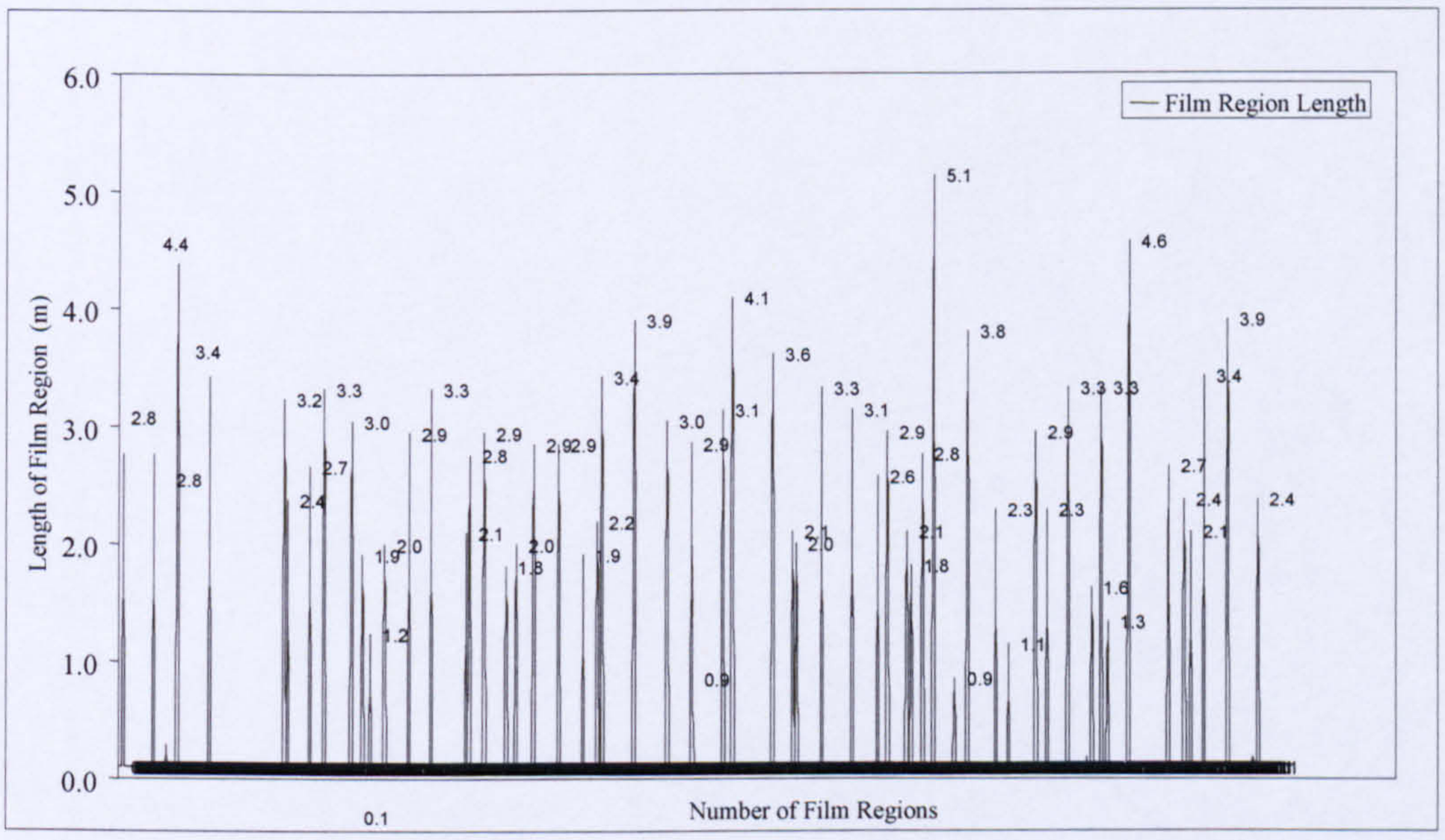

Figure 5-25: Film Regions Length Measurements by Ultrasonic Technique for V_{SL}=0.5 ms^{-1} and V_{SG}=0.8 ms^{-1}

The average slug length data for different experimental campaigns is presented in Figure 5-26. The average slug length data appears to be reasonably independent of the superficial gas velocities as stated by Nydal (1992). The standard deviation with 95.4% confidence (±2σ) of the slug bodies which were measured by ultrasonic techniques was ±2.41%, see Appendix A. The average slug length obtained by non-invasive ultrasonic technique was around 16 diameters (or 0.8 m) as shown in Figure 5-27.

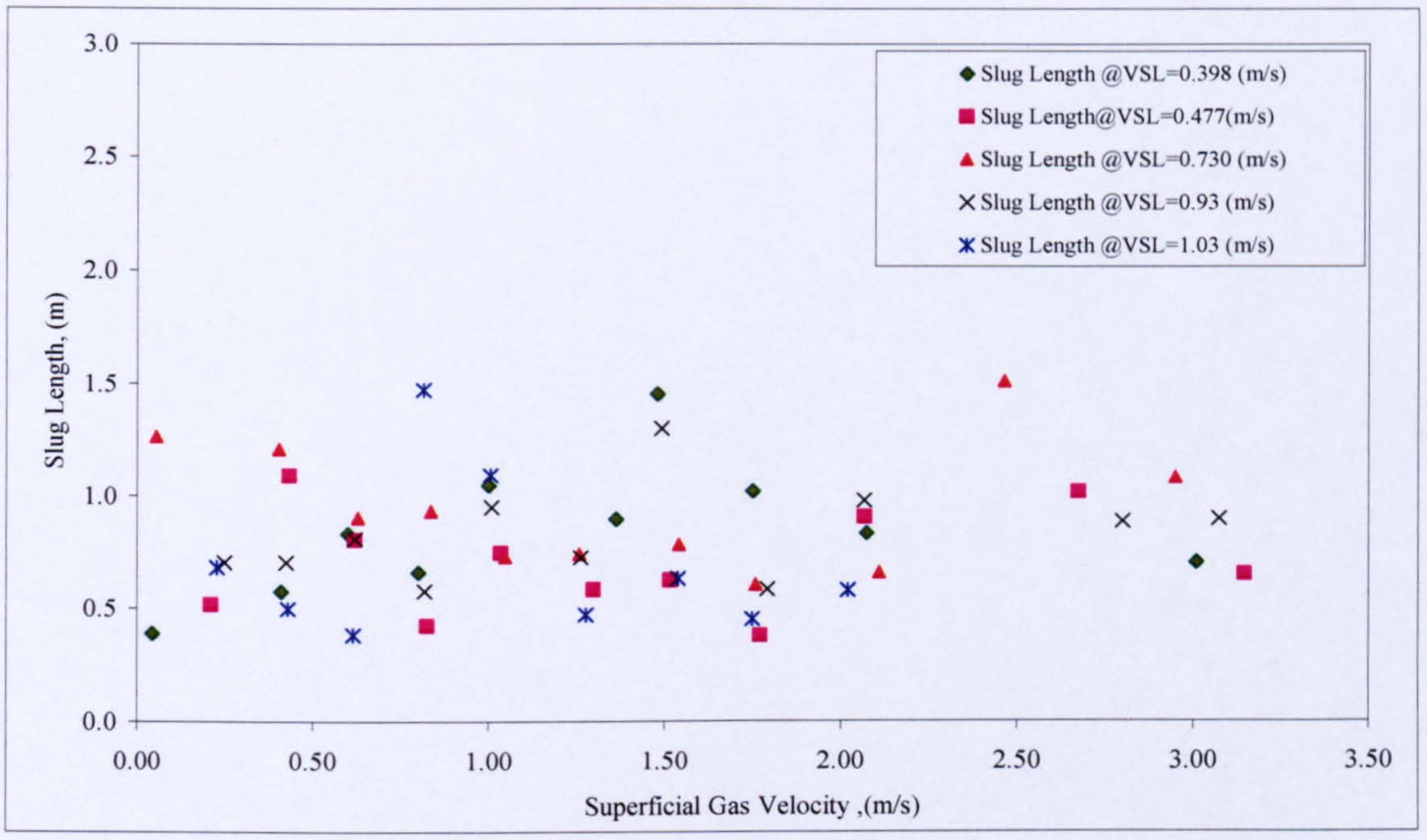

Figure 5-26: Slug Bodies Length by Ultrasonic Technique

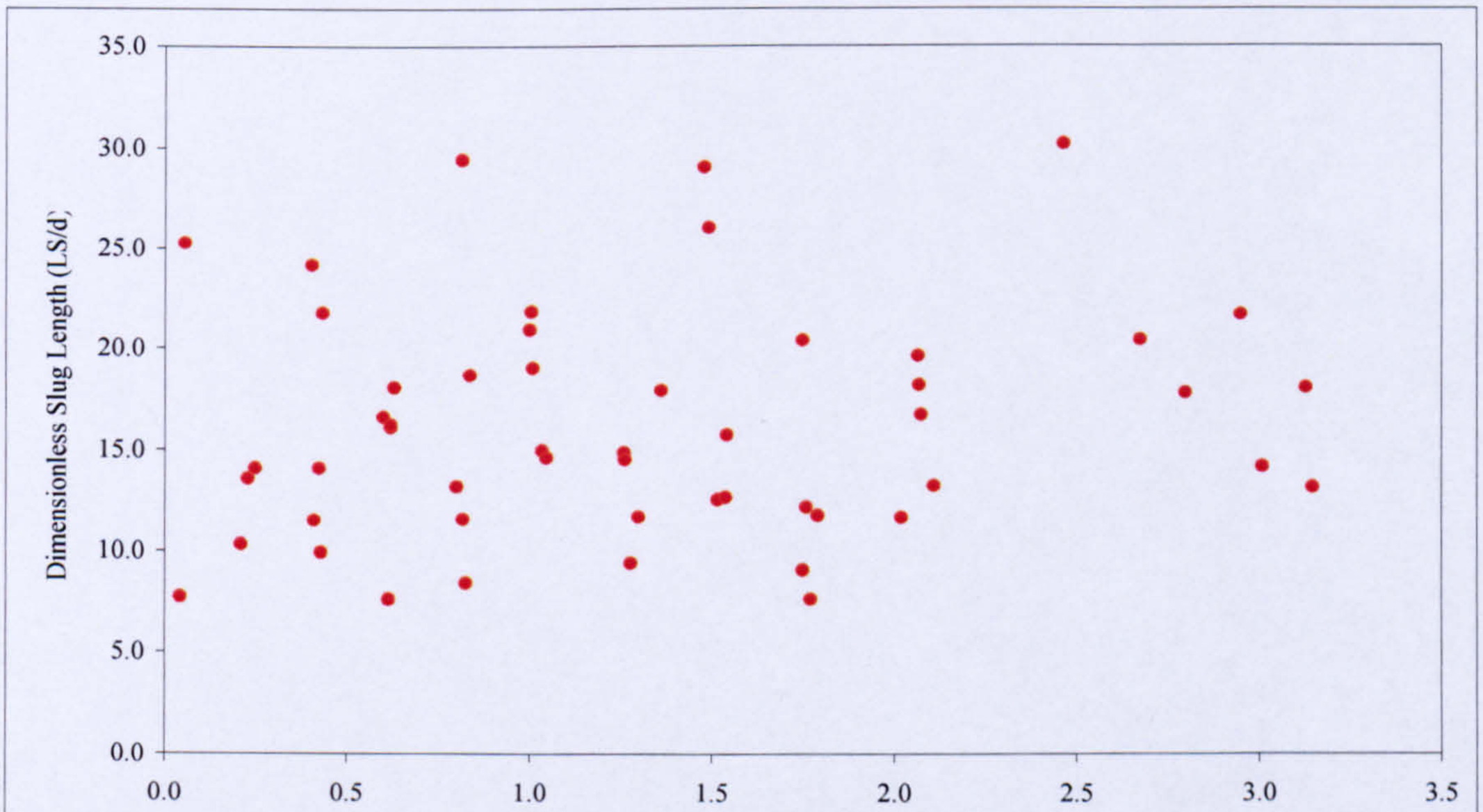

Figure 5-27: Dimensionless Slug Length vs. Superficial Gas Velocity

The average slug body lengths obtained by non-invasive ultrasonic technique was approximately (16d) and it is within the range of slug lengths reported by Dukler and Hubbard (1975) and Nicholson *et al*. (1978) of (12d-30d).

The model of Dukler *et al.* (1985) indicates that a minimum stable slug length for horizontal flow is approximately (8d).

In Figure 5-28 the measured film region length by non-invasive ultrasonic technique is plotted against the gas superficial velocity for the experimental tests at different superficial liquid velocities.

The film region length, L_F, increased as the superficial gas velocities increased. Manolis (1995) also reported similar findings for a "3-inch" horizontal pipe under slug conditions.

By adopting the same threshold level analysis technique on conductivity probe $C_{(C)}$, the slug body length and film region length were extracted.

In Figure 5-29, the threshold level analysis applied on the conductivity probe $C_{(C)}$ is presented. The slug lengths and film region lengths measured by the conductivity probe $C_{(C)}$ at V_{SL}=0.5 ms^{-1} and V_{SG}=0.8 ms^{-1} test condition are shown in Figures 5-30 and 5-31.

The average slug lengths obtained by the conductivity probe technique has approximately (17d) and it is within the range of slug lengths of (12d-30d) reported by Dukelr and Hubbard (1975) and Nicholson *et al.* (1978).

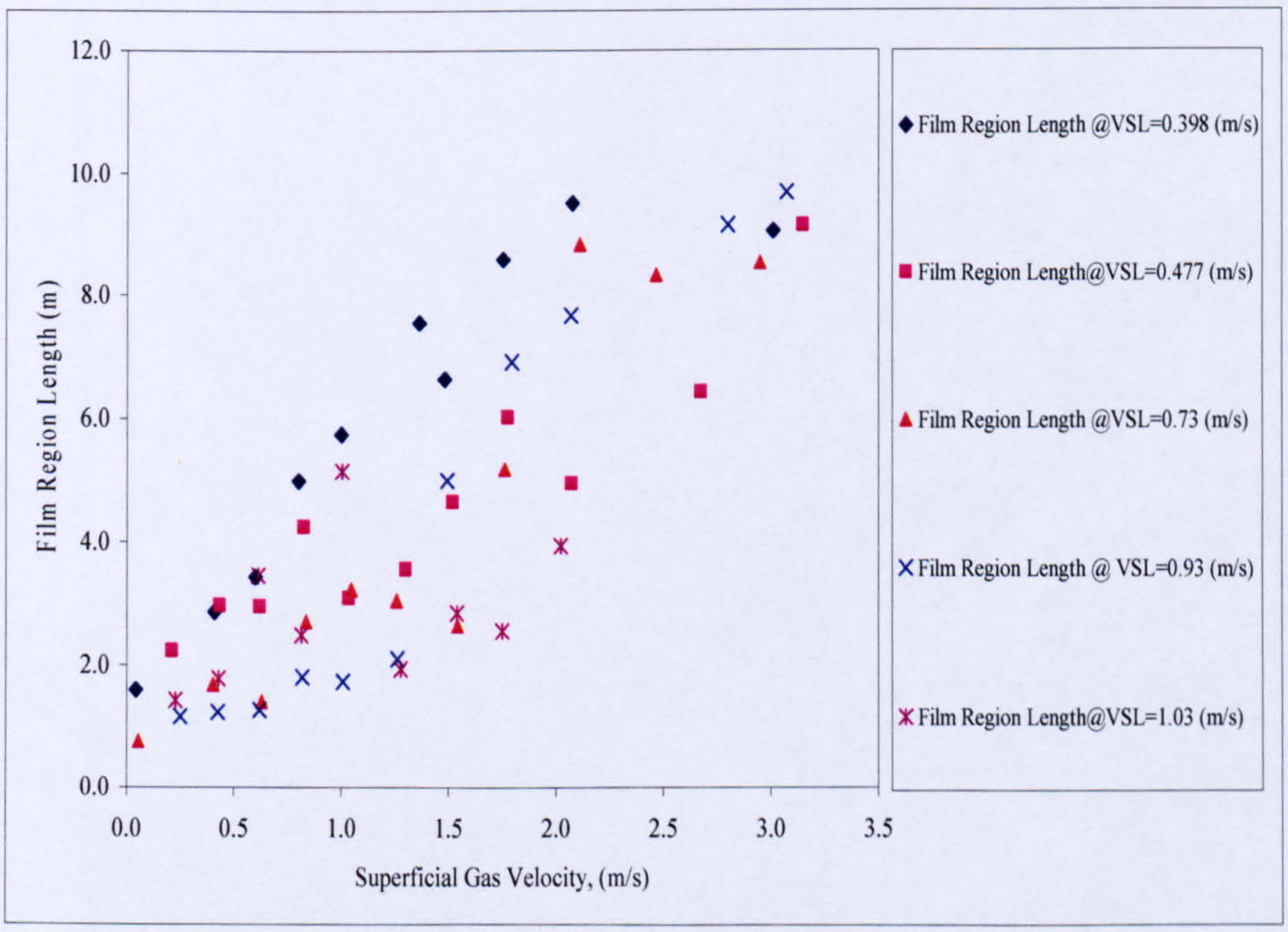

Figure 5-28: Film Region Length vs. Superficial Gas Velocity

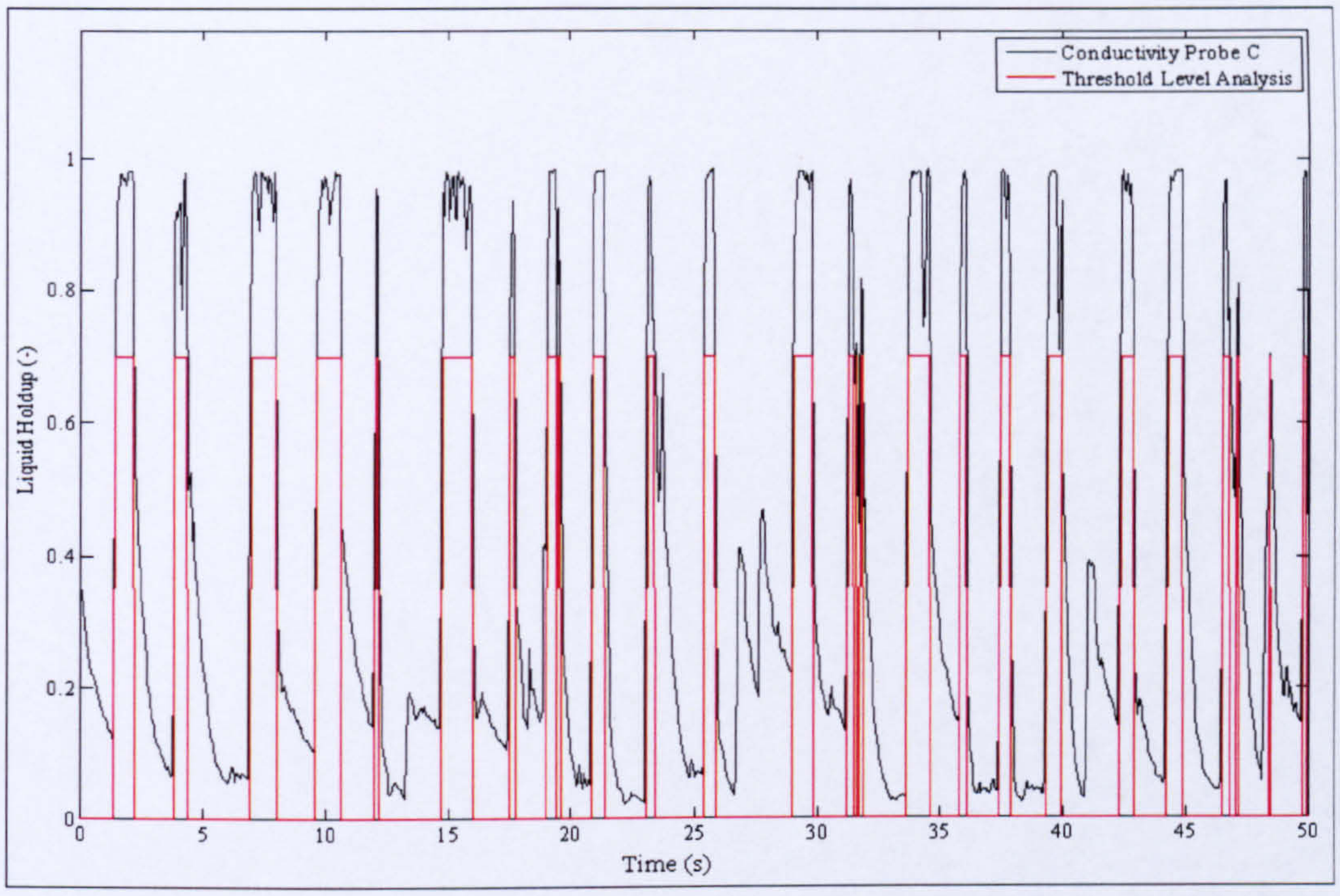

Figure 5-29: Slug Body and Film Region Passing Time Measurements

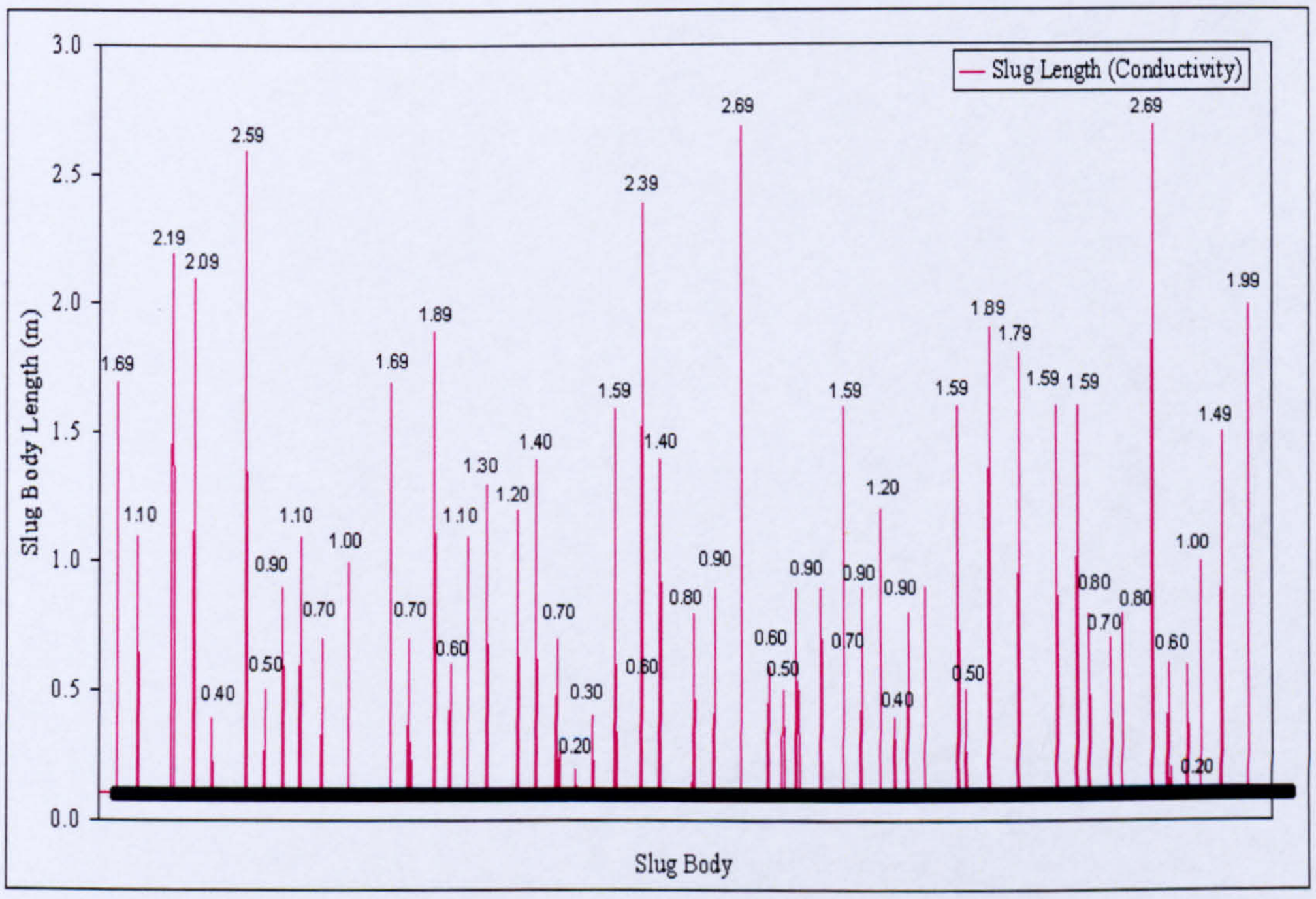

Figure 5-30: Slug body Lengths Measurements by Conductivity Sensor $C_{(C)}$ V_{SL}=0.5 ms^{-1} and V_{SG}=0.8 ms^{-1}

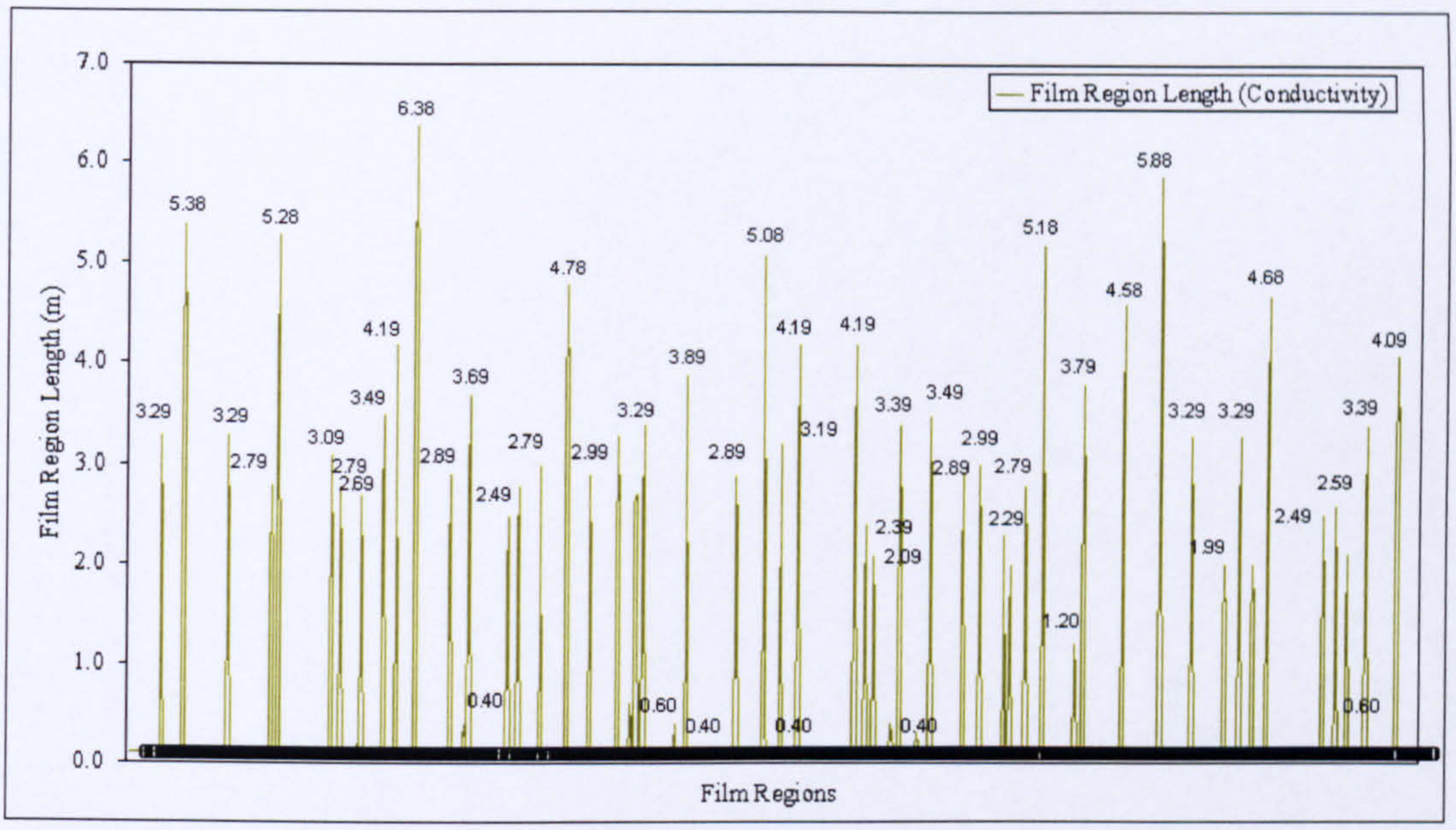

Figure 5-31: Film Regions Lengths Measurements by Conductivity Sensor $C_{(C)}$ V_{SL}=0.5 ms^{-1}, V_{SG}=0.8 ms^{-1}

The measurements of the non-invasive ultrasonic technique for slug length achieved good agreement with the non-intrusive conductivity technique with percentage error ranged from 3.77 % to 10% as is presented in Figure 5-32.

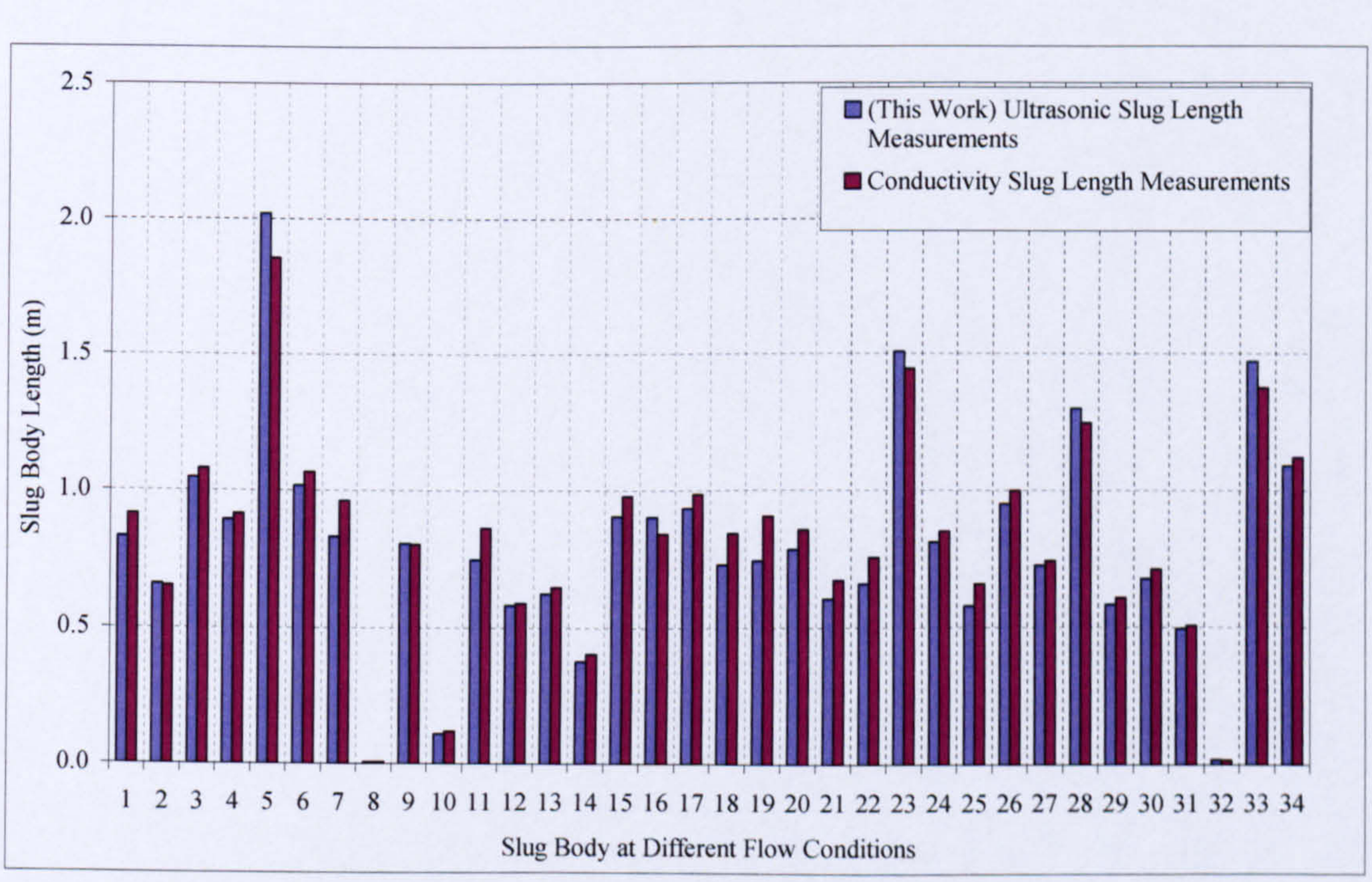

Figure 5-32: Ultrasonic Slug Body Length Measurements Comparison with Conductivity Measurements

5.5 Slug Body and Film Region Liquid Holdup Measurements

The slug body liquid holdup and film liquid holdup were deduced from the non-intrusive ultrasonic pulse-echo mode system as explained previously in section 4.1.2.3.

The system consists of an ultrasonic pulser–receiver which was used to excite the ultrasonic transducer (2.25 MHz), to receive and amplify the reflected signals and an electronic circuit to measure the time of transmitted and reflected ultrasound wave in liquid phase.

The liquid holdup measurements were validated against the non-intrusive conductivity probe and compared with correlations from the literature, see Figure 5-33.

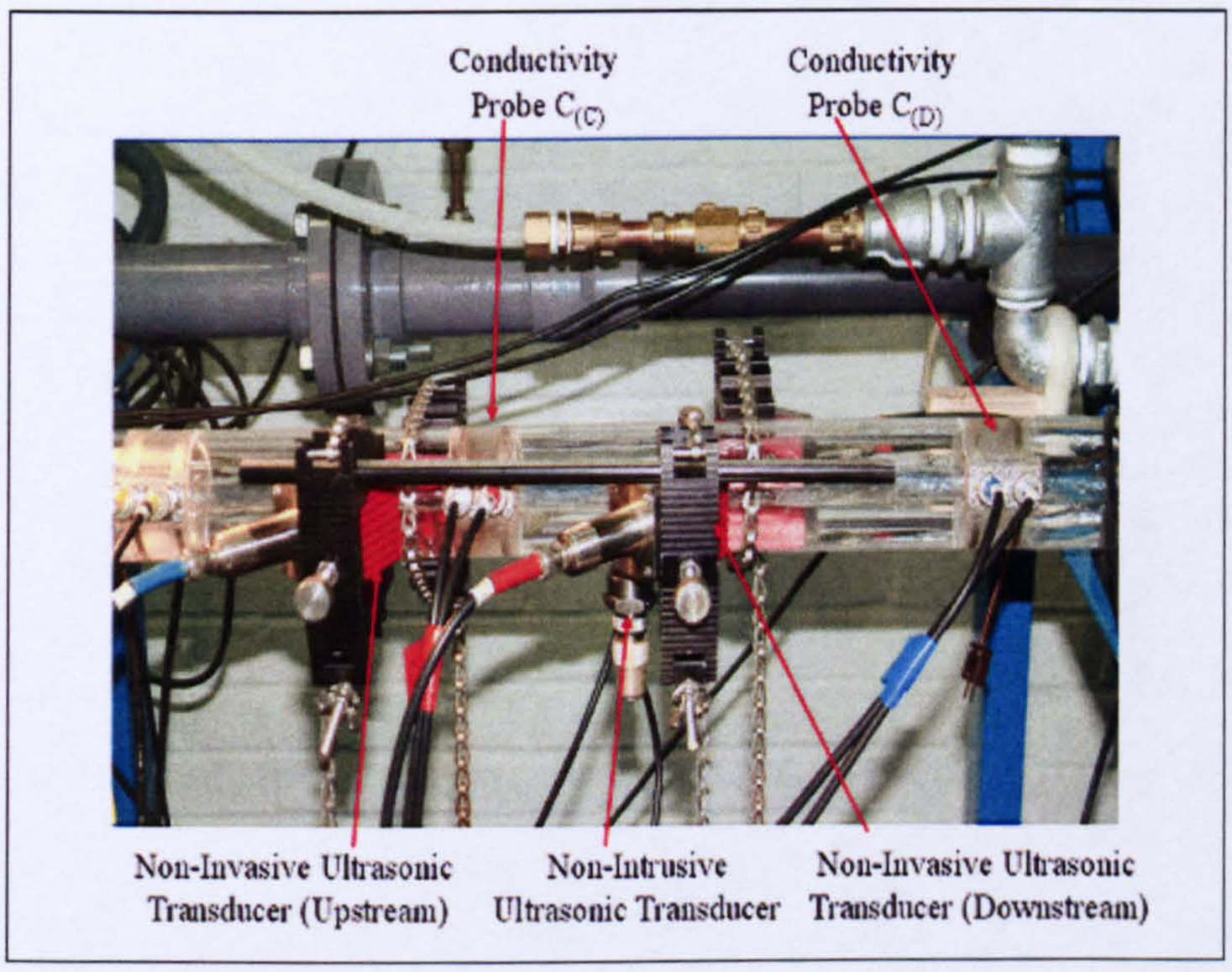

Figure 5-33: Ultrasonic and Conductivity for Liquid Holdup Measurements

Figure 5-34 shows the liquid holdup measurements by both the non-intrusive ultrasonic and conductivity techniques at V_{SL}= 0.5 ms^{-1} and V_{SG}= 1.25ms^{-1}. In this figure it can be seen that the slug body and film region trace by non-intrusive ultrasonic measurements follow the same trend as the one by the conductivity probe.

However, at the slug body tail, fluctuations of ultrasonic signal are present. These fluctuations were caused by the scatter of the reflections of the transmitted ultrasonic signals at the tail of the slug as the liquid surface was not horizontal to the pipe wall. .

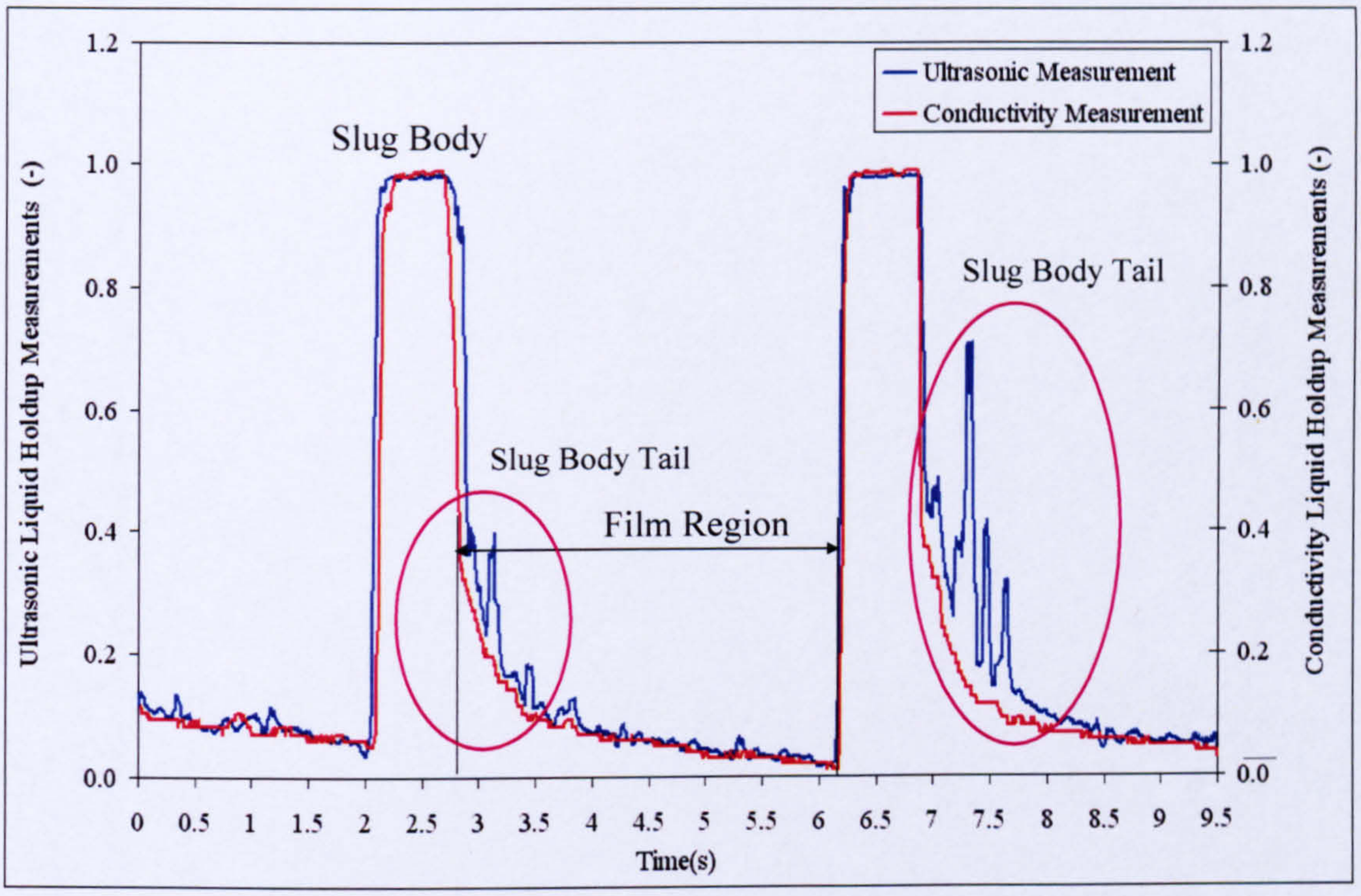

Figure 5-34: Liquid Holdup Measurements at (V_{SL}=0.5 ms^{-1}, V_{SG}=1.25ms^{-1})

Liquid heights in both the slug body, $h_{LS(U)}$, and the film region, $h_{LF(U)}$, were firstly inferred from the analogue voltage of the non-intrusive ultrasonic electronic circuit as given in the following equations:

$$h_{LS(U)} = \frac{V_{(U)} - V_{(U)(min)}}{V_{(U)(max)} - V_{(U)(min)}} \times d \;;\; h_{LF(U)} = \frac{V_{(U)} - V_{(U)(min)}}{V_{(U)(max)} - V_{(U)(min)}} \times d \qquad (5.9)$$

The slug body liquid holdup and film region liquid holdup were then obtained from the equations (5.10) and (5.11) respectively:

$$E_{LS(U)} = \frac{1}{\pi} \times \left(\pi - \cos^{-1}\left[2 \times \left(\frac{h_{LS(U)}}{d} \right) - 1 \right] + \left[2 \times \left(\frac{h_{LS(U)}}{d} \right) - 1 \right] \times \sqrt{1 - \left[2 \times \left(\frac{h_{LS(U)}}{d} \right) - 1 \right]^2} \right) \qquad (5.10)$$

$$E_{LF(U)} = \frac{1}{\pi} \times \left(\pi - \cos^{-1}\left[2 \times \left(\frac{h_{LF(U)}}{d} \right) - 1 \right] + \left[2 \times \left(\frac{h_{LF(U)}}{d} \right) - 1 \right] \times \sqrt{1 - \left[2 \times \left(\frac{h_{LF(U)}}{d} \right) - 1 \right]^2} \right) \qquad (5.11)]$$

In the slug body, the liquid holdup becomes less than unity at high superficial gas velocities since gas is entrained in the slug body and tends to concentrate near the top of the pipe (King *et al.* 1997).

Figure 5-35 presents the validations of the ultrasonic slug body liquid holdup measurements against the conductivity measurements; where it is obvious that the slug body liquid holdup measurements by ultrasonic techniques give satisfactory results in to comparison the conductivity technique measurements and the relative error was mostly within a range of 0.162% to 5 % and with standard deviation of ±0.1 %as presented in Appendix A.

In Figure 5-36, the slug body liquid holdup measurements by ultrasonic were compared with a set of correlations from literature including Gregory *et al.* (1978), Malnes (1979) and Paglianti *et al.* (1993). These correlations are given as:

Gregory *et al.* (1978)

$$E_{LS} = \frac{1}{1+\left(\frac{V_{mix}}{8.66}\right)^{1.39}} \tag{5.12}$$

Malnes (1979)

$$E_{LS} = 1 - \frac{V_{mix}}{C_M + V_{mix}} \quad \text{and} \quad C_M = 83 \times \left(\frac{g\sigma}{\rho_L}\right)^{1/4} \tag{5.13}$$

Paglianti *et al.* (1993)

$$E_{LS} = \frac{1}{\left(1+\frac{Fr^2 \times Bo^{0.2}}{625}\right)^2} \tag{5.14}$$

where Fr is Froude number defined as:

$$Fr = \frac{V_{mix}}{\sqrt{gd}} \tag{5.15}$$

and Bo is Bond number defined as:

$$Bo = \frac{\Delta\rho \times g \times d^2}{\sigma} \tag{5.16}$$

The correlation of Greogry *et al.* (1978) performs the best against the data set, see Table 5-3, although all correlations have comparable performance. The correlation of Malnes (1983) being slightly less accurate. This is probably because the correlation was based on modified interpretation of the data of Greogry *et al.* (1978). However, the correlation of Paglianti *et al.* (1993) performs the worst with a standard deviation of 15.17 %, and this is probably due to the value of the coefficients A and β in Paglianti *et al.* (1993) correlation.

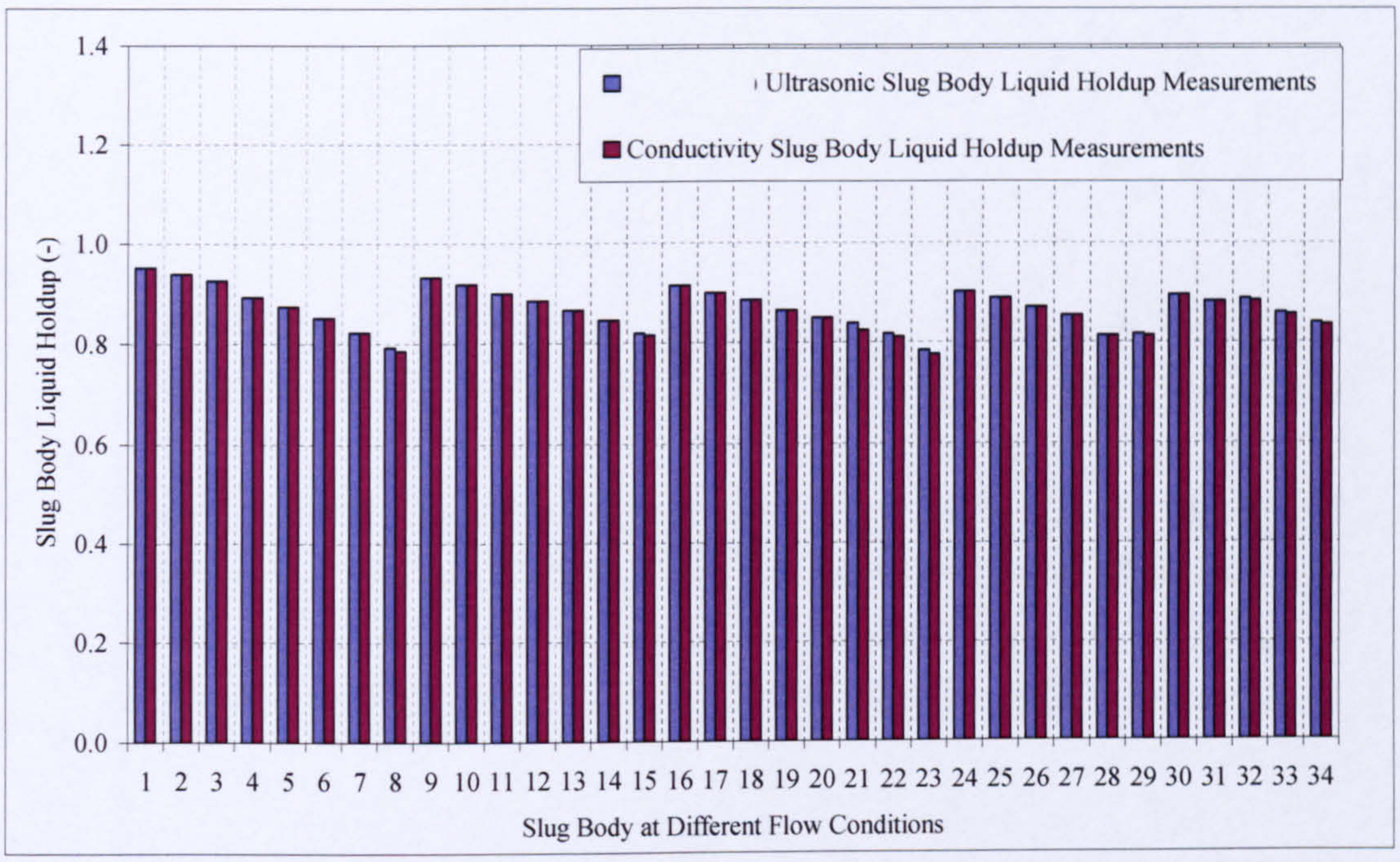

Figure 5-35: Ultrasonic Slug Body Liquid Holdup versus Conductivity Measurements

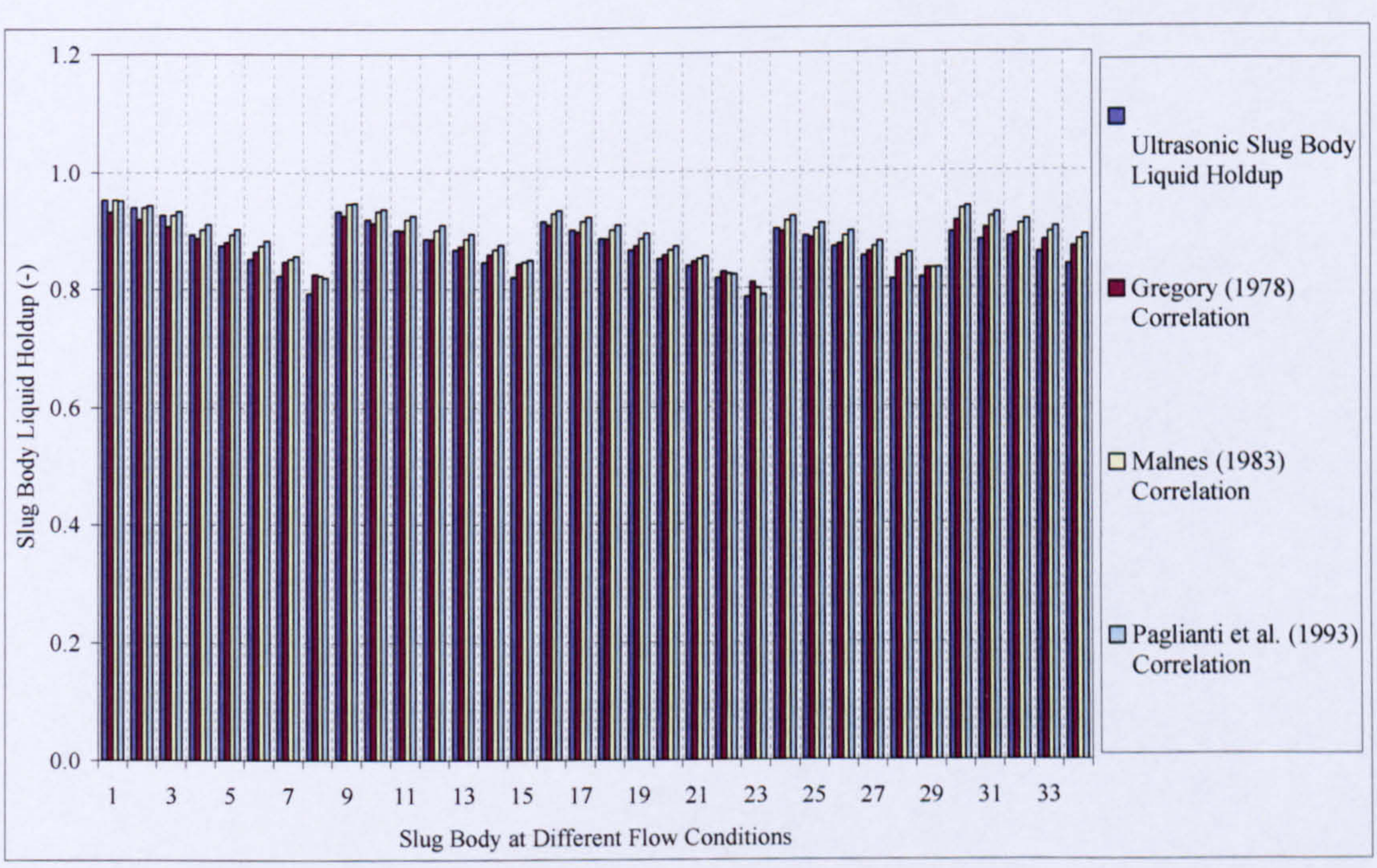

Figure 5-36: Ultrasonic Slug Body Liquid Holdup compared with Correlations

Table 5-3: Statistical Results of Ultrasonic Slug Body Holdup Measurements Performance

Correlations	Average Percentage Error	Standard Deviation
Gregory *et a*l. (1978)	-0.515%	±3.29%
Malnes (1983)	-1.978%	±12.66%
Paglianti *et al*. (1993)	-2.371%	±15.17%

The film liquid holdup was measured using conductivity ring electrodes under slug flow conditions at different gas and liquid superficial velocities by Stewart (2001). He stated, based on experimental investigations that the film liquid holdup reduced as the gas superficial velocities increase.

In Figure 5-37, the film liquid holdup measurements by non-intrusive ultrasonic under different slug conditions and the one obtained by Stewart (2001) are presented. It is clear from this figure that the film liquid holdup measured by ultrasonic technique decreased as the superficial gas velocities increased.

The film liquid holdup which was measured by non-intrusive ultrasonic technique has standard deviation of ± 0.1% with 95.4% confidence as presented in appendix A.

Conductivity probe measurements were used to validate the ultrasonic film liquid holdup measurements as is shown in Figure 5-38.

It is found that the film liquid holdup relative error is of the order of 1.14 % at low superficial gas velocity; however, at higher superficial gas velocity the error increases up to 5 %.

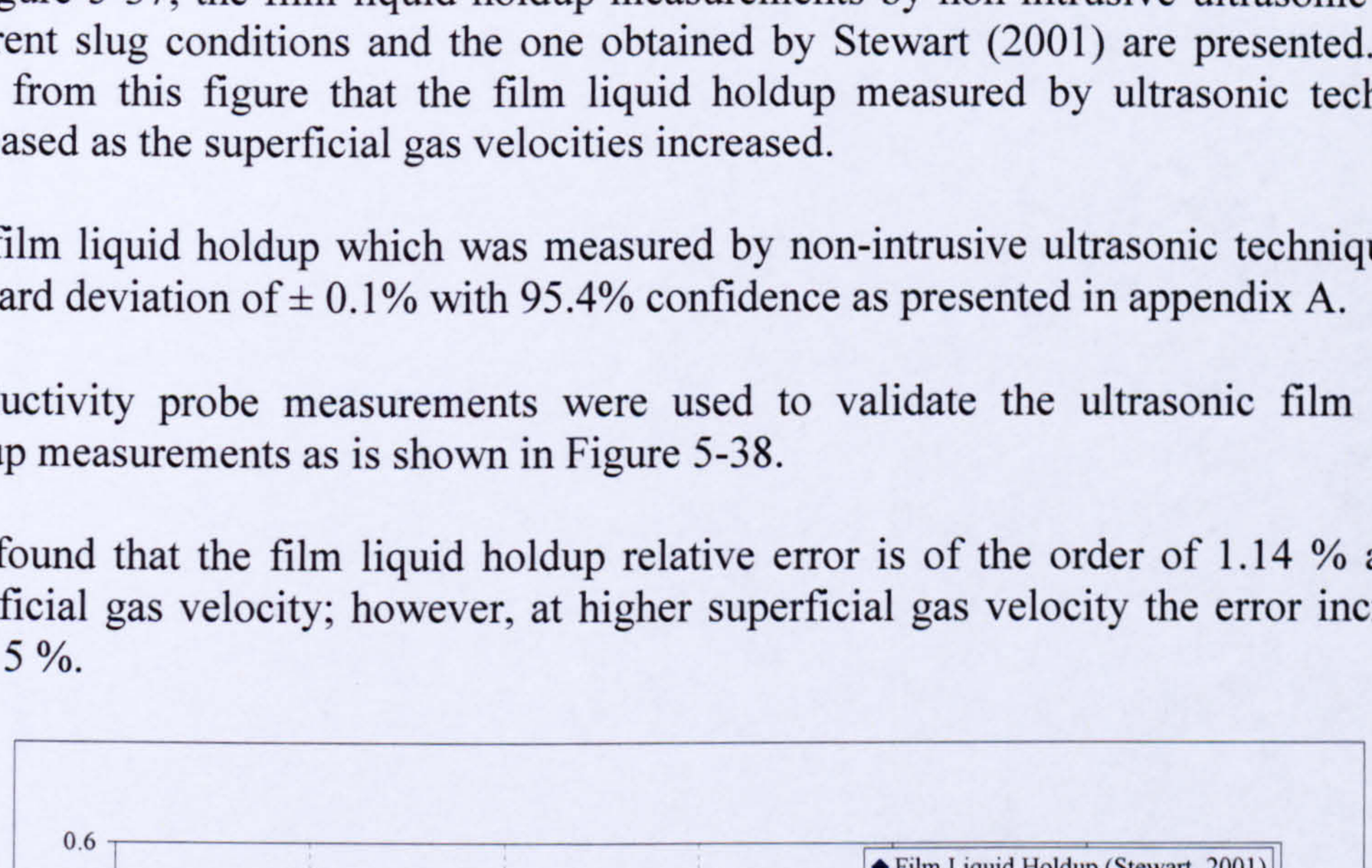

Figure 5-37: Ultrasonic Film Liquid Holdup Measurements

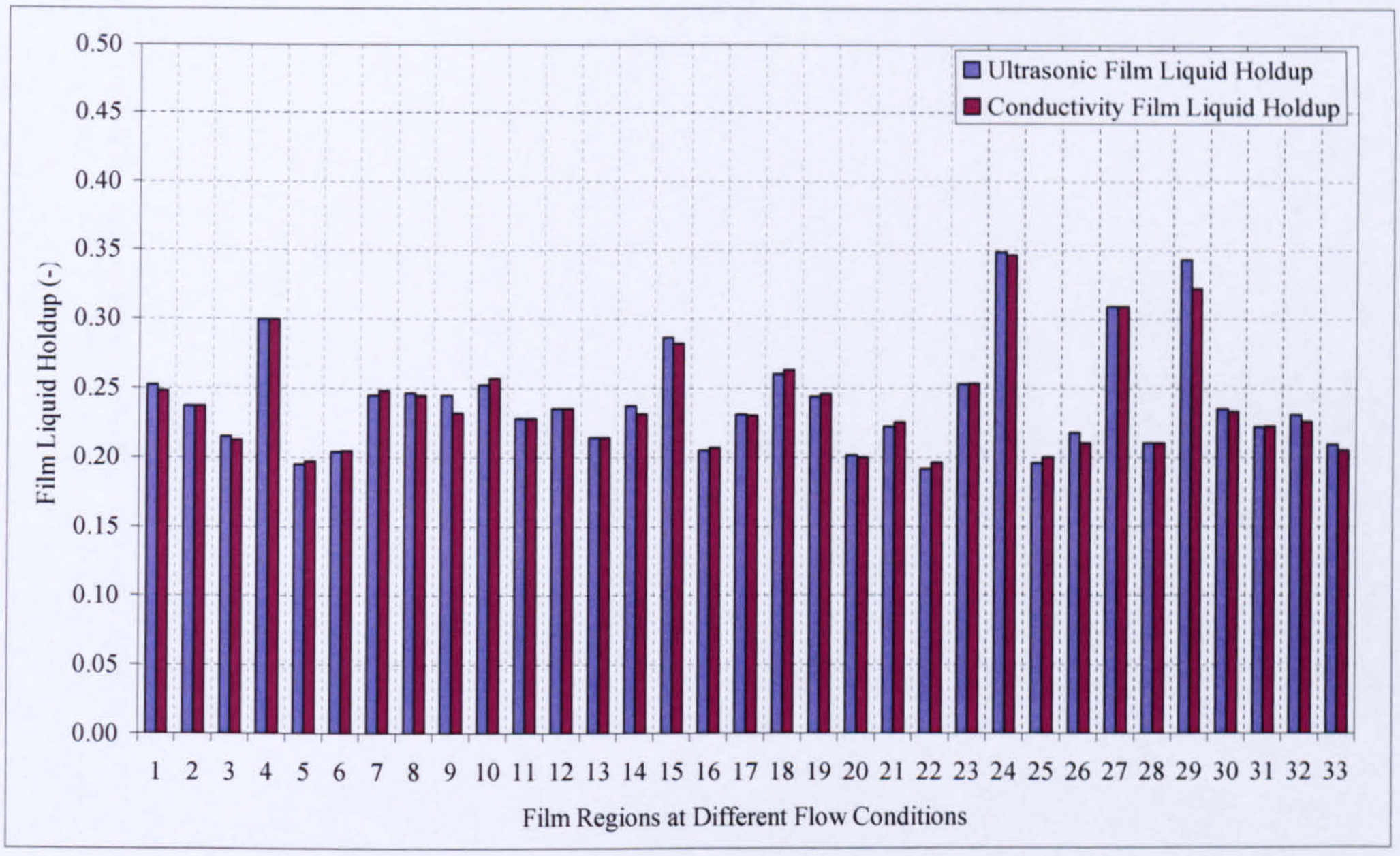

Figure 5-38: Ultrasonic Film Liquid Holdup Measurements Validations with Conductivity Measurements

5.6 Slip Ratio and Coefficient C_o, and Drift Velocity V_d

There is considerably less data available for the slip parameter s, due to the difficulty in its measurements. Dukler and Hubbard (1975) proposed that the gas and liquid phases in the slug body are a homogenous mixture, therefore (s=1). In this work, we also considered that the phases in slug body are a homogenous mixture.

The parameter, C_o, in the translational velocity equation (5.17) is a distribution coefficient related to the velocity profiles in dispersed systems. It may be closely approximated by the ratio of the maximum to the mean velocity in the liquid ahead of the bubble.

$$V_T = C_o V_{mix} + V_d \tag{5.17}$$

From various expressions found in the literature, the coefficients C_o and V_d can be expressed through the following general expression:

$$\begin{aligned} C_o &= C_o(Fr, Re_S, \sigma, \varphi) \\ V_d &= V_d(Fr, Re_S, \sigma, \varphi) \end{aligned} \tag{5.18}$$

where
φ is the pipe inclination,

σ is the surface tension,
Fr is a Froude number and is given as:

$$Fr = \frac{V_{mix}}{\sqrt{gd}} \tag{5.19}$$

and Re_S is the slug Reynolds number defined by:

$$Re_s = \frac{\rho_l V_{mix} d}{\mu_l} \tag{5.20}$$

In the present work, a correlation for the motion of the elongated gas bubble based on a linear fit to experimental data was developed. The data of slug translational velocity measured by ultrasonic technique is plotted versus the mixture velocity in Figure 5-39. The values of the slug translational velocities increase by increasing the gas and liquid flowrates.

However in order to extract the coefficients C_o and V_d from the slug translational velocities data, Ferre (1979) and Bendiksen (1984) plotted Froude number for mixture velocity versus slug translational velocity as is presented in Figure 5-40. Based on the value of Froude number, three groups of data are identified and listed as following:

Group	Froude Number Values Range
Group#1	$Fr < 2$
Group#2	$2 < Fr < 4$
Group#3	$Fr > 4$

Based on mixture Froude number analysis, the coefficients C_o, and drift velocity V_d obtained for each group based on a linear fit to group data (Figure 5-41). From Figure 5-41, correlations for slug translational velocity for each group is obtained and is given as:

$$\begin{aligned} &\text{Group 1: } V_T = 1.141 V_{mix} + 0.2017 \\ &\text{Group 2: } V_T = 1.1891 V_{mix} + 0.0285 \\ &\text{Group 3: } V_T = 1.2064 V_{mix} \end{aligned} \tag{5.21}$$

Therefore the values of the coefficients C_o, and drift velocity V_d are given in equation (5.22):

$$\begin{cases} C_o = 1.141 & V_d = 0.2017 & Fr_M < 2 \\ C_o = 1.1891 & V_d = 0.0285 & 2 \le Fr_M < 4 \\ C_o = 1.2064 & V_d = 0 & Fr_M \ge 4 \end{cases} \tag{5.22}$$

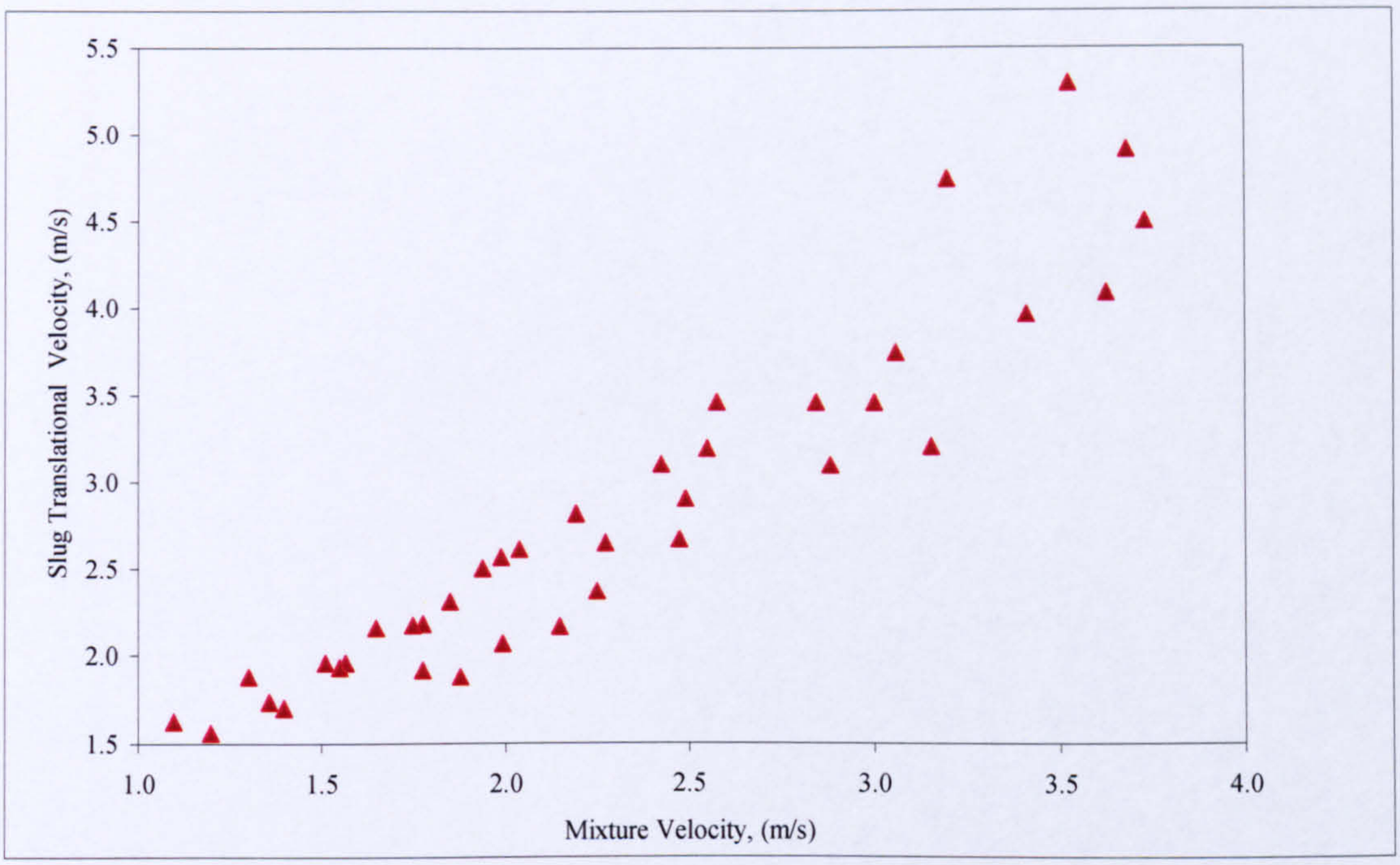

Figure 5-39: Slug Translation Velocity Measured vs. Mixture Velocity

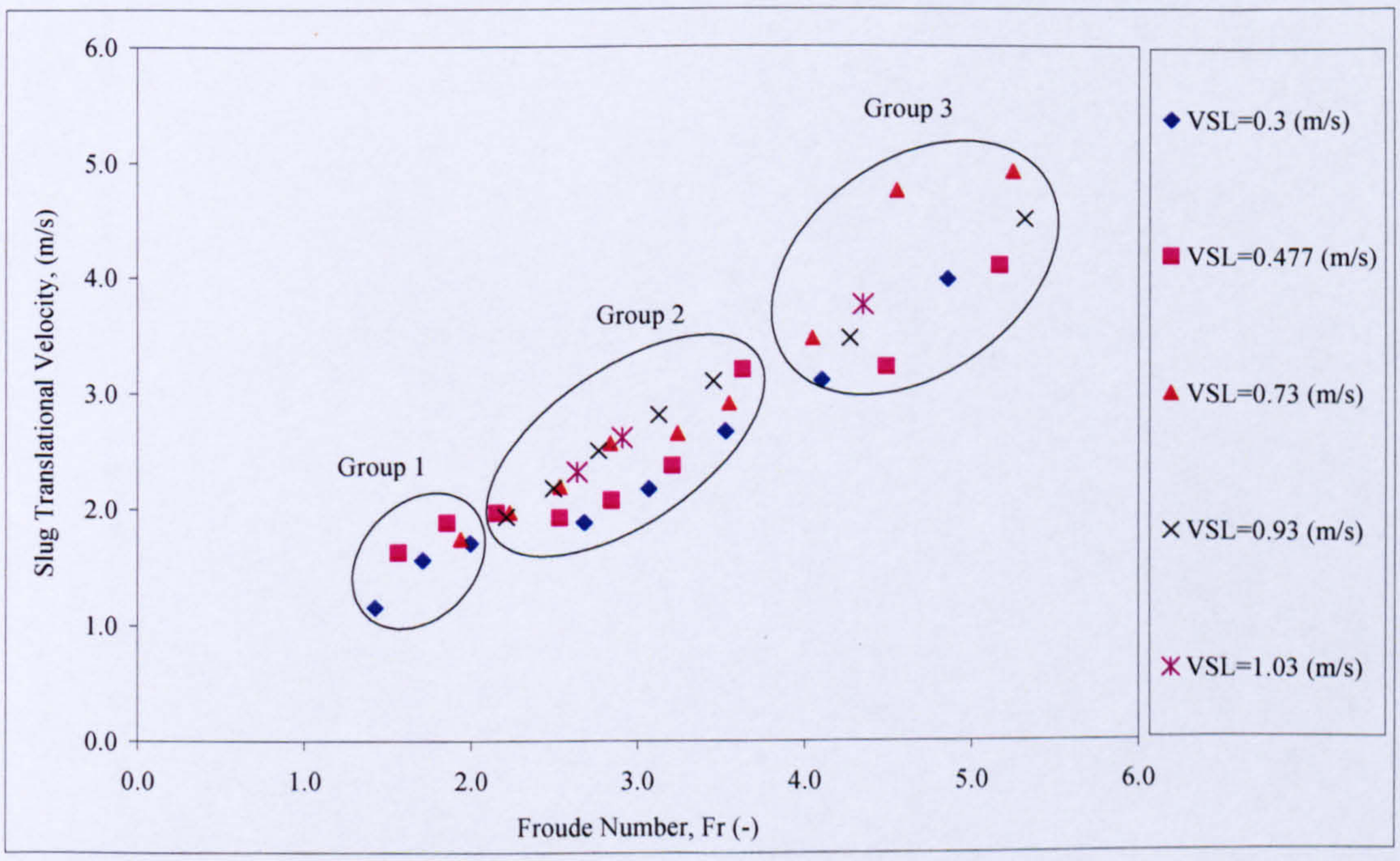

Figure 5-40: Slug Translation Velocity measured vs. Froude Number

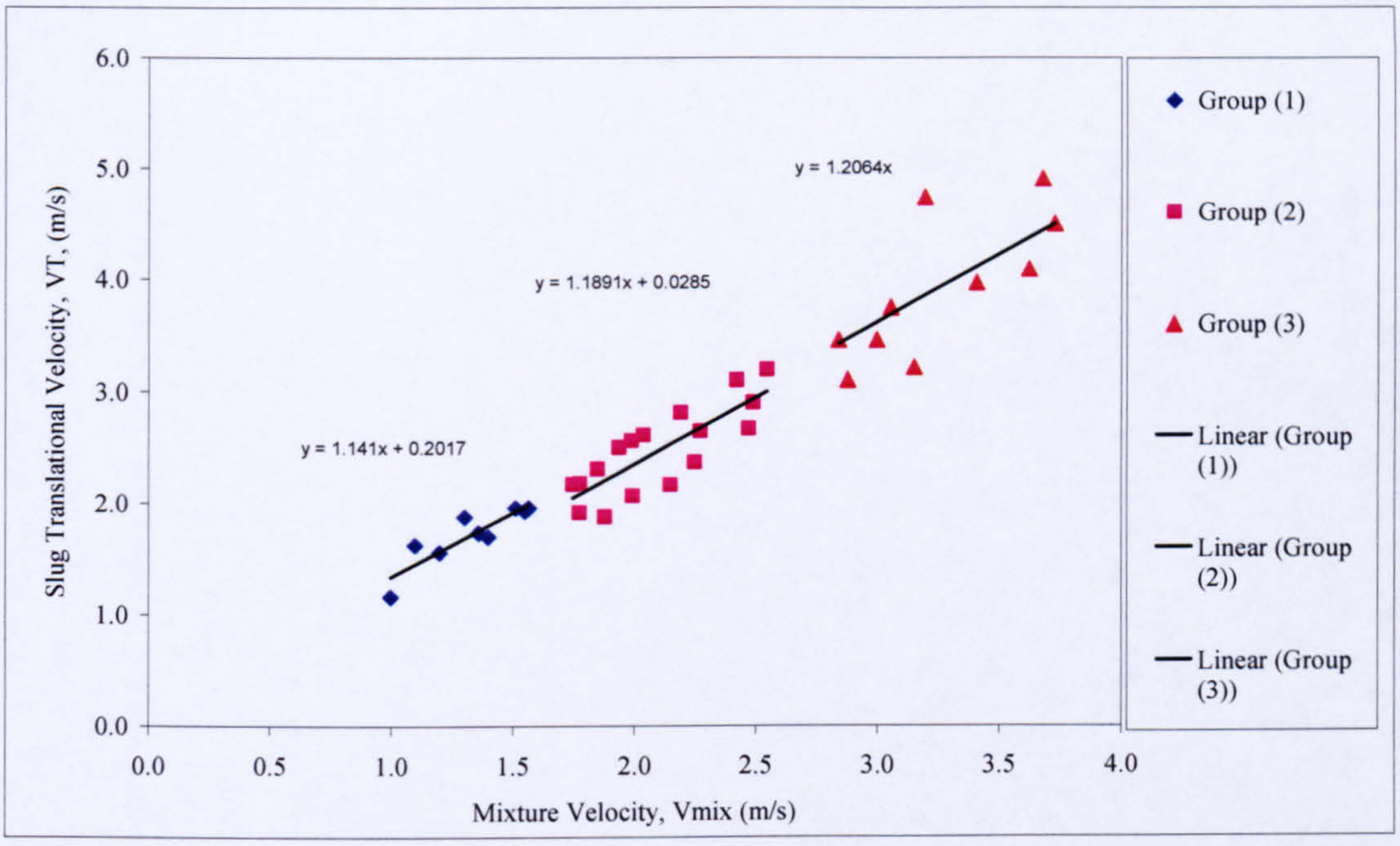

Figure 5-41: Extractions of Coefficients C_o and V_d

5.7 Summary

In this work, the slug characteristics measurements are of importance in order to achieve the final two-phase gas/liquid volumetric flowrates by implementing the slug closure model developed and presented in Chapter 3.

The measurements of the slug characteristics were achieved by using non-invasive and non-intrusive ultrasonic techniques. The slug characteristics measured were slug frequency, slug translational velocity, slug body length, film region length, slug body liquid holdup and film liquid holdup.

To extract the slug parameters, different analysing techniques were applied including, signal cross-correlation for slug translational velocity measurements, threshold level analysis for slug body and film region passing time..

The slug characteristics measured by non-invasive and non-intrusive ultrasonic techniques were compared with the slug characteristics measurements by conductivity probes and with a number of correlations from the literature. The performance assessment of the non-invasive and non-intrusive ultrasonic techniques for slug characteristics measurements are summarised in the following:

- The slug frequency increases rapidly from 0.13 Hz to 1.5 Hz with the superficial liquid velocity V_{SL}, though it changes only modestly with the superficial gas

velocity V_{SG}. Based on the Strouhal number analysis, Gregory and Scott (1969) correlation provides a good match to the present data.

- The slug translational velocity percentage error is of the order of 2.3 % to 18 % for the full range of test conditions and with standard deviation of ±2.9%.

- The average slug length obtained by ultrasonic is around 16d, comparing to 17d average slug length obtained by conductivity measurements with standard deviation of ± 2.5%.

- The slug body liquid holdup measurements by ultrasonic techniques give satisfactory results in comparison with the conductivity technique measurements, and the relative error was mostly within 0.162 %. The correlation of Greogry *et al.* (1978) performs the best against the data of this work.

- The film liquid holdup measured by ultrasonic technique decreased as the superficial gas velocities increased. The film liquid holdup relative error is of the order of 1.14 % at low superficial gas velocity, however, at higher superficial gas velocity the error increases up to 5 %.

- The coefficients C_o and V_d were extracted from the data based on the Froude number analysis proposed by Ferre (1979) and Bendiksen (1984). The values of flow profile C_o lied within the range 0.98-1.5 also reported discussed by Hale (2000).

Chapter 6

Ultrasonic Multiphase Metering Performance Assessment

The ultrasonic multiphase flow metering concept developed in this work was assessed for a two-phase air/water system under slug flow conditions. The operating principle of the developed ultrasonic multiphase flowmeter is presented in section 6.1.

Section 6.2 describes the experimental investigations conducted in this work on a commercial clamp-on transit time ultrasonic flowmeter and discusses the operational limitations of this flowmeter under slug flow conditions.

In section 6.3, the concept of the slug closure model, the data acquisition system and software code to obtain the gas and liquid phase volumetric flowrates are presented.

Section 6.4 presents the performance assessment of ultrasonic multiphase flowmeter. The assessment procedures include assessment of the error of slug characteristics measurements, the slug closure model factors ($K_{1\ (Liquid)}$, $K_{2\ (Liquid)}$, $K_{3\ (Gas)}$ and $K_{4\ (Gas)}$) and the error of the measurements prediction for the flowmeter using reference flowmeters.

Section 6.5 compared the performance errors of the developed ultrasonic multiphase flowmeter with the industrial requirements. Finally, the chapter summary is presented in section 6.6

6.1 Introduction

As discussed in Chapter 3, a slug closure model has been developed. The slug characteristics obtained by non-invasive and non-intrusive ultrasonic techniques (discussed in chapter 5) form inputs to this model. Using these inputs, the slug closure model calculates the factors $K_{1\,(Liquid)}$, $K_{2\,(Liquid)}$, $K_{3\,(Gas)}$ and $K_{4\,(Gas)}$.

These factors are a function of the slip ratio in the slug body, flow profile C_0, drift velocity V_d, slug body liquid holdup, gas void fraction in slug body, slug length, film length, and the total length of the slug unit. From these factors and the slug translational velocity, the slug closure model calculates the gas and liquid phase volumetric flowrates.

6.2 Ultrasonic Multiphase Flowmetering Concept

The operation system of the ultrasonic multiphase flowmetering concept developed in this work consists of slug closure model, data acquisition system and software to extract slug characteristics measurements and Matlab codes to calculate the gas and liquid phase volumetric flowrates. This system is schematically presented in Figure 6-1.

Initially, the raw signals from the non-invasive ultrasonic sensors were filtered, amplified and positive full wave rectified in the signal conditioning unit and were sent to the data acquisition system. The signals from non-intrusive ultrasonic sensors were sent through the time elapsed measurement unit and then to the data acquisition system. Conductivity probes output was also sent to the data acquisition system for the comparison

The data acquisition system, which is shown in Figure 6-2, consists of the following components:

- A BNC-2090 connector board (National Instruments) interfaces the raw signals from non-invasive and non-intrusive ultrasonic sensors as well as conductivity probes using BNC coaxial cables.

- A standard PC system (1.7GHz Dell PC) with 10 GB hard disk and 520 Mb of RAM.

- An AT-M10 data acquisition (DAQ) card to digitise the analogue data from each channel output from BNC-2090. This card samples the input data to 16-bit accuracy, at frequencies of up to 20 KHz.

Data acquisition software, written in the graphical programming language Labview 'Virtual Instrument' 6.2 Version (National Instruments). As each test run may result a considerable amount of data to be generated, this software is designed to write data

continuously to the computer hard disk and save them as txt file so it can be read by the Matlab.

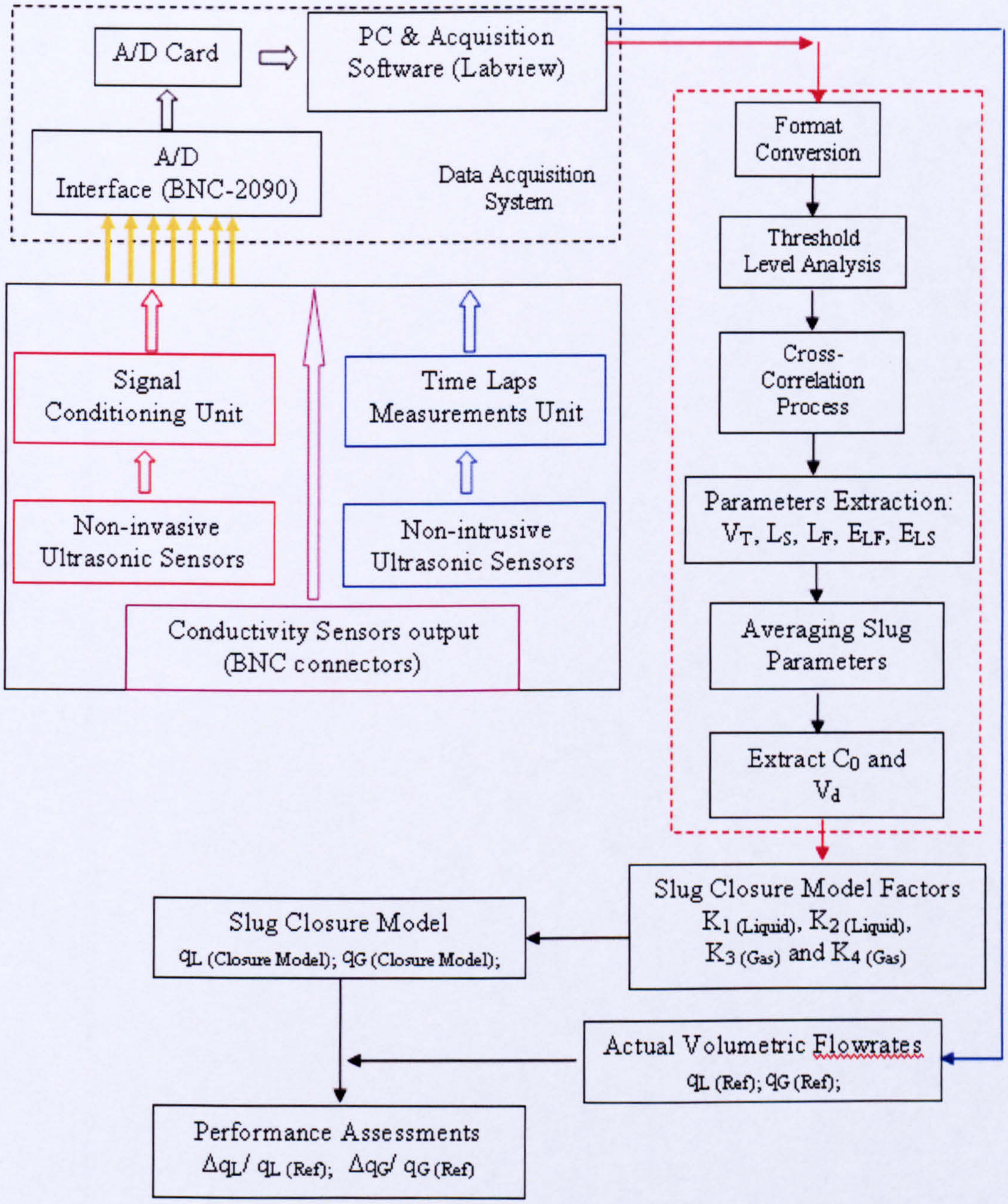

Figure 6-1: Schematic Diagram of Ultrasonic Multiphase Concept

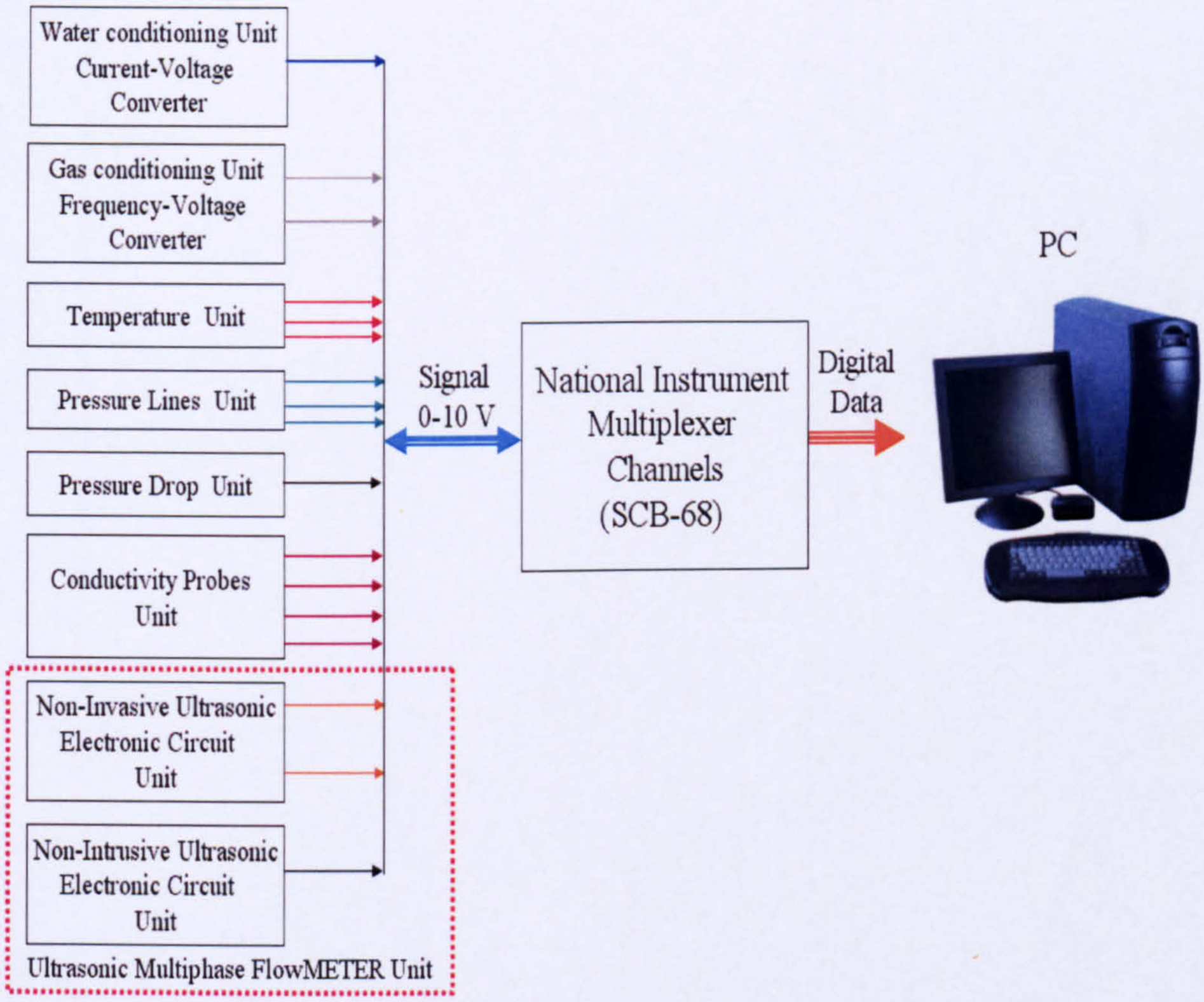

Figure 6-2: Data Acquisition Unit in Two-Phase Air/Water Facility

The data analysis was done using a set of software codes generated in Matlab which involved format conversion, threshold level analysis and cross-correlation process. The parameters extracted using Matlab codes were the average slug characteristics, including slug translational velocity ,V_T, slug length ,L_S, film zone length ,L_F, slug body holdup ,$E_{LS,}$ and film liquid holdup E_{LF}.

In order to obtain the gas and liquid phase volumetric flowrates from the slug closure model equations, the factors $K_{1(Liquid)}$, $K_{2(Gas)}$, $K_{3(Liquid)}$ and $K_{4(Gas)}$ must be calculated. Therefore, the coefficients,$C_{o,}$ and ,V_d, were derived based on slug translational velocities ,V_T, and mixture velocities ,V_{mix}, data. The gas and liquid flowrates obtained using this metering concept was validated with the reference gas and liquid phase measurements.

The concept of the slug closure model developed in this work is schematically presented in Figure 6-3. The input parameters for this model are the slug characteristics and the outputs results are the gas and liquid phase volumetric flowrates.

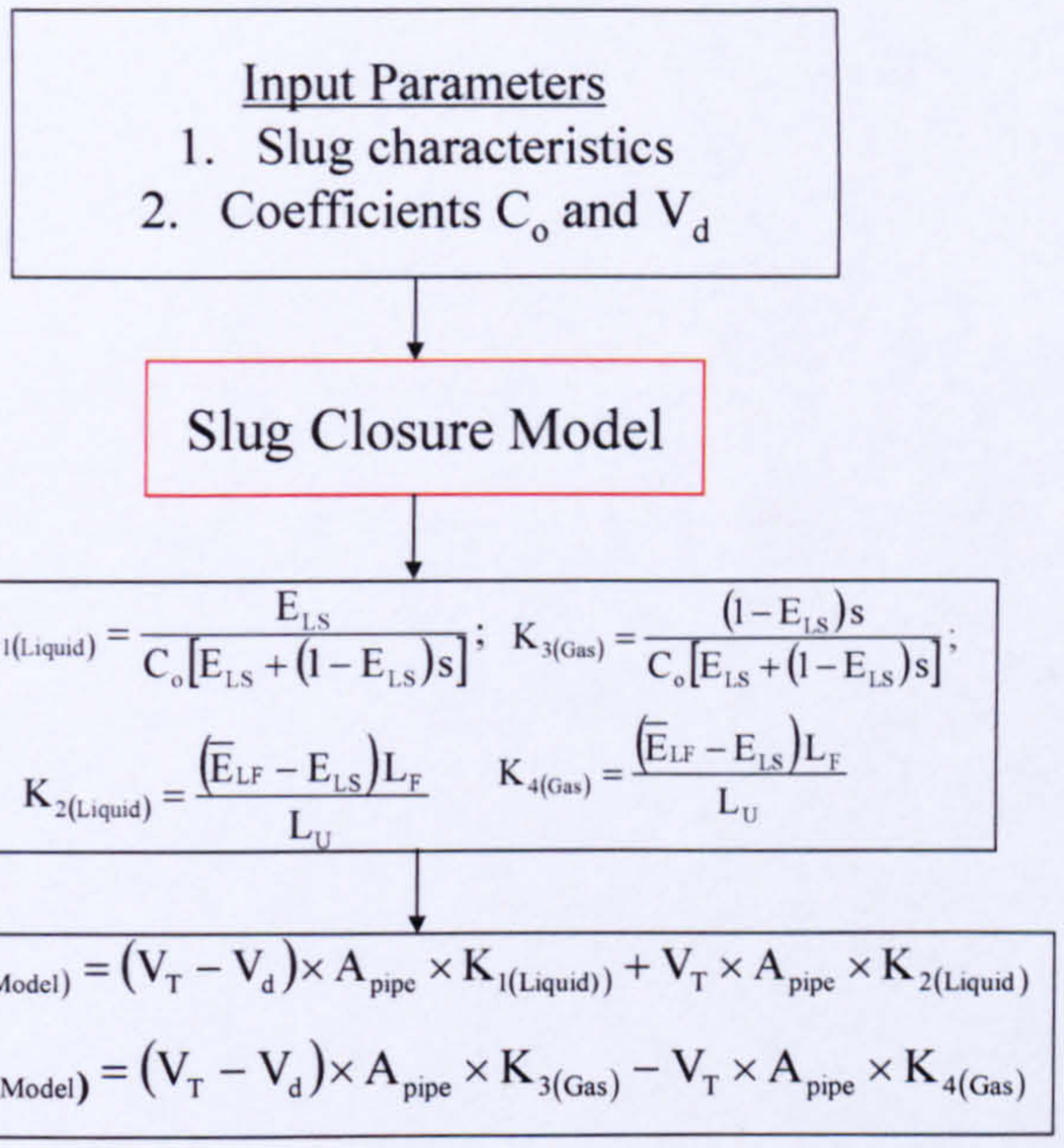

Figure 6-3: Schematic Diagram of the Concept of Ultrasonic Flowmeter

6.3 Performance of Ultrasonic Multiphase Metering Concept

The two-phase gas/liquid slug flow conditions tests campaigns performed in order to test the concept of the ultrasonic multiphase developed in this work are listed in Table 1 in Appendix A. These tests covered the range of 0.3-1.03 ms^{-1} and 0.6-3.0 ms^{-1} superficial liquid and gas velocities respectively as is presented in Figure 6-4.

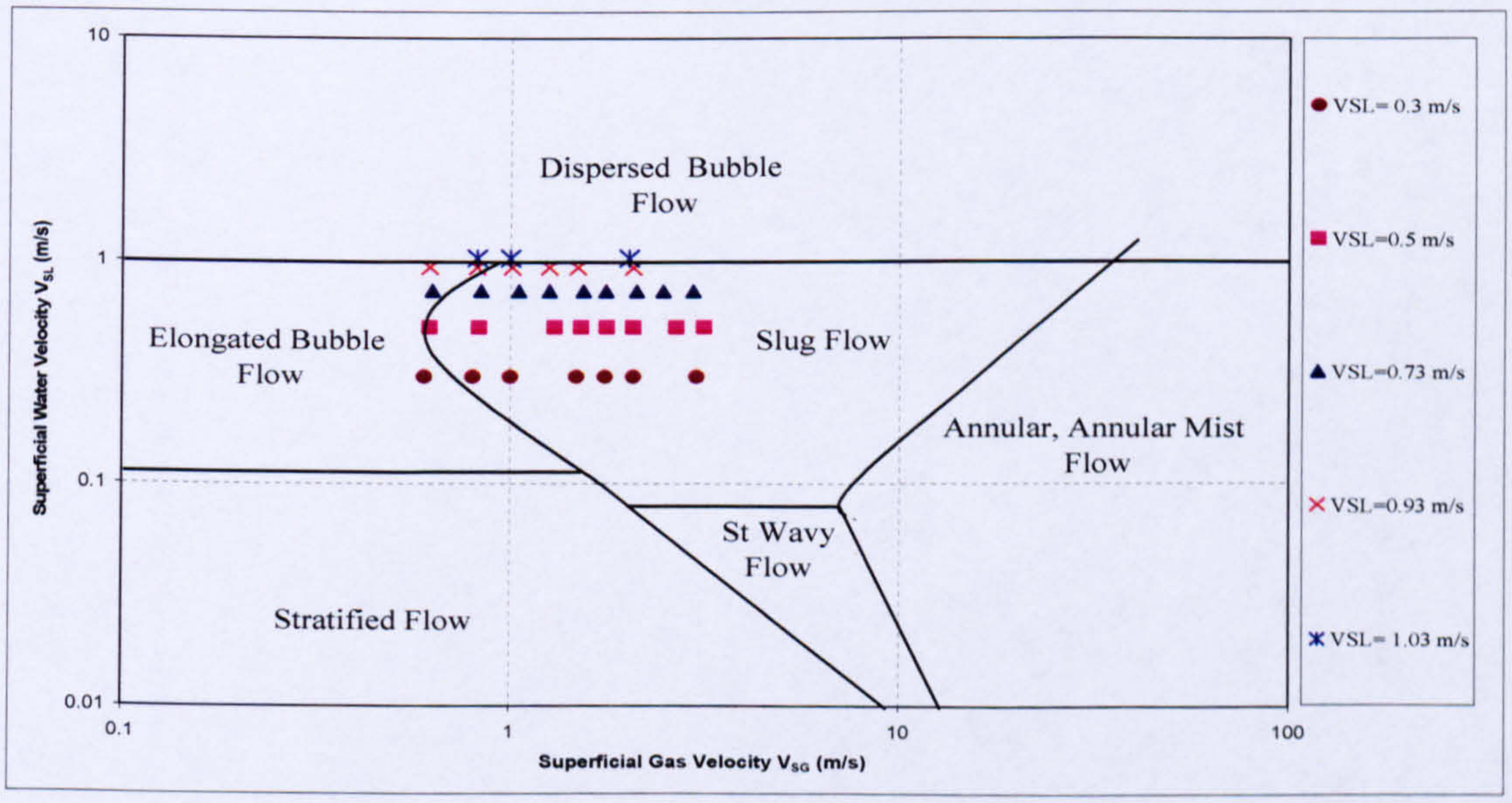

Figure 6-4: Two-Phase Water/Air Experimental Campaigns Flow Map

These tests range concentrates upon the slug flow conditions. Test phases were air (density 1.2 kg m^{-3}, viscosity 1.8×10^{-5} kg ms^{-1} at 20 °C and atmospheric pressure) and water (density 998.2067 kg m^{-3}, viscosity 9.772×10^{-4} kg ms^{-1}). The tests matrix covered the following slug flow points:

$$V_{SL} \in \{0.3, 0.5, 0.73, 0.93, 1.03\}$$
$$V_{SG} \in \{0.63, 0.84, 1.05, 1.26, 1.54, 1.76, 2.11, 2.47, 2.95, 3.15\}$$

6.3.1 Model Factors $K_{1\,(Liquid)}$, $K_{2\,(Liquid)}$, $K_{3\,(Gas)}$ and $K_{4\,(Gas)}$

The values of the factors $K_{1\,(Liquid)}$, $K_{2\,(Liquid)}$, $K_{3\,(Gas)}$ and $K_{4\,(Gas)}$ were obtained at different slug flow conditions as presented in Table 3 in Appendix A. These factors are calculated based on the slug body liquid holdup, slug length, film length, coefficients C_0, V_d and the slip ratio. The factors $K_{1\,(Liquid)}$ and $K_{3\,(Gas)}$ are given in equation (6.1):

$$K_{1(Liquid)} = \frac{E_{LS}}{C_o\left[E_{LS} + (1 - E_{LS})s\right]};$$
$$K_{3(Gas)} = \frac{(1 - E_{LS})s}{C_o\left[E_{LS} + (1 - E_{LS})s\right]}; \qquad (6.1)$$

where E_{LS} is the slug body liquid holdup and s is the slip ratio with the slug body.

These factors are function of slug body holdup, gas void fraction in slug body, flow profile, $C_{o,}$ and slip ratio between the gas and liquid phases in the slug body. In Figure 6-5, the factors are plotted against the mixture velocity.

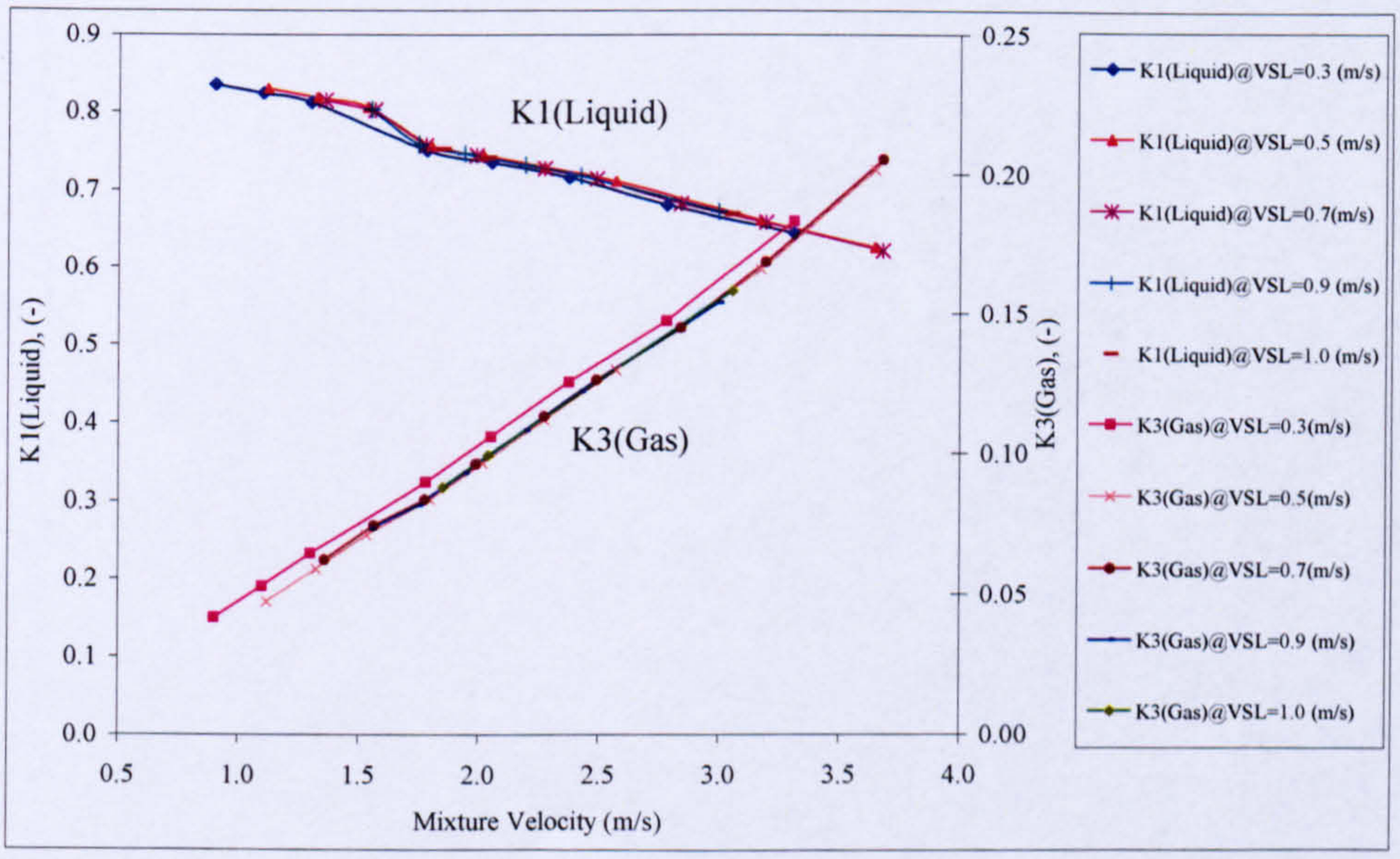

Figure 6-5: Slug Closure Model Factors $K_{1\,(Liquid)}$ and $K_{3\,(Gas)}$ versus Mixture Velocity

It can be seen from Figure 6-5 that the values of the $K_{1\ (Liquid)}$ decreases with increasing the mixture velocity. This is probably due to the increase of the gas void fractions in the slug body as is shown in Figure 6-6.

However, as the mixture velocity increases, the $K_{3\ (Gas)}$ factor strongly increases because of the increase of the gas void fraction values in the slug body.

The $K_{1\ (Liquid)}$ factor behaves similarly when it is plotted against the water flowrates obtained by slug closure model in Figure 6-7, therefore, it can be concluded that the factor $K_{1\ (Liquid)}$ is dominated by the values of the slug body liquid holdup.

However, the $K_{3\ (Gas)}$ is basically dominated by the value of the gas void fraction within the slug body as is shown in Figure 6-8, where the variation of the gas flowrates obtained by slug closure model with $K_{3\ (Gas)}$ is presented.

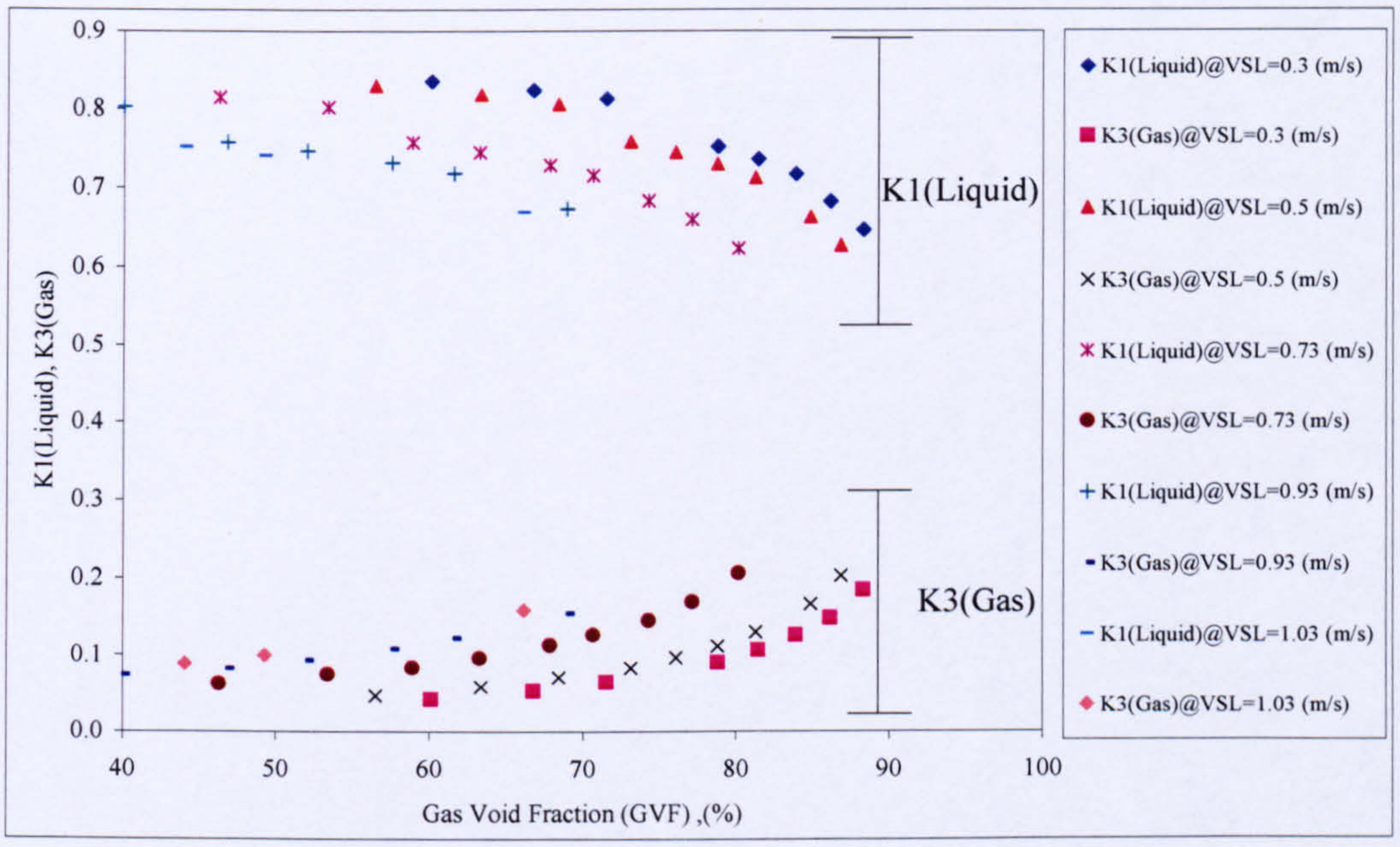

Figure 6-6: Slug Closure Model Factors $K_{1\ (Liquid)}$ and $K_{3\ (Gas)}$ versus GVF

The factors $K_{2\ (Liquid)}$ and $K_{4\ (Gas)}$ are given in equation (6.2):

$$K_{2(Liquid)} = \frac{(E_{LF} - E_{LS})L_F}{L_U} \qquad (6.2)$$

$$K_{4(Gas)} = \frac{(E_{LF} - E_{LS})L_F}{L_U}$$

where
E_{LF} is the average liquid film holdup,
E_{LS} is the slug body liquid holdup, L_F is the film zone length and
L_U is the total length of the slug unit.

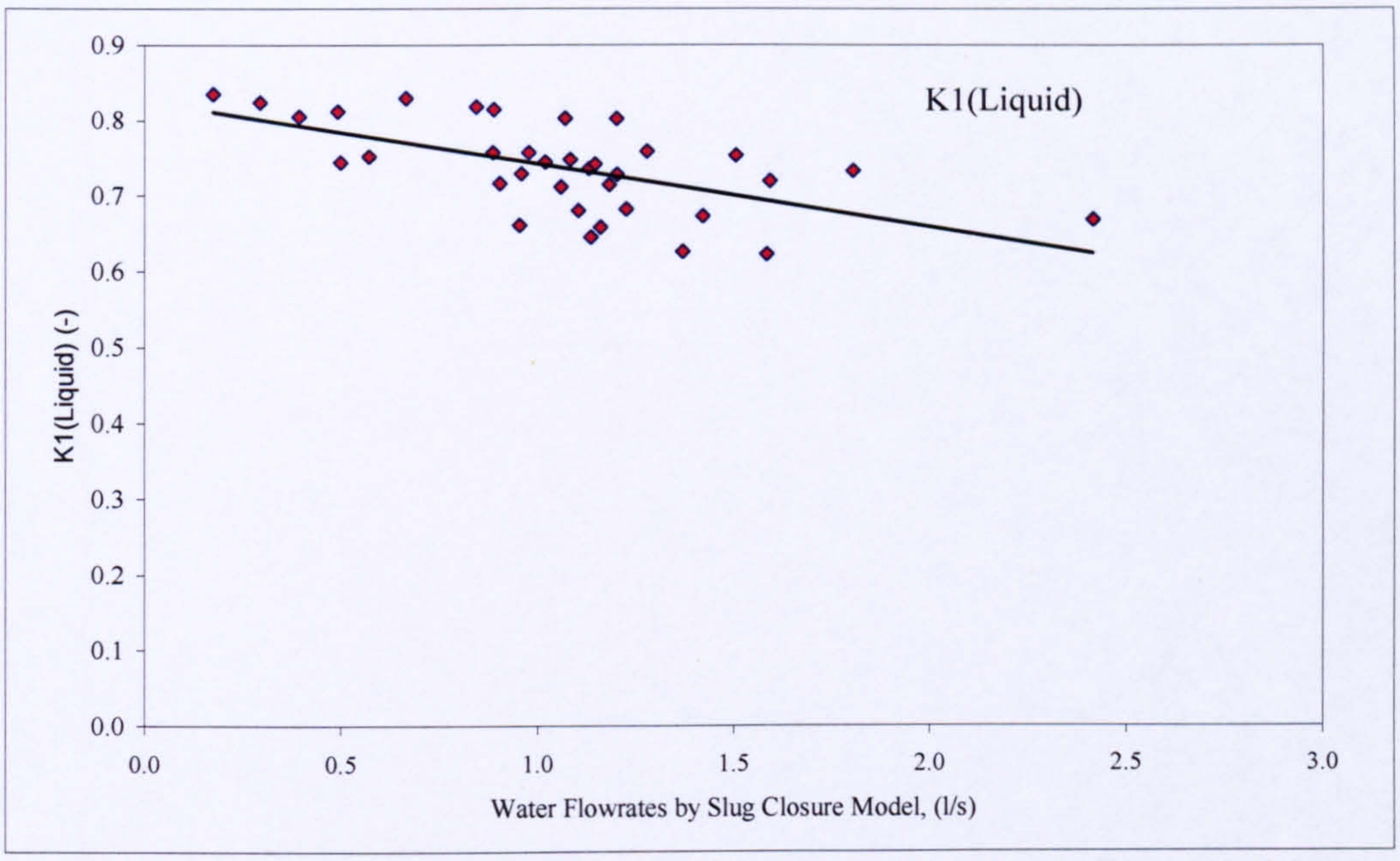

Figure 6-7: Water Flowrates by Slug Closure Model vs. $K_{1\ (Liquid)}$ Factor

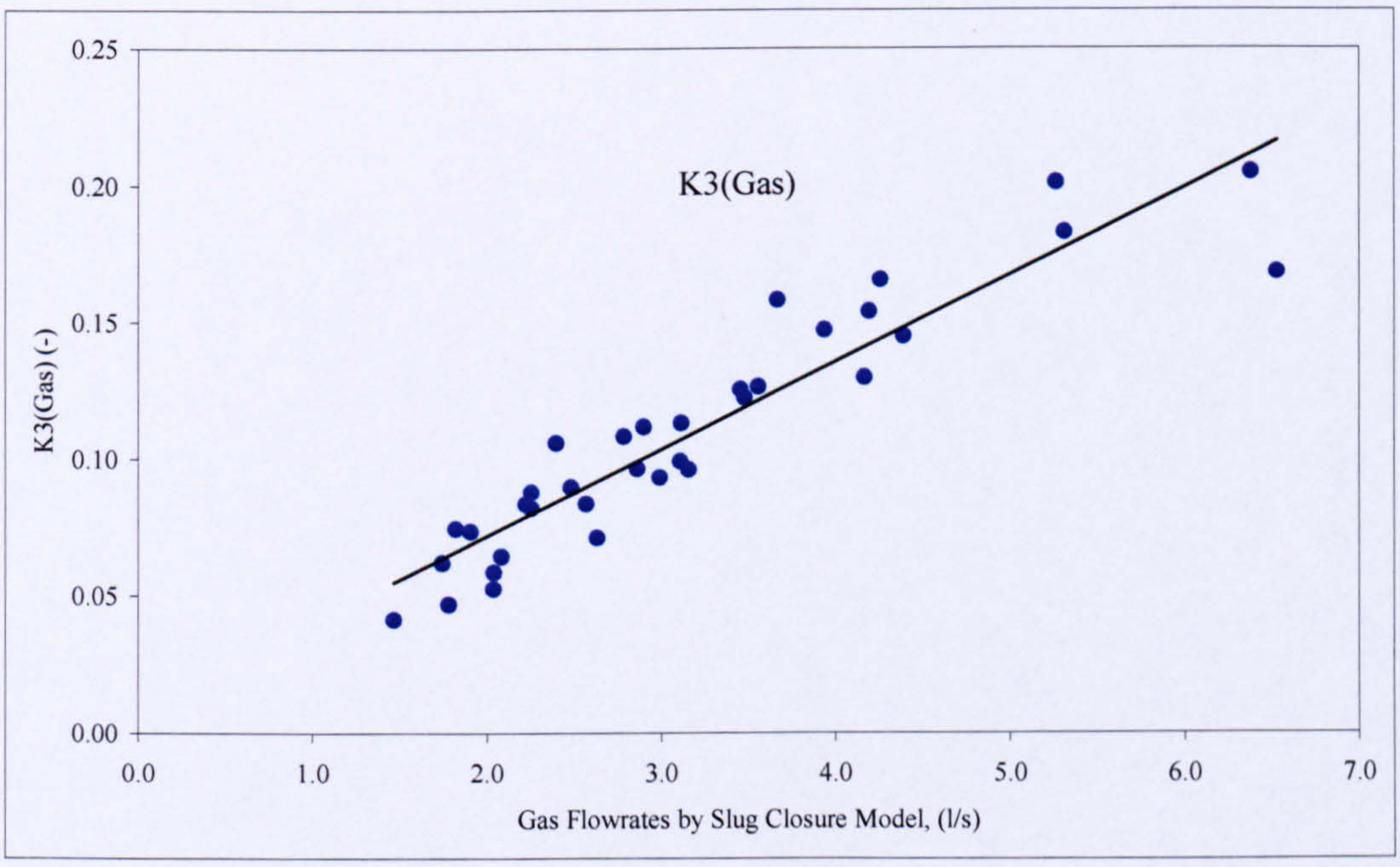

Figure 6-8: Gas Flowrates by Slug Closure Model vs. $K_{3\ (Gas)}$ Factor

The factors $K_{2\ (Liquid)}$ and $K_{4\ (Gas)}$ are equal and they are function of the film length, total slug unit length, slug body liquid holdup and average liquid film holdup in the film

region. The values of these factors are negative and that is due to the dominated values of the slug body liquid holdup.

However, the values of these factors increase with increasing the water flowrates obtained by the slug closure model mainly due to the increase of the gas void fractions in the slug body and decrease of the slug body liquid holdup and also due to the increase of the film region length (Manolis, 1995), which is shown in Figure 6-9.

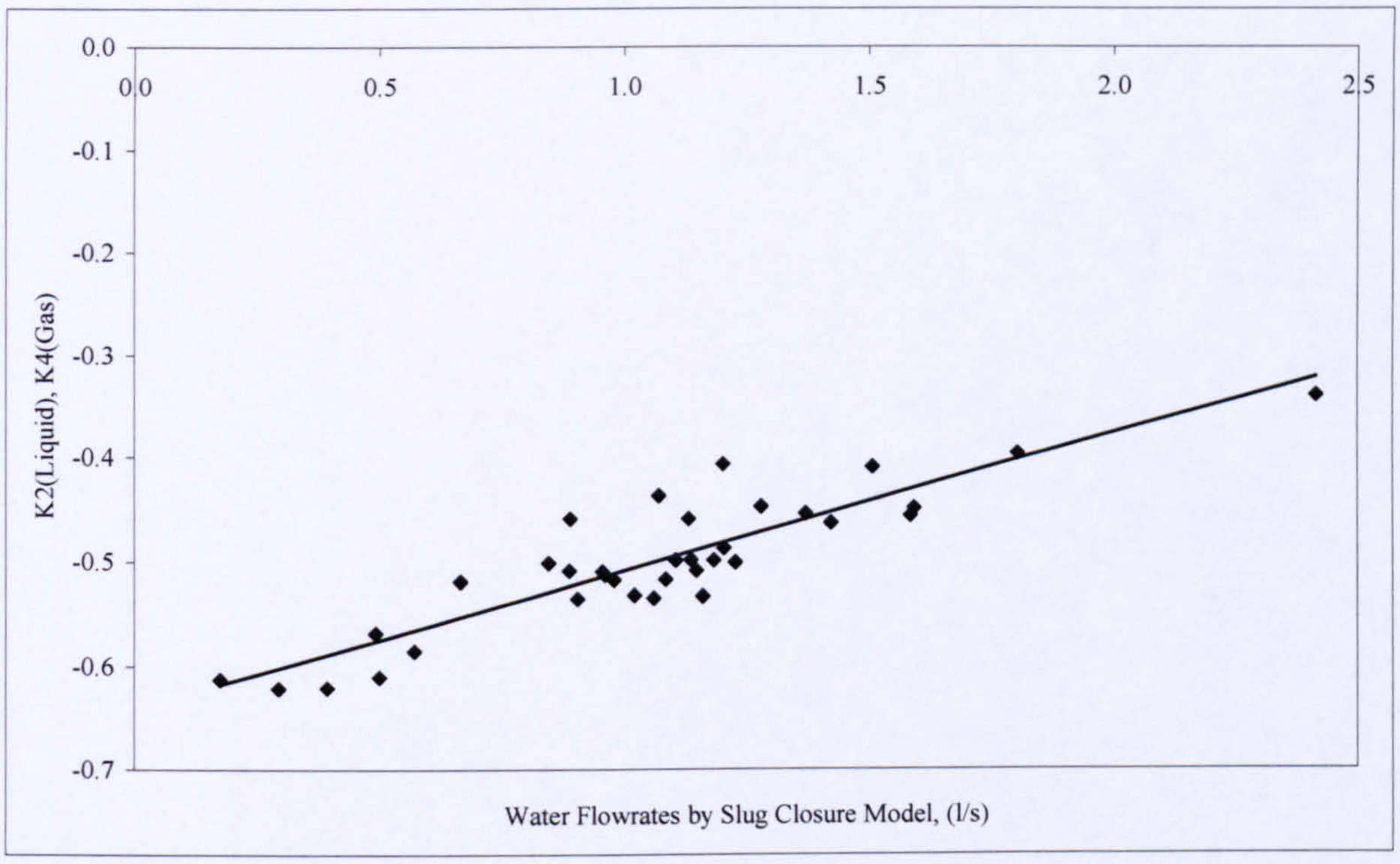

Figure 6-9: Water Flowrates by Slug Closure Model vs. $K_{2\,(Liquid)}$, $K_{4\,(Gas)}$ Factors

6.3.2 Assessment of the Ultrasonic Multiphase Metering Concept

The proposed ultrasonic multiphase flowmetering concept for the gas and liquid volumetric flowrates measurements performance is determined by examining the relative prediction errors following two methods:

1. Validate the proposed ultrasonic flowmetering system performance using reference flowmeters (electromagnetic water flowmeter and air turbine flowmeter) by applying the equation (6.3):

$$PE_{\text{Liquid Phase}} = \frac{q_{L(\text{Ultrasonic})} - q_{L(\text{Reference})}}{q_{L(\text{Reference})}} \times 100$$

$$PE_{\text{Gas Phase}} = \frac{q_{G(\text{Ultrasonic})} - q_{G(\text{Reference})}}{q_{G(\text{Reference})}} \times 100 \qquad (6.3)$$

where PE is the percentage error.

2. The performance of the proposed ultrasonic flowmetering concept can be determined by assessing the slug closure model under different two-phase flow conditions for different pipe geometry. For this reason, different values of the coefficient C_0 (slug profile) and the drift velocity V_d were chosen from Stewart (2001), Nydal *et al.* (1992) and Manolis (1995) correlations and used in the slug closure model developed in this work

6.3.2.1 Performance Assessment compared with Reference Flowmeters

As explained in Chapter 4, the setup of the experimental facility, the individual phases (water and air) volumetric flowrates were metered before mixing with the second phase as shown in Figure 6-10.

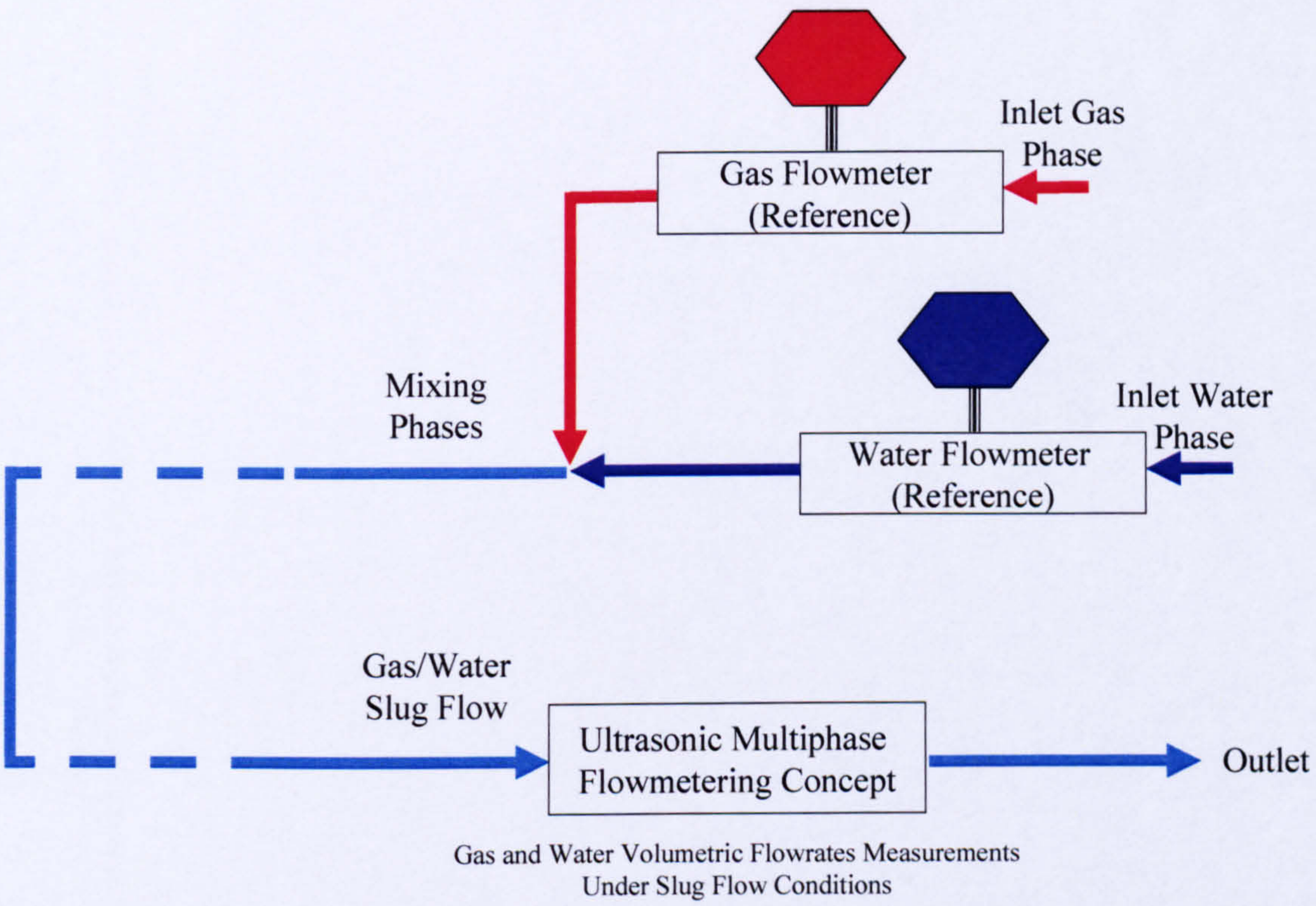

Figure 6-10: Reference Flowmeters and the Proposed Ultrasonic Multiphase Metering Concept Schematic Diagram

Table 4 in Appendix A displays the relative errors for the gas and liquid phase volumetric flowrates measured by the proposed ultrasonic multiphase metering system under slug flow conditions and the following trends are observed:

In general, the error of the liquid phase volumetric flowrate exceeds the error in the gas phase, over most of the experimental test range.

The liquid and gas phase relative errors are the largest at low gas and low liquid superficial velocities (about 42% and 63 % respectively) as shown in Figures 6-11 and 6-12.

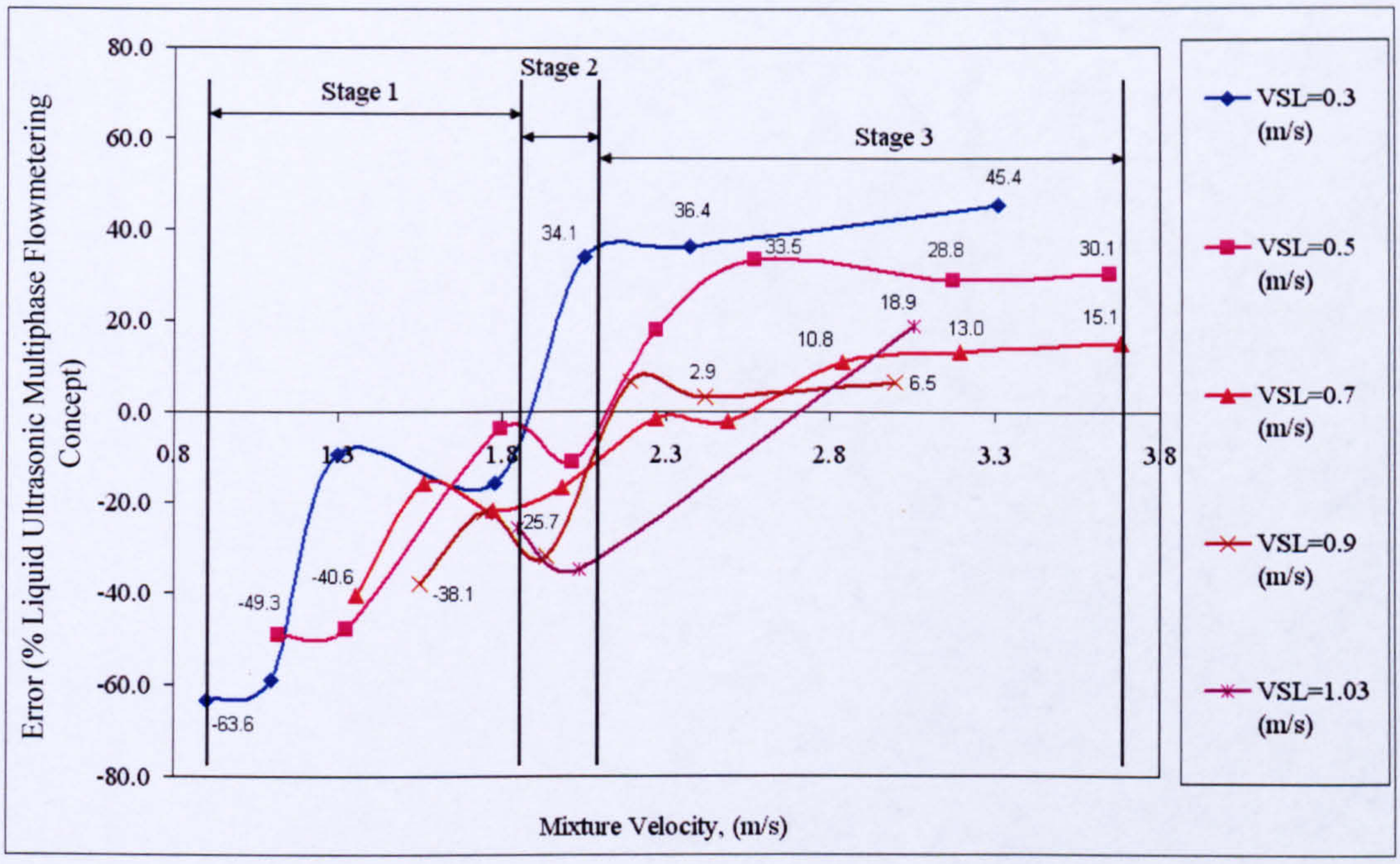

Figure 6-11: Liquid Phase Relative Prediction Error

For liquid phase error analysis at stage1 (see Figure 6-11), increasing the gas superficial velocity causes the liquid phase prediction error to fall from an average value of -47 % and -15%.

In stage 1, the slugs begin to develop and the gas bubbles changes from plug shape to slug shape with a very low percentage of bubbles in the liquid slug body. However by further increasing the gas superficial velocity, stage 2 (see Figure 6-11) a rise in the liquid phase relative error was observed for most of the test conditions.

However, in this stage the error has a reverse relationship with the superficial liquid velocity. That means, at a fixed value of superficial gas velocity, the error reduces by increasing the superficial liquid velocity. This can be explained by the slug growth model presented by Hale (2000). In this model Hale stated, based on the experimental investigations, that increasing the superficial liquid velocity within slug flow conditions pushes the slug to reach its well developed state.

In stage 3 (see Figure 6-11), after the slug passed from growth to developed state at stage 2, the liquid phase error reaches stable conditions apart from Campaign #5 (V_{SL}= 1.03 ms^{-1}) where the flow is in transition mode from slug to bubbly flow. The error of the liquid phase in stage 3 ranges from 45.4 % at V_{SL}= 0.3 ms^{-1} to 6.5 % at V_{SL}= 0.9 ms^{-1}.

Figure 6-12 presents the same liquid phase percentage errors at different slug flow test conditions which were presented in Figure 6-11, but in three dimension plotting method.

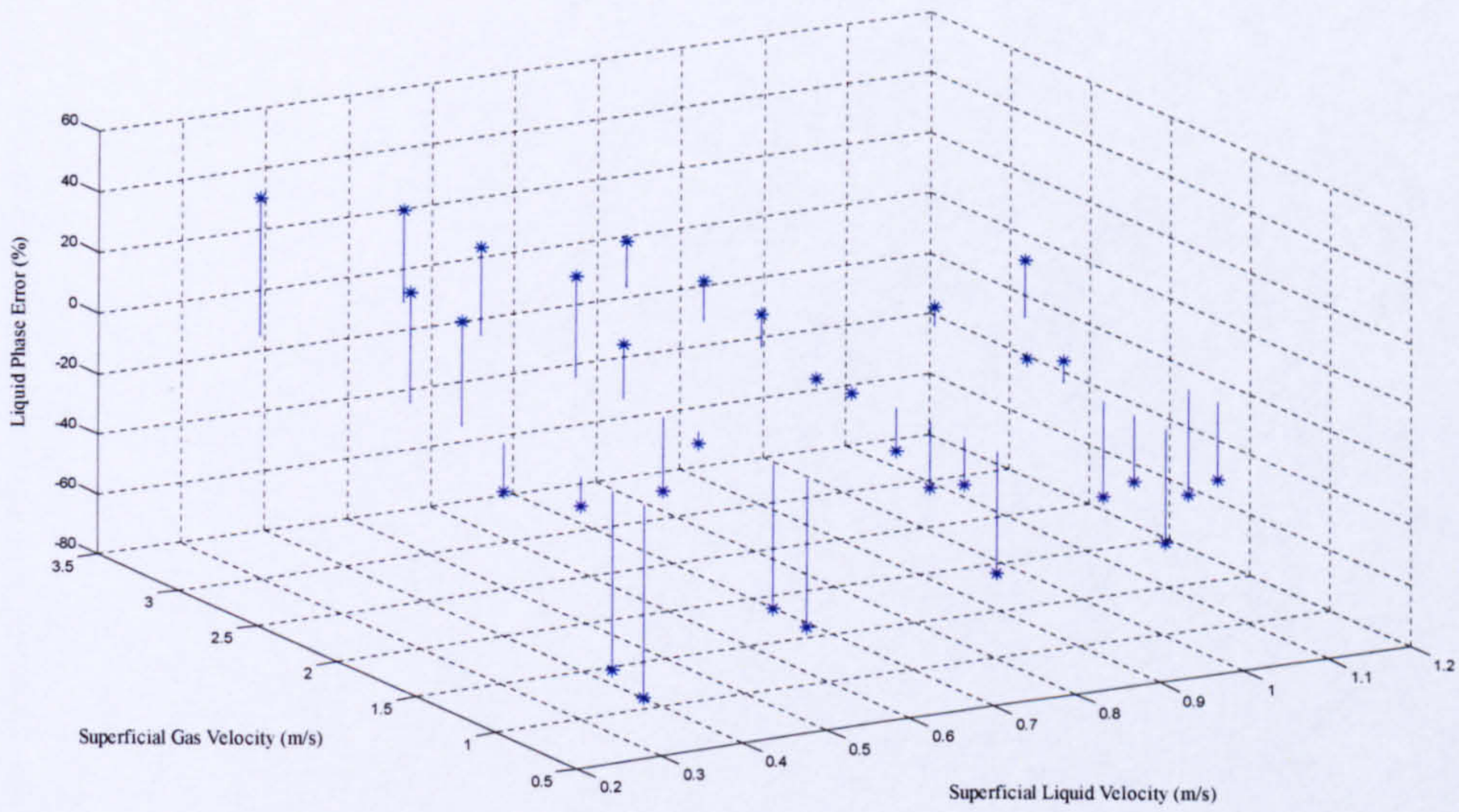

Figure 6-12: 3Dimension Liquid Phase Relative Prediction Error

Increasing the liquid superficial velocity towards bubbly flow conditions causes the gas phase relative error for most tests points to decrease from 42% to 22 %,(see Figure 6-13),. Increasing the gas phase superficial velocity causes the gas phase relative error to decrease considerably to 10 %. Figure 6-14 presents three dimensions plotting of the gas phase percentage errors which were presented in Figure 6-13.

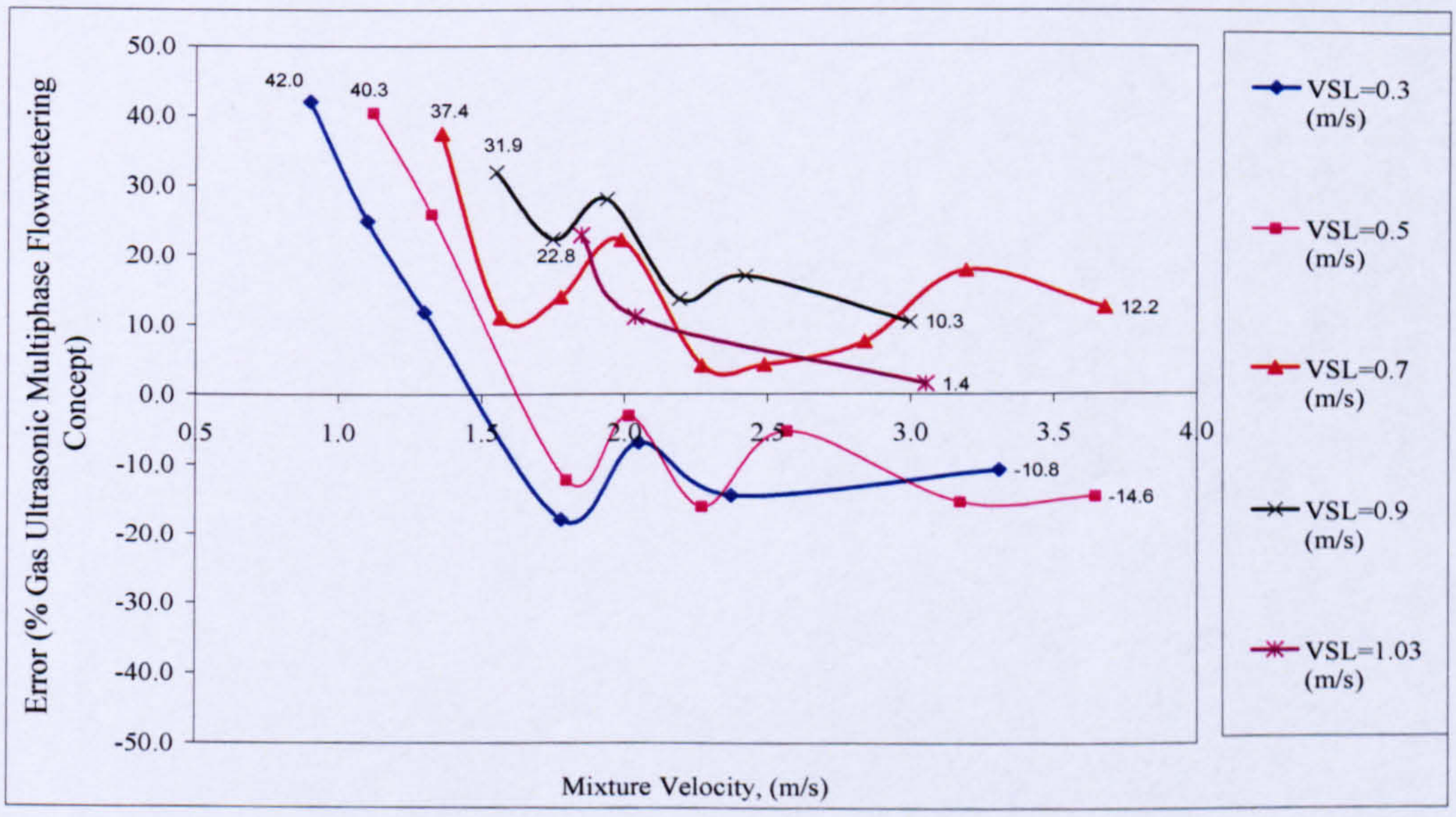

Figure 6-13: Gas Phase Relative Prediction Error

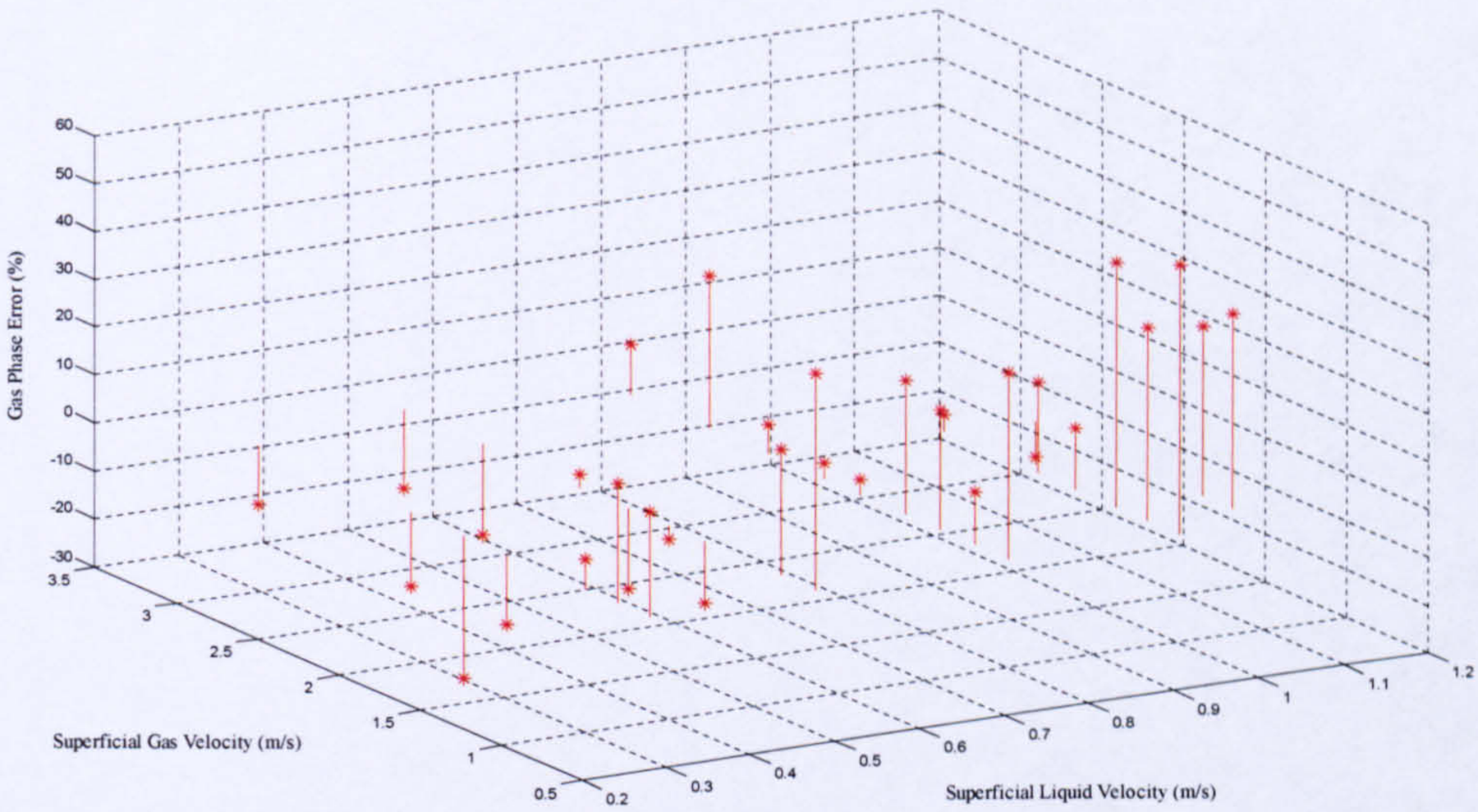

Figure 6-14: 3Dimension Gas Phase Relative Prediction Error

6.3.2.2 Performance Assessment Based on C_0 and V_d from Literature

In order to assess the performance of the proposed ultrasonic multiphase flowmeter concept under different flow conditions, the ultrasonic metering system was tested against different values of C_0 and V_d from previous experimental work including Stewart (2001), Nydal *et al.* (1992) and Manolis (1995) as listed in Table 6-1.

Table 6-1: C_o and V_d values

Reference	C_o	V_d
Stewart (2001)	1.29	1.09
Manolis (1995)	1.033 (Fr < 2.86)	0.33 (Fr < 2.86)
Manolis (1995)	1.216 (Fr > 2.86)	0.0 (Fr >2.86)
Nydal *et al* (1995)	1.2	0.0
This Work	1.14 (Fr < 2)	0.2017 (Fr < 2)
This Work	1.1891 (2 ≤ Fr < 4)	0.0285 (Fr < 2)
This Work	1.206 (Fr ≥4)	0.0 (Fr < 2)

Based on the coefficients C_0 and V_d assessments, the following trends are observed:

For the liquid phase, the values of $\underline{q_L}$ obtained from the slug closure model using C_0 and V_d coefficients from this work are in a good agreement with the that obtained using coefficients from Manolis (1995) and Nydal *et al.* (1992).

This agreement holds good for the whole range of mixture velocity studied. It can be noticed that by increasing the superficial liquid velocity, the error decreases as shown in

Figure 6-15. However, using coefficients from Stewart (2001) in the slug closure model results into high errors in the range of 100% to 250% as shown in Figure 6-16. Obviously, this error range falls from (265 % to 165 %) to another level (145% to 102%) by increasing the superficial liquid velocity from (0.3 to 0.7 ms^{-1}). The high error of the liquid phase volumetric flowrate obtained from the slug closure model using Stewart (2001) C_o and V_d coefficients, was a result of the high drift velocity value (V_d=1.09 ms^{-1}) compared to the other researchers as listed in Table 6-1.

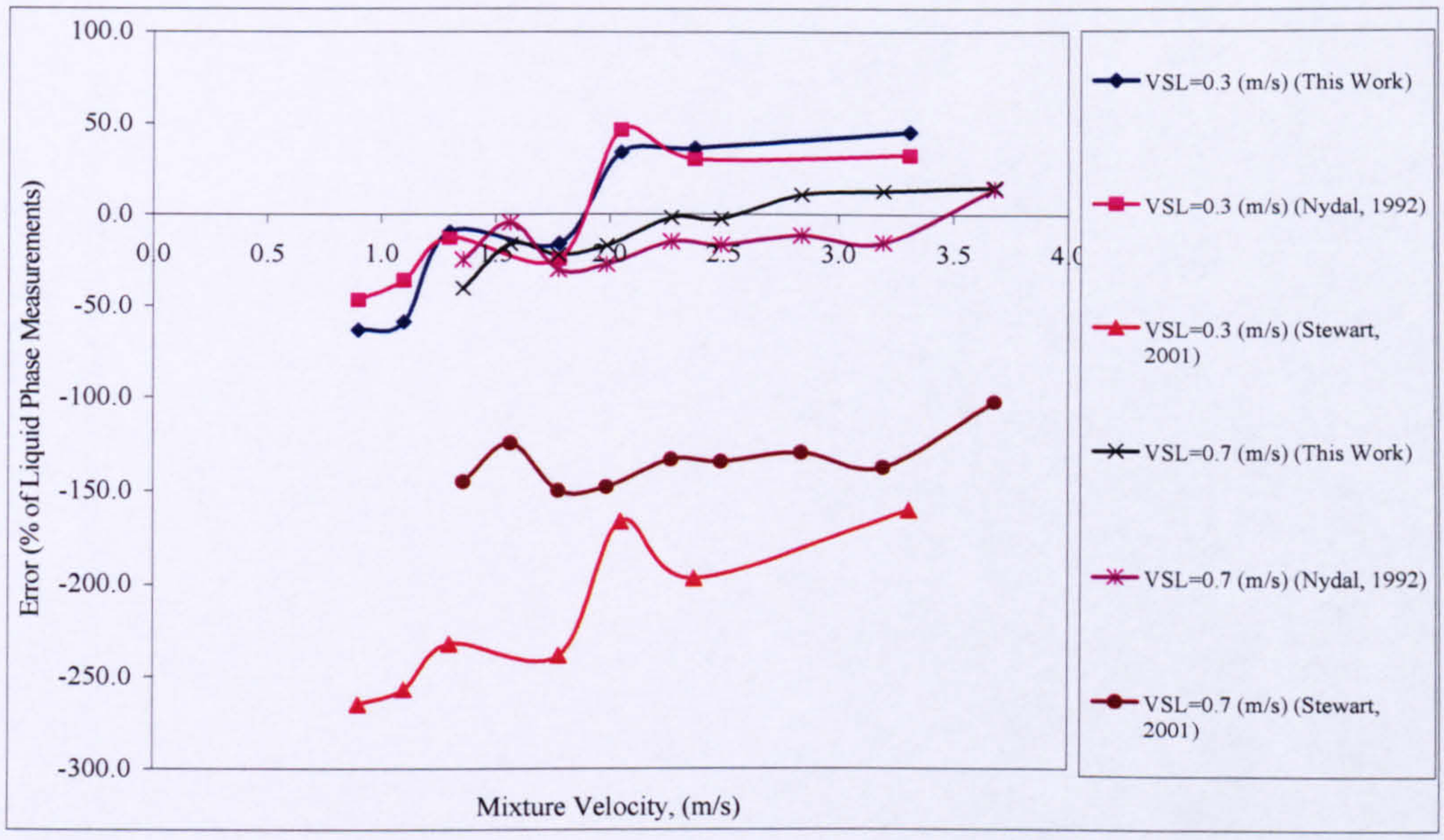

Figure 6-15: Liquid Phase Error using C_o and V_d Values at (V_{SL}=0.3, 0.7 ms^{-1})

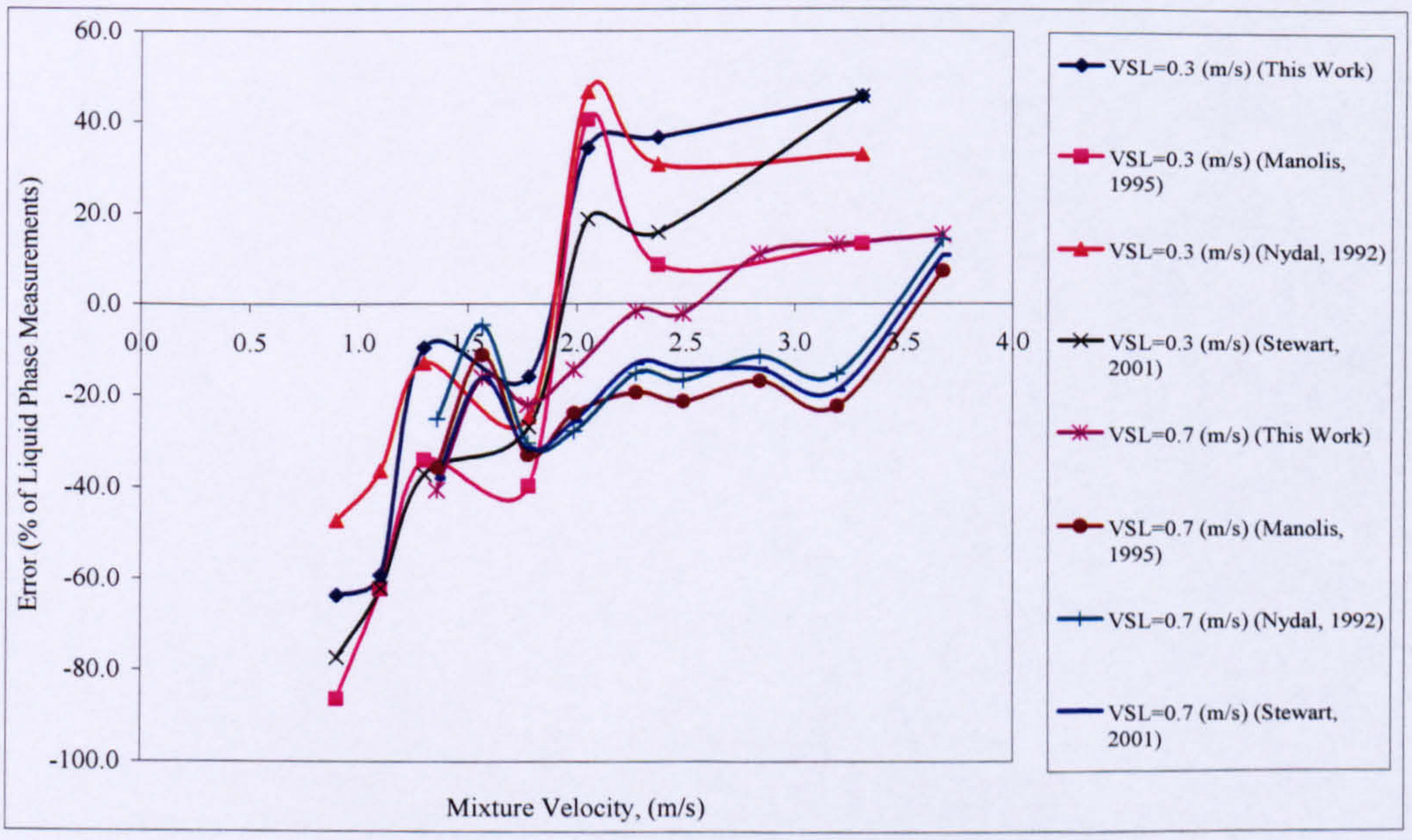

Figure 6-16: Liquid Measurements at (V_d=0 ms^{-1}) using (Stewart, 2001) Coefficients

6.4 Summary

In this chapter, an ultrasonic multiphase metering concept is proposed and assessed. The error assessments of the proposed ultrasonic metering system for the gas and liquid phase volumetric flowrates were performed by the determinations of the relative errors compared with the reference flowmeters.

A considerable degree of success had been achieved for both gas and liquid phase volumetric flowrate. However, the overall industrial requirements were not achieved by the proposed ultrasonic metering for most test conditions.

Chapter 7

Conclusions and Recommendations for Future Work

7.1 Conclusions

Multiphase flowmetering has been the centre of attention in the oil and gas industry. Because multiphase flowmeters do not use large volume separators, the response time of multiphase flowmeter is much faster than that of test separators. In addition to providing more temporal information than conventional well test systems, multiphase meters can also provide other real-time information such as water content. Such information allows rapid operator intervention and optimisation of production. However, multiphase flowmeter do not perform well during the production of intermittent slug due to the unpredictable nature of slug flow through its growth and dissipation process. The key objectives of this thesis were to:

- Review of the multiphase metering systems.

- Review of ultrasonic applications in multiphase flow measurement.

- Development of a slug closure model to estimate the gas and liquid phase volumetric flowrates from slug flow parameters determined by ultrasonic sensors.

- Measurement of the slug flow characteristics by non-invasive and non-intrusive ultrasonic sensors.

- Design and build a two-phase gas/liquid facility and its associated instrumentations to assess the performance of the proposed ultrasonic multiphase flowmetering concept under different two-phase gas/liquid slug flow conditions.

- Assessment of the performance of the proposed ultrasonic multiphase flowmetering concept.

The thesis has demonstrated:

- The implementation of the current ultrasonic measuring techniques under slug flows is difficult to achieve, due to the unpredictable and complicated nature of slug flow.as well as the disability of the current ultrasonic techniques to continue to function under this regime. Therefore, an approach based on combination of slug flow modelling and direct slug characteristics measurements by ultrasonic techniques was proposed in this work.

- A slug closure model to infer the gas and liquid phase volumetric flowrates has been developed based on the "slug unit" model.

- The proposed ultrasonic metering strategy was based on the combination of the non-invasive and non-intrusive ultrasonic sensors and the slug closure model to obtain the phase volumetric flowrates. The slug characteristics obtained by non-invasive and non-intrusive ultrasonic techniques form inputs to slug closure model. Using these inputs, the slug closure model calculates the factors $K_{1\,(Liquid)}$, $K_{2\,(Liquid)}$, $K_{3\,(Gas)}$ and $K_{4\,(Gas)}$. These factors are a function of the slip ratio in the slug body, flow profile (C_0), drift velocity (V_d), slug body liquid holdup, gas void fraction in slug body, slug length, film length, and the total length of the slug unit. From these factors and the slug translational velocity, the slug closure model calculates the gas and liquid phase volumetric flowrates

- To extract the slug parameters, a range of analysing techniques were applied. These include, signal cross-correlation for slug translational velocity measurements and threshold level analysis for slug body passing time and film region passing time measurements. The slug characteristics measured by non-invasive and non-intrusive ultrasonic techniques were compared with the slug characteristics measurements by conductivity probes and with a number of correlations from the literature.

- The slug characteristics measured were slug frequency, slug translational velocity, slug body length, film region length, slug body and film liquid holdup. The performance assessment of the non-invasive and non-intrusive ultrasonic techniques for slug characteristics measurements are summarised in the following:

    - The slug frequency increases rapidly from 0.13 Hz to 1.5 Hz with the superficial liquid velocity, V_{SL}, but changes only marginally with the

superficial gas velocity V_{SG}. Based on the Strouhal number analysis, the Gregory and Scott (1969) correlation provides a good match to the present data.

- For the translational velocity which was measured by non-invasive ultrasonic technique, percentage error is of the order of 2.3 % to 18 % for the full range of test conditions and with standard deviation of ±2.9%.

- The average slug length obtained by ultrasonic is around 16d, compared to 17d average slug length obtained by conductivity measurements. The small difference in the slug length can be attributed to the difference in the pulse width and pulse shape of both signals. This affects the slug length predictions using threshold technique.

- The slug body liquid holdup measurements by ultrasonic techniques give satisfactory results in comparison with the conductivity technique measurements, and the relative error was mostly within 0.162 %.

- The film liquid holdup measured by ultrasonic technique decreased as the superficial gas velocities increased. At low superficial gas velocity, the film liquid holdup error is of the order of 1.14 % in comparison to the conductivity measurements, however, at higher superficial gas velocity the error increases up to 5 %.

- The coefficients C_0 and V_d were extracted from the data based on the Froude number analysis proposed by Ferre (1979) and Bendiksen (1984). The values of flow profile C_0 is within the range 0.98-1.5 also reported discussed by Hale (2000).

The proposed ultrasonic multiphase flowmetering concept was assessed using the two-phase gas/liquid flow under slug flow conditions. Gas-water slug flow data were gathered from the data acquisition system and processed through the software code for a range of superficial velocities V_{SL}=0.3 to 1.03 ms^{-1} and V_{SG}=0.6 to 3.01 ms^{-1}. Based on the relative error assessments performed for gas and liquid phase volumetric flowrates, the followings findings were made:

- The performance of the proposed ultrasonic multiphase flowmeter system is seriously affected at low liquid and air flows in the region that the slugs were still developing. However, the performance improved and stabilised when slugs became well developed.

- Under bubbly flow conditions V_{SL}=1.03 ms^{-1} the performance of the ultrasonic multiphase flowmeter system did not stabilise and that demonstrated the limitation of this proposed meter under different flow conditions.

- The gas and the liquid phase volumetric flowrates measurements by the proposed ultrasonic multiphase flowmetering concept, did not achieve the overall goal of a 5% relative error for the tests conditions.

- The liquid phase percentage errors using the proposed ultrasonic metering concept were ranged from -63.6% to 45.4%. However, the gas phase percentage errors using the proposed ultrasonic metering concept were ranged from 42% to -14.6%.

7.2 Future Work

The present work attempted to develop an ultrasonic multiphase flowmetering system to measure the gas and liquid phase volumetric flowrates with better accuracy than the other multiphase flowmetring devices currently available in the market. The proposed ultrasonic multiphase metering concept presented in this work could measure the liquid with percentage errors ranged from -63.6% to 45.4% and the gas phase with percentage errors ranged from 42% to -14.6%.

The overall goal of a 5% relative error metering for both phases was not achieved for the conditions tested. Therefore, further improvements to the proposed ultrasonic multiphase metering are required. The possible improvements are summarised as following:

- Improve the performance of the ultrasonic multiphase flowmeter to function under different flow regime conditions including the stratified, bubble and annular flow regimes. This can be achieved by an additional array of non-intrusive ultrasonic sensors around the outside and along the length of the pipe to determine the parameters associated with each flow regime (Figure 7-1).

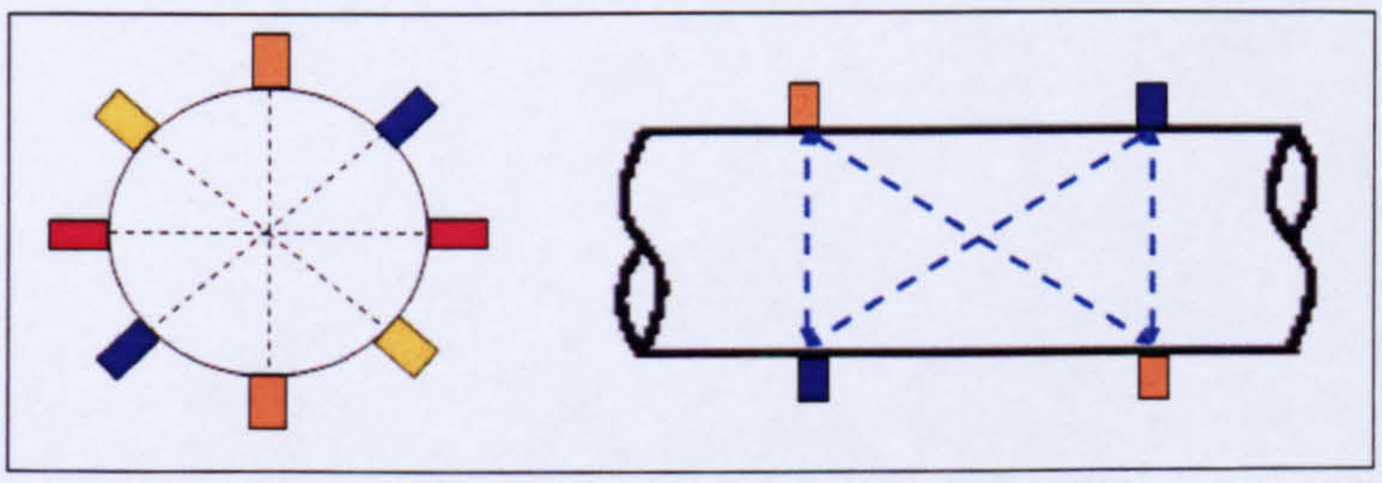

Figure 7-1: Arrangement of Ultrasonic Transducers

- Reduce the relative error in the gas and liquid phase volumetric flowrates to $\pm 5\%$ in compliance with the industrial requirement by improving the functionality of the data processing system by using Dedicated Ultrasonic Signal Control and Acquisition Processer (DUSCAP) which is associated with each transducer or transducer pair and act as central processor.

- The central processor will have the task of combining and processing the information to give the best estimate of the phases flow rate, and phase fraction and other parameters.

- Develop or implement extra instrumentation for the measurement of an oil phase, therefore completing the development of an ultrasonic multiphase flowmeter for three phase system. This can be achieved by using another gamma ray densitometer.

- Improvement of the performance of the ultrasonic techniques in two-phase and multiphase gas/liquid flow can be achieved by changing the complex and unpredictable intermittent slug flow regime to stratified and stratified wavy flow using sudden expansion.

Reference

Abouelwafa, M. S. A. and Kendall, E. J. M. (1980). The measurement of component rations in multiphase systems using gamma ray attenuation. *Journal of Physics E: Science Instruments.* 13, 341-345.

Al-lababidi, S. and Sanderson, M.L., Closure model for two-phase liquid-gas measurement under slug flow conditions. In: *Proceedings of the 11th International Conference on Flow Measurement, FLOMEKO'03*, Groningen, Netherlands, May 12-14, 2003.

Al-lababidi, S., and Sanderson, M.L. Transit Time Ultrasonic Modelling in Gas/Liquid Intermittent Flow Using Slug Existence Conditions and Void Fraction Analysis". In: *Proceedings of the 12th International Conference on Flow Measurement, FLOMEKO'04,* Guilin, China, Sep12-17 2004.

Andreussi, P. and Bendiksen, K. H. (1989). An Investigation of void fraction in liquid slugs for horizontal and inclined gas-liquid pipe flow. *International Journal of Multiphase Flow*, 15(6), 937-946.

Andreussi, P., Donfrancesco, Di. and Messia, M. (1988) . An Impedance Method for the Measurement of Liquid Holdup in Two-Phase Flow. *International Journal of Multiphase Flow*, 14(6), 777–787.

Barnea, D. and Taitel, Y. (1993). A model for slug length distribution in gas-liquid slug flow. *International Journal of Multiphase Flow*, 19(5), 829–838.

Beck, M.S., and Plaskowski, A. (1987). *Cross-Correlation Flowmeters: Their Design and Application.* Bristol, UK: Adam Hilger.

Bendiksen, K. H. (1984). An experimental investigation of the motion of long bubbles in inclined tubes. *International Journal of Multiphase Flow*, 10(4), 467-483.

Bendiksen, K. H., Malnes, D. and Nydal, O.J. (1996). On the modelling of slug flow. *Journal of Chemical Engineering Communications,* 141, 71-102.

Bignell, N. and Choi, Y. M. (2001). Volumetric positive-displacement gas flow standard. *Journal of Flow Measurement and Instrumentation,* 12(4), 245–251.

Brill, J. P., Schmidt, Z., Coberly, W. A., Herring, J. D. and Moore. D.W. (1981). Analysis of two-phase tests in large-diameter flow lines Prudhoe Bay Field. *SPE Journal,* 1981, 363-377.

Cheng, W., Murai, Y., Sasaki, T. and Yamamoto, F. (2005). Bubble velocity measurement with a recursive cross correlation PIV technique. *Journal of Flow Measurement and Instrumentation,* 16 (1), 35-46.

Corneliussen, S., Couput, J., Dahl, E., Dykesteen, E., Frøysa, K. E., Malde, E., Moestue, H., Moksnes, P. O., Scheers, L. and Tunheim, H. (2005). *Handbook of Multiphase Flow.* Norwegian Society for Oil and Gas Measurement (NFOGM) and The Norwegian Society of Chartered Technical and Scientific Professionals (Tekna), Norway, Revision 2, March 2005.

Costigan, G. and Whalley, P. B. (1997). Slug Flow Regime Identification From Dynamic Void Fraction Measurement in Vertical Air-Water Flows. *International Journal of Multiphase Flow*, 23(2), 263-282.

Coull, C. and Sattary, J. (2004). Evaluation of Ultrasonic Technology for Measurement of Multiphase Flow. National Engineering Laboratory, UK, Report No2004/230, November, 2004.

Davies, S. R. (1992). *Studies of Two-Phase Intermittent Flow in Pipelines.* PhD Thesis, Imperial College, London, UK, 1992.

Dong, F., Xu, Y. B., Xu, L. J., Hua, L. and Qiao, X. T. (2005). Application of dual-plane ERT system and cross-correlation technique to measure gas-liquid in vertical upward pipe. *Journal of Flow Measurement and Instrumentation*, 16(2-3), 191-197.

Dukler, A. E. and Hubbard, M. G. (1975). A model for gas-liquid slug flow in horizontal tubes. *Industrial and Engineering Chemistry Fundamental.* 14 (4), 337-347.

Fan, Z., Lusseyran, F. and Hanratty, T. J. (1993a). Initiation of slugs in horizontal gas-liquid flows. *Journal of American Institute of Chemical Engineering* . 39, 1741-1753.

Fan, Z., Ruder, Z. and Hanratty, T. J. (1993b). Pressure profiles for slugs in horizontal pipelines. *International Journal of Multiphase Flow*, 19(3), 421-437.

Ferschneider, G. (1983). 'Ecoulements Diphasiques Gas-Liquid á Poches et á Bouchon en Conduits. Cited in: **Hale, C. P. (2000).** *Slug Formation, Growth and Decay in Gas-Liquid Flow, chapter 3, p211.*PhD Thesis, Imperial College, London, UK, 2000.

Fossa, M., Guglielmini, G., and Marchitto, A. (2003). Intermittent flow Parameters from Void Fraction Analysis. *Journal of Flow Measurement and Instrumentation*, 14, 161–168.

Fossa, M. (1998). Design and Performance of a Conductance Probe for Measuring the Liquid Fraction in Two-Phase Gas-Liquid Flows. *Journal of Flow Measurement and Instrumentation*, 9, 103-109.

Ghassan, H. and Majeed, A. (1999). Liquid slug holdup in horizontal and slightly inclined two-phase slug flow. *Journal of Petroleum Science and Engineering* 27, 27-32.

Gopal, M. and Jepson, W. P. (1997). Development of digital image analysis techniques for the study of velocity and void profiles in slug flow. *International Journal of Multiphase Flow*, 23(5), 945-965.

Graham, B; Wallis, G. B. and Dobson, J. E. (1973). The onset of slugging in horizontal stratified air-water flow. *International Journal of Multiphase Flow*, 1(1), 173-193.

Gregory, G.A. and Scott, D. S. (1969). Correlation of liquid slug velocity and frequency in horizontal cocurrent gas-liquid slug flow. *Journal of AIChE,* 15, 933-935.

Gregory, G.A., Nicholson, M. and Aziz, K. (1978). Correlation of the liquid volume fraction in the slug for horizontal gas liquid slug flow. *International Journal of Multiphase Flow*, 4(1), 33–39.

Gurevich, Y. (2001). Performance evaluation and application of clamp-on ultrasonic cross-correlation flow meter CROSSFLOW. In: *Proceedings of the International Conference of Flow Measurement,* Sao Paolo, Brazil, (date), 2000.

Hale, C. P. (2000). *Slug Formation, Growth and Decay in Gas-Liquid Flow*, PhD Thesis, Imperial College, London, UK, 2000.

Hammer, E. A. and Nordtvedt, J. E. (1991). The Application of a Venturi Meter to Multiphase Flow Meters for Oil Well Production. In: *Proceedings of the 5th Conference on Sensors and their Applications,* London, UK, September 22-25 (Bristol: Adam Hilger).

Hewitt, G. F., Harrison, P. S., Parry, S. J. and Shires, G. L. (1995). Development and Testing of the 'Mixmeter' Multiphase Flowmeter. In: *Proceedings of the 13th North Sea Flow Measurement Workshop*, Lillehammer, Norway, October 24-26 1995.

Jepson, W. P. and Gopal, M. (1998). Ultrasonic Measuring System and Method of Operation. U.S Patent, Patent No 5,719,329, (February. 17, 1998).

King, M. J. S., Hale, C. P., Roberts, I. F., Fisher, S. A., Lawrence, C. J., Mendes-Tatsis, M. A. and Hewitt, G. F. (1997). Experimental investigations of flowrate Transients in horizontal pipes. In: *Proceedings of the 8th International conference on Multiphase Production*, Cannes, France, June 18-20, 1997.

King, N.W. (1990). Subsea multi-Phase Flow Metering a Chanllenge for the Offshore Industry. In: *Subsea 90 International Conferences,* London, England, December 11-12, 1990.

Kordyban, E. S. (1961). A flow modle for two-phase slug flow in horizontal tubes. *Journal of Basic Engineering, TASME,* 83, 613-618.

Kordyban, E. S. and Ranov, T. (1970). Mechanism of Slug Formation in Horizontal Two-Phase Flow. *Journal of Basic Engineering.* 92, 857-864.

Letton, W. (2003). Technique for Measurement of Gas and Liquid Flow Velocities, and Liquid Holdup in a Pipe with Stratified Flow. U.S Patent, Patent No 6,550,345 B1, (Aprial 22, 2003).

Lunde, O., Asheim, H. (1989). An Experimental Study of Slug Stability in Horizontal Flow. In: *Proceedings of the* 4th *International conference Multiphase Production,* Nice, France, June 19-21, 1989.

Malnes, D. (1979). Slip relations and momentum equations in two-phase flow. Cited in: **Bendiksen, K. H., Malnes, D. and Nydal, O.J. (1996).** On the modelling of slug flow. *Journal of Chemical Engineering Communications,* 141, 71-102.

Manfield, P. (2000). *Experimental, computational and analytical studies of slug flow.* PhD Thesis, Imperial College, London, UK, 2000.

Manolis, I. G. (1995). *High Pressure Gas-Liquid Slug Flow.* PhD Thesis, Imperial College, London, UK, 1995.

Mehdizadeh, P. and Williamson, J. (2004). *Principles of Multiphase Measurements.* Alaska Oil & Gas Conservation Commission, Alaska, USA.

Merilo, M., Dechene, R. L. and Cichowlas, W.M. (1977). Void Fraction Measurement with a Rotating Electric Field Conductance Gauge. *ASME Journal of Heat Transfer* 99, 330-332.

Mishima, K. and Ishii, M. (1980). Theoretical prediction of onset of horizontal slug flow. *Journal of Fluids Engineering, Transactions of the ASME* . 102, 441-445.

Moore, P. I. (2000). *Modelling of Installation Effects on Transit Time Ultrasonic Flow Meters in Circular Pipes.* PhD Thesis, University of Strathclyde, UK.

Moura, L. F. M. and Marvillet, C. (1997). Measurement of Two-phase Mass Flow Rate and Quality Using Venturi and Void Fraction Meters. In: *Proceedings of the 1997 ASME International Mechanical Engineering Congress and Exposition,* Dallas, TX, USA, November 16-21, 1997, The Fluids Engineering Division, FED, 1997, Vol. 244, 363-368.

Mwambela, A.J. and Johansen, G.A. (2001). Multiphase flow component volume fraction measurement: experimental evaluation of entropic thresholding methods using an electrical capacitance tomography system. *Journal of Measurement Science and Technology,* 12, 1092-1101.

Nadler, M. and Mewes, D. (1995). Effect of the viscosity on the phase distribution in horizontal gas-liquid flow. *International Journal of Multiphase Flow*, 21(2), 253-266.

Nicholson, M. K., Aziz, K. and Gregory, G. A. (1978). Intermittent two-phase phase flow in horizontal pipes: predictive models. *The Canadian Journal of Chemical Engineering*, 56 (6), 653-663.

Nydal, O.J., Pintus, S. and Andreussi, P. (1992). Statistical characterisation of slug flow in horizontal pipes. *International Journal of Multiphase Flow*, 18(3), 439-453.

Olsen, A.B. (1993). Framo Subsea Multiphase Flow Meter System Proc.Sem.Multiphase Meters and their Subsea Application, London, England.

Ong, K.H. (1975). *Hydraulic Flow Measurement Using Ultrasonic Transducers and Correlation Techniques*. PhD thesis. University of Bradford, UK.

Paglianti, A., Andreussi, P.and Nydal, O. J. (1993). The Effect of Fluid Propoerties and Geometry on Void Distribution in Slug Flow. In: *Proceedings of the 6th International Conference on Multiphase Production,Cannes*, France, June 16-18, 1993.

Pan, L. (1996). High Pressure Three-phase (gas-liquid-liquid) flow. PhD Thesis. Imperial College, London.

Rafa, K., Tomoda, T. and Ridley, R. (1989). Flow Loop Field Testing of a Gamma Ray Compositional Meter. In: *Proceedings of the ASME Energy Sources Technology Conference and Exhibition*, paper no.89-Pet-7, Houston, Texas, Jan 22-25, 1989.

Reis, E. dos. and Goldstein Jr. L. (2005). A non-intrusive probe for profile and velocity measurement in horizontal slug flows. *Journal of Flow Measurement and Instrumentation*, 16 (4), 229-239.

Roach, G. J. and Watt, J. S. (1996). Current status development of CSIRO gamma-ray multiphase flow meter. In: *Proceedings of the 14th North Sea Flow Measurement Workshop,* Peebles, Scotland, October 27-30, 1996.

Ruder, Z., Hanratty, P. H. and Hanratty, T. J. (1989). Necessary conditions for the existence of stable slugs. *International Journal of Multiphase Flow*, 15(2), 209-226.

Sanderson, M. L. and Yeung, H. (2002). Guidelines for the use of ultrasonic non-invasive metering techniques. *Journal of Flow Measurement and Instrumentation*, 13: 125–142.

Scott, S. L., Shoham, O. and Brill, J. P. (1986). Prediction of slug length in horizontal large-diameter pipes. In: *Proceedings of the 56th Regional Meeting on the Society of Petroleum Engineers*, Oakland, CA, April 2-4 (SPE 15103).

Singh, G. and Griffith, P. (1970). Determination of the Pressure Drop Optimum Pipe Size for Two-Phase Slug Flow in an Inclined Pipe. Cited in: **Hale, C. P. (2000).** *Slug Formation, Growth and Decay in Gas-Liquid Flow, chapter 3, p211.*PhD Thesis, Imperial College, London, UK, 2000.

Stanislav, J. F. Kokal, S. and Nicholson, M.K. (1986). Intermittent gas-liquid flow in upward inclined pipes. *International Journal of Multiphase Flow*, 12(3), 33–39.

Steven, R. N. (2002). Wet gas metering with a horizontally mounted Venturi meter. *Journal of Flow Measurement and Instrumentation*, 12(5-6), 361-372.

Stewart, C. (2001). *Instrumentation for the Measurement of Slug Flows.* PhD thesis, University of Strathclyde, UK.

Taitel, Y. and Barnea, D. (1990). Two-phase slug flow. *Advances in Heat Transfer,* 20, 83-132.

Taitel, Y. and Dukler, A. E. (1976). A model for predicting flow regime transitions in horizontal and near horizontal gas-flow. *Journal of American Institute of Chemical Engineering.* 22(1), 47-55.

Theuveny, B. C., Segeral, G. and Pinguet, B. (2001). Multiphase Flowmeters in Well Testing Applications. In: *Proceedings of the SPE Annual Technical Conference and Exhibition,* New Orleans, Louisiana, USA, September 30-October 3, 2001, SPE Paper 71475.

Thompson, E. J. (1978). Mid-radius ultrasonic flow measurement *FLOMEKO* ed H H Dijstelbergen and E A Spencer, pp 153–61.

Thorn, R., Johansen, G. A., and Hammer, E. A. (1997). Recent developments in three phase flow measurement. *Measurement Science and Technology*, 8(7), 691–701.

Tuss, B., Perry, D. and Shoup, G. (1996). Field tests of the high gas volume fraction multiphase meter. In: *Proceedings of the SPE Annual Technical Conference and Exhibition.* Denver, USA, October 6-9, 1996, SPE Paper 36594.

Van Santen H., Kolar, Z. I. and Scheers, A.M. (1995). Photo Energy Selection for Dual Energy Gamma and /or X-ray Absorption Composition Measurement in Oil-Water-Gas Mixtures. *Journal of Nuclear .Geophysics*, 9(3), 193-202.

Vedapuri, D. and Gopal, M. (2003). Determining Gas and Liquid Flow Rates in A Multi-Phase Flow. U.S Patent, Patent No 6,502,465 B1, (January 7, 2003)

Woods, B. D. and Hanratty, T. J. (1996). Relation of Slug Stability to Shedding Rate. *International Journal of Multiphase Flow*, 22(5), 806-828.

Xie, C. G, Stott, A. L., Plaskowski, A. and Beck, M. S. (1990). Design of capacitance electrodes for concentration measurement of two-phase flow. *Journal of Measurement Science and Technology*, 1, 65-78.

Xu, L.J., Xu, J., Dong, F. and Zhang, T. (2003). On fluctuation of the dynamic differential pressure signal of Venturi meter for wet gas metering. *Journal of Flow Measurement and Instrumentation*, 14(4-5), 211-217.

Yang, W. Q. and Beck, M. S. (1997). An intelligent cross correlation for pipelines flow velocity measurement. *Journal of Flow Measurement and Instrumentation*, 8(2), 77-84.

Zhang, H.J., YUE W.T. and HUANG, Z.Y. (2005). Investigation of Oil-Air Two-Phase Mass Flow rate Measurement using Venturi and Void Fraction Sensor. *Journal of Zhejiang University SCIENCE*,6A(6),601-606.

Appendix A

Table 1: Slug Flow Test Conditions

Test#	V_{SL} (ms^{-1})	V_{SG} (ms^{-1})	V_{mix} (ms^{-1})	Sample rate (Hz)	Test Duration (s)	GVF (%)	Flow Regime
1	0.30	0.60	0.90	500	180	60.12	SLUG
2	0.30	0.80	1.10	500	180	66.78	SLUG
3	0.30	1.00	1.40	500	180	71.53	SLUG
4	0.30	1.48	1.78	500	180	78.81	SLUG
5	0.30	1.75	2.37	500	180	83.90	SLUG
6	0.30	2.07	2.78	500	180	86.17	SLUG
7	0.30	3.01	3.31	500	180	88.32	SLUG
8	0.50	0.62	1.12	500	180	56.52	SLUG
9	0.50	0.83	1.33	500	180	63.36	SLUG
10	0.50	1.03	1.53	500	180	68.43	SLUG
11	0.50	1.52	2.02	500	180	76.07	SLUG
12	0.50	1.77	2.27	500	180	78.79	SLUG
13	0.50	2.07	2.57	500	180	81.26	SLUG
14	0.50	2.67	3.17	500	180	84.86	SLUG
15	0.50	3.15	3.65	500	180	86.84	SLUG
16	0.73	0.63	1.36	500	180	46.28	SLUG
17	0.73	0.84	1.57	500	180	53.38	SLUG
18	0.73	1.05	1.78	500	180	58.90	SLUG
19	0.73	1.26	1.99	500	180	63.28	SLUG
20	0.73	1.54	2.27	500	180	67.86	SLUG
21	0.73	1.76	2.49	500	180	70.67	SLUG
22	0.73	2.11	2.84	500	180	74.30	SLUG
23	0.73	2.47	3.20	500	180	77.15	SLUG
24	0.73	2.95	3.68	500	180	80.16	SLUG
25	0.93	0.62	1.55	500	180	40.00	SLUG
26	0.93	0.82	1.75	500	180	46.80	SLUG
27	0.93	1.01	1.94	500	180	52.01	SLUG
28	0.93	1.26	2.19	500	180	57.55	SLUG
39	0.93	1.49	2.42	500	180	61.60	SLUG
30	0.93	2.07	3.00	500	180	68.97	SLUG
31	1.03	0.82	1.85	500	180	44.08	Slug-Bubble
32	1.03	1.00	2.03	500	180	49.27	Slug-Bubble
33	1.03	2.02	3.05	500	180	66.15	Slug-Bubble

Table 2: Mean Values for Slug Characteristics Measurement by Ultrasonic

V_{SL}=0.3 (ms^{-1})

Test#	V_{SL} (ms^{-1})	V_{SG} (ms^{-1})	V_T (ms^{-1})	E_{LS} (-)	E_{LF} (-)	L_S (m)	L_F (m)	υ (Hz)
1	0.30	0.60	1.16±0.136	0.95±0.14	0.19 ±0.06	0.83±0.953	3.42±0.4	0.27
2	0.30	0.80	1.56±0.493	0.94±0.12	0.28±0.14	0.66±0.683	9.72±1.16	0.15
3	0.30	1.00	1.70±0.249	0.93±0.1	0.26±0.15	1.05±0.656	5.75±0.34	0.25
4	0.30	1.48	1.88±0.409	0.89±0.1	0.24±0.12	0.90±0.66	7.55±2.11	0.22
5	0.30	1.75	2.67±2.335	0.85±0.12	0.25±0.1	1.02±2.415	8.59±0.51	0.28
6	0.30	2.07	3.10±2.939	0.82±0.16	0.28±0.2	0.83±1.807	9.51±0.34	0.30
7	0.30	3.01	3.97±0.04	0.79±0.12	0.29±0.14	0.01±0.145	15.87±1.45	0.25

V_{SL}=0.5 (ms^{-1})

Test#	V_{SL} (ms^{-1})	V_{SG} (ms^{-1})	V_T (ms^{-1})	E_{LS} (-)	E_{LF} (-)	L_S (m)	L_F (m)	υ (Hz)
8	0.50	0.62	1.62±0.271	0.95±0.04	0.24±0.16	1.09±1.564	2.97±0.35	0.40
9	0.50	0.83	1.88±0.277	0.93±0.04	0.30±0.08	0.81±1.769	2.95±0.44	0.50
10	0.50	1.03	1.96±0.251	0.92±0.04	0.28±0.1	0.11±1.737	4.24±0.61	0.45
11	0.50	1.52	2.07±0.296	0.89±0.04	0.18±0.12	0.58±1.434	3.55±1.72	0.50
12	0.50	1.77	2.37±0.445	0.87±0.06	0.29±0.08	0.63±1.187	4.64±0.09	0.45
13	0.50	2.07	3.20±0.361	0.85±0.06	0.28±0.18	0.38±0.74	6.02±0.93	0.50
14	0.50	2.67	3.21±1.486	0.80±0.18	0.20±0.06	0.91±1.609	4.94±0.43	0.55
15	0.50	3.15	4.09±1.837	0.77±0.04	0.24±0.16	1.02±2.15	6.42±0.66	0.55

V_{SL}=0.73 (ms^{-1})

Test#	V_{SL} (ms^{-1})	V_{SG} (ms^{-1})	V_T (ms^{-1})	E_{LS} (-)	E_{LF} (-)	L_S (m)	L_F (m)	υ (Hz)
16	0.73	0.63	1.73±0.0751	0.93±0.04	0.14±0.08	1.21±1.158	1.68±0.07	0.60
17	0.73	0.84	1.96±0.14	0.92±0.04	0.25±0.14	0.90±1.209	1.40±0.22	0.85
18	0.73	1.05	2.18±0.127	0.90±0.08	0.20±0.12	0.93±1.204	2.70±0.77	0.60
19	0.73	1.26	2.56±0.229	0.89±0.06	0.23±0.1	0.73±1.213	3.21±0.4	0.65
20	0.73	1.54	2.65±0.496	0.87±0.08	0.26±0.12	0.74±1.429	3.04±0.31	0.70

21	0.73	1.76	2.90±0.585	0.85±0.06	0.20±0.12	0.78±1.393	2.63±0.77	0.85
22	0.73	2.11	3.46±1.138	0.82±0.06	0.27±0.1	0.61±1.480	5.17±0.31	0.60
23	0.73	2.47	4.74±0.942	0.80±0.06	0.23±0.1	0.66±1.342	8.82±0.24	0.50
24	0.73	2.95	4.91±0.575	0.77±0.1	0.23±0.1	1.51±0.583	8.32±0.43	0.50

V_{SL}=0.93 (ms^{-1})

Test#	V_{SL} (ms^{-1})	V_{SG} (ms^{-1})	V_T (ms^{-1})	E_{LS} (-)	E_{LF} (-)	L_S (m)	L_F (m)	υ (Hz)
25	0.93	0.62	1.93±0.107	0.92±0.06	0.23±0.08	0.70±1.044	1.23±0.2	1.00
26	0.93	0.82	2.17±0.128	0.90±0.02	0.17±0.16	0.81±0.763	1.26±0.42	1.05
27	0.93	1.01	2.50±0.187	0.89±0.04	0.21±0.18	0.58±0.835	1.80±0.11	1.05
28	0.93	1.26	2.81±0.249	0.87±0.1	0.26±0.04	0.95±0.925	1.73±0.24	1.05
29	0.93	1.49	3.10±0.261	0.85±0.08	0.25±0.1	0.73±0.845	2.09±0.42	1.10
30	0.93	2.07	3.46±0.598	0.81±0.06	0.23±0.14	1.30±1.111	4.99±0.51	0.55

V_{SL}=1.03 (ms^{-1})

Test#	V_{SL} (ms^{-1})	V_{SG} (ms^{-1})	V_T (ms^{-1})	E_{LS} (-)	E_{LF} (-)	L_S (m)	L_F (m)	υ (Hz)
31	1.03	0.82	2.31±0.154	0.90±0.04	0.29±0.18	0.68±0.857	1.42±0.46	1.10
32	1.03	1.00	2.61±0.213	0.88±0.04	0.23±0.1	0.50±0.694	1.77±0.32	1.15
33	1.03	2.02	3.75±0.06	0.81±0.08	0.27±0.1	1.47±0.203	2.48±0.59	0.95

Table 3: Slug Closure Model Factors $K_{1\ (Liquid)}$, $K_{2\ (Liquid)}$, $K_{3\ (Gas)}$ and $K_{4\ (Gas}$

Test	V_{SL} (ms^{-1})	V_{SG} (ms^{-1})	$K_{1(Liquid)}$ (-)	$K_{2\ (Liquid)}$ (-)	$K_{3\ (Gas)}$ (-)	$K_{4\ (Gas)}$ (-)
1	0.30	0.60	0.835	-0.612	0.041	-0.612
2	0.30	0.80	0.824	-0.621	0.053	-0.621
3	0.30	1.00	0.812	-0.568	0.064	-0.568
4	0.30	1.48	0.751	-0.585	0.090	-0.585
5	0.30	1.75	0.716	-0.536	0.125	-0.536
6	0.30	2.07	0.680	-0.499	0.147	-0.499
7	0.30	3.01	0.644	-0.499	0.183	-0.499
8	0.50	0.62	0.829	-0.518	0.047	-0.518
9	0.50	0.83	0.818	-0.501	0.059	-0.501
10	0.50	1.03	0.805	-0.621	0.071	-0.621
11	0.50	1.52	0.744	-0.610	0.097	-0.610
12	0.50	1.77	0.729	-0.513	0.112	-0.513
13	0.50	2.07	0.711	-0.535	0.130	-0.535
14	0.50	2.67	0.661	-0.510	0.166	-0.510
15	0.50	3.15	0.625	-0.454	0.201	-0.454
16	0.73	0.63	0.814	-0.459	0.062	-0.459
17	0.73	0.84	0.802	-0.407	0.074	-0.407
18	0.73	1.05	0.757	-0.518	0.084	-0.518
19	0.73	1.26	0.744	-0.532	0.096	-0.532
20	0.73	1.54	0.727	-0.487	0.113	-0.487
21	0.73	1.76	0.714	-0.499	0.126	-0.499
22	0.73	2.11	0.682	-0.501	0.145	-0.501
23	0.73	2.47	0.658	-0.533	0.169	-0.533
24	0.73	2.95	0.621	-0.457	0.205	-0.457
25	0.93	0.62	0.803	-0.437	0.073	-0.437
26	0.93	0.82	0.758	-0.448	0.082	-0.448
27	0.93	1.01	0.747	-0.517	0.093	-0.517
28	0.93	1.26	0.732	-0.397	0.108	-0.397
29	0.93	1.49	0.718	-0.450	0.122	-0.450
30	0.93	2.07	0.673	-0.463	0.154	-0.463
31	1.03	0.82	0.752	-0.410	0.088	-0.410
32	1.03	1.00	0.741	-0.509	0.099	-0.509
33	1.03	2.02	0.668	-0.340	0.158	-0.340

Table 4: Relative Error for Gas and Liquid Phase Volumetric Flowrates

Test#	V_{SL} (ms^{-1})	V_{SG} (ms^{-1})	GVF (%)	Liquid Phase Error (%)	Gas Phase Error (%)
1	0.30	0.60	60.12	-63.60	22.03
2	0.30	0.80	66.78	-59.20	24.93
3	0.30	1.00	71.53	-9.60	6.12
4	0.30	1.48	78.81	-16.00	-14.65
5	0.30	1.75	81.47	34.13	-29.74
6	0.30	2.07	83.90	36.40	-15.19
7	0.30	3.01	88.32	45.44	-12.24
8	0.50	0.62	56.52	-49.30	44.92
9	0.50	0.83	63.36	-48.00	25.83
10	0.50	1.30	73.13	-4.00	-12.81
11	0.50	1.52	76.07	-25.10	-2.69
12	0.50	1.77	78.79	17.83	-16.75
13	0.50	2.07	81.26	33.52	2.56
14	0.50	2.67	84.86	28.87	-18.87
15	0.50	3.15	86.84	30.10	-16.19
16	0.73	0.63	46.28	-40.60	38.94
17	0.73	0.84	53.38	-16.15	10.90
18	0.73	1.05	58.90	-22.16	24.97
19	0.73	1.26	63.28	-14.52	27.97
20	0.73	1.54	67.86	-1.72	3.12
21	0.73	1.76	70.67	-2.30	3.20
22	0.73	2.11	74.30	10.80	5.97
23	0.73	2.47	77.15	13.00	31.85
24	0.73	2.95	80.16	15.10	10.20
25	0.93	0.62	40.00	-38.10	56.36
26	0.93	0.82	46.80	-22.40	40.28
27	0.93	1.01	52.01	-32.10	51.07
28	0.93	1.26	57.55	7.50	12.52
29	0.93	1.49	61.60	2.90	18.69
30	0.93	2.07	68.97	6.50	3.35
31	1.03	0.82	44.08	-25.76	40.76
32	1.03	1.00	49.27	-35.00	35.15
33	1.03	2.02	66.15	18.99	-7.50